Postcranial indicators of primate sexual dimorphism: implications for reconstructing fossil hominin sexual dimorphism and hominin palaeoecology

Thesis submitted in accordance with the requirements of the University of Liverpool for the degree of Doctor in Philosophy by Shelley Anne Farrar Stoakes

August 2019

This thesis is dedicated to

John Barrie Ferguson

Abstract

Sexual dimorphism can be used to reconstruct various aspects of hominin palaeoecology; however, previous studies have highlighted problems with the current methodologies for estimating both sex and body mass. This includes the influence of body mass estimation techniques on the prediction of dimorphism and choosing the correct comparative sample. Increased understanding of sexual dimorphism within the primate order may improve the accuracy of methods used for estimation. Here the structure of sexual dimorphism for nine primate species was investigated through twelve postcranial indicators of skeletal dimorphism. Discriminant function analysis was used to assess the best metric discriminators of sex and was evaluated as a method for classifying sex in fossil hominin specimens. Differences in skeletal metric pair correlation coefficient values between the sexes were also used to investigate variation in the structure of sexual dimorphism.

Skeletal dimorphism within the primate order was found to be non-isometric, with upper limb metrics being generally better discriminators of sex for dimorphic primates. This includes *Homo sapiens* upper limb metrics, although femoral head diameter is a higher ranked discriminator of sex for *Homo sapiens* than it is for other dimorphic primates. Discriminant function analysis achieves greater accuracy in estimating sexual dimorphism than previous methods and accuracy is sustained when using a smaller number of the best skeletal metric discriminators. The pattern of skeletal metric correlation coefficient difference between males and females varies across the primate order and similarities between species do not consistently reflect phylogenetic relationships.

Separating the estimation of body mass and the determination of sex within fossil hominin species is important because it reduces the risk of error being introduced through the prediction of sex from body mass. The sustained accuracy of sex estimation through the best skeletal metric discriminators makes discriminant function analysis a practicable method of classifying sex for fossil hominin specimens. Patterns of shape dimorphism, analysed through skeletal metric correlation coefficient values, supplies another method for analysing the complexities of scaling relationships in males and females. Increased accuracy in estimation will lead to greater confidence when inferring various aspects of hominin palaeoecology.

Acknowledgments

Firstly, I would like to express gratitude to my supervisor Dr Matt Grove for his guidance, insight and good sense. I really appreciate each piece of constructive feedback and discussion. I also wish to thank my secondary supervisor Dr Jessica Pearson for every important suggestion that vastly improved the structure of the thesis. The Department of Archaeology, Classics and Egyptology at the University of Liverpool has produced an encouraging academic culture that strives to get the best out of everyone and I really value the work they do.

I wish to thank the Smithsonian NMNH, in particular Rick Potts, Jennifer Clark and Kristofer Helgen, for their kind support as I collected data at the museum. Thanks to David Hunt for providing me with access to the Robert J. Terry Collection. The three months I spent in Washington D.C. were some of the most enjoyable in my life thanks to the friendships made with fellow scholars on the AHRC IPS Scholarship. I would also like to thank Inbal Livne for organising access to the primate collection at the Powell-Cotton Museum. I am grateful to the North West Consortium Doctoral Training Partnership for funding the project and for the additional funds provided through the NWCDTP Fieldwork Fund and AHRC IPS Scholarship.

I am grateful to all my friends for their encouragement, especially my tribe of ambitious women who have always pushed each other in their achievements. I am ever thankful for my Husband for understanding the trials that come with having "the same piece of homework every day for four years". Thank you for coming home and cooking me delicious meals even though my workspace is by the kitchen. I also appreciate the fact that you learnt the names of hominins and very rarely mixed them up. Thanks to my parents for providing a place with clean sea air to escape to, critical thinking skills and a childhood library membership that started everything.

Finally, a special thanks to every Ferguson, Farrar, Stoakes and Bell who have supported me along the way. We are all bound together through marriage and a shared love of knowledge. I could not have asked for better supporters.

Contents

List of figures in text

Chapter 2: A review of literature relevant to the study

Chapter 3: Materials and methodology

Chapter 4: Defining the structure of sexual dimorphism in the primate order through discriminant function analysis

Chapter 5: Evaluation of sexual dimorphism estimation methods

Chapter 6: Scaling of skeletal dimorphism within the primate order

List of tables in text

Chapter 2: A review of literature relevant to the study

Chapter 3: Materials and methodology

Chapter 4: Defining the structure of sexual dimorphism in the primate order through discriminant function analysis

Chapter 5: Evaluation of sexual dimorphism estimation methods

Chapter 6: Scaling of skeletal dimorphism within the primate order

List of appendices

Chapter 1:

Introduction

1.1: Introduction

Body mass dimorphism can be used to reconstruct many aspects of hominin palaeoecology, including breeding systems, social dynamics and energetic requirements. Both body mass and canine tooth dimensions are employed in analysing the ecological correlates of extinct hominin sexual dimorphism; however, there is an imbalance in the application of dental metrics over postcranial indicators of sexual dimorphism. Given that sexual dimorphism in body mass is so prevalent among the extant primates, and has such clear ecological correlates, this imbalance is surprising. Evaluating sexual dimorphism through postcranial indicators of sexual dimorphism has the advantage of employing statistical models with multiple skeletal measurements to reduce uncertainty, whilst allowing canine tooth dimensions to be used as an independent test.

Nonetheless, the palaeoecological inferences produced from current methods of estimating fossil hominin sexual dimorphism are insecure as a result of the accumulation in error formed through the two-step process of estimating body mass and then predicting the level of sexual dimorphism from a pooled sample. As the ecological correlates of fossil hominin body mass dimorphism are dependent on the strength of prediction, there is a need for more accurate methods of estimation. Many studies have focused on improving the accuracy of body mass estimation but a greater understanding of sexual dimorphism within the primate order is required if there is to be improved techniques for determining the level of sexual dimorphism within fossil hominin species. Previous studies have shown that the use of sex-combined formulae for body mass estimation tends to influence calculations of body mass dimorphism. Separating body mass estimation from the prediction of sex and sexual dimorphism level could therefore improve studies of fossil hominin body mass dimorphism. The broad aim of this study is to increase understanding of sexual dimorphism within the primate order and improve the accuracy of methods used to estimate body mass dimorphism through a comparative analysis.

1.2: Aims of the study

This study aims to:

1. Investigate the structure of sexual dimorphism within the primate order through an analysis of postcranial skeletal dimorphism.
2. Evaluate how greater understanding of primate sexual dimorphism could be applied to the estimation of sexual dimorphism within fossil hominin species.
3. Explore the similarities and differences between species in terms of how skeletal metric scaling varies between males and females.

Previous studies have highlighted problems with the current methodology for hominin dimorphism estimation. Error is introduced from the two-step procedure of predicting body mass from FHD and then estimating the level of dimorphism within a pooled sample. Sexual dimorphism estimation methods also have reduced accuracy when applied to moderately dimorphic species. Comparing the level of dimorphism for skeletal metrics in different primate species can increase understanding of whether there is a pattern to the structure of sexual dimorphism across the primate order. Findings from the investigation into the structure of primate sexual dimorphism could be used to improve estimation techniques for fossil hominin species by either enhancing current methods or providing a new methodology.

A further exploration of how scaling between elements of the skeleton varies between males and females can provide a novel approach for interpreting sexual dimorphism. Previous research has focused on the scaling of body mass from individual skeletal metrics or joint size dimorphism. Here skeletal dimorphism will be evaluated in terms of variation in the extent to which skeletal metrics covary in males and females. This approach can be used to examine whether males are just larger females in terms of postcranial metric proportions or whether there are more complex scaling patterns underpinning sexual dimorphism. Any variation between species can also be inferred along with direct comparisons to *Homo sapiens.* This is particularly useful in understanding the differences between *Homo sapiens* and *Pan troglodytes* sexual dimorphism in greater detail, potentially providing a further aspect for interpreting fossil hominin sexual dimorphism.

1.3: Thesis structure

Chapter 2: *A review of literature relevant to the study* provides a review of the literature, highlighting the current problems in estimating body mass dimorphism, before an evaluation of how primate sexual dimorphism could be employed in improving the methodology. Chapter 3: *Materials and methodology* describes the sample collected for the study including descriptions of the primate species chosen and the postcranial skeletal metrics measured. Chapter 4: *Defining the structure of sexual dimorphism in the primate order through discriminant function analysis* investigates the structure of sexual dimorphism within the primate order through an analysis of postcranial skeletal dimorphism and answers the following questions:

1. Are there differences in the level of sexual dimorphism between skeletal metrics for a given species?
2. What is the structure of sexual dimorphism within the primate order (in terms of the variation and patterns between primate species as well as differences and similarities between skeletal metrics within the same species)?
3. Does the structure of sexual dimorphism in humans differ greatly in comparison to other primate species?

Discriminant function analysis was employed to highlight the most and least dimorphic skeletal elements within each species. The models produced were then compared to each other to see if there is any overall pattern across the primate order. Monomorphic species were also analysed, acting as a comparative sample for the evaluation of discriminant power. The discriminant function analysis results were tested through a comparison to binomial logistic regression.

Chapter 5: *Evaluation of sexual dimorphism estimation methods* assesses how greater understanding of primate sexual dimorphism could be applied to the estimation of sexual dimorphism within fossil hominin species and answers the following questions:

1. How does discriminant function analysis compare to previous methods of estimating sexual dimorphism?
2. For *Homo sapiens* samples, is there a distinct advantage to selecting skeletal metrics other than FHD as discriminators of sex?
3. Can choosing the most dimorphic skeletal metrics be applicable to fossil hominin cases as a way of estimating sexual dimorphism?

The methods most commonly used in previous studies of hominin dimorphism estimation were tested. The discriminant function analysis method of classifying sex was compared to the best previous method of defining the level of sexual dimorphism within a sample. The chapter also evaluates how discriminant function analysis can be practically used as an estimation technique by comparing accuracy percentages produced from discriminant functions employing a smaller number of skeletal metrics. The use of FHD as a classifier of sex in the discriminant function model was also investigated, noting its use in body mass estimation methods.

Chapter 6: *Scaling of sexual dimorphism in the primate skeleton* explores the similarities and differences between species in terms of how skeletal metric scaling varies between males and females and answers the following questions:

1. How variable is sexual dimorphic scaling between metrics within the skeleton of primate species?
2. Does the difference in scaling between males and females vary depending on the area of the skeleton?
3. How similar are humans to other species in the primate order in terms of sexual dimorphism scaling?

The first analysis in Chapter 6 involved the regression of all skeletal metrics to each other to determine the scaling relationship between them. Sexual dimorphism for the primate order was evaluated through a comparison between male and female correlation coefficients. The correlation coefficient difference results were then compared across species through hierarchical clustering. The similarities and differences between results for *Homo sapiens* and *Pan troglodytes* were evaluated in greater detail. Chapter 7: *Discussion* reviews all findings including the implications for hominin sexual dimorphism estimation procedures and potential future studies.

Chapter 2:

A review of literature relevant to the study

2.1: Literature review introduction

Accurate estimation of body mass has important implications for the field of palaeoanthropology for a variety of reasons. The first is that body mass is related to a range of life history characteristics including scaling relationships between increasing adult female body size and longer life spans, greater age at first reproduction and lower annual fertility in primates, as suggested by Charnov's Model (Charnov, 1993; Robson and Wood, 2008; Jones, 2011). The difference in body mass between males and females of a species is also associated with socioecological characteristics such as mating systems (Plavcan, 2012a) and so can be used to predict these characteristics in fossil species. Fossil hominin body mass estimation can also be utilised as a way of assessing trends in evolution, such as encephalization, tooth and gut size (McHenry, 1984; Aiello and Wheeler, 1995; Lacruz et al. 2008). Body mass has been used as a factor for defining hominin taxonomic classification and tracing geographical differences in population morphology. For example, Ruff (2010) analysed the relatively complete early *Homo* pelvis from Gona, Ethiopia and estimated the body mass of the specimen to around 33.2kg, which is far lighter than any previously known *Homo* specimen. This finding increases variation in body mass for the *Homo erectus* species to a level far greater than any other hominin taxon. The author concludes that the specimen may not belong to the genus, *Homo*, but in fact represent another contemporaneous hominin taxon. To continue implementing the estimation of body mass in such ways and to use such predictions for determining the level of sexual dimorphism, confidence in the accuracy of estimation must be affirmed. This chapter will aim to analyse the methods of estimating fossil hominin body mass and highlight any problems found in their execution and accuracy. As estimating body mass dimorphism within fossil species has the potential to aid in the inference of breeding structures and behaviours, this chapter will also examine methods of estimating body mass dimorphism and their accuracy, as well as highlighting the socioecological importance such estimations can have.

2.2: The socioecological importance of body mass dimorphism estimation

Estimating the level of dimorphism has important socioecological implications and is often used to increase understanding of the breeding systems and associated behaviour of a species. Body size dimorphism is linked to the sexual selection theory as proposed by Darwin (1871), where males are thought to compete for reproductive advantage as access to females is limited, and a larger body size increases the chances of success (van Schaik et al. 1999). Studies have shown that in highly dimorphic anthropoids this pattern fits, with male reproductive advantage achieved through the winning of fights with other males or by reaching the top of the social hierarchy, both allowing for better access to females (Cowlishaw and Dunbar, 1991). On average, monogamous anthropoids have been found to be less dimorphic on average, although new evidence from autosomal DNA studies has called the classification of some of these species into question (Di Fiore, 2003). Wittenberger and Tilson (1980) defined monogamous mating as an exclusive mating relationship between a single male-female pair, including prolonged association with one another. However, primate species that are often classified into this social system no longer fit this criterion in light of new evidence of extrapair copulations (EPC) (Morino, 2009). Genotyped fecal sampling in a wild white-handed gibbon (*Hylobates lar*) population found evidence of 7.1% EPCs in a dataset of 41 offspring, contradicting the traditionally-thought single male-single female mating strategy (Barelli et al. 2013). Kenyon et al. (2011) had previously discovered 1% extrapair paternity (EPP) in a golden cheeked gibbon (*Nomascus gabriellae*) population that was gradually recovering numbers due to forest regeneration. EPCs have also been observed in long term studies of Indri lemurs (*Indri indri*) and suggest that females may copulate with non-bonded males of superior genetic quality to increase genotypic fitness and variability of offspring (Bonadonna et al. 2014). Studies of the white handed gibbons of Khao Yai, Thailand suggest female cyclic sexual swellings do not accurately indicate time of ovulation and may be associated with paternity confusion, as swellings during pregnancy continue male interest and copulations when fertilisation is no longer possible (Barelli et al. 2008). Such studies also indicate that sexual swellings in gibbons are analogous to the greater sexual swellings found in Old World monkeys and great apes, as there is correlation between the size of sexual swellings and the frequency of copulation (Reichard et al. 2012). The male ability to increase reproductive success through extra matings is another obvious reasoning for EPC, but this is balanced by the cost of pursuing additional copulations and the gains from parental effort (Bonadona et al. 2014). The full extent of EPCs in supposedly monogamous anthropoid species is currently unknown, but the current evidence suggests that the

percentages are small and may be indicative of increasing genetic diversity when population numbers have fallen.

In 2013, two studies analysed the causation behind social monogamy in mammals, questioning whether selection for paternal care (contributions to the rearing of young), male protection against infanticidal competitors or male guarding strategy as a consequence of increasingly solitary female home ranges were the basis for a transition to social monogamy. Lukas and Clutton-Brock (2013) used Bayesian and Maximum Likelihood statistics to compare the social systems of 2500 mammalian species based on their own classifications of social systems. They found that in five out of six socially monogamous primate species, the ancestral condition would have been females living in individual home ranges, where males would be unable to defend access to more than one female.

Analysis of evolutionary transitions to social monogamy in mammals indicated that paternal care is a consequence rather than a causal factor of social monogamy (Opie et al. 2013a). The authors believe the dataset used does not indicate that infanticide was a causal factor but again a consequence of the transition to social monogamy. Opie et al. (2013a) also used Bayesian likelihood statistics but on a different data set of 230 primate species. Whilst the study agreed that paternal care was a consequence of and did not precede social monogamy, the authors also suggest that discrete female ranges were not a causal factor. The ancestral reconstructions and models indicate that male infanticide preceded social monogamy and that social monogamy with high infanticide creates an unstable state. This is because there is considered to be little evidence of transitions from polygyny to monogamy with low rates of infanticide and a small probability of transitioning back to polygyny as a consequence of the reduction in male infanticide. The study also indicates that the mechanism through which social monogamy decreased male infanticide is by the creation of shorter lactation periods in comparison to gestation periods, as males kill weaning infants to hasten oestrous resumption in non-seasonally breeding females.

A paper by de Waal and Gavrilets (2013) reviewed the conclusions of the two studies and suggests that caution should be taken when creating analyses from unreliable male infanticide data and that through removing this data, the correlation between male infanticide as a causal factor of social monogamy in primates is reduced. Dixson (2013) also critiqued the Opie et al. (2013a) results believing that much of the infanticide data was simulated via the correlation with ‘infanticide risk’- the ratio between gestation in addition to lactational length and the duration of lactation. The author suggests that the ratio is

affected by phylogeny as different evolutionary pressures have created the selection for variation in the ratio. The example provided is that the ratio is unlikely to be linked to male infanticide in the case of monogamous New World Callitrichids, which present no delayed ovulation during lactation, but lactate well into conception and have a cooperative breeding system. This is in comparison to monogamous Old World Hylobatids, which display a shorter interbirth interval in the event of infant death, and so male infanticide would be linked. Opie et al. (2013b) replied to this criticism by stating there was no confliction of Callitrichid monogamy with other primate species in the dataset. Moreover, the data set used to determine male infanticide included both observational data from wild populations and Van Schaik's index of infanticide. Lukas and Clutton-Brock (2014) believe that differences in the classification of social systems produced the differing results seen in the 2013 papers and suggest using models that do not assume constant change is better.

Lukas and Huchard (2014) formed phylogenetic analyses to identify social organisation and mating systems favoured by males in 260 mammals. The results suggested that the ratio of lactation duration to gestation is weakly correlated with infanticide risk and appear to confirm that female ability to breed throughout the year was the only factor able to explain distribution of male infanticide and that it occurs more frequently where reproduction is monopolised by a few males in stable mixed-sex groups. Therefore, infanticide is a consequence of contrasts in social and mating systems and not a causal factor of social monogamy.

Kappeler (2014) attempted to illuminate the issue through the analysis of Madagascan lemur behaviour (with variable intersexual cohesion amongst pair-living lemurs) to model the step-wise evolution towards monogamy in primates. Data from these variable behaviours suggested that female territoriality was the first step with females joined by males who shared ranges but with minimal interaction, which developed into the need for male mating strategies as the amount of social units containing two females decreased. This in turn would lead to the increased need for paternal care as male-female cohesion became more permanent. The requirement for female competition and interspecific competition also increased in group settings as did the need for infanticide avoidance. Whilst it should be noted that the life history data of lemurs is associated with individual ecological factors that are not representative of the whole primate order, the evidence does substantiate the Lukas and Huchard (2014) finding that selection for reduced infanticide risk will have limited importance when pair living and will gain greater importance in larger groups.

An attempt at analysing molecular sequence variation as a genetic indicator of the selective forces effecting social monogamy was published in 2014 (Ren et al. 2014). AVP (arginine vasopressin) is a hormone that has been found to affect various behavioural systems including social behaviour (Caldwell et al. 2008) and the study analysed genetic variation of the AVP coding regions with monogamous New World monkeys and other primate taxa. The results of the study found that there are genetic substitutions at six positions in Callitrichine primates, with four associated with possible functional change in the receptor subtype AVPR1a. However, only one substitution was noted in any other monogamous New World monkey and the authors caution that the results may be just a consequence of phylogeny and not linked to social monogamy.

Polygynous anthropoids do not always follow the predicted trend of having greater body mass dimorphism than monogamous species, provided by sexual selection theory, as studies have found that some polygynous anthropoid species participate in large amounts of intrasexual competition without showing associated body mass dimorphism (Martin et al. 1994). There are other proposed factors influencing the variability of body mass amongst anthropoids. Early research indicated that a principle factor affecting body size dimorphism is the level of dimorphism in ancestor species (Cheverud et al. 1985). This finding was refuted by Ely and Kurland (1989), who calculated that the amount of sexual dimorphism variation that is directly derived from phylogenetic inheritance amounts to only 1% and cannot be the main factor contributing to body mass dimorphism in anthropoids. Other factors highlighted in the literature include allometric effects (where the amount of sexual dimorphism accumulates as body size increases), energetic constraints associated with diet (found to be the second most important contributing factor to platyrrhine sexual dimorphism), the cost of lactation in females (with female *Papio* size reduced to absorb the cost of lactation) and the degree of arboreality and predation (Godfrey et al. 1993; Ford, 1994; Dement, 1983; Plavcan, 2001).

A study by Mitani et al. (1996) analysed the relationship between the above factors and body mass dimorphism. The effects of allometry and phylogeny were controlled in a sample of 18 anthropoid species, where the amount of females in estrus that could be monopolised by a male, depending on the timing of possible conception, was tested. The results showed that sexual selection was the principle factor influencing body mass dimorphism in polygynous anthropoids. Plavcan and van Schaik (1997) critiqued this study and indicated that caution was required as the study used operational sex ratios from a small sample, which is not

enough to clearly define relationships. The authors repeated the test with an increased sample size and found that the strongest relationship (between body mass dimorphism and possible male-male competition, substrate, diet, allometry and phylogenetics) was between male-male competition and body mass dimorphism. It was therefore concluded that the greatest influence on body weight dimorphism is male-male competition as predicted by sexual selection theory.

Plavcan (2001) had noted, however, that the absence of body mass dimorphism in anthropoid species was not indicative of monogamy or that there is male-male competition in a species. Lawler (2009) suggested two socioecological mechanisms that control the evolution of extant anthropoid male-male competition, one being extra pair paternities as previously discussed. Sexual selection is affected as the reproductive skew is reduced for a group when a male is unsuccessful in reproduction but is successful at extra-group fertilisations, reducing the possibility of sexual selection taking effect. The author notes that as the amount of extra-group fertilizations differ at the individual level, predicting the significance for fossil species is impossible. The second proposed socioecological mechanism controlling the evolution of extant anthropoid male-male competition is stabilising selection, which acts on males and alleviates the selective pressure for greater body mass. Evidence from observations of Verreaux's sifaka (*Propithecus verreauxi*), suggests that in certain environments an intermediate body size provides a reproductive advantage and for Verreaux's sifaka, as male-male fighting involves bouts of arboreal chasing, selection for a larger body to increase success in fights is stabilised by the need to be light and swift during arboreal locomotion. In terms of fossil species, Lovejoy (1981) proposed that differential exploitation of niches in *Australopithecus afarensis* may have produced selective pressure variation, leading to body mass dimorphism.

Recently the contribution of factors affecting female body mass have been highlighted with some authors indicating that there may be some correlation between male and female body size, as females would have to increase body size to give birth to larger offspring even if selection for increased body size acted only on males (Plavcan, 2011). It should be noted, however, that DeSilva (2011) found a negative allometric relationship between maternal and neonatal size across primates and Smith and Leigh (1998) had previously observed that more dimorphic species did not birth correspondingly dimorphic neonates. The Lande (1980) model suggests that the reason for these findings is that there is a correlated response to a larger male body size, as increasing the female size beyond the optimal size standard will

eventually select for a return to the standard, forming dimorphism. This is because large size decreases birth rates as stated in Charnov's life history model and so selective pressure for increasing the birth rate may have brought the female size back to its optimum standard (Charnov, 1993; Martin et al. 1994). It should be noted that the contribution of these factors to body mass dimorphism is likely to be small, as most sexual dimorphism will develop through the process of sexual maturation.

Female resource competition is another factor that may have affected the selection for larger female size. Dimorphism will be reduced if competition is formed between antagonistic females competing for resources and an increase in size provides an advantage in fights. Evidence for this has been suggested in *Pan troglodytes* populations as Leigh and Shea (1995) indicated that the extended growth period for female chimpanzees may be correlated with limited fruit resources. Studies analysing the relationship between female group size and body size in anthropoid species did not find any significant correlation between the two, although when folivores (with little observed resource competition) were removed from the sample, significant correlation between the two was formed (Lindenfors, 2002; Plavcan, 2011). Gordon (2006a) observed that if selection for large body size targets males then dimorphism will scale positively and males will show less body size variability. When selection targets females, the dimorphism will scale negatively and female body size will show less variability. Therefore, there is the potential to infer which selective forces influenced body mass dimorphism in a species from the level of body size variability presented. It should be noted, however, that there would be difficulty in acquiring the necessary data to apply this to fossil species.

2.3: Examples of the socioecological implications of body size dimorphism inferred from fossil hominins

The potential for predicting the above socioecological factors and the underlying evolutionary mechanisms for them in fossil species is particularly appealing. For example, there have been attempts to interpret the behaviour of *Australopithecus afarensis* from fossil evidence. The variation between small canine dimorphism and some estimates of body mass dimorphism in the species have been highlighted (see Section 2.2.4: *Examples of studies utilising fossil hominin body mass and dimorphism level estimation*). Small canine size is associated with a monogamous mating strategy or low levels of male-male competition as

per the weapon replacement theory, where weapons are thought to have replaced the use of canines in intrasexual competition and larger bodies were also more likely to not be selected for (Wolpoff, 1976). As australopithecines are generally associated with relatively low crowned maxillary canines, it has been suggested that species in the genus typically had low levels of intrasexual competition and therefore a monogamous social structure (Plavcan and van Schaik, 1997). As previously discussed, many of the studies analysing body mass dimorphism in *Australopithecus* suggest that the canine dimorphism is contrasted with larger levels of body mass dimorphism (Richmond and Jungers, 1995; Lockwood et al. 1996; Harmon, 2006). However, the results of Reno et al. (2003, 2010) provided further evidence of a monogamous mating strategy for *Australopithecus afarensis* as the level of dimorphism was found to be within the modern human range and not as great as *Gorilla* or *Pongo*. Furthermore, studies analysing the earlier *Ardipithecus ramidus* species suggest that it was minimally dimorphic and may be an indication that minimal to moderate dimorphism was selected for early in the lineage and retained later in *Australopithecus afarensis* (White et al. 2009). The work of Nelson et al. (2011) was also found to imply monogamy in *Australopithecus afarensis* as 2:4 digit ratios correlate with intrasexual competition and mating systems in the haplorhines, and whilst the digit ratios of *Aridipithecus ramidus* were consistent with polygynous extant species, the ratios of *Austalopithecus afarensis* were more consistent with monogamous extant species; it should be noted, however, that the results were speculative due to low sample sizes.

Plavcan (2001) questioned whether the relationship between sexual dimorphism and mating systems is strong enough to support such behavioural inferences in fossil species. After analysing canine and body mass dimorphism in relation to a range of behavioural correlates for 76 anthropoid species, the results suggested that dimorphism is of limited use for inferring behaviour as the estimated levels of dimorphism can mostly be found in more than one mating system or behaviour. Smaller amounts of body mass dimorphism were not found solely in species with monogamous mating strategies and so low dimorphism levels cannot discount polygynous behaviour, as previously thought. Moreover, there are other factors beyond sexual selection that have been found to affect the level of body mass in extant species, as discussed previously and summarised in Andersson (1994). The author has indicated that in future, studies should concentrate on defining the causal relationships between sexual selection and behaviour, social systems and the life histories of anthropoids before attempting to infer them in fossil species (Plavcan, 2012a). To produce more secure socioecological inferences based on sexual dimorphism, more accurate methods of

estimating fossil hominin sexual dimorphism must be developed first. This is because research that fully defines the causal relationship between sexual selection and behaviour will have limited value if it cannot be applied to fossil hominin cases.

2.4: Methods of estimating body mass

There are two types of body mass estimation techniques: morphometric and biomechanical. The theory behind morphometric body mass estimation is that the human body can be modelled on the shape of a cylinder. Body mass can therefore be calculated from the combined function of height (measured as stature) and width (measured as bi-iliac breadth) in an attempt to directly reconstruct body size. Ruff et al. (1991) developed equations that are sex specific due to variation in shoulder-to-hip ratio between sexes. Ruff et al. (1997) later added skeletal bi-iliac breadth to soft-tissue measurement conversion. This morphometric technique was tested on a sample of adults from Karkar Island and a sample of US Marine Corps. On average, the equations overestimated body mass by only 2-5%, apart from male marines in the sample who were underestimated by 9% on average. Ruff (2000a) examined whether the equations would be valid for use in estimating body mass for early human samples, considering the fact that they may differ in some aspect of body proportion or size in comparison to the populations used to develop the equations or the populations that had been used to test their accuracy. The study assumes that earlier humans would have a condition matched more closely with modern day athletes and so tested the estimation technique on measurement data from a sample of Olympic level athletes. The average for both sexes had a prediction error of less than 3%, although individuals specialising in weightlifting were underestimated and those who specialised in long distance events were overestimated. As the author believes that early humans would have a generalised body condition between those of the weight lifters and long distance eventers, the morphometric equations were considered suitable for estimation of early human samples. It should be noted, however, that the sample tested in the study was based on living measurements and error of estimation would increase for any skeletal sample, as the estimation methods for stature necessary for this technique have their own confidence interval and the morphometric technique still relies on reconstructing the living body width from bi-iliac breadth.

Ruff et al. (2005) wanted to test the morphometric equations on higher latitude populations using a sample of Alaskan Inupiat and Finnish adults, distinctive in being broad bodied as well as relatively tall in the Finnish sample. Whilst the results showed small directional error, for male Finns the error was larger and new equations were formulated from the data in the study to increase the accuracy of prediction for early high latitude humans. The differences between old and new estimates of various specimens were found to be small, although as expected, were greater for two specimens that were proportionally taller, wider bodied and considered closer to the added Finnish male data in the reference sample (noting the difference was still below 2%). The authors suggest using these new equations as they increase the range of body types in the reference sample. The study also highlights the difficulties of shoulder breadth variation on estimation accuracy. Although having separate equations for males and females goes some way to solve this problem, there is still a challenge in calculating absolute or relative shoulder breadths from fragmentary skeletal remains.

The morphometric equations have been used to estimate body mass in studies with early modern human samples (e.g. Holt, 2003) and for other *Homo* specimens (e.g. Rosenburg, 2005; Ruff et al. 2006). Body mass estimation of a probable *Homo heidelbergensis* specimen was attempted in 1999 after Pelvis 1 from the Sierra de Atapuerca site in Spain was reconstructed. An associated femur was used to estimate stature and through the combined stature and bi-iliac breadth equation, the body mass of the individual was estimated at between 93.1kg and 95.4kg (Arsuaga et al. 1999). The same researchers later revised the reconstruction of Pelvis 1 after the discovery of an associated complete lumbar spine. The corrected bi-iliac breadth and modified stature (now estimated from more than one possibly associated femur) created a body mass estimation range between 90.3kg and 92.4kg, smaller than the earlier estimation (Bonmati et al. 2010). Nonetheless, the estimated ranges from the two studies are similar, with ranges that almost overlap, which provides greater confidence in the estimation from the reconstructed pelvis.

The method has not frequently been employed for estimating the body mass of earlier hominins because of the variation in body form compared to modern humans. Ruff (1998) produced an estimate of body mass for the *Australopithecus afarensis* specimen A.L. 288-1 'Lucy' through a morphometric methodology. The study required modifications to the stature/bi-iliac breadth calculation because of the more elliptical shape of the *Australopithecus afarensis* pelvis. A correction factor was produced through measurement

of the external anteroposterior breadth of the pelvis along with bi-iliac breadth from a modern human sample. The resulting body mass estimate was close to the midpoint of previous estimations.

Brassey et al. (2018) applied a new type of morphometric body mass estimation employing convex hull modelling. The method utilises the relationship between body mass and an estimated 'shrink-wrapped' volume of the outer skeleton in extant species. A predictive model was produced from computed tomography scans of fifteen primate species. When applied to A.L. 288-1, the estimated body mass was found to be lower than all previous estimates, indicating that the technique does not have an appropriate conversion factor between the outer boundary volume and body mass for early hominin applications. The method requires validation through a larger comparison of species with different body shapes and volumes. The rarity of hominin specimens with enough remaining skeletal material, alongside the reduced accuracy in estimation due to the increased confidence interval caused by the approximation of separate elements, signifies the limitations of the morphometric method for use in estimating hominin body mass.

Biomechanical methods of body mass estimation are based on the mechanical relationship between a load-bearing skeletal element and body size and are implemented through the formation of equations, obtained by the regression of body mass onto the skeletal metric. Articular surface dimensions are less influenced by activity level and subsequent mechanical loading and so are preferred in comparison to diaphyseal breadths or cross-sectional dimensions (Trinkaus et al. 1994; Lieberman et al. 2001). Femoral head diameter (FHD) is often the skeletal metric of choice for biomechanical estimation as it is frequently found in skeletal assemblages and can be easily measured. This skeletal metric was used in the production of three biomechanical body mass estimation formulae. Ruff et al. (1991) developed a formula using a sample from modern US Baltimore with a body mass range of 42-135kg with a mean of 77kg (which in comparison to preindustrial Holocene samples is actually higher than average, probably due to the higher average age and fat deposits in the modern sample (Auerbach and Ruff, 2004)). The body mass range for the sample is within the range for modern humans, though it does not encompass the body mass of Pygmy and Andaman females. The formulae have an in-built adjustment for increased adiposity in modern U.S. adults that produces a downward correction factor of about 10%. This adjustment for adiposity is limited as the systematic error of the equation in each

preindustrial population is unknown and the 10% correction factor was chosen to create consistent results between the populations in the study.

McHenry (1992) created a formula from four sample means for modern humans, including African Pygmies and the small bodied Khoisan population. The body mass range for this sample was 30.4kg to 64.9kg. The new prediction equation was compared to an equivalent developed from all-hominoid regressions and found that the human sample formula was likely to outperform the all-hominoid formula in estimating fossil hominins.

Grine et al. (1995) developed a body mass estimation equation from ten sex/sample means that represented larger bodied humans and had a body mass range between 54kg and 84kg. This was used to estimate body mass from the large Berg Aukas proximal femur from northern Namibia. Trinkaus et al. (1999) indicate that the large femoral head diameter relative to femoral length may have been due to high levels of mechanical loading before maturation. Therefore, the method would have provided an overestimation of body mass for the Berg Aukas individual. However, Churchill et al. (2012) argue that previous studies have proven joint size to be independent of the amount of mechanical loading and highly active populations still show estimation from femoral head diameter equations that coincide with those from morphometric estimates. Ruff et al. (1997) compared the body mass estimations of each biomechanical formula with estimations from the morphometric formulae in a sample of Pleistocene *Homo* specimens. For all techniques, the mean absolute difference of estimates was found to be a non-statistically significant 5kg (7.6%) with the mean directional difference of 1kg (1.1%). Therefore, whilst morphometric and biomechanical methods use different skeletal elements and have different rationale for their use, the estimations were similar and with little systematic bias, increasing confidence in both methods.

Auerbach and Ruff (2004) noted the small sample size of the Ruff et al. (1997) study and the potential problems with the amount of skeletal elements in some specimens. They attempted to test the accuracy of the three biomechanical formulae using a sample of around 1000 Holocene human specimens and compared the body mass estimation with morphometric estimations (noting that this does not provide true body mass to compare with). The results showed that overall, the biomechanical methods estimated body mass for a large range of Holocene humans with little mean directional bias, in comparison to estimates using the morphometric method. There were, however, some differences between the biomechanical body mass estimation formulae. The morphometric equation

and stature estimation equations used for the technique are all formed from a worldwide sample. The three biomechanical equations do not show the full range of body size and shape diversity in the human species and so differ in accuracy depending on the size of the sample being estimated. The Ruff et al. (1991) formula had the best performance in terms of smaller mean directional bias in comparison to the estimated body mass from the morphometric formula, but performed less well at the extremes of the body mass range sample. McHenry (1992) was closest in accuracy to the morphometrically estimated body mass of female African Pygmies and Andaman Island samples, and is therefore more suitable for estimating smaller bodied samples. Grine et al. (1995) was closest in accuracy to the morphometrically estimated body mass of larger specimens used in the study and is most suitable for estimating larger bodied samples. Auerbach and Ruff (2004) suggest averaging the estimations from the three formulae when using data from the middle of the range, but not at the extremes.

The biomechanical estimation techniques have been tested in their accuracy when estimating specific human population samples. Pomeroy and Stock (2012) analysed the estimated body mass results from a sample of coastal and mid-altitude Andean populations. The pattern of the Ruff et al. (1991) formula giving greater bias at the extremes of the sample range, McHenry (1992) equation underestimating body mass in the sample and the Grine et al. (1995) equation overestimating body mass in the sample was repeated. But averaging the estimations from the three formulae did reduce bias at the extremes of the range in the Andean sample, noting that the population was in the middle of the human body mass range as expected from these results.

Kurki et al. (2010) examined the estimations of body mass from small bodied individuals in a southern African Holocene population, which had a smaller than average stature and narrower pelves. As expected, the McHenry (1992) formula was more appropriate for the smaller females in the population and the smaller average body size meant the Ruff et al. (1991) formula tended to overestimate body mass. Population specific equations developed for European Holocene specimens were found to have greater prediction accuracy than previous methods (Ruff et al. 2012). Whilst these new equations have the advantage of being more representative of European Holocene body size, there are weaknesses with these formulae as they were developed using morphometric estimates of true body mass and so the accuracy of predictions will be reduced.

The use of craniometrics has been considered an alternative method for estimating fossil hominin body mass, using elements more likely to survive in fossil assemblages. Aiello and Wood (1994) and Kappelman (1996) believed measurements from the orbital region can be used as an alternative to femoral head diameter when estimating body mass through biomechanical techniques. Spoctor and Manger (2007) found upper facial breadth and orbital height to have strong correlation with body mass and formed regression equations, developed from a primate sample, for the estimation of fossil hominin body mass. However, a later study tested the scaling of postcranial, dental and cranial metrics in a Cercopithecoid sample and found orbital dimensions provided low correlation with body mass, although neurocranial lengths had higher correlation (Delson et al. 2000). Plavcan (2003) decided to look at the taxonomic differences in scaling between craniofacial variables and body mass for a primate sample that included Cercopithecoids, Platyrrhines and Hominoids. The results showed significant taxonomic differences in scaling between craniofacial metrics and body mass, whilst the existing equations for the prediction of body mass from craniofacial metrics produced high levels of error. More recently, Elliot et al. (2014) noted the problem of using estimation equations formed from the means of various primate species to predict the body mass of a single specimen. They decided to test the above sets of prediction equations, and as modern humans were within all the reference samples used to formulate equations, the use of modern human CT scans to analyse the accuracy of estimation was deemed acceptable. The results showed the method had large amounts of error in estimation and suggested the original small size of the reference sample formulating the equations caused the reduced prediction accuracy.

Therefore, whilst methods of estimating body mass from craniometric variables would be useful in the field of palaeoanthropology, the problem of wide taxonomic differences in scaling relationship make developing accurate estimation equations difficult. Morphometric equations have noted limitations including: unsolved problems with error due to shoulder breadth variation, potential differences in relative muscularity between specimens and the need to match with a reference sample containing the same body proportions (especially in terms of stature) to reduce the effects of error from predicting the necessary elements of the equation. Consequently, most studies undertaking estimations of fossil hominin specimens have used biomechanical body mass regression equations.

The latest studies in body mass estimation have attempted to develop biomechanical body mass regression equations different to the conventionally used Ruff et al. (1991), McHenry,

(1992) and Grine et al. (1995) equations. Squyres and Ruff (2015) developed a body mass estimation technique based on knee breadth rather than FHD. A new technique was deemed necessary because of the potential differences in mechanical loading of the femoral head due to variation in the morphology of the hip and gait between Australopithecines and *Homo* species. Joints articulations do not change in response to mechanical loading throughout adulthood. Therefore, joint size will reflect young adult body mass rather than the modern human trend for increased body mass in old age. This makes articulations more suitable for the archaeological record as extreme adiposity and old age are unlikely.

The Squyres and Ruff (2015) study compared the new knee regression formulae (from a sample of living human subjects using radiographs) to estimate body mass on fossil hominin specimens. Because many of the fossil knee measurements were below the modern human sample range, the choice of reduced major axis regression was made over least squares regression when developing the formulae. This follows the suggestion by Konigsberg (1998), due to the calibration that reduces the limitation problem of only being applicable to cases derived from the same sample of data used to form the equations (see Section 2.2.2: *Problems with estimating fossil hominin body mass*). The results were comparable to estimations using FHD with absolute error between 7% and 9%. As with FHD, estimation equations from knee measurements were found to be more correlated with young body mass.

The method was suggested as being less problematic than estimating body mass from FHD because of the potentially different hip mechanics during weight support as hip joint loading relative to body mass is reduced in Australopithecines. Ruff and Higgins (2013) compared the cortical thickness of the femoral neck for two Australopithecine species using CT scans and found them to be generally closer in morphology to humans than apes, although some values were intermediate and the midneck was found to be closer in morphology to apes. By comparing proximal femur metrics of Australopithecines and *Homo* specimens the study found that in comparison to modern humans, Australopithecines have a femoral neck with superoinferior length that is relatively larger than femoral head breadth. This pattern was not found in early *Homo* specimens. This observation, combined with their smaller femoral heads, suggest Australopithecines had a slightly altered gait involving the centre of gravity positioned more laterally over the lower limb. The knee is therefore considered less problematic for use in body mass estimation equations as it is positioned under the centre of gravity for the body.

The use of other articular metrics than FHD for body mass estimation was also explored by Ruff (2002a). The study analysed the body mass of Old World monkeys and apes using both cross-sectional diaphyseal and articular metrics. Data from sex/species means in comparison to known body mass when forming regression equations was used to assess choice of reference sample. Least squares regression was applied and the percentage standard error of estimation was calculated. The tibia was found to provide less precise body mass estimations than the femur apart from proximal tibial articular breadth. The femur is generally better than the humerus, lengths are poor estimators and articular breadths were better than surface areas. Ruff (2003) suggests linking species by locomotion and structural proportions when choosing a comparative sample and metric for regression. Fossil anthropoid specimens may have intermediate morphology or unknown locomotion so the best choice for an equation may be an average of estimates derived from different reference groups. A multivariate approach was also tested but adding more than one metric was not found to increase predictive power, although some of the worst predictors may be made better with additional metrics.

More recent body mass estimation methods note the importance of avoiding extrapolation beyond the size range of the reference sample, especially for studies estimating early fossil hominin body mass. Dagosto et al. (2018) avoided extrapolation beyond the size range of the reference sample in a study estimating the body mass of early Eocene primates, *Teilhardina* and *Archicebus*. The comparative sample used to develop estimation equations included a variety of small-bodied mammals. Tests of models with varying taxonomic and size compositions indicated that the choice of variable was more critical for estimation than the choice of model. The most reliable variables, which produced body mass estimates of *Teilhardina* and *Archicebus* within the expected range of mouse lemurs, were mediolateral breadth across the femoral condyles and the area of the calcaneocuboid facet of the calcaneus. Ruff and Niskanen (2018) note that the choice of variable and reference sample are interrelated as the choice of reference sample will have less importance for estimation produced by the best performing variables. Therefore, the relationship between the best predictive variables and body mass is more constant across taxa. Perry et al. (2018) also found the mediolateral breadth of the knee joint to be the best variable for estimating body mass with consistent results across taxonomic groupings in a large sample of catarrhine and platyrrhine primates. The results of both Dagosto et al. (2018) and Perry et al. (2018) corroborated earlier evidence of the strong relationship between knee traverse breadth and

body mass for catarrhine species (Ruff, 2003). This suggests that knee morphology and function is conserved in many primate species.

Body mass estimation methods were reviewed by Grabowski et al. (2015) and noted that, since McHenry (1992;1994), the number of fossils found has increased with more taxa defined and there are now better human comparative samples especially including smaller bodied humans. They also note that the work of Uhl et al. (2013) offers better scaling testing when producing estimation equations (see Section 2.3: *Problems with estimating fossil hominin body mass*). The study used a large (n=220) sample of modern humans with known body mass to create estimation equations used to predict hominin species body mass averages. The method used meant it was possible to provide confidence intervals, determine traits with some scaling relationships and use inverse calibration as suggested by Uhl et al. (2013). However, the reference sample only employed modern humans and the authors reasoned that chimpanzees could not be used as their lower limbs do not have critical adaptations for bipedalism, although this may only make a difference for hominins that appear to be bipedal and human samples may potentially be less appropriate for the earliest fossils of our clade. The study also notes the requirement for actual body mass data for the reference sample and this is difficult to acquire from chimpanzee data. It should be noted that there were no known body masses for smaller bodied modern human populations used in this study, and smaller bodied individuals from the Terry Collection were chosen to provide less biased body mass estimates for smaller bodied hominins, although there may be issues with limb scaling differences between smaller bodied individuals in the Terry Collection and smaller bodied modern human populations. The study also only focused on lower limb measurements for estimation, reasoning that bipedal locomotive adaptations would be shared with early hominins that connect to weight distribution. However, there will be differences between taxa depending on the amount of retained arboreal locomotion, although the upper limb was not used because the relationship between body size and upper limb morphology in early hominins is unknown.

Ruff et al. (2018) developed new body mass estimation equations from femoral head diameter and proximal tibial plateau breadth. The reference sample was derived from diverse modern human populations with the aim of applying the methodology to hominin specimens. An adjustment was built into the equations to account for the smaller femoral head diameters of non-*Homo* taxa through the observed difference between joint scaling in the hip and knee. The correction compensates for the assumed relative reduction in hip

loading expected for australopiths. The Ruff et al. (2018) estimation equations are dependent on the accuracy of the morphometric method of estimating body mass as the stature/bi-iliac breadth equations were employed in determining the body mass of specimens within the modern human reference sample. This means that some error was already introduced in the development of the equations, before they were applied to hominin specimens.

There is a difference in the hominin body mass estimations developed from Ruff et al. (2018) and those produced by Grabowski et al. (2015). The lower body mass estimates of Grabowski et al. (2015) were attributed to the use of a larger-bodied reference sample. Ruff et al. (2018) argued that the discrepancy in body mass estimates was due to body mass being derived from the cadaveric measurements of the Terry and Hamann-Todd osteological collections in the Grabowski et al. (2015) study. A previous use of cadaveric samples for body mass estimation procedures displayed reservations as to the accuracy of the recorded cadaver weights in these collections (Churchill et al. 2012). Comparison of the recorded weights to estimations from stature/bi-iliac breadth found an underestimation of cadaveric body mass of 29%. Ruff et al. (2018) suggested that the lower weight may be due to postmortem processing procedures. This means that although error may be introduced through the development of a reference sample with body mass determined by stature/bi-iliac breadth, the opposing use of cadaveric body mass may produce more inaccurate body mass estimations. A summary of studies utilising body mass estimation equations is provided in Table 2.1.

Table 2.1: Summary of body mass estimation methods evaluated in this chapter.

Studies with body mass estimation equations from morphometric, biomechanical and craniometric methods	
Morphometric	Ruff et al. (1991) Ruff et al. (1997) Ruff et al. (2005) Brassey et al. (2018)
Biomechanical	Ruff et al. (1991) McHenry (1992) Grine et al. (1995) Squyres and Ruff (2015) Ruff (2002a) Dagosto et al. (2018) Perry et al. (2018) Grabowski et al. (2015) Ruff et al. (2018)
Craniometric	Aiello and Wood (1994) Kappelman (1996) Spoctor and Manger (2007)

2.5: Problems with estimating fossil hominin body mass

Whilst biomechanical methods can, on the whole, be considered more practical for palaeoanthropological studies, there are underlying problems with the use of estimation formulae. Smith (1996) examined the reliance on proxies of body mass for fossil specimens, which generates additional error when estimating body mass for fossil hominin taxa, as the estimation is based on methods created through the use of data from other species. The author also describes how the analysis of ecological correlates is restricted through the uncertainty caused by the multiplication of regression error when approximating body mass dimorphism. The author shows that the cumulative effects of confidence intervals means that the predictions often have little value as each predicted step in the method multiplies the error in estimation. The width of the CI provides an indication of how useful the regression model is for estimating body mass, with a wider CI suggesting a less precise estimation. Therefore, inferred ecological correlates can greatly differ depending on which prediction in the range is chosen for analysis. Studies that infer socioecological traits from predicted body mass are also limited because of interspecies differences in the relationships

between body mass and certain traits. As a result, predicting traits in fossil hominins is dependent on which comparative relationship is chosen as a reference.

Studies have shown that skeletal metrics scale to body mass differently between taxa with modern humans showing positive allometry between femoral head diameter and body mass whilst gibbons, siamangs and great apes show a close to isometrical scaling relationship between femoral head diameter and body mass (Ruff 1988; Jungers, 1990a; Ruff and Runestead, 1992). Gordon et al. (2008) suggests only using postcranial data where the skeletal metric scales isometrically with body mass in all comparative taxa or choosing metrics that scale allometrically equivalent for all comparative taxa. However, this is not possible when estimating fossil hominin body mass as the correct scaling relationship may be unknown. Nonetheless, Gordon et al. (2008) do indicate a solution by scaling sexual dimorphism for each measurement by the allometric scaling relationship of the the comparative sample. All possible extant scaling patterns would then be applied to the fossil sample to determine if the results are consistent. The authors indicate that for analysing dimorphism level, the method used by McHenry (1992, 1994) for *Australopithecus afarensis* specimens was already implementing this technique, where allometric scaling relationships between skeletal metrics and body mass in both apes and humans were used to form separate estimations and analysed together.

There are also difficulties in the choice of regression techniques used to formulate body mass estimation equations. Konigsberg et al. (1998) believe that whilst estimation from regression equations is frequently used, the best use of the method is limited to the application of future cases that are derived from the same sample of data used to form the equations. The authors highlight the two potential calibrations that can be used. The first is inverse calibration as a Bayesian estimator, where the likelihood of observing a fixed data point is conditional on the unobservable value, but with relation to prior probability, creating a regression of the greater unobservable value onto the smaller value. The second is classical calibration as a Maximum Likelihood estimator, which forms the maximum probability of obtaining a particular data set, where the fixed data point is conditional on the unobservable value, creating regression of the greater unobservable value onto the smaller value and then solving for the unobservable value. Whilst the study utilised stature estimation as an example, the points raised do extend to other types of estimation including body mass. Inverse calibration was found to be suitable when the distribution being analysed is similar to the reference sample. Classical calibration should be used when the estimation is likely to

be beyond the useful limits set by the reference sample. Hens et al. (2000) also found that classic calibration was best for body mass estimation extrapolated from a reference sample not similar in terms of either size or shape to the target specimen.

Auerbach and Ruff (2004) noted the findings of Konigsberg et al. (1998) and Hens et al. (2000) when analysing the results of their comparison of estimation formulae. The problem of data extremes when using the Ruff et al. (1991) equation, where smaller individuals were overestimated, was thought to be caused by the use of inverse calibration when formulating the regression equation. This again signifies that that the method works best when the sample being estimated is closest to the centre of distribution in the reference sample. The authors note the alternative method of extrapolating beyond the ends of the reference sample by Konigsberg et al. (1998) and Hens et al. (2000), as well as using the reduced major axis as supported by Aiello (1992). It should be noted, however, that Konigsberg et al. (1998) believe the use of the reduced major axis will simply mean a compromise between inverse and classical calibration that cannot extrapolate around the mean to the extent of classical calibration.

Uhl et al. (2013) suggest R and R_x statistics (Brown and Sundberg, 1987) as a way of comparing size and shape differences between the target specimen and the reference sample to evaluate how much extrapolation will be needed for estimation. This prior analysis to estimation can be used for palaeoanthropological estimations where unknown body mass is estimated through the use of a reference sample with known body mass. This is due to the fact that the R statistic provides a measure of allometric differences whilst the R_x statistic provides a measure of size extrapolation. The choice between inverse and classical calibration can be based on the R_x statistic, where significant values dissuade from the use of inverse calibration. The Uhl et al. (2013) study applied this technique to a *Homo erectus* specimen, KNM-WT 15000, and the R_x statistic found a significant allometric departure between femoral head diameter and body size, with the femoral head diameter being significantly larger than expected.

Each of the highlighted difficulties in the use of biomechanical methods can reduce the accuracy of body mass estimations. Whilst this is important to note in itself, most studies attempt body mass predictions of fossil species for the application of further analysis. Estimating the level of body mass dimorphism in a species is often the next step in palaeoanthropological studies.

2.6: Estimating body size dimorphism in fossil hominins

Sexual dimorphism can be defined as the absolute differences in size and shape between males and females of a species. For fossil hominins, there are complications in analysing the level of sexual size dimorphism for a species because the small number of available specimens can cause taphonomic bias towards one sex rather than the other. Problems with the taxonomic classification of specimens and the fragmentary nature of many fossil hominin assemblages are other reasons why accurately estimating the level of sexual dimorphism in fossil hominin species is particularly difficult. As the sex of fragmentary fossil specimens is often unknown, because no sex specific morphological traits are preserved, most studies analyse fossil hominin dimorphism by assuming larger specimens are male and smaller specimens are female. Any overlap in size between the sexes will be ignored in analysis and so the methods used tend to overestimate the level of dimorphism; this is particularly enhanced when the level of true dimorphism is small (Plavcan, 1994).

When attempting to determine the amount of sexual dimorphism in a fossil sample, there needs to be confidence that any dimorphism observed is not the result of two separate, but morphologically similar species or two geographically divided groups of the same species. A simple solution was developed through graphic analysis where continuity in a bivariate plot can be used to indicate a single species and a break in the plot is considered an indication of two species within the sample (Fernandez and Monchot, 2007). However, it has been shown that such patterns may simply be a reflection of sampling error and that a sample of closely related species may not always produce increased sample variation. This is because higher levels of variation can be considered an indication of two separate species within the sample, but low levels of variation cannot provide full confidence that the sample contains only one species (Plavcan and Cope, 2001; Cope and Lacy, 1992; 1995). As the likelihood of sexes and species being equally represented in a fossil sample are low, non-sexually dimorphic traits are often chosen as a way of determining whether the sample contains taxonomically different specimens.

When sex is known sexual dimorphism is measured as the ratio of mean male size to mean female size. For fossil species this is rarely the case and so other methods of estimating the level of sexual dimorphism must be undertaken. Once of the simplest techniques is the mean method, based on the principle that as male and female distributions should not intersect, the combined sample with unknown sex can be divided at the mean (Godfrey et al. 1993). The larger subsample is then considered male and the smaller subsample is considered

female. The mean of the larger subsample is then divided by the smaller subsample to calculate dimorphism. An associated technique, the median method, works under the same principle but uses the median to divide the combined sex sample. Tests of comparison have found the median method to be less reliable than the mean method (Plavcan, 1994). Josephson et al. (1996) highlights the difficulties with the method due to the fundamental assumption that the sample in question will show clear bimodal distribution. Accuracy in estimating the level of dimorphism within the sample will be reduced if male and female values overlap in the distribution, meaning graphic representation of the data will still be needed for confirmation. The authors therefore developed the mean-of-moments method. A form of finite mixture analysis, the technique assumes that the sample is made up of two normal distributions, one male one female. Three moments around the mean of the combined sex sample are used to estimate the mean and standard deviation of the two distributions (Josephson et al. 1996). The method still suffers from its sensitivity to sample size, where accuracy is reduced in smaller samples and from fluctuations in the ratio between males and females, where accuracy is decreased depending on fluctuation in the sample ratio, which in terms of application for fossil samples, are both common potential problems. Rehg and Leigh (1999) tested these methods with actual data in a large sample consisting of 42 anthropoid species with known body mass. Although the mean method was the most consistent (in comparison to median and method of moments) it was inaccurate for 25% of the cases and tended to overestimate dimorphism when true dimorphism was low. Averaging all three did not increase prediction accuracy.

The use of the coefficient of variation is another method that is often exercised as a way of estimating the level of dimorphism in a sample. Fleagle et al. (1980) and Kay (1982) noted the correlation between mean male and female canine dimension ratios and the combined sample coefficient of variation for Oligocene anthropoids and Miocene hominoids, respectively. A further study went on to analyse canine sizes in species of *Australopithecus,* utilising the coefficient of variation (Leutenegger and Shell, 1987). The theory behind the method is that as the distance between the means of the male and female distributions in the sample increases, the standard deviation increases. This can be measured as the standard deviation divided by the mean, otherwise known as the coefficient of variation. Coefficients of variation for extant species with known dimorphism can then be used to estimate fossil coefficients of variation through the development of regression equations. Josephson et al. (1996) tested the method using an optimized artificial sample where the numbers of species used to develop the regression equations were greater than the amount

actually implemented, each species was made to have the same within sex coefficient of variation and the sample sizes were large. The method was found to overestimate dimorphism level at low levels of dimorphism, independent of sample size. The authors also note the problem of choosing the correct comparative species for determining the level of dimorphism from the coefficient of variation, as there are differences in coefficients of variation between extant species. Plavcan (1994) had also found that the method is sensitive to fluctuations in ratio and unable to provide reliable dimorphism estimations when true sexual dimorphism in the sample is low.

Another technique used to estimate the level of sexual dimorphism in a combined sex sample is the binomial dimorphism index. This technique is similar to the mean method in terms of fundamentally splitting the combined sample and dividing the mean of the larger subsample by the mean of the smaller subsample. The binomial index works by arraying the data according to increasing size and the weighted mean of all the ratios is calculated from a sample of n-1 sex allocations (Reno et al. 2003). This technique was compared to the mean method and another method of sexual dimorphism estimation, maximum/minimum ratios. These ratios estimate the dimorphism level by simply dividing the largest value by the smallest value (Richmond and Jungers, 1995). The technique was found to be especially poor as it ignored other values in the sample beyond the maximum and minimum and therefore tended to overestimate the amount of dimorphism in the sample (Plavcan, 1994). Gordon et al. (2008) compared multivariate postcranial size dimorphism in an *Australopithecus afarensis* fossil sample and a comparative sample made up of *Homo sapiens, Pan troglodytes, Gorilla gorilla* and *Pongo pygmaeus*. The mean method, binomial dimorphism index and max/min ratios were tested on the comparative extant all hominoid sample. Max/min ratios were again found to overestimate postcranial sexual dimorphism. The mean method and binomial dimorphism index were found to produce acceptable estimations for *Gorilla gorilla* and *Pongo pygmaeus*, but overestimated the dimorphism level in *Homo sapiens*. The coefficent of variation was analysed separately as the technique does not produce ratio values for comparison directly, and were found to share the estimation accuracy pattern of the mean method and binomial dimorphism index. Therefore, this test again reproduced the result that methods formed from dividing the largest value from the smallest overestimate sexual dimorphism level when male and female values overlap in the sample distribution.

A further problem for estimating fossil hominin body mass dimorphism is that the methods for estimating body mass influence the predicted level of sexual dimorphism. Ruff et al.

(2012) found that combined-sex body mass equations increased sexual dimorphism in mean body mass up to 3% whilst the sex-specific body mass equations reduced sexual dimorphism up to 0.3%. A recent 2018 study also found that sex-specific femoral head equations reduced differences in mean body mass between males and females (Sládek et al. 2018). Moreover, the resulting sexual dimorphism calculation from the sex-specific body mass estimations produced a better agreement with sexual dimorphism obtained through a morphometric reference test than estimated from combined-sex equations. A test of body mass estimation equations noted that as there is positive allometry of femoral head diameter relative to body mass, the use of one formula for both sexes tends to overestimate body mass in males as they generally have larger femoral head diameters than females (Kurki et al. 2010). This indicates that frequently used methods of estimating body mass are influencing the level of sexual dimorphism determined within a combined sex sample, creating greater uncertainty for studies estimating fossil hominin sexual dimorphism where sex is unknown. There is therefore a need to separate the determination of body mass estimation and the prediction of sexual dimorphism level as combined in the current procedure:

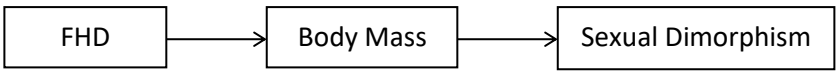

Figure 2.1: The current procedure of estimating body mass from FHD before using the body mass estimation values to predict sexual dimorphism.

Overall, techniques used to estimate the level of sexual dimorphism in a sample are restricted in terms of accuracy when values overlap between sexes in the distribution and sample sizes are small. Both problems are likely when estimating fossil hominin dimorphism as the amount of specimens with necessary elements for estimation are small and usually without morphological characteristics used to determine sex. This, along with the error accumulated from estimating body mass, widens the confidence interval (as noted by Smith, 1996) to a point that makes the results questionable.

2.7: Examples of studies utilising fossil hominin body mass and dimorphism level estimation

The discussed issues with estimation accuracy are problematic for the field of palaeoanthropology due to the large extent they are used to estimate hominin body mass and species dimorphism level. McHenry (1992) provided an estimation of average female *Australopithecus afarensis* body mass at 29kg using a modern human reference regression and 36kg from a hominoid reference regression. Specimen A.L. 288-1 was estimated by McHenry (1992) as having a body mass of 27.9kg using a human reference sample and was estimated by Jungers (1990b) at 29.5kg from a non-human hominoid sample. The average male body mass was given as 45kg with a human reference sample and 60kg using a hominoid reference sample. However, the large (and probably male) A.L. 333 specimen is 50kg using the human reference and 68.6kg from the all hominoid formula. Jungers (1990) provided a much larger estimated body mass of 81.9kg for this specimen. Holliday (2012) highlighted the problem of estimating australopithecine body mass as femoral head diameters are smaller than humans so the question of whether a non-human hominoid reference or an all hominoid reference sample is more appropriate for developing estimation equations must be asked. This is especially problematic with larger specimens, as seen in the estimations of the A.L. 333 specimen.

The large variation in skeletal size and morphology, along with differences in estimated body mass between specimens of *Australopithecus afarensis,* has led researchers to estimate the level of size dimorphism in the species. Richmond and Jungers (1995) examined the likelihood that variation between the extremes in size of *Australopithecus afaresnsis* specimens could be matched to the levels found in extant hominoids. The study recorded skeletal metrics for all the species being compared and an exact randomization procedure was implemented. This allowed for the analysis of probabilities through max/min ratios, where only the largest and smallest metrics contribute to the estimation of dimorphism level. Therefore, whilst the accuracy of max/min ratios is limited when estimating fossil species dimorphism, by using a method that considers a given metric as one of many, equally possible outcomes, the study can analyse how these possible outcomes compare to the distribution of other possible findings. The results found that the femoral skeletal metric ratios formed between the maximum, large specimen A.L. 333-3 and the minimum, small A.L. 288-1 specimen had a small probability of being found within a *Pongo* or *Gorilla* sample, but were never found in samples of *Homo sapiens* or *Pan troglodytes*.

A further study by Lockwood et al. (1996) moved away from simply analysing the maximum and minimum cases in a distribution to estimate the level of dimorphism in *Australopithecus afarensis*. The authors state that as only the probability of the most extreme dimorphic level was calculated, the average level of dimorphism for the species is unknown and would be more informative. The Lockwood et al. (1996) study compared the total distribution of all pairwise comparisons amongst the fossil sample with those from the extant hominoid reference sample. The probability that a pair of specimens from an extant hominoid species has greater variation than that shown in the fossil sample was calculated. The study found that there was a 59.9% probability of measuring a coefficient of variation as high as those found in 1000 samples of the fossil sample than in 17 *Gorilla* samples and a 49.8% probability of this pattern being found in the *Pongo* samples (Lockwood et al. 1996). However, the authors indicate that the results may simply be due to an unusual sampling event or that the coefficient of variation is a better measure of dimorphism level than max/min ratios, which is supported by comparative studies by Gordon et al. (2008).

A new approach was taken by Harmon (2006) who tested whether proximal femoral size and shape variation is consistent with the level found in a single extant species. Variation in the metrics from both the *Australopithecus afarensis* fossil and the comparative extant species samples were examined via the coefficient of variation of geometric means. Three quarters of the simulations found comparable skeletal size variation between *Australopithecus afarensis* and *Gorilla/Pongo* samples, although one simulation did suggest that the level of variation was greater in the fossil sample and it was noted that this trial contained the extremes of the sample, A.L. 333-3 and A.L. 288-1. Shape variation was also found to be within the extant hominoid range. Harmon (2006) suggested that the importance of these results is dependent on the scaling relationship between proximal femoral dimensions and body mass, which is discussed in Section 2.2.1: *Methods of estimating body mass*.

Whilst such studies indicate a relatively large level of dimorphism for *Australopithecus afarensis*, within the range of *Gorilla* and *Pongo* species, consensus has not been reached. Reno et al. (2003) estimated the dimorphism level of an enlarged *Australopithecus afarensis* sample through the use of a template specimen (A.L. 288-1). Specimens from the Afar Locality 333 were chosen as they are thought to be from a simultaneous death assemblage, meaning any temporal or geographic variation is negated in the study (Behrensmeyer, 2008). The amount of measurable material available was increased by the estimation of missing elements using A.L. 288-1 as a template, through the use of ratios between skeletal metrics.

Therefore, femoral head diameters for all the specimens in the sample were produced and body mass estimated, with dimorphism level predicted from the binomial dimorphism index, coefficient of variation and max/min ratio methods and compared to dimorphism levels in *Homo sapiens, Pan troglodytes* and *Gorilla gorilla* samples. The study found that by estimating sexual dimorphism level for the A.L. 333 sample, through the use of both the binomial dimorphism index and the coefficient of variation, the results found the level for *Australopithecus afarensis* to be closer to modern humans than *Gorilla* or *Pongo* as previous studies suggested. A combined sample of *Australopithecus afarensis* specimens from other Afar localities indicated a higher level of dimorphism, but the authors attribute this to temporal and geographic factors.

The results of the study were critiqued by Plavcan et al. (2005) who suggested that the A.L. 333 sample did not represent as many individuals as previously thought and that the sample included a male bias as there were more specimens with relatively higher skeletal metrics. If true, then the estimated level of dimorphism would be far smaller than in actuality. The Reno et al. (2003) study did simulate a sample with an added eight smaller A.L. 288-1 sized individuals to the A.L. 333 sample, with the results signifying that the sexual dimorphism level is closer to *Gorilla.* The authors believe this finding to be inconclusive as the sample is artificial and therefore the results could not be representative of an actual *Australopithecus afarensis* population. Placan et al. (2005) refute this and indicate that the use of the A.L. 333 sample for the study, believed to be from one simultaneous death assemblage, is not representative of the whole species. Plavcan et al. (2005) also questions whether there is enough evidence to suggest that the combined Afar sample variation in dimorphism level is caused by temporal differences, as the estimated body size range for the two samples should be greater and with more overlap between male and female clusters, which was not found. Also, whilst a modern human-like scaling relationship between femoral head diameter and body mass was assumed, the femoral head diameters may in fact be placed in the *Pan* range, which has a different scaling relationship. Reno et al. (2010) do not believe the A.L. 333 sample was biased and added 12 additional specimens from other localities, with the results suggesting that this combined sample had a dimorphism level similar to modern humans, although it should be noted that increasing the sample with four intermediate sized specimens increased the sexual dimorphism level to the *Gorilla* range. This may be due to the sensitivities caused by small sample sizes and not representative of the species.

Studies have attempted to further our understanding of early *Homo* body size and proportions, as well as analysing whether transitional *Homo* species were more similar to *Australopithecus* body sizes and had limb proportions suggesting a potentially retained arboreal locomotive component, or if they were more similar to modern humans potentially indicating full bipedal terrestriality. McHenry (1992, 1994) also suggested there is less body size dimorphism in *Homo erectus* than in australopiths, because of differentially larger female *Homo erectus* body mass. Pontzner (2012) analysed ecological correlates of *Homo* body size (through the underground storage organ model, increased female size and delayed life history characteristics, the grandmother hypothesis, etc.) using evidence from Plio-Pleistocene fossil hominin body mass estimation data provided by McHenry (1992). An increase in body mass was found with the mean australopith body mass being 36.8kg increasing to the mean *Homo* body mass of 48.8kg, fitting many models of ecological change. The average male *Homo* body mass was found to be 56.4kg, whilst the average female *Homo* body mass was 40.7kg, although it should be noted that the sample included the notably smaller than average specimens from Dmanisi and Gona. Body estimation has been attempted for the fragmentary remains of *Paranthropus robustus* and *Homo erectus* specimens from Swartkrans Cave, South Africa. *Paranthropus robustus* body mass estimations were formed from McHenry (1992) and Grine et al (1995), and dimorphism was estimated by classifying the larger femoral heads as male and the smaller femoral heads as female, with a male mean of 40kg and a female mean of 30kg. The fragmentary material classified as *Homo erectus* by morphology were estimated from metrics other than femoral head diameter and gave a male mean of 55kg and female mean of 30kg. Therefore, the evidence for decreasing dimorphism through increased female body mass in *Homo erectus* is not shown in specimens from the Swartkrans site, although there are obvious potential sources in error from the fragmentary remains and use of different estimation methods for comparison.

Holliday (2012) also used McHenry (1992) to predict body mass in a wide range of fossil hominin species. *Australopithecus* species included *Australopithecus afarensis* with a mean of 41kg, *Australopithecus africanus* (37.3kg), *Paranthropus robustus* (37.0kg), *Paranthropus boisei* (38.5kg). Early *Homo* (specimens from 1.8-1.5 Ma) were estimated to have a mean of 54.5kg, less heavy than neanderthals (73.6kg), late Pleistocene humans (64.1kg) and high latitude modern humans (59.9kg). Consequently, the study again suggests that *Homo* specimens from 1.8-1.5 Ma had greater average body mass than australopith specimens. Antón (2012) analysed *Homo erectus/ergaster* specimens and found southern African and

eastern African fossils shared a similar body size, although there are few southern African postcranial remains. Georgian *Homo erectus* was found to be 17-24% smaller (between 40-50kg) than eastern African fossils (between 51-68kg), with the range depending on whether the Gona pelvis is included. The author suggests there may be bias in taxonomic classification of specimens in Africa where smaller isolated postcrania are classified as early *Homo* and larger specimens are classified as *Homo erectus.* The study of cranial variation in Dmanisi specimens may also be seen as evidence in favour of this view (Lordkipanidze et al. 2013).

Plavcan (2012) analysed the estimated fossil body sizes calculated by Pontzner (2012) and compared them to examples of extant primate body size (*Hylobates lar, Pongo abelii, Pongo pygmaeus, Nasalis larvatus, Papio anubis*). Sexual dimorphism in australopith species (*Australopithecus afarensis* and *Australopithecus africanus*) and *Homo habilis*/*rudolfensis* appears well defined and with no overlap, but the author notes this is probably due to the fact that sex was determined by size for these cases, so strong size dimorphism cannot be inferred from this pattern. Furthermore, the *Homo habilis*/*rudolfensis* combined sample can be considered taxonomically two separate species and so cannot be used to analyse dimorphism without secure taxonomic classification of each specimen. This remains unlikely as the sample size is very small and the addition of one or two new specimens would change the results dramatically. However, even with these caveats the range of the sample is comparable to the range of specimens in the *Hylobates lar* sample. When utilising the total of the four fossil samples the range is still within the total for the extant species. The *Homo erectus* sample was found to be within the range of a single sex of *Hylobates lar* and *Pongo abelii*, noting that this included the smaller Dmanisi specimens. The results of the Plavcan (2012) comparison also indicate that if the sex allocation for the Dmanisi specimens is correct, this will expand the male and female range for *Homo erectus*, although again no more than for extant species, and as they are temporally and geographically divided from the rest of the sample, the size difference may be unrelated to dimorphism. The McHenry (1992) suggestion of a female *H. erectus* body size increase lowering dimorphism level is slightly supported by the pattern found in the study with *H. habilis*/*rudolfensis* males found to have a body mass average similar to *H. erectus* males, but *H. habilis*/*rudolfensis* females are smaller than the female *H. erectus*, even when the *H. erectus* sample contains the Dmanisi specimens. The author concludes that whilst temporal differences in *H. erectus* can be affected by variation in diet, ecology and disease, as the findings suggest variation is well within the range for normal intrapopulation variation in a species understanding the importance of such factors in the evolution of the genus *Homo* will be difficult.

Will and Stock (2015) analysed the body mass of early *Homo* using a 'taxon free' approach where temporal and geographical variation in body size were investigated. Body mass was estimated from new regression equations based on a sample of globally representative hunter gatherers, through the reasoning that locomotion and subsistence strategies would compare with those of early *Homo*. The study also included estimates of FHD for some specimens and the evaluation of the method was based on comparisons of size estimations using the same method rather than absolute values. Body size increase in Africa was found to have occurred after the establishment of the Dmanisi population, so the Eurasian expansion was not dependent on a larger body size. The study also indicated regional size differences in African populations.

Jungers et al. (2016) applied the data set from the Grabowski et al. (2015) paper to analyse the body mass of hominin fossils. The study found the fossil hominin record to be dominated by small bodied individuals that fit within the range of the smallest modern human populations, although the two smallest- *Orrorin tugenensis* and *Ardipithecus ramidus* were smaller than previously published estimates (at the lower modern human 'pygmy' range). The authors state that this is a possible ramification of modelling such early hominins as true bipeds and that chimpanzee reference samples were found to increase the size estimate. *Australopithecus afarensis* was found to be the most variable with some larger individuals overlapping with later *Homo erectus*, presumably male. All early *Homo* samples were found to be small bodied, negating the hypothesis that the emergence of the genus *Homo* was correlated with larger body size, which is consistent with the finding of Will and Stock (2015). Furthermore, the Dmanisi fossils may also have been small bodied suggesting that the increase in body size of African *Homo erectus* happened later than the expansion out of Africa, as indicated in Will and Stock (2015). Jungers et al. (2016) suggest that the larger bodied hunter gather sample used in Will and Stock (2015) overestimates body mass due to the biased effects of inverse calibration.

The 2016 study also analysed size and shape differences through estimations of body mass index (BMI) and ponderal index. Specimen of both *Homo floresiensis*- LB1 and *Australopithecus afarensis*- AL 288-1 were found to have unusually high BMIs and ponderal indices beyond the range of smaller modern human populations. This indicates more mass on stocky frames than would be predicted by stature alone. Size and limb proportion were also analysed via the humerofemoral index. Both specimens had indices higher than modern humans, and a further specimen of *Ardipithecus ramidus* had a higher index than LB1 and Al

288-1, suggesting limb proportions facilitating climbing. The femur was found to be especially short in LB1 and Al 288-1, therefore they had unhuman-like limb proportions, although their body mass appears to be in the smaller modern human population range. A larger (possibly male) specimen of *Australopithecus afarensis* had a femur size within the modern human range, suggesting sexual dimorphism is related to possible differences in size, shape or locomotor function within the species.

Will et al. (2017) looked at long-term trends in body mass evolution from hominin specimens dating between 4.4Ma and the Holocene, including body estimates for *Homo naledi.* A general pattern was inferred of significantly larger average body mass for *Homo* in relation to australopithecines but with retention of diversity, including small body sizes. The study also indicates that there was a general increase in body mass in Mid-Pleistocene *Homo* compared earlier *Homo*, including Early Pleistocene *Homo erectus*. A decrease in relative size variability in later *Homo* compared to australopithecines is suggested to be associated with selection against small-bodied individuals after 1.4Ma. Small-bodied *Homo naledi* and *Homo floresiensis* are important exceptions to this trend. Ruff et al. (2018) agree that there was an increase in early *Homo* size relative to australopithecines but question the increase in body mass in Mid-Pleistocene *Homo*. It is believed that this result was due to an underestimation of the Early Pleistocene Gona specimen through the calculations of Will and Stock (2015), which used the slender femoral shaft to predict femoral head size for body mass estimation.

The mean method of determining body mass dimorphism has recently been applied to a study of *Homo naledi* (Garvin et al. 2017). Dimorphism in skeletal dimensions has been found to be within the range of *Homo sapiens*. The previously reported body mass for the species by Grabowski et al. (2015) indicated that *Homo naledi* had an average body mass above confidence intervals for *Australopithecus sediba* and below confidence intervals for Asian, and Georgian *Homo erectus.* The estimates were found to overlap with the range for Dmanisi *Homo erectus.* Garvin et al. (2017) reported that the estimated sexual dimorphism index indicates that male *Homo naledi* were only on average 20% heavier than females. The authors note that the use of the mean method to determine the level of sexual dimorphism and that the fact that body mass estimates were close to unimodal, suggest sexual dimorphism within the species is likely to have been overestimated. If the individual specimens of the *Homo naledi* sample were found to have been represented more than once in body mass estimates, then this may also invalidate the estimation of a human-like level of dimorphism. Considering the relatively late geological date of the *Homo naledi* specimens

provided by Dirks et al. (2017), the level of dimorphism within the species indicates a scenario where either *Homo naledi* retained reduced dimorphism from a common ancestor with *Homo erectus* or an independent evolution.

Such studies show the extent to which body mass estimation and dimorphism level predictions are being applied to the fossil record. Whilst nearly all the studies add a caveat about the accuracy of prediction, the results are still being used to reconstruct important information about hominin fossil species. The temptation to do so is more understandable when some of the socioecological implications are highlighted.

2.8: Ecological correlates of body mass

Body mass is connected to a wide range of ecological variables including type of locomotion, predation, life history variables, home range size and diet. Body mass is also used as a way of assessing trends in evolution such as encephalization. The ability to accurately estimate body mass for fossil hominin specimens allows for greater understanding of these correlates.

2.8.1: Correlation with locomotion and predation

Locomotion style varies with body mass in the primate order. Napier and Walker (1967) provide categories for primate locomotion: quadrupedalism, vertical clinging and leaping, brachiation and bipedalism. Quadrupedalism is subdivided into terrestrial and arboreal quadrupedalism. In arboreal habitats, gaps between trees can either be bridged through leaping or climbing. Larger primates with longer limb dimensions have the greater ability to cross gaps through climbing whilst smaller primates can cross through leaping (Cartmill and Milton, 1977). For smaller animals, leaping carries a reduced risk as smaller body size means a lower amount of energy absorbed on impact in comparison to larger animals (Schmidt, 2010). As expected for primates, leaping behaviour increases with a decrease in body size whilst climbing behaviour increases with an increase in body size (Fleagle and Mittermeier, 1980). Suspensory behaviour is also connected to body size as it is easier for larger animals to hang below a small branch than to balance their weight above it. Studies have also confirmed positive correlation between suspensory behaviour and body size in the primate order (Schmidt, 2010).

Body size constrains arboreal locomotion in great apes. Doran (1993) observed that for Tai chimpanzees, 84% of their locomotion was terrestrial quadrupedalism. Significant sex differences were found in arboreal feeding locomotion. Males use less quadrupedalism and more climbing, tree-swaying and bipedalism than females. There were no differences in the type of substrates used for arboreal feeding, but there were differences in terms of which branches are used and how. Female chimpanzees are smaller and so there are more branches that can support their weight during arboreal quadrupedal locomotion. As there are fewer stable weight bearing branches for males to use, they require other methods of locomotion than quadrupedalism when feeding arboreally. As predicted by their body size, males also display more suspensory behaviour during feeding than females. Gorillas travel between trees less frequently than chimpanzees, although female suspensory behaviour is similar in frequency to chimpanzees (Remis, 1995). Scrambling behaviour (suspension from forelimbs with substantial support from the hind limbs) is an adaptation for larger bodied animals to distribute their body weight over small substrates. Female gorillas were observed using scrambling behaviour as well as bipedal posture (for greater reach when feeding) more frequently than males, although the differences were not statistically significant.

Primate body size is also linked to protection from predators. There is a general trend for larger predators to target larger prey, which was ascertained in a study of neotropical primates and predators (Libório and Martins, 2013). Eisenburg et al. (1972) observed that successful predator escape often requires mobility and agility as well as relative group uniformity. An equalization of body size in males and females is one way of providing group uniformity, making it difficult for a predator to single out an individual. Whilst selection for monomorphism involves a number of factors, it is also advantageous in predator protection. Leutenegger and Kelly (1977) found that for chimpanzees, which use trees for refuge and as a food resource, larger body size for predator defence is constrained by the need for limited arboreal locomotion.

2.8.2: Correlation with life history

Life history theory approaches the understanding of how an organism and population of organisms live and reproduce, the different evolutionary strategies that form these life cycles and their variety between species. Life history variables that are used to study variation in life cycle strategies include: maximum lifespan, age at first reproduction, adult body mass,

gestation time, weaning age, the mass of weaning offspring, litter size and birth intervals (Borries et al. 2013). Mammalian life histories involve a period of growth until maturity is reached where growth ceases and energetic effort is transferred to reproduction. Primate life histories are characterised by relatively long lives, a longer growth period with later ages of first reproduction, low reproductive rates and extended parental care in comparison with other mammal species (Harvey and Clutton-Brock, 1985). Such a strategy exemplifies one extreme, with the other represented by rodent species with shorter lifespans and increased reproductive rates. For primate species, the fact that females have relatively long life spans but low reproduction levels equates to a life-history tactic with low reproductive effort (Jones, 2011). It has been shown that delayed reproduction is favoured in environmental conditions where variability affects juvenile survival rates more than adult survival rates (Charnov and Schaffer, 1973). Jones (2011) notes that as primates are primarily frugivores and fruiting seasons are variable, this may represent part of the environmental pressure that led to this life history trend. The paper notes the study by Morris et al. (2011) which indicates that adult primate survival variance is lower than other mammals and that Janson and van Schaik (1993) found juvenile frugivorous primates to have lower foraging success due to their smaller body size and scramble competition.

Skinner and Wood (2006) divide life history variables as either first order life history variables (gestation length, age at weaning, age at reproduction, interbirth interval, mean life span, maximum life span) or life history related variables (body mass, brain mass, dental crown and root formation times and dental eruption times). Great ape life histories generally follow the primate life history pattern although they are long lived and late maturing compared to other primates. Gorillas are the exception to this general great ape trend with fast growth (rather than the more usual slow growth) paired with a large size. Robson and Wood (2008) found that body size is still the best predictor of great ape life history as brain size does not correlate with the length of subadulthood between chimps and modern humans and dental variables are weakly correlated with life history variables. Modern human life histories are distinct from other great apes through characteristics that include higher rates of survival, longer lifespans, later age at first reproduction, shorter interbirth intervals and a postreproductive period (Kaplan et al. 2000; Leigh, 2001).

In relation to body mass, Charnov's life history model states that a larger body mass is indicative of a delayed age at maturity, which is connected to a reduction in adult mortality and increased lifespans (Charnov, 1993). This is due to the fact that selection for a longer

period of ontogeny and larger adult body mass can only occur when there are low levels of adult mortality and so early reproduction is not advantageous. The model also emphasises that a larger body size provides advantages to females as a larger mother should deliver more energy to her offspring, although this is dependent on the energetic costs of maintaining a large body mass.

Hawkes at al. (1998) noted that human longevity may have been extended by grandmothering, where a grandmother aids in the provision of food for her daughter's offspring, allowing the daughter to have a shorter interbirth period, which would increase selection against senescence. Whilst modern humans have a similar reproductive timespan as chimpanzees, their lifespans are much larger with menopause occurring at around 50 years of age, with a postreproductive period equaling the reproductive period in some modern hunter gatherer populations and exceeding it in industrial populations. The longer human lifespan is related to low adult mortality levels in comparison to those of chimpanzees. The selection for menopause is related to the grandmothering hypothesis, as females can increase fitness through aiding their daughter's reproductive potential rather than continuing to produce offspring of their own. As larger mothers produce larger but fewer babies, their fertility would be increased as grandmothers are able to provide food to weaned infants meaning they were capable of producing another offspring faster. Kim et al. (2014) used a probabilistic agency based model to simulate conditions necessary for the evolution of postmenopausal longevity and found that with fewer than 1% of females living past their fertile period, this would still change the equilibrium of the population from the ancestral ape equilibrium to one found in modern hunter-gatherer populations where 40% the population are females at an age post their reproductive period. Noting that if the same method is used for each hominin species, the error in body mass estimation should be equal and so general trends can be inferred. Aiello and Key (2002) note that *Homo erectus* females would be over 50% heavier than australopithecine females meaning there would be a significant increase in daily energy requirements, higher still during gestation and lactation. They conclude therefore, that shortening the interbirth interval would reduce the energetic costs per offspring, providing the selective pressure for the menopause and a postreproductive period. It should be noted, however, that relationships between life history variables are confounded and causal relationships are difficult to determine.

2.8.3: Correlation with home range size and diet

As body size increases, the space used by an animal also increases. Body size has been shown to scale allometrically to population density, home range and day range (Isaac et al. 2012). However, the allometric scaling exponents obtained from analysis have been higher than the predicted 0.75, which would have suggested that home range size is directly proportional to energetic requirements as basal metabolic rate scales to body mass by an exponent of 0.75 (Kelt and van Vuren, 2001; Isaac et al. 2012). It has been suggested that this discrepancy is due to areas shared with conspecifics and that home range overlap increases with body size. Jetz et al. (2004) modelled the frequency of interaction, spatial overlap and loss of resources to neighbours, and showed that the ability to defend a territory is constrained by the amount of space and that the exclusivity of a home range decreases with increased body size. Pearce et al. (2012) analysed home range overlap between 100 primate species and found home range overlap to be highest for larger bodied species living in large home ranges at high population densities. The authors note the difficulty in studying animal space use and the importance of other factors than body size, for example group living will confound the relationships between body size, home range size and overlap if mean group size scales with body size.

Diet also influences home range area, with folivorous primates having smaller home ranges for their body weight than frugivores and omnivores. Fruiting trees are widely dispersed in space and so the frugivorous resource pattern requires a larger home range size. Arboreal omnivorous primates have larger home ranges for their body weight equal to terrestrial omnivorous primates (Milton and May, 1976). Diet has also been associated with body size and other life history variables as folivorous primates consume leaves that are available year round and so are expected to have faster growth rates in comparison to frugivorous primates whose diet is limited by the seasonal nature of fruits (Leigh, 1994). However, when a sample of Asian colobines and Asian macaques were controlled for body mass, a longer gestation length was found in the folivorous colobines and another study on folivorous lemurs found all life history variables to be longer than those of frugivores (Godfrey et al. 2004; Borries et al. 2011).

2.8.4: Body mass and encephalization

Body mass is the size variable used to assess other morphological characteristics including encephalization. Encephalization is the increase in ratio of brain mass to total body mass that has occurred in the evolutionary history of a number of species. The encephalization quotient (EQ) provides a quantitative value that allows for relative brain mass to be compared across species. It is determined by calculating the ratio of observed brain mass to expected brain mass in accordance with the animal's body mass (Jerison, 1973). Therefore, species with an EQ >1 have brains that are larger than expected for their size, whilst species with an EQ <1 have brains that are smaller than expected for their size. Primates have one of the widest ranges of EQs for mammals, and there is evidence of both increasing and decreasing relative brain mass within primate lineages (Boddy et al. 2012). Studies have consistently shown that modern humans are the most encephalized species (with a brain mass that on average is six times larger than expected for a mammalian species of its size) (Jerison, 1973; Marino, 1998).

Brain size correlates with several primate life history traits including life span, gestation length and age at first reproduction, with a trend for larger brained primates generally having long lives with slow growth and sexual maturation (Ross, 2003). There have been attempts to evaluate whether the link between brain size and life history is independent of body size. A procedure to statistically remove body mass was produced by 'the residuals method', where variables are regressed on body mass to create 'residual' values. It has been noted that this method is vulnerable to species-specific body mass estimation error, where overestimates or underestimates of true body size will bias both residuals by being either smaller than expected (with an overestimation) or larger than expected (with an underestimation) (Harvey and Krebs, 1990). Independent estimates of body size for each variable were used in a further study to reduce the effects of an over- or underestimation and found brain mass to be positively correlated with life span, gestational length and age at first reproduction residuals (Deaner et al. 2003).

The larger encephalization found in humans has also been extensively studied. Comparisons between humans and chimpanzees found no association between longer periods of postnatal brain growth and longer periods of subadulthood, no association between longer postnatal brain growth and a smaller percentage of adult brain size at birth and no association between longer subadult period and a slower brain growth rate (Leigh, 2004; Robson and Wood, 2008). This indicates that humans and chimpanzees have similar brain

ontogeny and that it is the faster rate in modern humans that is different and so juvenility being longer does not seem to be correlated with brain growth requirements.

This can be taken as evidence refuting the idea that longer juvenility allows for more learning time and that this was the causal factor in delaying maturity and increasing lifespans in humans. Hawkes et al. (1998) argues that other species have an increased period of ontogeny without associated brain growth and learning and that ethnographic data does not indicate a consistent time spent learning adult skills in hunter-gatherer societies. They argue that longer lifespans may have caused increased learning capabilities as a consequence of increased lifespans favouring delayed maturity, rather than a necessary learning period being the causal factor.

A variety of hypotheses have been developed to explain the evolution of increased brain size in mammals generally. Firstly, encephalization has also long been considered a function of cognitive buffering, where a large brain buffers against environmental variation by allowing for a larger range of behavioural responses (Allman et al. 1993; Sol, 2009). There is a general trend for behaviourally innovative animals to have larger brains, and it has been proposed that as larger brains contain more neurons, this allows for a greater capacity to gather, store and process data (Herculano-Houzel et al. 2006). An analysis of over 400 mammalian 'introduction events', where a mammal had been introduced to a new environment outside their current native range, found that larger brained mammals were more successful in establishing populations in their new environments (Sol et al. 2008). The study, however, notes that the cognitive mechanism that allows for flexible behavioural responses is still unknown.

The maternal energy hypothesis proposes a link between offspring brain development and the metabolic capacity of the mother. Martin (1996) notes that mothers with low quality diets such as folivores, will have less metabolic capacity to provide nursing infants with the energy required for larger brains, therefore constraining brain size. Kleiber's Law states that for the vast majority of organisms, basal metabolic rate scales to the 0.75 power of the organism's body mass (Kleiber, 1961, cited in Martin, 1996). In the primate order, prosimians generally have low basal metabolic rates whilst haplorhines typically follow Kleiber's law and folivores tend to have lower basal metabolic rates than frugivores (Ross, 1992). Furthermore, folivorous primates generally have smaller brains than frugivorous primates. In support of this hypothesis, Isler at al. (2008) found that both BMR and gestation length correlated with brain size in a study that compared endocranial volumes in primate species.

The expensive tissue hypothesis (Aiello and Wheeler, 1995) suggests that there was an evolutionary trade-off between the energetic needs of digestion and those for an increased brain size. If other processes in anthropoid primates allowed for the reduced size of the digestive tract, then the energy previously required for digestion would permit an increase in brain size. Navarrete et al. (2011) investigated whether there was correlation between the size of energetically expensive organs and the size of the brain for 100 mammalian species including 23 primates. The data was controlled for body size using a fat-free measurement of body mass to avoid effects caused by variation in adiposity. The study found no correlation between the relative size of the brain and digestive organs or any other energetically expensive organ. Studies suggest a link between larger brains compensated for by a permanent increase in net energy, as indicated through basal metabolic rate (BMR) (Isler and van Schaik, 2006; Navarrette et al. 2011). As an energetic trade-off between expensive organs and larger brain sizes does not appear to have occurred, other possible factors accounting for this net energy increase include moving towards a diet with increased quality food such as meat and later methods of processing food (Wrangham, 2009). Other potential factors include provisioning and food sharing through cooperation (Burkart et al. 2009), reducing variation in energy budgets via cognitive buffering (see above), and reduced energetic costs with more efficient bipedal locomotion in hominins (Pontzer et al. 2009).

Another possible explanation for encephalization in primates, which is not based on either ecological problem solving or constraints on development, is the social brain hypothesis. For primates, mean social group size has been found to correlate with the relative neocortex volume of the brain (Dunbar, 1998). Correlation between relative neocortex volume and a number of other traits of social complexity including the number of females in a group, size of grooming groups, male mating strategies and numbers of coalitions, the amount of observed social-play and social-learning and the frequency of tactical deception (Dunbar and Shultz, 2007). Social complexity has therefore been proposed as the causal factor promoting an increase in brain size during primate evolution. For other mammals and birds, whilst social group size does not correlate with brain size, species with pairbonded social systems tend to have the largest brains. Dunbar (2009) proposes that pairbonding was the first step for increasing brain size, as it requires greater cognitive ability to choose a strong mate as well as the need to coordinate and synchronize behaviour. Pairbonding requires 'perspective-taking' or the ability to be attentive to a partner's needs and this may be the foundation for more complex cognition found in primates. The complex social groups of primates have developed beyond singular social bonding with a mate, with social bonding occurring

between all members of a group, with many primate species having female-bonded social groups (Dunbar and Shultz, 2007). As the amount of social bonds is constrained by group size, increased brain size and associated cognition would be required to navigate increasingly complex social dynamics as group size increased, meaning greater social complexity may have produced selection for increased brain size. All studies of encephalization require an increase in brain size to be assessed in relation to total body mass. This highlights the importance of accurate estimation in cases where body mass is unknown.

2.9: Literature review conclusion

Fossil hominin body mass dimorphism methodology combines estimation of body mass with the prediction of dimorphism level from a pooled sample. Body mass is related to a range of life history characteristics but error in estimation is derived from the problem of confidence intervals and how the regression-based methods employed are based on comparative samples. There are also differences in the scaling relationship of skeletal metrics and body mass between modern humans and ape species, meaning the choice of regression method is also dependant on whether the distribution being analysed is similar to the reference sample in terms of size and shape.

As body mass estimation is used to analyse dimorphism level in fossil hominin species, the error in estimation is accumulated as the various methods used to estimate the dimorphism level have their own confidence interval. The accuracy of sexual dimorphism methods are significantly reduced when there is overlap in the distribution of values between sexes where dimorphism tends to be overestimated. This problem is exacerbated by small sample sizes, a prevalent occurrence in fossil hominin species. Nonetheless, this has not stopped such methods being applied widely to the fossil record. Body mass dimorphism estimations have been carried out for early fossil hominin species and the results have been used to predict palaeoecological correlates. Whilst such studies almost always provide caveats about the degree of accuracy in estimation, there is still a dependency on utilising inaccurate methods to try to understand important socioecological implications. To be able to correctly predict body mass dimorphism may provide clues about the earliest hominin mating systems and behaviour as well as the selective forces acting to drive their evolution.

There have been numerous studies devoted to improving the accuracy of body mass estimation but few have concentrated on the second part of the two-step body mass

dimorphism estimation procedure: predicting the level of sexual dimorphism from the sample of predicted body mass. A greater understanding of sexual dimorphism within the primate order is required if there is to be an improved methodology for determining the level of sexual dimorphism within fossil hominin species. Gordon et al. (2008) and Plavcan (2012) also noted the importance of comparative studies for understanding sexual dimorphism across the primate order. The overall aim of this study is to explore sexual dimorphism through such a comparative analysis in an attempt to increase understanding of sexual dimorphism within the primate order and to improve the level of accuracy in estimation methods.

Chapter 3:

Materials and methodology

The overall aim of this study is to increase understanding of sexual dimorphism within the primate order and improve the accuracy of methods for estimating body mass dimorphism through a comparative analysis. This study utilises postcranial indicators of skeletal dimorphism to investigate the structure of sexual dimorphism within the primate order. This chapter will describe the species and skeletal metrics chosen, sample locations and the methodology for forming the database of postcranial measurements.

3.1: Species chosen for the study

Postcranial measurements were taken from a range of species in the primate order including prosimians, Old World monkeys, New World monkeys and non-human apes. Both monomorphic and dimorphic species were chosen for comparison and to investigate the differences between male and female specimens once the factor of size is removed in the final analysis. The species also display a diverse range of traits including social systems, locomotor behaviour and geographic range (see Table 3.1., Table 3.2. and Table 3.3.). Species choice was also dependent on practicality where there were enough specimens with the required postcranial skeletal elements and known sex. The three tables (Table 3.1., Table 3.2. and Table 3.3.) are grouped into the three monomorphic prosimian and New World monkeys, three dimorphic Old and New World monkeys and three dimorphic hominids.

3.1.1: Southern needle-clawed bushbaby (*Euoticus elegantulus)*

The southern needle-clawed bushbaby (*Euoticus elegantulus*) is a nocturnal primate species in the Galagidae family. They inhabit the upper African rainforest canopy of Southern Cameroon, Mainland Equatorial Guinea, Gabon, Congo and South Nigeria (Macdonald, 2009) and are considered vertical clingers and leapers that can also move quadrupedally through the canopy, making horizontal leaps of up to 2.5 metres (Charles-Dominique, 1977; Klopfer and Boskoff, 1979). *Euoticus* is an exudate

gum and resin dependent genus, with 75% of their diet composing of exudate gums. *Euoticus elegantulus* possess a longer toothscraper than other galago species, which is used for gouging bark to retrieve gum (Stephenson et al. 2010). *Euoticus elegantulus* is a monomorphic, medium sized galago species with an average body mass of 270-360g (Charles-Dominique, 1977). Galago species are proportioned with a long tail, relatively long lower limbs in comparison to the upper limbs and an elongated tarsus portion of the foot. *Euoticus elegantulus* have specialised pointed and keeled nails allowing them to vertically climb larger trunks, which reduces resource competition with other galago species (Stephenson et al. 2010).

The social structure of the species consists of philopatric female groupings where social activity between females occurs in matriarchal groupings. The territories of the males overlap with the females (Charles-Dominique and Bearder, 1979). Charles-Dominique (1977) studied the behaviour of nocturnal prosimian species, including *Euoticus elegantulus,* and found active competition between males for access to females, with the smallest, weakest males prevented from contact with female home ranges. Dixson (2012), however, believes that the difficulties of mate guarding spatially separated females in their home ranges, in the active hours of darkness, would indicate that the species is unlikely to be strictly polygynous. Life history traits are typical for a primate of its size, with a gestation period of 122 days, one offspring born per gestation and an inter-litter period of 182 days (Ernest, 2003). They have a lifespan of around 15 years in captivity but their lifespan in the wild is expected to be much lower due to predation (Grzimek, 1990). Home range size is unreported. Combined sex averaged brain mass is 7.2g and resting metabolic rate is calculated as 25.1kcal/day (Stephan et al. 1981; Snodgrass et al. 2009).

3.1.2: Three-striped night monkey (*Aotus trivirgatus*)

The three-striped night monkey or three-striped owl monkey (*Aotus trivirgatus*) is a nocturnal New World monkey. Their habitat range covers most of tropical South America (Macdonald, 2009). Although preferring large canopied fruit trees, *Aotus trivirgatus* can be found in environments ranging from rainforest to near savannah. Their lower limbs are relatively longer than their upper limbs to assist in quadrapedal locomotion across branches and leaping between trees (Baer et al. 1994). The diet of *Aotus trivirgatus* is

primarily frugivorous, although supplemented with insects, leaves, nectar and small animals such as lizards and frogs (Wright, 1994).

Aotus trivirgatus is a monomorphic species with an average body mass between 800g-1kg for both sexes (Ford and Davis, 1992). The species does not display canine dimorphism (Kay et al. 1988). Their monogamous social system consists of a breeding pair and their offspring. Juveniles remain with parents past infancy, helping to care for younger siblings and leave the group between 2.5 and 3.5 years, with both males and females dispersing. Wright (1994) suggests that this extended dependency on the family group is due to the high energy costs of infant care and the predictable patterns of seasonal food in their home range. Males are the primary care givers who carry infants (until four months of age) and guard, play and share food after weaning. Mothers nurse unweaned infants between 2 and 3 hours per day, therefore infant care is probably the biggest factor influencing the evolutionary development of a monogamous mating strategy in *Aotus trivirgatus* (Kinzey, 1997). There is little social grooming reported in the species although territorial behaviour from both males and females has been described when defending their average nine hectare home range from other groups (Wright, 1978). *Aotus trivirgatus* have a lifespan in the wild between 12 and 20 years. Both males and females reach sexual maturity at around two years. The gestation period for the species is 142 days with one offspring usually born per gestation and the litter interval is 269 days (Ernest, 2003). Combined sex averaged brain mass is 16g and rest metabolic rate is calculated as 52.4kcal/day (Stephan et al. 1981; Snodgrass et al. 2009).

3.1.3: Cotton-topped tamarin (*Saguinus oedipus*)

The cotton-topped tamarin (*Saguinus oedipus*) is a diurnal New World monkey that is located in northwest Colombia. They inhabit tropical rainforests, dry deciduous woodland as well as secondary, remnant forest (Kinzey, 1997). As with other arboreal quadrupedal primates, their locomotor morphological characteristics include: grasping hind feet, a diagonal-sequence gait, a posterior weight shift and a 90^{o} humeral protraction (Schmidt, 2005). This allows them to primarily run through the canopy along medium to small branches as well as leaping between trees. *Saguinus oedipus* travel between multiple layers of tropical forest but are more commonly found to utilise the lower vertical levels (Kinzey, 1997). Callitrichid primates have claw-like nails called tegulae, rather than the flat nails

(ungulae) of most other primates. *Saguinus oedipus* use their curved tegulae to enable climbing on vertical substrates as well as aiding in clinging, running and leaping through trees (Smith and Smith, 2013).

Saguinus oedipus are a monomorphic species with a body mass range for captive animals between 250-500g, whilst the average body mass in the wild is 416.5g and they do not display canine dimorphism (Kay et al. 1988; Willemet, 2013). Garber (1980) defined their diet as being primarily insectivorous (40%) with the rest composing of small fruits (38.4%) and exudate gum (14.4%). *Saguinus oedipus* are considered opportunistic exudativores as they do not have the relatively longer tegulae found in the *Callithrix* genus, which along with the use of longer incisors, allows *Callithrix* species to specialise in gouging tree bark to retrieve exudate gum (Smith and Smith, 2013). Their home range is between 0.078 and 0.1km^2 with foraging travel between 1.5 and 1.9km per day. Travel time is interspersed with rest and grooming periods every hour (Neymann, 1977). *Saguinus oedipus* live in groups of 3 to 13 individuals.

They were previously thought to be a monogamous species, but in both captive and wild groups, a polyandrous social system has been observed with only one reproductively active adult female in the group (Savage et al. 1996a). Reproduction is suppressed in other group females, who do not demonstrate normal ovarian cycles until placed outside of their natal group with an unrelated male, where fertility commences (Ziegler et al. 1987). There have been reports of two pregnant females in the same group, but there have been no observations of two females rearing infants at the same time (Savage et al. 1996a). *Saguinus oedipus* display cooperative infant care, with fathers and sibling helpers contributing the most, via food sharing and infant carrying (Washabaugh et al. 2002). Following the birth of infants, males in groups with fewer helpers lost more weight than those with higher numbers of helpers, with maximum weight loss ranging from 1.3-10.8% of prebirth weight, indicating the energetic cost of infant caregiving (Achenbach and Snowdon, 2002). *Saguinus oedipus* females usually give birth to twins, doubling the amount of investment in infant care. Twinning and the need for increased predator detection are provided as reasons for cooperative infant care in the species (Savage et al. 1996b). Furthermore, there is evidence for learned parenting skills within groups, which increases infant survival rates, as adults with no parenting experience of either sex are more likely to have offspring that are rejected or neglected. The lower infant survival rates in captivity also provide an indication of the importance of learned caregiving proficiency, where the

amount of parenting experience is limited due to little to no chance of dispersal between groups (Savage et al. 1996b; Bardi et al. 2001).

There is a dominance hierarchy with the primary breeding male and sole breeding female codominant over the other group members, although the breeding female in feeding contexts maintains dominant access to food resources (Garber, 1996). Both males and females emigrate out of their natal groups in equal numbers; groups display territorial behaviour and maintain social bonds through grooming (Kinzey, 1997). The average lifespan for *Saguinus oedipus* is 13.5 years (Rowe, 1996). Both males and female reach sexual maturity at around 1.5 years (although age at first reproduction for females may be extensively delayed for reasons explained above). The gestation period for the species is 178 days, with an average of two offspring born per gestation and the litter interval is 244 days (Ernest, 2003). Combined sex average brain mass is 10g and basal metabolic rate is calculated at 449.5 ml oxygen/hour (Willemet, 2013; Jiménez-Arenas, 2013).

Table 3.1: Descriptions of traits for *Euoticus elegantulus*, *Aotus trivirgatus* and *Saguinus oedipus*.

Species	*Euoticus elegantulus*	*Aotus trivirgatus*	*Saguinus oedipus*
Common name	Southern needle-clawed bushbaby	Three-striped night monkey	Cotton-topped tamarin
Taxonomy	Suborder: Strepsirrhini, Family: Galagidae	Suborder: Haplorrhini, Parvorder: Platyrrhini, Family: Aotidae	Suborder: Haplorrhini, Parvorder: Platyrrhini, Family: Callitrichidae
Nocturnal/Diurnal	Nocturnal	Nocturnal	Diurnal
Geography	Cameroon, Mainland Equatorial Guinea, Gabon, Congo, South Nigeria	Most of tropical South America	Colombia
Habitat type	Upper rainforest canopy	Prefer canopied rainforest, but also found in near savannah habitats	Tropical rainforests, dry deciduous woodland, secondary remnant forest
Locomotor behaviour	Arboreal quadruped with adaptations for clinging and leaping	Aboreal quadruped with adaptations for leaping	Arboreal quadruped with adaptations for clinging and leaping
Diet	Exudate gum and resin dependant, with small amounts of insects and fruit	Primarily frugivorous	Primarily insectivorous with fruits exudates
Home range size (km^2)	Unknown	0.9	0.078-0.1
Dimorphic/ Monomorphic	Monomorphic	Monomorphic	Monomorphic
Average male weight (kg)	0.27-0.36	0.8-1	0.25-0.5
Average female weight (kg)	0.27-0.36	0.8-1	0.25-0.5
Social system type	Not confirmed. Evidence of male-male competition but not likely to be strictly polgynous	Monogamous	Monogamous, with usually one breeding pair in a group
Life history traits	Lifespan average: 15 years, sexual maturity: unknown, gestation: 122 days, interlitter period: 182 days, one offspring	Lifespan: between 12 and 20 years, sexual maturity: 2 years, gestation: 142 days, interlitter period: 269 days, one offspring	Lifespan: 13.5 years, Sexual maturity: 1.5 years (although age at first reproduction often suppressed in females), gestation: 178 days, interlitter period: 244 days, two offspring

3.1.4: Rhesus macaque (*Macaca mulatta*)

The rhesus macaque (*Macaca mulatta*) is a diurnal Old World monkey that inhabits western Afghanistan, India, northern Thailand as well as small populations remaining in southern China and Tibet (Smith and McDonough, 2005). *Macaca mulatta* live in lowlands and higher altitudes of up to 3000m in the Himalayas and are able to survive in a wide variety of climates and habitats, including urban areas (Grzimek, 1990). They are quadrupedal primates that are also adept at swimming. Small variation in anatomical proportions between populations has been recorded with northern populations found to have shorter tails than southern populations (Hamada et al. 2005). A further study found that female macaques from the Indochinese border had relatively longer limb lengths than other rhesus macaques, closer in proportion to long tailed female macaques; the study did not find variation in rhesus macaques large enough to suggest significant amounts of hybridisation (Hamada et al. 2006).

Female *Macaca mulatta* weigh 5.5kg on average, whilst males weigh between 6.5 and 12kg. Adult male *Macaca mulatta* decrease in weight during the breeding season and regain body mass during the non-breeding season (Bernstein et al. 1989). Studies found indirect hormonal regulation of seasonal weight variation and group activity patterns, along with individual behaviour, influencing seasonal weight changes. They are omnivorous, eating a wide variety of foods dependent on habitat including, roots, fruits, insects and small animals (Grzimek, 1990). Seasonal variation in diet has been observed, with an increased need to consume lower quality food sources during the winter months, which is associated with a decrease in body weight. Home range sizes are habitat dependent with more urbanised populations having smaller home ranges (less than $3km^2$, although the forested areas of India can provide a home range of up to $15km^2$) (Lindberg, 1971).

Macaca mulatta live in multi-male, multi-female groups of between 8-180 members, with two to four times as many females than males. After leaving their natal group, males that do not fully join another mixed-sex group become either solitary or peripheral members of another group (Boinski et al. 2005). Females mate with multiple males (Bercovitch, 1997). Male-male competition is characterised by age and endurance rivalry rather than antagonistic competition. Higham et al. (2011) found reproductive success to be associated with feeding patterns and body condition. Good male body condition including increased body weight during the non-breeding season allowing for the increased cost of numerous copulatory activities. *Macaca mulatta* have an average lifespan in the wild of 15 years,

although in captivity this is increased to 20-25 years. Females reach maturity at around three years of age and males mature at around five years of age. The gestation period for the species is 165 days, with one offspring usually born per gestation and the litter interval period is around 444 days (Ernest, 2003). Combined sex averaged brain mass is 110g and resting metabolic rate is calculated as 231.9kcal/day (Stephan et al. 1981; Snodgrass et al. 2009).

3.1.5: Squirrel monkey (*Saimiri sciureus*)

The squirrel monkey (*Saimiri sciureus*) inhabits the majority of tropical rainforest in South America (except southeastern Brazil) (Groves, 2001). They use quadrapedal locomotion to move through the forest, walking on branches 1-2cm thick, with small amounts of leaping (less than 2 metres) towards lower levels of the forest (Boinski et al. 1998). *Saimiri sciureus* have a slender build with a non-prehensile tail and sexually dimorphic teeth (males have larger upper canines).

Females have an average weight of 650g, whilst males have an average weight of 950g (Rowe, 1996). *Saimiri sciureus* also show seasonal variation in male body weight, which is characterised by an increased storage of water and fat in the upper arms, shoulders and torso proceeding and continuing into the breeding season (Schiml et al. 1996). A study by Stone (2014) suggests seasonal fattening is associated with male-male competition, as well as female preference. *Saimiri sciureus* diet is both frugivorous and insectivorous, although supplemented with small vertebrates, leaves, seeds, nectar and gum. They preferentially consume small berries that are around 1cm in diameter, caterpillars and grasshoppers (Janson and Boinksi, 1992). The species has a home range size of 2.5-3km^2 and live in multi-male and multi-female groups with around 15-30 members on average (Boinski et al. 2002).

Saimiri sciureus breed seasonally and have concealed ovulation. Both sexes emigrate from their natal group, although females may spend their first mating season in their natal group (Boinksi et al. 2005). The females nurse and provide infant care without male help until their offspring reach independence. Alloparental care has been observed with adult females caring for infants that are not their own offspring (Tardif, 1994). The young reach independence between 5-8 months of age (Aruguete and Mason, 1996). They have a reported average lifespan in the wild of 15 years and 20 years in captivity (Rowe, 1996).

Females reach maturity at around two or three years of age, whilst males reach maturity at around four or five years of age. The gestation period is 161 days, with one offspring usually born per gestation and the litter interval period is around 365 days (Ernest, 2003). Combined sex averaged brain mass is 22g and resting metabolic rate is calculated as 68.8kcal/day (Stephan et al. 1981; Snodgrass et al. 2009).

3.1.6: Vervet monkey (*Chlorocebus pygerythrus*)

The vervet monkey is an Old World monkey of the family Cercopithecidae. Whilst many studies classify vervet/grivet/green monkey as one species, *Cercopithecus aethiops*, there have been more recent taxonomic re-classifications of the species. Groves (2001) divides vervet/grivet/green into three separate species within the genus, *Chlorocebus*. The grivet monkey (found in the northern range of Ethiopia, Sudan, Djibouti, Eritrea) is given the species name, *Chlorocebus aethiops*, whilst the vervet monkey (found in the southern range) is given the species name, *Chlorocebus pygerythrus*. Napier (1981) and Grubb et al. (2003), however, consider the superspecies to be *Cercopithecus aethiops* with five subspecies due to the difficulty in defining population boundaries and areas of hybridisation. Considering all species/subspecies of vervet/grivet/green monkey, they have a wide geographic range from Senegal in the west of the continent to Ethiopia in the east as well as south towards South Africa. They are found in environments including savannah and riverine woodland, but are primarily found close to water sources (Groves, 2005). They have also been introduced to the Caribbean islands of the West Indies.

Chlorocebus pygerythrus move quadrapedally across both terrestrial and arboreal environments. Anapol et al. (2005) compared the anatomy of *Cercopithecus aethiops* with another *Cercopithecus* species, the blue monkey (*Cercopithecus mitis*) and found that *Cercopithecus aethiops* has a shorter trunk that may reduce spinal flexibility when running on the ground and longer distal limb segments suggest adaptations towards terrestrial quadrapedlism as well as arboreal movement. Their diet is omnivorous consisting mainly of fruit, but is supplemented by food items such as insects, leaves, resins, seeds, invertebrates, small mammals and birds. In dry seasons more time per day is spent drinking, resting and grooming in the mornings with a reduction in time spent travelling and feeding (Adeyemo, 1997). Home range size varies by geography, with populations in Senegal having home ranges as large as 1.78km^2 (Harrison, 1983).

They are sexually dimorphic with males weighing between 3.9-8.0kg and females weighing between 3.4-5.3kg (Skinner and Chimimba, 2005). *Chlorocebus pygerythrus* live in multi-male/multi-female groups of around 7-76 individuals (Isbell et al. 1991). Females remain in their natal groups with males emigrating when they reach sexual maturity. Females have a linear dominance hierarchy with higher ranking females having priority access to food and are the most sought after grooming partners, with daughters inheriting rank from their mothers and kin supporting each other in agonistic interactions (Isbell et al. 1999). Males emigrate to a new group every two years, usually with another male and move into a neighbouring group with male kin, which is thought to reduce the risk of predation when transferring and decrease the likelihood of conflicts in their new group (Cheney and Seyfarth, 1983). It has been suggested that males are limited in terms of dispersal because of the habitat being restricted to close water sources, meaning groups will line up along rivers, which reduces the options for transfer movement (restricted along the waterfront) (Isbell et al. 2002). Whilst females hold the highest ranking in a group overall, males also have their own dominance hierarchy with the highest ranking male reducing interactions between females and lower ranking males. Rank is defined by agonistic behaviour between males as well as being influenced by supportive high ranking female coalitions during dominance interactions (Hector and Raleigh, 1992).

Alloparental care is common with females caring for offspring not their own, although care from nulliparous elder sisters is more common as they are able to practice mothering skills (Fairbanks, 1990). High predation rates reduce lifespans in the wild but individuals have reached around 23 years of age in captivity (Hakeem, 1996). Females reach sexual maturity at around three years of age and males reach sexual maturity at around five years of age. The gestation period is 162 days, with one offspring usually born per gestation and the litter interval period is around 357 days (Ernest, 2003). The combined sex averaged brain mass is 80.81g, basal metabolic rate is unknown for this species (Navarette et al. 2011).

Table 3.2: Description of traits for *Macaca mulatta*, *Saimiri sciureus* and *Chlorocebus pygerythrus*.

	Macaca mulatta	*Saimiri sciureus*	*Chlorocebus pygerythrus*
Common name	Rhesus macaque	Squirrel monkey	Vervet monkey
Taxonomy	Suborder: Haplorrhini, Parvorder: Catarrhini, Family: Cercopithecidae	Suborder: Haplorrhini, Parvorder: Platyrrhini, Family: Cebidae	Suborder: Haplorrhini, Parvorder: Catarrhini, Family: Cercopithecidae
Nocturnal/Diurnal	Diurnal	Diurnal	Diurnal
Geography	Afghanistan, India, northern Thailand, southern China and Tibet	The majority of South America (apart from southeastern Brazil)	Northern Ethiopia, Sudan, Djibouti, Eritrea
Habitat type	Wide variety of habitats, including forests, high altitudes and urban environments	Tropical rainforest	Forests, savannah and riverine woodland
Locomotor behaviour	Primarily terrestrial quadruped	Arboreal quadruped with small amounts of leaping	Arboreal and terrestrial quadruped
Diet	Omnivorous	Frugivorous and insectivorous	Omnivorous
Home range size (km^2)	Varies with urban areas: <3.0, forested areas: <15.0	2.5-3	<1.78
Dimorphic/ Monomorphic	Dimorphic	Dimorphic	Dimorphic
Average male weight (kg)	6.5-12.0	0.95	3.9-8.0
Average female weight (kg)	5.5	0.65	3.4-5.3
Social system type	Multi-male, multi-female groups	Multi-male, multi-female groups	Multi-male, multi-female groups
Life history traits	Lifespan: 15 years in the wild, female sexual maturity: 3 years, male sexual maturity: 5 years, gestation: 165 days, interlitter period: 444 days, one offspring	Lifespan: 15 years in the wild, female sexual maturity: 2-3 years, male sexual maturity: 4-5 years, gestation: 161 days, interlitter period: 365 days, one offspring	Lifespan: 23 years in captivity, female sexual maturity: 3 years, male sexual maturity: 5 years, gestation: 162 days, interlitter period: 357 days, one offspring

3.1.7: Western gorilla (*Gorilla gorilla*)

The western gorilla (*Gorilla gorilla*) is a diurnal great ape, with the species subdivided into two subspecies, the western lowland gorilla (*G. g. gorilla*) and the cross river gorilla (*G. g. diehli*). The species inhabits the lowland, swamp and montane forests of Africa, including Nigeria, Cameroon, the Central African Republic, Equatorial Guinea, Gabon, the Republic of Congo, Angola and the Democratic Republic of Congo (Wilson and Reader, 1993). *Gorilla gorilla* locomotion is primarily quadrapedal knuckle walking on the ground, with some climbing ability and the capacity to stand bipedally for small amounts of time. Adults are too large to climb beyond the main trunk branches, although juveniles are more agile (Rowe, 1996).

Gorilla gorilla display the greatest amount of body mass dimorphism amongst hominoid primates, with male average weight around 140kg and female average weight around 75kg (Estes, 1992). Males have larger canines and jaw musculature as well as relatively increased amounts of facial prognathism (O'Higgins and Dryden, 1993). The large level of dimorphism is associated with male-male competition (Kappeler, 2000). Their diet is folivorous, consisting of leaves and stems from herbaceous terrestrial vegetation. The daily activity pattern of *Gorilla gorilla* includes feeding in the morning and afternoon with rest periods and travel time in between (Stewart, 2001). Rogers et al. (2004) found that western gorillas exploit both common and rare food resources in the forest, with fruits being the most diverse and eaten throughout most of the year, although this is a smaller percentage of overall diet than seen in other species such as chimpanzees. *Gorilla gorilla* also construct nests from plant material for day and night time use (Fruth and Hohmann, 1996). Average home ranges are between 7-14km^2, with an average daily travelling distance of 1105m and both home range and travelling distances are on average larger than those of the eastern gorilla (*Gorilla beringei*) (Tutin, 1996).

Gorilla gorilla typically live in one male, multi-female groups of about 8-10 individuals, including offspring (Robbins et al. 2004). Large mature silverbacks (usually over 12 years of age) benefit from long term associations with females and many maintain sole reproductive access to the females in their group. Infanticide of unweaned infants occur when there is a newly dominant male, returning all lactating females to their reproductive cycle and increasing the chance of the male producing his own offspring (Stokes et al. 2003; Robbins et al. 2004). Permanent associations between females and males have been hypothesised as a way for females to avoid infanticide by extra group males and to increase

protection against predators. Harcourt and Greenberg (2001) modelled encounter rates of lone females and males and found that a lone female would mate with so few males that infanticide rates would increase by three times the rate when associated with one male. Therefore, whilst protection from predators is still a possible hypothesis (as both females and their offspring are protected by the larger male), there is support for the infanticide hypothesis.

Both males and females emigrate from their natal groups and relationships between infants and adult females other than their mother are usually weak, due to small amounts of female kin that remain in a social group (Tutin, 1996). Whilst mothers remain an important social partner throughout their offspring's infancy, time spent with the silverback increases in late infancy. Silverbacks have been known to show increased affiliative behaviour towards juveniles that have lost their mothers (Watts and Pusey, 1993). The lifespan of *Gorilla gorilla* in the wild averages between 30-40 years of age and in captivity at around 55.4 years of age (Hakeem et al. 1996). Females reach sexual maturity at around seven years of age and males reach sexual maturity at around 11 years. The gestation period is 256 days, with one offspring usually born per gestation and the litter interval period is around 1397 days (Ernest, 2003). The *Gorilla gorilla* brain size combined sex average is 500g (Stephan et al. 1981). There are few accurate resting metabolic rate calculations, although it is noted that from their large bodies and relatively small brain mass, they are expected to have relatively low BMR (Steele, 1996).

3.1.8: Chimpanzee (*Pan troglodytes*)

Pan troglodytes is a diurnal great ape with four recognised subspecies: *P. t. troglodytes, P. t. verus, P. t. ellioti, P. t. schweinfurthii.* Studies suggest there is little morphological difference between subspecies (Rowe, 1996). *Pan troglodytes* range across equatorial Africa with the majority of populations found in Gabon, Cameroon and Congo (Cowlishaw and Dunbar, 2000). They live mostly in tropical rainforests but are also found in forest-savannah mosaic areas and montane forest (Nowak, 1999). The species is both terrestrial and arboreal, with locomotion predominantly consisting of quadrapedal knuckle walking, although they do display limited bipedalism. Their lower limbs are relatively shorter than their upper limbs, which aids in quadrapedal locomotion. Whilst much of their hand morphology is adapted for arboreal activity (including the ability to hold on to branches), the increased curling of the fingers necessary for knucklewalking has also been noted

(Jones et al. 1996). Males have moderately larger canines than females, used for intrasexual agonistic competition and during predation (Leutenegger and Kelly, 1977).

Pan troglodytes display slight body mass dimorphism with an average male weight of 40-60kg and an average female weight of 32-47kg (Rowe, 1996). They have an omnivorous diet primarily consisting of fruit, although they also eat leaves, bark, resin, seeds and insects as well as supplementing their main diet with small vertebrates and medium sized mammals, such as red colobus monkeys. Diet varies between populations with possible cultural differences influencing variation in diet between populations, even when the same types of food is available in each environment (Tomasello, 1994). There is also variation in hunting strategies, with chimps on the Ivory Coast using a more cooperative strategy, hunting in groups of three or four, whilst in Tanzania, there is a higher frequency of single males hunting. Boesch (1994) suggest that this is due to factors such as canopy density, where the denseness of the Ivory Coast canopy can allow prey to escape to higher canopy levels so cooperative tactics are necessary. In Tanzania, however, the canopy is less dense and hunting by a single chimp can be successful. *Pan troglodytes* exhibit nesting behaviour, constructing nightly nests made from plant material in trees (Stewart et al. 2007).

Pan troglodytes live in multi-male/multi-female communities. Group size varies greatly with large populations of 150 individuals having previously been observed (Watts, 2002). Females transfer from their natal group, forming bonds with resident males in their new group before any new relationships with resident females are formed. Their fission-fusion social system (where individuals form smaller subgroups that change in size throughout the day) has been proposed as a way of reducing intragroup feeding competition and increasing foraging efficiency (Doran, 1997). Males have a linear dominance hierarchy with common competition related aggression observed between males as a way of re-establishing rank that is difficult to maintain in a fission-fusion society (Muller and Wrangham, 2004). Male intrasexual competition is also associated with mating success as dominant males generally sire more offspring, although there are male-male coalitions who use grooming as a way to strengthen bonds. Such bonds are important for hunting activities and coalitionary mate guarding (Watts, 1998). Females in Gombe were also found to have a linear dominance hierarchy, with higher ranking females supporting each other in food competition (Pusey et al., 1997).

Pan troglodytes use four reproductive strategies: opportunistic mating, with females mating with many males, consortship, where a male and female leaves the group for a

period of time, mate guarding (plus coalitionary mate guarding) and extragroup mating (Tutin, 1979). Infanticide rates vary, with lower rates in western chimpanzees where there is increased female-male sociality (van Schaik, 1996). Home range size also differs between populations and habitats. In forest environments, the average home range is 12km^2, whilst in savannah environments, where there is a greater spread of food resources and home ranges can be 120-560km^2 (Nowak, 1999). *Pan troglodytes* life spans in the wild average between 40-50 years and in captivity, between 50-60 years (Macdonald, 2009). Females reach sexual maturity at around 9 years of age, whilst males reach sexual maturity at around 8 years of age. The gestation period is 229 days, with one offspring usually born per gestation and the litter interval period is around 840 days (Ernest, 2003). Combined sex averaged brain mass is 420g and resting metabolic is calculated as 581.9kcal/day (Stephan et al. 1981; Snodgrass et al. 2009).

3.1.9: Modern humans (*Homo sapiens*)

Modern humans (*Homo sapiens*) have a current population size of around 7.6 billion and inhabit all terrestrial environments with permanent populations in every continent, except Antarctica (Population Reference Bureau, 2018). The use of technology has allowed *Homo sapiens* to both adapt and modify a large variety of habitats (Boaz and Almquist, 2002). *Homo sapiens* are a unique species of great ape that display habitual terrestrial bipedalism as well as significantly reduced body hair. *Homo sapiens* are a morphologically diverse species, with physical attributes varying between populations. Size variation has been attributed to ecogeographical principles such as Allen's and Bergmann's rules, long-term trends in diet and nutrition, selection for particular size standards associated with environmental and behavioural factors and sexual dimorphism, as well as being connected to phenotypic and developmental plasticity triggered by various environmental stimuli (Ruff, 2002b; Kuzawa and Bragg, 2012).

Homo sapiens show moderate skeletal size dimorphism that is slightly greater than chimpanzees but have been found to be proportional in terms of lean body mass dimorphism (Gordon et al. 2008; Plavcan, 2012b). Wang et al. (2000) provides body mass averages from a sample of modern humans from a variety of populations, including African-American, Asian, Caucasian and Hispanic groups, with males averaging at 80.5kg and females averaging at 67.3kg. *Homo sapiens* have a variable omnivorous diet with food

often extensively prepared and stored. In comparison to other primates, modern humans have a higher level of carnivory with between 20% and 50% of modern hunter gatherer diet consisting of meat. For chimpanzees, meat accounts for just 5% of their diet on average (Stanford, 2001). Mating strategies also vary with culture, including: monogamy, polygyny and polyandry, although most involve some form of cooperative infant care (Boaz and Almquist, 2002).

Homo sapiens display an unusual mix of mostly slow life history strategy (low mortality rates and extended growth periods, with higher infant dependence) but with some fast life history traits, for example contemporary foraging populations have a fertility rate that is twice as fast as other great apes. This is associated with weaning offspring and the shortened interbirth period (see grandmothering hypothesis in Chapter 2: *A review of literature relavant to the study*, section 2.8.2: *Correlation with life history*). There are differences in average lifespan between populations due to variance in amounts of trauma, disease and nutritional deprivation. Gurven and Kaplan (2007) assessed the human mortality profile using a cross-cultural approach, including data from modern hunter-gatherer populations. They found that modal adult life span is between 68 and 78 years old. Gestation is around 280 days and typically with one offspring per gestation. Litter-interval, time of weaning and time of sexual maturity vary through nutritional status and cultural practices, although puberty typically begins in females at around 13 years and in males at around 14 years (Boaz and Almquist, 2002). Combined sex average brain mass is 1295g and rest metabolic rate is calculated at 1400kcal/day (Stephan et al. 1981; Snodgrass et al. 2009).

Table 3.3: Description of traits for *Gorilla gorilla, Pan troglodytes* and *Homo sapiens*.

	Gorilla gorilla	*Pan troglodytes*	*Homo sapiens*
Common name	Gorilla	Chimpanzee	Modern Humans
Taxonomy	Suborder: Haplorrhini, Parvorder: Catarrhini, Family: Hominidae	Suborder: Haplorrhini, Parvorder: Catarrhini, Family: Hominidae	Suborder: Haplorrhini, Parvorder: Catarrhini, Family: Hominidae
Nocturnal/Diurnal	Diurnal	Diurnal	Diurnal
Geography	Various countries in Central Africa	Gabon, Cameroon and the Congo	All continents apart from Antarctica
Habitat type	Lowland, swamp and montane forest	Tropical rainforest, forest-savannah mosaic areas and montane forest	All terrestrial environments
Locomotor behaviour	Quadrupedal knucklewalking	Quadrupedal knucklewalking	Terrestrial bipedalism
Diet	Folivorous	Omnivorous	Omnivorous
Home range size (km^2)	7.0-14.0	12	Unlimited
Dimorphic/ Monomorphic	Dimorphic	Dimorphic	Dimorphic
Average male weight (kg)	140	40-60	80.5
Average female weight (kg)	75	32-47	67.3
Social system type	One male, multi-female groups	Multi-male, multi-female groups	Monogamy, polygyny, polyandry
Life history traits	Lifespan: 30-40 years in the wild, female sexual maturity: 7 years, male sexual maturity: 11 years, gestation, 256 days, interlitter period: 1397 days, one offspring	Lifespan: 40-50 years in the wild, female sexual maturity: 9 years, male sexual maturity: 8 years, gestation: 229 days, interlitter period: 840 days, one offspring	Lifespan: modal lifespan between 68 and 78 years, female sexual maturity: 13 years, male sexual maturity: 14 years, gestation: 280 days, interlitter period: variable, one offspring

3.2: Data collections used

The osteological material used for this project was collected from the Smithsonian National Museum of Natural History, Washington D.C., USA and the Powell-Cotton Museum, Kent, UK. The modern human sample was collected from the Robert J. Terry Collection at the Smithsonian Institution. The Robert J. Terry Collection consists of 1728 specimens, with a demographic spread that includes 461 white males, 546 black males, 323 white females, 392 black females. Age at death ranges from 16 years to 102 years. The collection was assembled between 1921 and 1946 at the Washington University Medical School in St. Louis, Missouri. Further work was undertaken by Dr. Mildred Trotter between 1941 and 1967, where the collection was expanded to include younger individuals (Hunt and Albanese, 2005).

Though anthropometric data, including weight, is provided for some specimens from the Robert J. Terry Collection, it should be noted that many individuals were undernourished and death was often caused by the wasting effects of chronic diseases. The weights of specimens in the records therefore do not represent the normal healthy weight of the individual. Moreover, postmortem problems such as loss of water and muscle mass after death reduce the accuracy of weight measurements (Hunt and Albanese, 2005). Recorded weights are not used in this study due to these limitations.

Understanding the history and demographic composition of the Terry Collection is useful for evaluating the implications of using the Terry collection as a representative sample for modern humans. The specimens do not reflect all the variation within modern humans and the level of sexual dimorphism in this sample will not be representative of *Homo sapiens* as a whole. Ideally, a broader sample of modern humans should be used to provide more generalised results.

The majority of primate postcranial data was obtained from specimens based at the Smithsonian Institution's National Museum of Natural History. The Mammals Collection was developed under the former name of the United States National Museum, with the collection developing from U.S Exploring Expeditions from 1838, the William L. Abbott collection of mammals from central and southeast Asia in the early 1900s, the Smithsonian African Expedition, which collected African mammals between 1909 and 1911, as well as the Smithsonian Venezuelan Project and the African Mammal Project from the 1960s. For this project, samples of *Euoticus elegantulus*, *Aotus trivirgatus*, *Saguinus oedipus*, *Macaca*

mulatta, *Saimiri sciureus*, *Chlorocebus pygerythrus*, *Pan troglodytes* and *Gorilla gorilla* were obtained from this collection.

The Powell-Cotton Museum houses almost 2,000 primate specimens collected by Major Powell-Cotton during his trips to Africa in the early 1900s. Each specimen has detailed records including longitude and latitude locations, sex and any external pathologies. For this project, samples of *Euoticus elegantulus*, *Gorilla gorilla* and *Pan troglodytes* were obtained from this collection. Where possible, specimens for each species were chosen from records of the same geographic location but it should be noted that there may be variability in populations. This means that the effects of population variability will not be analysed in this study.

3.3: Measurements

Twelve metrics dimensions were taken from the skeletal remains of nine species in the primate order where available (see Table 3.4.). The measurements were chosen because of their previous use in fossil hominin sexual dimorphism studies (Reno et al. 2003; 2010). Moreover, most of the metrics are articular dimensions and therefore have a greater association with size; articular dimensions are also less affected by the variation in the frequency and intensity of loading than diaphyseal dimensions (Gordon et al. 2008). The sample size of the project and sample source locations can be found in Table 3.5. and Table 3.6.

Only adult individuals were chosen with age determined by the observation of fully fused epiphyses of the long bones. Known sex was provided from museum records, based on primary and secondary sexual characteristics at the time of collection. Sex was also confirmed through cranial assessment where available, using the scoring system for humans by Walker in Buikstra and Ubelaker (1994) and primate sexing techniques described by the National Research Council (1981). Skeletons with known pathologies on the bones, including trauma, age related degeneration of the bone or disease were removed from the study. The subsample of humans from the Robert J. Terry Collection was chosen at random after the removal of specimens with pathology and age-related degeneration. The 12 skeletal dimensions were measured in millimetres using digital callipers. Measurements were taken from right sided bones where available. The full data spreadsheet and histograms of postrcranial metrics are provided in Appendix 1 and 2.

The average level of sexual dimorphism, as described in the literature, is presented in Table 3.7. For this study, monomorphic species were defined as having sexual dimorphism indices of 1.0, while the dimorphic species were defined as having sexual dimorphism indices over 1.0.

Table 3.4: List of skeletal metrics and descriptions taken from Reno et al. (2003; 2010) and Buikstra and Ubelaker (1994).

Metric	Skeletal region	Bone Area	Description
HHD	Upper limb	Proximal humerus	Maximum diameter of humeral head
OLCB		Distal humerus	Mediolateral width of the distal humerus, measured at the superior margin of the olecranon fossa
CAPD		Distal humerus	Maximum diameter of the capitulum
RHD		Proximal radius	Maximum diameter of the radial head
ULB		Proximal ulna	Mediolateral width of the ulna immediately distal to the radial facet
FHD	Lower limb	Proximal femur	Maximum diameter of femoral head
TRCD		Proximal femur	Maximum femoral shaft diameter immediately below the lesser trochanter
CNDC		Proximal tibia	Mediolateral distance between the centres of the medial and lateral tibial condyles
PRXTB		Proximal tibia	Maximum mediolateral tibial bicondylar breadth
DSTTB		Distal tibia	Anteroposterior articular length of the distal tibia taken from the mediolateral mid-point of the articular surface
FIBD		Distal fibula	Maximum diameter of the distal fibula
TAL		Talus length	Maximum anteroposterior length of the talus

Table 3.5: The sample size for each species divided into sex and skeletal metrics, with location of sample source.

	Sample Size		
	Euoticus elegantulus	*Aotus trivirgatus*	*Saguinus oedipus*
Males	26	29	28
Females	26	29	28
HHD	52	58	56
OLCB	52	58	56
CAPD	52	58	56
RHD	52	58	56
ULB	52	58	56
FHD	52	58	56
TRCD	52	58	56
CNDC	52	58	56
PRXTB	52	58	56
DSTTB	52	58	56
FIBD	47	56	56
TAL	8	50	42
Sample source	Powell-Cotton Museum, Smithsonian	Smithsonian	Smithsonian
	Chlorocebus pygerythrus	*Saimiri sciureus*	*Macaca mulatta*
Males	30	30	18
Females	30	30	18
HHD	60	60	36
OLCB	60	60	36
CAPD	60	60	36
RHD	60	60	36
ULB	60	60	36
FHD	60	60	36
TRCD	60	60	36
CNDC	60	60	36
PRXTB	60	60	36
DSTTB	60	60	36
FIBD	52	60	34
TAL	39	60	2
Sample source	Smithsonian	Smithsonian	Smithsonian

Table 3.6: The sample size for each species divided into sex and skeletal metrics, with location of sample source continued.

	Sample Size		
	Pan troglodytes	*Gorilla gorilla*	*Homo sapiens*
Males	29	30	30
Females	29	30	30
HHD	58	60	60
OLCB	58	60	60
CAPD	58	60	60
RHD	58	60	60
ULB	58	60	60
FHD	58	60	60
TRCD	58	60	60
CNDC	58	60	60
PRXTB	58	60	60
DSTTB	58	60	60
FIBD	55	60	60
TAL	51	54	60
Sample source	Powell-Cotton Museum	Powell-Cotton Museum	Smithsonian

Table 3.7: Sexual dimorphism index (male - female) based on average male and female weights provided in the literature.

	Male (kg)	Female (kg)	SDI	References
Euoticus elegantulus	0.315	0.315	1.00	Charles-Dominique (1977)
Aotus trivirgatus	0.900	0.900	1.00	Ford and Davis (1992)
Saguinus oedipus	0.417	0.417	1.00	Kay et al. (1988); Willemet (2013)
Macaca mulatta	6.500	5.500	1.18	Rowe (1996)
Saimiri sciureus	0.950	0.650	1.46	Rowe (1996)
Chlorocebus pygerythrus	5.950	4.350	1.37	Skinner and Chimimba (2005)
Gorilla gorilla	140.00	75.00	1.87	Estes (1992)
Pan troglodytes	50.00	39.50	1.26	Rowe (1996)
Homo sapiens	80.50	67.30	1.19	Wang et al. (2000)

3.4: Intra-evaluator error

Intra-evaluator error (variation in repeated measurements by the measurer) was calculated as the standard error of measurement (Arroyo et al. 2010; Popovic and Thomas, 2017). Each of the metrics was taken from one *Homo sapiens* specimen, one *Gorilla gorilla* specimen and one *Euoticus elegantulus* specimen twice, with a week-long separation between sets of measurements. The three specimens were chosen as examples for evaluating intra-evaluator error in a human sample, the largest non-human species and the smallest non-human species (see Table 3.8., Table 3.9. and Table 3.10.). The intra-evaluator error was calculated as follows:

$$SEM = \frac{\sqrt{[(A-B)^{2)}/2]}}{\left[\frac{A+B}{2}\right]}$$

Where:

A is the measurement from the first day

B is the measurement from the second day

Table 3.8: Intra-evaluator error calculation as SEM for *Homo sapiens* specimen examples.

H. sapiens	1st day (mm)	2nd day (mm)	Individual SD (mm)	Mean (mm)	SEM (%)
HHD	42.69	42.61	0.06	42.65	0.13
OLCB	30.53	30.46	0.05	30.50	0.16
CAPD	19.56	19.56	0.00	19.56	0.00
RHD	20.92	20.89	0.06	20.91	0.30
ULB	14.82	14.81	0.01	14.82	0.05
FHD	42.87	42.81	0.04	42.84	0.10
TRCD	31.34	31.76	0.30	31.55	0.94
CNDC	39.09	39.13	0.03	39.11	0.07
PRXTB	66.22	66.68	0.33	66.45	0.49
DSTTB	28.15	28.21	0.04	28.18	0.15
FIBD	18.90	19.00	0.08	18.95	0.45
TAL	49.08	48.94	0.10	49.01	0.20

Table 3.9: Intra-evaluator error calculation as SEM for *Gorilla gorilla* specimen examples.

G. gorilla	1st day (mm)	2nd day (mm)	Individual SD (mm)	Mean (mm)	SEM (%)
HHD	68.00	67.97	0.02	67.99	0.03
OLCB	58.43	58.49	0.04	58.46	0.07
CAPD	32.12	32.11	0.01	32.12	0.02
RHD	39.06	39.06	0.00	39.06	0.00
ULB	26.06	26.00	0.04	26.03	0.16
FHD	51.60	51.71	0.08	51.66	0.15
TRCD	42.19	41.88	0.22	42.04	0.52
CNDC	53.95	53.99	0.03	53.97	0.05
PRXTB	91.15	91.57	0.30	91.36	0.33
DSTTB	34.72	34.73	0.01	34.73	0.02
FIBD	34.55	34.57	0.01	34.56	0.04
TAL	65.29	65.40	0.08	65.35	0.12

Table 3.10: Intra-evaluator error calculation as SEM for *Euoticus elegantulus* specimen examples.

E. elegantulus	1st day (mm)	2nd day (mm)	Individual SD (mm)	Mean (mm)	SEM (%)
HHD	4.97	5.00	0.02	4.99	0.43
OLCB	6.15	6.11	0.03	6.13	0.46
CAPD	2.10	2.08	0.01	2.09	0.68
RHD	2.69	2.72	0.02	2.71	0.78
ULB	1.06	1.05	0.01	1.06	0.67
FHD	4.58	4.59	0.01	4.59	0.15
TRCD	3.52	3.47	0.04	3.50	1.01
CNDC	3.62	3.58	0.03	3.60	0.79
PRXTB	7.00	7.08	0.06	7.04	0.80
DSTTB	3.53	3.56	0.02	3.55	0.60
FIBD	3.69	3.64	0.04	3.67	0.96
TAL	7.10	7.08	0.01	7.09	0.20

The intra-evaluator error calculated as the standard error of measurement was less than 1% for all metrics of the *Homo sapiens* and *Gorilla gorilla* specimens. Only *Euoticus elegantulus* TRCD produced a SEM value greater than 1% at 1.01%. This means that the intra-evaluator error is under the acceptable maximum SEM value of 1.5% for intra-evaluator error as given by Perini et al. (2005).The SEM values also show that there is little

difference in error produced from measuring human, large non-human or small non-human species.

Inter-evaluator error was not calculated because of the practical limitations of transporting another observer to sample locations. Previous studies have noted the importance of standard definitions for landmark and measurement items in reducing inter-evaluator error (Kouchi et al. 1999; Langley et al. 2018). The metrics utilised in this study are common measurements standardised in Buikstra and Ubelaker (1994) and employed in previous evaluations of fossil hominin sexual dimorphism (Reno et al. 2003; 2010). This means that replicability should be preserved with low inter-evaluator error when measured by another observer familiar with the anthropometric procedures of Buikstra and Ubelaker (1994). Though the metric standards produced by Buikstra and Ubelaker (1994) were developed for human samples, the anthropometric procedures have been successfully applied to primate samples for comparative studies (Swales and Nystrom, 2015). Some of the metrics, such as FHD and HHD, have been previously recorded and measured for specimens at the Powell Cotton Museum and Smithsonian National Museum of Natural History. Where possible, skeletal metric values were checked against measurements made by other observers and confirmed that the inter-evaluator SEM value was less than 2%, the limit defined by Perini et al. (2005).

3.5: Data analyses within the study

The methodology for each set of analyses is provided in the following chapters. All calculations and models were produced using SPSS 21.0 and MATLAB 9.1 software. The formulae used in analyses are given in the methodology section of each chapter where applicable. The code used to form models and graphs in MATLAB is reproduced in Appendix 3.

3.6: Chapter summary

This chapter details the species and skeletal metrics chosen and the methodology for forming the database of postcranial measurements. This includes recording of socioecological traits for the primate species chosen and descriptions of the collections that every specimen was derived from. Intra-observer error of measurement was calculated and

the results were under the maximum accepted standard error of measurement value. The database consists of more than 5800 datapoints that were used to produce detailed analysis of postcranial variation between males and females of nine primate species. The breadth of data collected allows for both inter- and intra-species analysis in terms of sexual dimorphism within the skeleton.

Chapter 4:

Defining the structure of sexual dimorphism in the primate order through discriminant function analysis

Previous studies have highlighted problems with the current methodology for hominin body mass estimation. This includes the use of comparative samples from species with differing amounts of sexual dimorphism and diverse scaling relationships between skeletal metrics and body mass. Comparing the level of dimorphism for skeletal metrics in different primate species can increase understanding of whether there is a pattern to the structure of sexual dimorphism within the primate species. Greater understanding of which areas of the skeleton differ in terms of their level of dimorphism and a comparison between species is an important first step for developing more accurate methods of estimating sexual dimorphism. Univariate plots of data do not always provide clear discrimination of sexual dimorphism and so other methods of evaluating sexual dimorphism are required (see histograms of data provided in Appendix 2).

This chapter aims to investigate the structure of sexual dimorphism within the primate order through an analysis of postcranial skeletal dimorphism by:

1. Utilising discriminant function analysis to define the most and least dimorphic elements within each species.
2. Examining similarities and differences to determine whether there is an overall pattern across primate species.
3. Evaluating the results of the discriminant function analysis through a comparison to binomial logistic regression.

The chapter will begin with an introduction to discriminant function analysis and previous applications of the method in archaeology and physical anthropology. The aims of the analyses are then highlighted before the results of both unstandardised and stepwise discriminant functions for each species are presented. The analyses will then be discussed in terms of their significance in defining the structure of sexual dimorphism within the primate order. A description of binomial logistic regression and its connection to discriminant function analysis is provided before a final comparative test of the two classification methods.

4.1: Introduction to discriminant function analysis

For this set of analyses, discriminant function analysis was used to discriminate between skeletal metrics to determine which skeletal metrics are the best predictors of sex. Discriminant function analysis determines the differences between groups in regards to the mean of a variable and then predicts group membership from that variable. A structure matrix is produced which provides a ranking of discrimination with coefficients that express the correlation between each metric and the discriminant function analysis. The coefficients can then be used to calculate a score which is compared against the group centroids to establish group membership. Stepwise discriminant function analysis evaluates variables in a series of steps, where at each step all variables not yet included in the model are evaluated in order to determine which variable is the best discriminator between groups. This variable is then added to a model of discrimination and the process is repeated during the next step. The stepwise method provides the number of variables required to form the best possible discrimination model for prediction of group membership. A ranking of best discriminators is supplied in a structure matrix and the percentage number of variables classified correctly is then calculated.

4.1.1: Discriminant function analysis in ecomorphology

Discriminant function analysis has been applied to studies from a wide range of archaeological fields including ecomorphology. Ecomorphology or 'ecological morphology' reconstructs palaeoenvironments from the functional morphology of mammalian postcrania. Habitat preferences can be predicted by the representative fauna found at archaeological and palaeontological sites (Kovarovic et al. 2011). Discriminant function analysis can be used to assign functional morphological variables, such as locomotor adaptations, with the environment they are selected for. This allows for the reconstruction of palaeoenvironments that maintained the same numbers and distributions of fauna used in the discriminant function analysis (DeGusta and Vrba, 2003). An advantage to this functional morphology approach is that it does not require large amounts of taxonomic or phylogenetic information. Characteristics can be chosen that correlate with habitat preference without the need to correct for phylogeny. This technique has mainly been applied to bovids as bovid taxa are typically under selection by predation and have specific

locomotor adaptations for escape strategies. Because these strategies can be specific to a habitat, this makes bovids good habitat predictors (Greenacre and Vrba, 1984). DeGusta and Vrba (2003) tested a discriminant function analysis of modern bovid astragali across four habitat categories via eight skeletal metric variables, which were found to produce a correct classification of 67%. The study also highlighted the importance of standardising the discriminant function analysis classification percentage in relation to chance. For a study with four groups a random specimen has a 25% chance of accuracy so an example classification percentage of 67% is 2.68 times greater than chance.

This type of ecomorphological study has also been applied to Old World monkeys. Elton et al. (2016) used discriminant function analysis to compare the habitat signals of cercopithecids, felids, suids and bovids from measurements of the humerus. Four habitat groups were discriminated, including open habitats with little tree cover, intermediate habitat groups and closed habitats with lots of forest. For cercopithecids, the closed forest group was split into 'forest terrestrial' for primarily forest floor dwellers and 'forest arboreal' for primarily arboreal forest dwellers. Bovids had the highest classification percentages, followed by felids and suids. The cercopithecids had the lowest discriminant function analysis classification percentages. This was expected as primates engage in behaviours that require fine upper arm motor control for purposes other than locomotion, such as grooming. Therefore, the habitat signal was expected to be weaker for species with a generalist forelimb that is used for a number of applications. Interestingly, metrics of the distal humerus were found to be key structures in determining locomotor strategy, in association with the elbow joint for all the mammalian groups. Metrics of the proximal humerus were found to diverge more between habitat groups in the cercopithecids and felids. The authors suggest this may be related to greater demands of the joint during arboreal activity, but it may also reflect other behaviours such as grooming or foraging.

Williams and Patterson (2010) attempted to define whether the South African habitat of the Taung child *Australopithecus africanus* fossil differs from present-day conditions. Dental microwear features from fossil papionins found at the site were compared with extant papionins from South Africa. A combination of principal components analysis and discriminant function analysis were used to evaluate species specific dietary signals and classify indeterminate species from Taung. The results found it was possible to distinguish between the microwear of extant and fossil species suggesting differences in the availability or exploitation of resources. *Papio ursinus*, however, differed from the fossil

species by a greater number of fine scratches only. Dental microwear can be used to infer the physical properties of food consumed, with lighter microwear mostly associated with softer foods. This in turn can be employed for identifying the type of habitat where such food was available. The distinct microwear of the fossil species from Taung in the study suggests the environment experienced by the Taung child would most likely have been open woodland with softer C_4 plants available.

A similar study (William and Geissler, 2014) used discriminant function analysis to compare the fossil colobine monkey, *Cercopithecoides williamsi,* found at Sterkfontein, South Africa to other fossil and extant primates from the area. The first discriminant function analysis categorised the species in terms of dietary proclivities from dental wear patterns. The highest rate of classification was for omnivores and frugivores at 70% and the lowest classification was for folivores at 37% that included *Cercopithecoides williamsi*. A second discriminant function analysis, which discriminated between arboreal and terrestrial habitats, had an overall classification rate of 86% with most of the *Cercopithecoides williamsi* specimens classified as terrestrial. A final discriminant function analysis categorised the sample into taxa and found only 46% of *Cercopithecoides williamsi* specimens were correctly identified (Williams and Geissler, 2014). These results suggest that dental microwear also provides a strong habitat signal without accurate phylogenetic information, similar to previous studies that evaluated locomotion as a habitat signal.

4.1.2: Discriminant function analysis in osteoarchaeology

Discriminant function analysis is also a widely used statistical tool in the field of osteoarchaeology. Constructing a biological profile from skeletal remains is a foundation of osteoarchaeological examinations. Sex determination is the first step during such assessments because estimations of age and stature generally require sex specific methodologies. Discriminant function analysis has been used to test the accuracy of common sex determination methods. Sexually diagnostic characteristics of the pelvis have been found to be the most accurate with discriminant function analysis classification percentages of up to 95.5% (Gonzalez et al. 2009; Patriquin et al. 2005; Steyn and Iscan, 2008). Sexually diagnostic characteristics of the skull have also been tested through discriminant function analysis with classification percentages up to 86.8% (Dayal et al. 2008; Green and Curnoe, 2009; Steyn and Iscan, 1998). Because skeletal assemblages in

archaeology can be fragmentary, other methods of determining sex are being developed and tested when elements of the pelvis or skull are not available. A study tested metrics of the clavicle from a British medieval population through the employment of discriminant function analysis and found that linear measurements of the clavicle had a classification percentage of 89.6%, indicating that methods of sexing using measurements of the clavicle can be appropriate for sex determination in British populations (Atterton et al. 2016). A more recent study (Sehrawat, 2018) also used discriminant function analysis to assess a multivariate method of sex determination for Northwest Indian populations. By combining measurements of both the sternum and the clavicle, a higher percentage accuracy was produced, although the clavicle provided greater sex estimation power than the sternum during individual analysis (Sehrawat, 2018). This is an example of improved performance using a multivariate approach through the discriminant function analysis equations formed from measurements of different bones.

Furthermore, discriminant function analysis has been employed to provide a quantitative method of categorising types of artificial cranial deformation, a permanent body modification that is applied to infants. The analysis of artificial cranial deformation is useful for archaeological investigations as it denotes a specific social identity. Rather than previous methods based on trait observation, O'Brien and Stanley (2013) categorised skulls into discrete categories, deformed or not-deformed as well as annular modification or tabular modification. Two discriminant functions were developed and a territory map of deformity types was created that can be used to classify other samples. The discriminant functions were tested on a comparative sample of non-deformed skulls from South America, and 100% of the sample was correctly classified as non-deformed. The method was also compared to a set of prior observations that were classified as non-deformed by an expert and the new method classified 81.3% as non-deformed. The O'Brien and Stanley (2013) set of discriminant functions has been used to classify other samples. McKenzie and Popov (2016) assessed the evidence for artificial cranial modification in Neolithic skulls from Primorye, in the far east of Russia. The discriminant functions classified six skulls as showing cranial modifications, confirming previous assessments of artificial cranial modification at the site. The results, however, differed from the previous visual observation of there being eleven skulls with cranial modifications. Further research will be required to determine whether this is because of normal variation within the population, the conservative nature of the discriminant functions or the discriminant functions being less accurate when applied to this population. It is also important that differences in the precise

nature of cranial deformation, such as severity and technique, are defined before quantitative methods for categorising artificial cranial modification are applied.

4.1.3: Discriminant function analysis in geometric morphometrics

Discriminant function analysis is also frequently utilised for studies with geometric morphometrics. The increased efficiency in separating size and shape and the ability to visualise the results has been applied to various subjects in archaeology (Rohlf and Marcus, 1993). Geometric morphometrics has been used to understand differences between groups whilst discriminant function analysis has been applied to the prediction of group affiliation from shape coordinates (Kovarovic et al. 2011). Viðarsdóttir et al. (2002) employed geometric morphometrics to analyse interpopulation variation in the facial skeleton of ten modern human populations. The geometric morphometric method of generalised Procrustes analysis removed size information by minimising the sum of squared differences between landmarks and a principal component score was produced by warping the triangulated surface of the mean shape. The discriminant function analysis then utilised the principal component scores to discriminate between populations. The result found that between 66.7% and 100% of individuals can be correctly classified by this method, with over half the populations having a classification percentage greater than 75%. The results were consistent regardless of age or sex, which suggests the early presence of differences. This indicates that modern human populations have similar postnatal facial ontogenetic trajectories and so distinctions in facial shape are probably present at birth.

Buck and Viðarsdóttir (2004) applied this technique to form a new method for race identification for subadult human skeletons. Multivariate statistics using adult linear distances of the craniofacial region are common, but the large scale ontogenetic allometric changes that occur between birth and adulthood mean the same methods cannot be applied to subadults (Thompson et al. 2003). The Viðarsdóttir et al. (2002) study found that once size is removed, the resulting craniofacial shape coordinates can be compared across a range of ages. This meant that a new method of estimating race for subadult populations could be developed. The Buck and Viðarsdóttir (2004) study compared mandibular shape coordinates from a sample of five morphologically distinct groups: African Americans, Native Americans, Caucasians, Inuit and Pacific Islanders. The resulting discriminant function analysis had a classification percentage of 70.1% for all individuals in the sample.

The Caucasian sample had the highest percentage accuracy whilst the Inuit sample had the lowest percentage accuracy. A smaller analysis with only three groups, African American, Native American and Caucasian provided a classification percentage of 87.6%.

Discriminant function analysis was also used to compare the ontology of craniofacial characteristics in African apes (Berge et al. 2014). Discriminant functions were used to identify taxonomic differences between *Pan troglodytes* and *Gorilla gorilla*. The discriminant function shape vectors allowed for the visualisation of shape changes. The results found statistically significant differences between *Pan troglodytes* and *Gorilla gorilla* with *Gorilla gorilla* having the size and shape that corresponds to older chimpanzees for each stage of growth. Shape changes were also found to be more extensive in *Gorilla gorilla* with 36% of total change, in comparison to *Pan troglodytes* with 29% of total change.

A further study assessed variation in Clovis point shape using geometric morphometrics and discriminant function analysis (Buchanan et al. 2014). A large sample of Clovis points were analysed to test whether Clovis points vary regionally. The first discriminant function analysis determined how well Clovis point shapes discriminate amongst the environmental regions east and west of the Mississippi River. The classification percentage of Clovis points from either the east or west, based on shape, was 88%. A further set of discriminant function analyses looked at variation within subregions. Within the eastern region, clovis point shapes were significantly different in the northeast area in comparison to the other subregions. In the western region, the northwest Clovis point shapes were significantly different from the southwest and southern plains, along with the northern plains being statistically different to the southern plains. This supports a regional environment adaptation hypothesis, particularly as the previous work of Buchanan et al. (2011) found that prey type is associated with the size and shape of Palaeoindian points, indicating that Clovis point differences are correlated with the type of prey targeted by Clovis hunters in each region and subregion.

4.2: Evaluation of discriminant function analysis

There have been discussions on the appropriate use of discriminant function analysis for archaeological studies. DeGusta and Vrba (2003) highlighted the fact that discriminant function analysis is designed to maximise the differences between groups and therefore

the results tend to correctly categorise specimens at a greater rate than expected by chance. This occurs even if the individual predictor variables used in the discrimination do not show separation between groups. Nonetheless, individual predictor variables may still contribute to the separation of groups when incorporated as part of a multivariate analysis. White and Ruttenberg (2007) noted the problem of sample size on accuracy rates. Structured resampling was suggested as a method of evaluating the analytical parameters of discriminant function analysis, although Kovarovic et al. (2011) suggest that the use of real data sets rather than simulated datasets will be better for determining these parameters as they more closely reflect the imperfect nature of archaeological assemblages. The study tested the parameters of discriminant function analysis on two faunal datasets and two simulated datasets and found small and unequal sample sizes were likely to over-fit the results. They provide the required number of predictors through the formula:

$$N - G \geq V$$

When:

N is the total number of individuals in the entire sample
G is the number of groups
V is the number of variables

Stepwise discriminant function analysis has been suggested as a method of analysis when the sample size does not conform to this equation. However, it has been found to be more sensitive to small variations in predictors that may exaggerate their importance in the model (Huberty and Hussein, 2003). Most archaeological studies applying discriminant function analysis to datasets also violate the assumption of equality of within-group variance-covariance matrices (homoscedasticity), or the assumption that the variation about the regression line is the same for all predictor values. Tabachnick and Fidell (2006) indicate that discriminant function analysis is robust to this violation when sample sizes are large. Kovarovic et al. (2011) also indicated the importance of comparing the classification percentages to chance, as applied to the work of DeGusta and Vrba (2003). For this analysis, discriminant function analysis is deemed appropriate because the sample size fits the required number of predictors and is large enough to reduce any effects caused by lack of normality or divergence from homoscedasticity.

4.3: Aims of the study

The structure of the data, consisting of multiple skeletal measurements taken for each species with sex determined for each specimen, is suitable for discriminant function analysis because it can predict the binary grouping variable (sex) by multiple continuous predictor variables (skeletal metrics). Discriminant function analysis assumes that the sample is normally distributed. Violations of the normality assumption are not considered 'fatal' and results can still be considered significant (Tabachnick and Fidell, 2006). Tests for normality found the majority of skeletal metric data for each species were normally distributed but non-normal distributions are highlighted in Appendix 4.

Discriminant function analysis was used to answer the following questions from the data:

1) Are there differences in the level of sexual dimorphism between skeletal metrics for a species and if so, which skeletal metrics are the best and worst discriminators of sexual dimorphism?

2) What is the structure of sexual dimorphism within the primate order (in terms of the variation and patterns between primate species as well as differences and similarities between skeletal metrics within the same species)?

3) Does the structure of sexual dimorphism in humans differ greatly in comparison to other primate species?

These questions are important for their application to body mass dimorphism estimation and in particular, hominin body mass dimorphism estimation. Current estimation procedures rely on a correctly chosen comparative sample. There is a presumption of isometry in relation to the scaling relationship between a chosen skeletal metric and body mass. Studies have shown that skeletal metrics scale to body mass differently between taxa. For example, humans show positive allometry between femoral head diameter and body mass whilst gibbons, siamangs and great apes show a close to isometrical scaling relationship between femoral head diameter and body mass (Ruff 1988; Jungers, 1990a; Ruff and Runestead, 1992). Gordon et al. (2008) noted the problem of fossil hominin dimorphism estimation requiring only the use of postcranial data where the skeletal metric scales isometrically with body mass in all comparative taxa or by choosing metrics that scale with equivalence for all comparative taxa. Through this analysis using discriminant functions, the structure of sexual dimorphism within the primate skeleton can be explored

and the question of whether sexual dimorphism varies within the skeleton can be answered.

If variation within the primate skeleton is found then this also has consequences for body mass dimorphism estimation methods. The background chapter evaluated the large amount of socioecological factors that are associated with body mass dimorphism. However, these factors are tempered by energetic, mechanical and locomotive restrictions. If sexual dimorphism within the primate skeleton is shown to vary then the factors restricting the equal scaling of skeletal metrics can be explored. The sample includes monomorphic species that can act as a control for the analysis. Their locomotion and morphology (including the presence or absence of a prehensile tail) are reflected in some of the species in the dimorphic sample. Therefore, the results can be compared to highlight differences between monomorphic species and dimorphic species, noting that certain aspects of locomotor morphology are controlled for.

If variation within the skeleton is found then this means it would be possible to determine which elements are more dimorphic and therefore which skeletal metrics are better characteristics for determining sex. Current estimation procedures require FHD to predict body mass and then the level of sexual dimorphism in a pooled group of predicted body masses is determined. Evaluating the discriminate power of FHD, along with other skeletal metrics, may present new methods of estimating body mass dimorphism. There may also be implications for hominin studies by evaluating the results of the human skeleton in comparison to other primate species. Whilst a common primate pattern across all primates could be identified, it is also possible that important variations between humans and other primates could be revealed. The results can be used to determine how strong the evidence is for using humans as a comparative sample for fossil hominin body mass dimorphism estimation. Discriminant function analysis is suitable for answering these questions as the rankings can be compared between species and the average ranking of skeletal metrics can be grouped and compared in order to explore any differences between species that are found.

4.4: Study sample

The discriminant function analysis was performed on data from twelve skeletal metrics that can be divided by skeletal region. Descriptions of the skeletal metrics utilised in the analysis

and the skeletal region from which they are derived can be found in Chapter 3: *Materials and Methodology*. Skeletal metrics with a low sample size were removed before the analysis commenced. The threshold for low sample size was classed as fewer than 15 metrics measured for each sex within a species. An equal number of measurements between males and females were maintained through the removal of skeletal metrics from randomly selected individuals of the opposite sex.

4.5: Intraspecies analysis

The intraspecies analysis of sexual dimorphism aims to answer the questions set out in section 4.3: *Aims of the study*. Forming discriminant function analysis rankings for each species provides the best and worst ranked discriminators of sexual dimorphism, which can be later compared to other species to form a general trend of best and worst discriminators for the primate order. This analysis answers the second question of the structure of sexual dimorphism by defining any variation in sexual dimorphism within a species through rankings. Ranking data for the comparison of humans with other primate species is also provided in this analysis.

4.5.1: Methodology for intraspecies analysis

Unstandardised discriminant function analysis and stepwise discriminant function analysis were both performed on data from each species. As the unstandardised method creates a model of discriminant function from all the variables and the stepwise method utilises variables that provide the best possible discrimination model for prediction of group membership, it is possible to explore differences in discrimination models and how this changes discrimination rankings. This analysis used the following methodology:

1. For each of the nine species (*Euoticus elegantulus, Aotus trivirgatus, Saguinus oedipus, Chlorocebus pygerythrus, Saimiri sciureus, Macaca mulatta, Pan troglodytes, Gorilla gorilla* and *Homo sapiens*) a separate discriminant function analysis was performed.
2. The structure matrix output determined which predictor variables were the best discriminators of sex by ranking the coefficients. The higher ranked skeletal metric variables are therefore the better discriminators of sex.

3. A table of canonical discriminant function coefficients was also produced that can be used to create the discriminant function equation from the model for the species being analysed.
4. This means that further cases can be classified by the discriminant function equation produced for that species.
5. A classification percentage is determined that states the percentage of correctly classified skeletal metrics by the discriminant function.
6. A further stepwise discriminant function analysis provides the same output of structure matrix rankings, discriminant function equation and classification percentage. The difference is that the stepwise discrimination model is formed from the best skeletal metrics for discriminating sex, rather than all the skeletal metrics being used as predictor variables.

The three best and worst discriminators of sex for each species are described from the structure matrix table. The structure matrix table displays the correlation of each variable with the discriminant function. The reported structure matrix coefficients can therefore be used to identify the largest absolute correlations with the discriminant function. The stepwise discriminant function analysis selects the best variables for a model of discrimination. The structure matrix coefficients calculated by the stepwise discriminant function analysis provide the correlation between each variable and the discriminant function model produced from the best variables. The stepwise procedure can lead to different rankings because it considers collinearity in choosing which variables to add, meaning that if two variables are very highly correlated only one is necessary for prediction. The best and worst discriminators of sex for each species can therefore also be described from the stepwise structure matrix table.

4.5.2: Results of the intraspecies analysis

4.5.2.1: *Euoticus elegantulus*

The unstandardised discriminant function analysis provided a ranking of skeletal metrics for *Euoticus elegantulus* apart from TAL, which was removed due to low sample size. TRCD was the best discriminator between sexes, with a structure matrix coefficient of 0.418. FHD was ranked second with a structure matrix coefficient of 0.364 and ULB was ranked third with a structure matrix coefficient of 0.340. PRXTB was the worst discriminator between sexes

with a structure matrix coefficient of 0.012. CAPD was ranked tenth with a structure matrix coefficient of -0.012 and CNDC was ranked ninth with a structure matrix coefficient of -0.013. The negative coefficient reflects the negative correlation between the variable and the discriminant function analysis. The classification percentage for this analysis was 74.5%, with six males incorrectly classified as female and six females incorrectly classified as males. The stepwise discriminant function analysis was unable to provide a ranking for the sample as the multivariate statistic, Wilks' Lambda, was not statistically significant and so the data did not qualify for stepwise analysis.

Table 4.1: Discriminant function analysis results for *Euoticus elegantulus*.

	Euoticus elegantulus	
	Discriminant Function Ranking	Structure Matrix Coefficients
HHD	6	-0.070
OLCB	5	0.138
CAPD	10	-0.012
RHD	7	0.062
ULB	3	0.340
FHD	2	0.364
TRCD	1	0.418
CNDC	9	-0.013
PRXTB	11	0.012
DSTTB	4	-0.284
FIBD	8	0.023
TAL	N/A	N/A
Classification Percentage (%)	74.5	

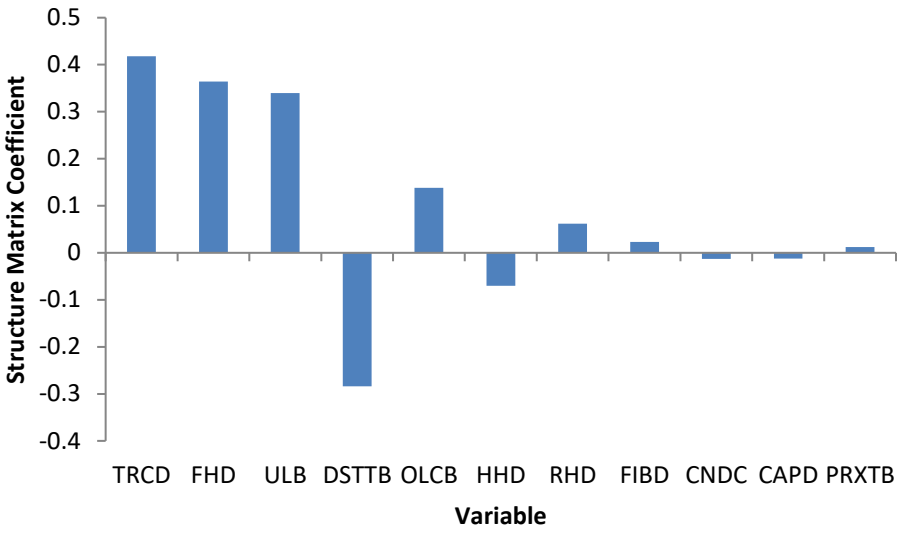

Figure 4.1: Discriminant function ranking results for *Euoticus elegantulus*, ranked from highest to lowest discriminatory power.

4.5.2.2: *Aotus trivirgatus*

The unstandardised discriminant function analysis provided a ranking of all skeletal metrics for *Aotus trivirgatus.* FHD was the best discriminator between sexes, with a structure matrix coefficient of 0.465. PRXTB was ranked second with a structure matrix coefficient of 0.329 and TRCD was ranked third with a structure matrix coefficient of 0.307. FIBD was the worst discriminator between sexes with a structure matrix coefficient of 0.005. DSTTB was ranked eleventh with a structure matrix coefficient of 0.077 and RHD was ranked tenth with a structure matrix coefficient of 0.109. The classification percentage for this analysis was 74%, with six males incorrectly classified as female and seven females incorrectly classified as male. The stepwise discriminant function analysis was unable to provide a ranking for the sample as the multivariate statistic, Wilks' Lambda, was not statistically significant and so the data did not qualify for stepwise analysis.

Table 4.2: Discriminant function analysis results for *Aotus trivirgatus*.

	Aotus trivirgatus	
	Discriminant Function Ranking	Structure Matrix Coefficients
HHD	6	0.251
OLCB	9	0.171
CAPD	7	0.248
RHD	10	0.109
ULB	5	0.268
FHD	1	0.465
TRCD	3	0.307
CNDC	8	0.189
PRXTB	2	0.329
DSTTB	11	0.077
FIBD	12	0.005
TAL	4	0.282
Classification Percentage (%)	74	

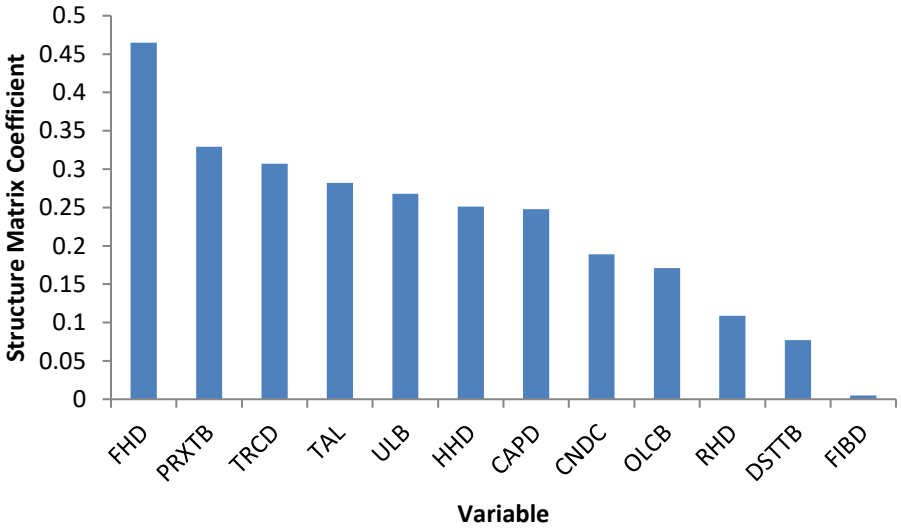

Figure 4.2: Discriminant function ranking results for *Aotus trivirgatus,* ranked from highest to lowest discriminatory power.

4.5.2.3: *Saguinus oedipus*

FIBD was the best discriminator between sexes of *Saguinus oedipus*, with a structure matrix coefficient of 0.488. HHD was ranked second with a structure matrix coefficient of 0.359 and ULB was ranked third with a structure matrix coefficient of 0.271. CAPD was the worst discriminator between sexes with a structure matrix coefficient of 0.008. PRXTB was ranked eleventh with a structure matrix coefficient of 0.052 and OLCB was ranked tenth with a structure matrix coefficient of -0.069. The classification percentage for this analysis was 81%, with three males incorrectly classified as female and seven females incorrectly classified as male.

The stepwise discriminant function analysis provided a ranking of all the skeletal metrics. The stepwise discriminant model only added FIBD to the discriminant function model, making it the only variable needed to produce the best model of discrimination. The structure matrix rankings provided FIBD with a structure matrix coefficient of 1.000 because it is the only predictor. PRXTB was still ranked second with a structure matrix coefficient of 0.730 but CNDC was ranked third with a structure matrix coefficient of 0.697. CAPD was still the worst discriminator between sexes with a structure matrix coefficient of 0.354. ULB was ranked eleventh with a structure matrix coefficient of 0.414 and RHD was ranked tenth with a structure matrix coefficient of 0.461. The classification percentage for this analysis was lower than the unstandardised discriminant function analysis at 60.7%, as expected because of the fewer independent variables in the analysis. The model of discrimination incorrectly classified ten males as female and twelve females as males.

Table 4.3: Discriminant function analysis results for *Saguinus oedipus*.

	Saguinus oedipus	
	Discriminant Function Ranking	Structure Matrix Coefficients
HHD	2	0.359
OLCB	10	-0.069
CAPD	12	0.008
RHD	9	-0.080
ULB	3	0.271
FHD	4	0.267
TRCD	5	0.196
CNDC	8	0.096
PRXTB	11	0.052
DSTTB	6	0.192
FIBD	1	0.488
TAL	7	0.114
Classification Percentage (%)	81	

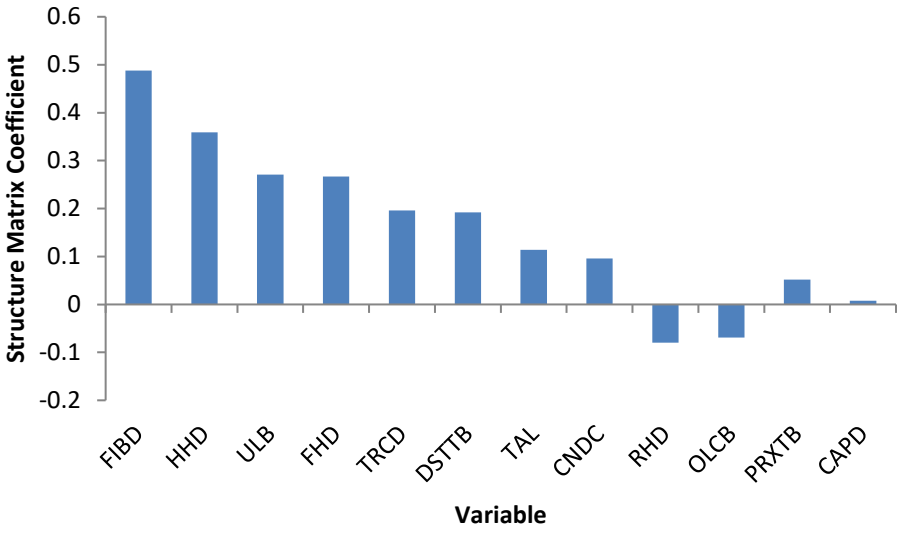

Figure 4.3: Discriminant function ranking results *for Saguinus oedipus,* ranked from highest to lowest discriminatory power.

Table 4.4: Stepwise discriminant function analysis results for *Saguinus oedipus.*

	Saguinus oedipus	
	Discriminant Function Stepwise Ranking	Structure Matrix Coefficients
HHD	5	0.595
OLCB	9	0.462
CAPD	12	0.354
RHD	10	0.461
ULB	11	0.414
FHD	6	0.591
TRCD	7	0.585
CNDC	3	0.697
PRXTB	2	0.730
DSTTB	8	0.493
FIBD	1	1.000
TAL	4	0.599
Classification Percentage (%)	60.7	

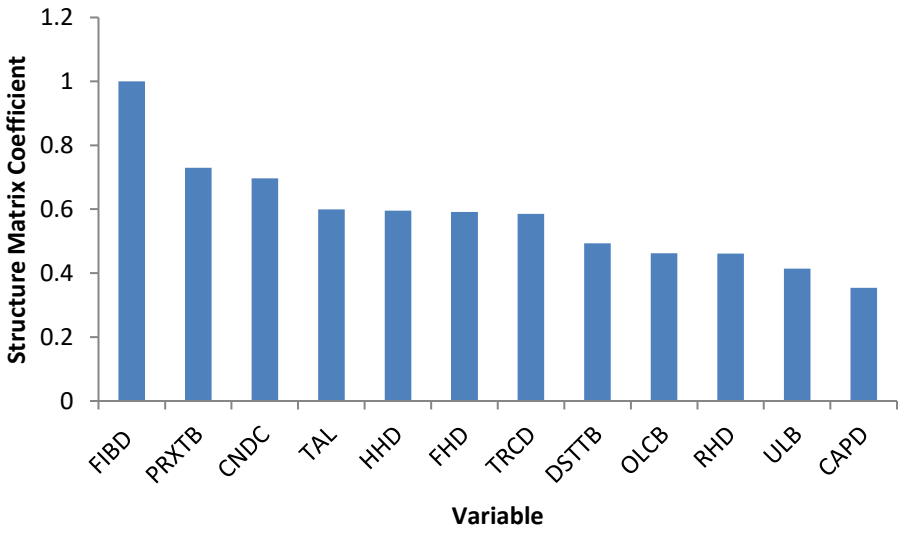

Figure 4.4: Stepwise discriminant function ranking results for *Saguinus oedipus*, ranking metric correlation with the stepwise model from highest to lowest.

.

4.5.2.4: *Chlorocebus pygerythrus*

HHD was the best discriminator between sexes of *Chlorocebus pygerythrus* with a structure matrix coefficient of 0.741. TAL was ranked second with a structure matrix coefficient of 0.532 and CAPD was ranked third with a structure matrix coefficient of 0.498. TRCD was the worst discriminator between sexes with a structure matrix coefficient of 0.269. ULB was ranked eleventh with a structure matrix coefficient of 0.274 and FIBD was ranked tenth with a structure matrix coefficient of 0.310. The classification percentage for this analysis was 100%.

The stepwise discriminant function analysis provided a ranking of all the skeletal metrics. The stepwise discriminant model only added HHD, to the discriminant function model making it the only variable needed to produce the best model of discrimination. The structure matrix rankings provided HHD with a structure matrix coefficient of 1.000 because it is the only predictor. PRXTB was ranked second with a structure matrix coefficient of 0.731 and RHD was ranked third with a structure matrix coefficient of 0.655. TAL was the worst discriminator between sexes with a structure matrix coefficient of 0.397. ULB was still ranked eleventh with a structure matrix coefficient of 0.432 and FHD was ranked tenth with a structure matrix coefficient of 0.436. The classification percentage for the stepwise discriminant function analysis was 98.3%, with one male incorrectly classified as female.

Table 4.5: Discriminant function analysis results for *Chlorocebus pygerythrus.*

	Chlorocebus pygerythrus	
	Discriminant Function Ranking	Structure Matrix Coefficients
HHD	1	0.741
OLCB	9	0.341
CAPD	3	0.498
RHD	7	0.368
ULB	11	0.274
FHD	8	0.345
TRCD	12	0.269
CNDC	4	0.460
PRXTB	6	0.399
DSTTB	5	0.414
FIBD	10	0.310
TAL	2	0.532
Classification Percentage (%)	100	

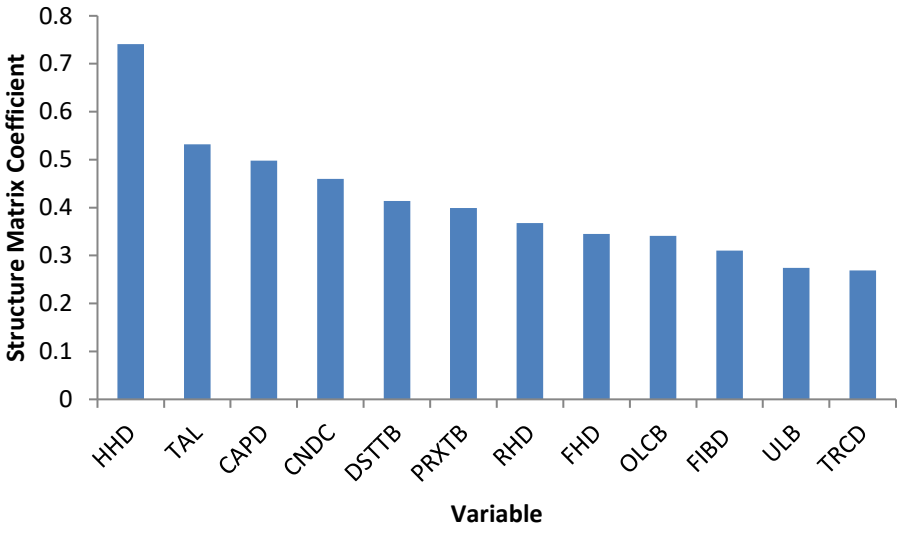

Figure 4.5: Discriminant function ranking results for *Chlorocebus pygerythrus,* ranked from highest to lowest discriminatory power.

Table 4.6: Stepwise discriminant function analysis results for *Chlorocebus pygerythrus.*

	Chlorocebus pygerythrus	
	Discriminant Function Stepwise Ranking	Structure Matrix Coefficients
HHD	1	1.000
OLCB	6	0.505
CAPD	4	0.517
RHD	3	0.655
ULB	11	0.432
FHD	10	0.436
TRCD	8	0.482
CNDC	5	0.507
PRXTB	2	0.731
DSTTB	7	0.485
FIBD	9	0.450
TAL	12	0.397
Classification Percentage (%)	98.3	

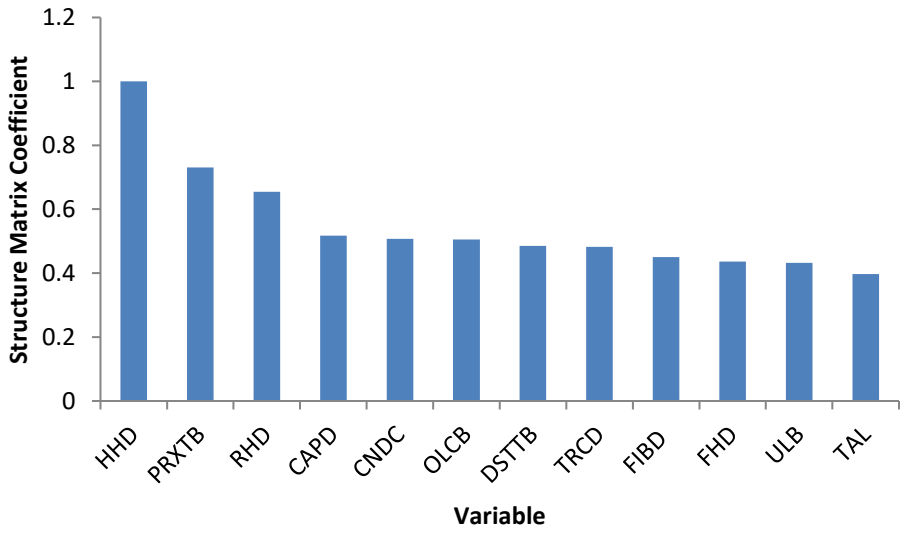

Figure 4.6: Stepwise discriminant function ranking results for *Chlorocebus pygerythrus,* ranking metric correlation with the stepwise model from highest to lowest.

4.5.2.5: *Saimiri sciureus*

OLCB was the best discriminator between sexes of *Saimiri sciureus* with a structure matrix coefficient of 0.753. HHD was ranked second with a structure matrix coefficient of 0.539 and CAPD was ranked third with a structure matrix coefficient of 0.425. FIBD was the worst discriminator between sexes with a structure matrix coefficient of 0.207. ULB was ranked eleventh with a structure matrix coefficient of 0.259 and TAL was ranked tenth with a structure matrix coefficient of 0.300. The classification percentage for this analysis was 100%.

The stepwise discriminant function analysis provided a ranking of all the skeletal metrics. The stepwise discriminant model used two metrics as predictors, with OLCB added in the first step, being the best discriminator of sexual dimorphism. TRCD was added in the second step, to form the best model of discrimination. The structure matrix rankings provided OLCB with a structure matrix coefficient of 0.950. RHD was ranked second with a structure matrix coefficient of 0.594 and HHD was ranked third with a structure matrix coefficient of 0.503. TRCD was only sixth in the structure matrix rankings with a structure matrix coefficient of 0.422. FHD was the worst discriminator between sexes with a structure matrix coefficient of 0.246. TAL was ranked eleventh with a structure matrix coefficient of 0.271 and DSTTB was ranked tenth with a structure matrix coefficient of 0.321. The classification percentage for the stepwise discriminant function analysis was 96.7%, with two males incorrectly classified as female.

Table 4.7: Discriminant function analysis results for *Saimiri sciureus.*

	Saimiri sciureus	
	Discriminant Function Ranking	Structure Matrix Coefficients
HHD	2	0.539
OLCB	1	0.753
CAPD	3	0.425
RHD	9	0.311
ULB	11	0.259
FHD	7	0.359
TRCD	8	0.334
CNDC	5	0.387
PRXTB	6	0.374
DSTTB	4	0.392
FIBD	12	0.207
TAL	10	0.300
Classification Percentage (%)	100	

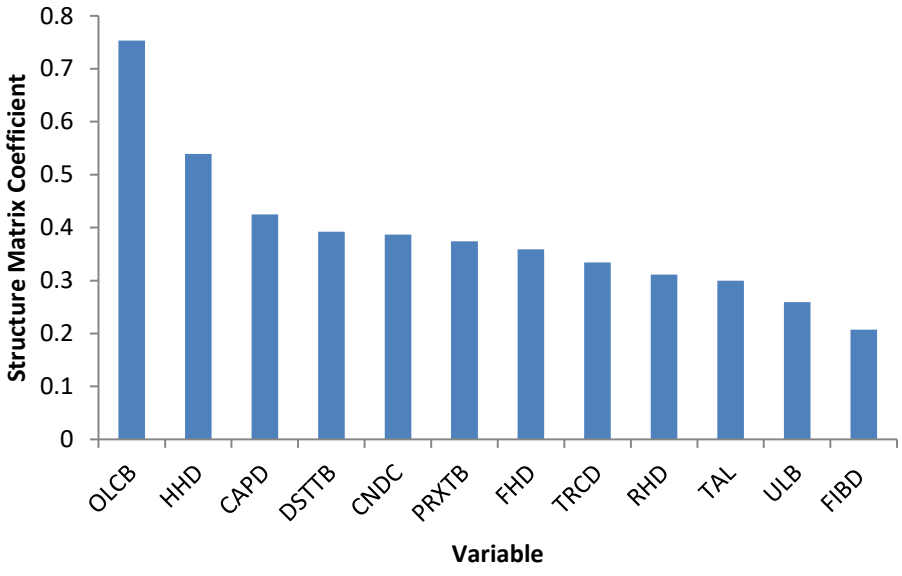

Figure 4.7: Discriminant function ranking results for *Saimiri sciureus,* ranked from highest to lowest discriminatory power.

Table 4.8: Stepwise discriminant function analysis results for Saimiri *sciureus.*

	Saimiri sciureus	
	Discriminant Function Stepwise Ranking	Structure Matrix Coefficients
HHD	3	0.503
OLCB	1	0.950
CAPD	5	0.424
RHD	2	0.594
ULB	9	0.364
FHD	12	0.246
TRCD	6	0.422
CNDC	8	0.371
PRXTB	4	0.469
DSTTB	10	0.321
FIBD	7	0.392
TAL	11	0.271
Classification Percentage (%)	96.7	

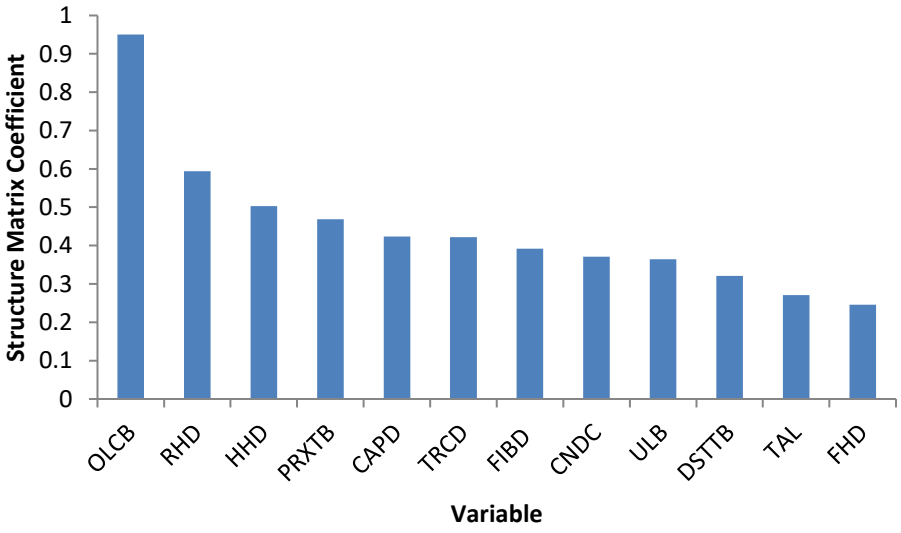

Figure 4.8: Stepwise discriminant function ranking results for *Saimiri sciureus,* ranking metric correlation with the stepwise model from highest to lowest.

4.5.2.6: *Macaca mulatta*

The unstandardised discriminant function analysis provided a ranking of skeletal metrics for *Macaca mulatta*, apart from TAL, which was removed due to low sample size. The threshold for low sample size was chosen as fewer than 15 measurements for each sex. HHD was the best discriminator between sexes with a structure matrix coefficient of 0.752. OLCB was ranked second with a structure matrix coefficient of 0.726 and CAPD was ranked third with a structure matrix coefficient of 0.687. ULB was the worst discriminator between sexes with a structure matrix coefficient of 0.135. DSTTB was ranked tenth with a structure matrix coefficient of 0.398 and FIBD was ranked ninth with a structure matrix coefficient of 0.467. The classification percentage for this analysis was 100%.

The stepwise discriminant function analysis provided a ranking of all skeletal metrics, apart from TAL, which was removed due to low sample size. The stepwise discriminant model used two metrics as predictors, with HHD added in the first step, being the best discriminator of sexual dimorphism. OLCB was added in the second step to make the best model of discrimination. The structure matrix rankings provided HHD with a structure matrix coefficient of 0.915. OLCB was still ranked second with a structure matrix coefficient of 0.884 but FHD was ranked third with a structure matrix coefficient of 0.840. ULB was still the worst discriminator between sexes with a structure matrix coefficient of 0.343. DSTTB was still ranked tenth with a structure matrix coefficient of 0.590 and FIBD was still ranked ninth with a structure matrix coefficient of 0.620. The classification percentage for the stepwise discriminant function analysis was 97.2%, with one male incorrectly classified as female.

Table 4.9: Discriminant function analysis results for *Macaca mulatta.*

	Macaca mulatta	
	Discriminant Function Ranking	Structure Matrix Coefficients
HHD	1	0.752
OLCB	2	0.726
CAPD	3	0.687
RHD	6	0.507
ULB	11	0.135
FHD	5	0.507
TRCD	4	0.640
CNDC	7	0.471
PRXTB	8	0.468
DSTTB	10	0.398
FIBD	9	0.467
TAL	N/A	N/A
Classification Percentage (%)	100	

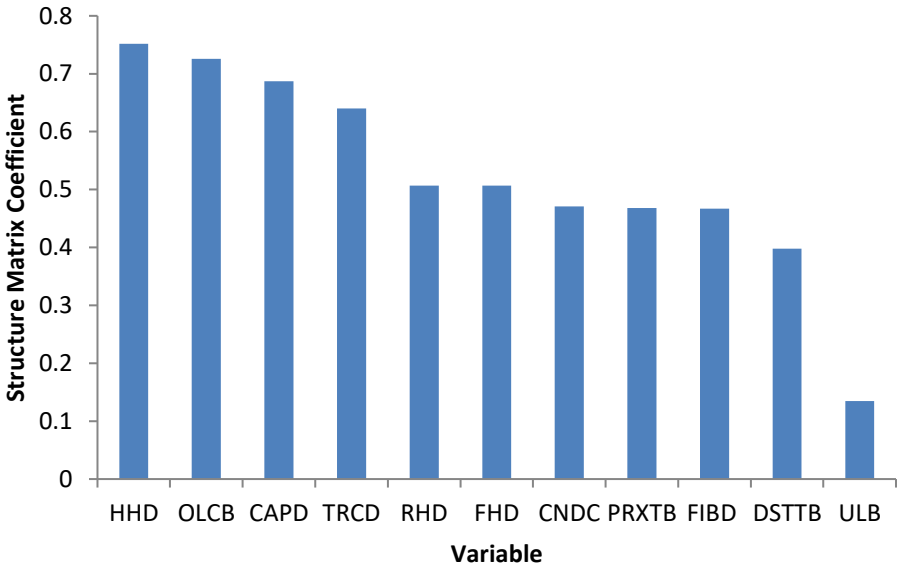

Figure 4.9: Discriminant function ranking results for *Macaca mulatta,* ranked from highest to lowest discriminatory power.

Table 4.10: Stepwise discriminant function analysis results for *Macaca mulatta.*

	Macaca mulatta	
	Discriminant Function Stepwise Ranking	Structure Matrix Coefficients
HHD	1	0.915
OLCB	2	0.884
CAPD	7	0.695
RHD	6	0.732
ULB	11	0.343
FHD	3	0.840
TRCD	8	0.663
CNDC	5	0.744
PRXTB	4	0.773
DSTTB	10	0.590
FIBD	9	0.620
TAL	N/A	N/A
Classification Percentage (%)	97.2	

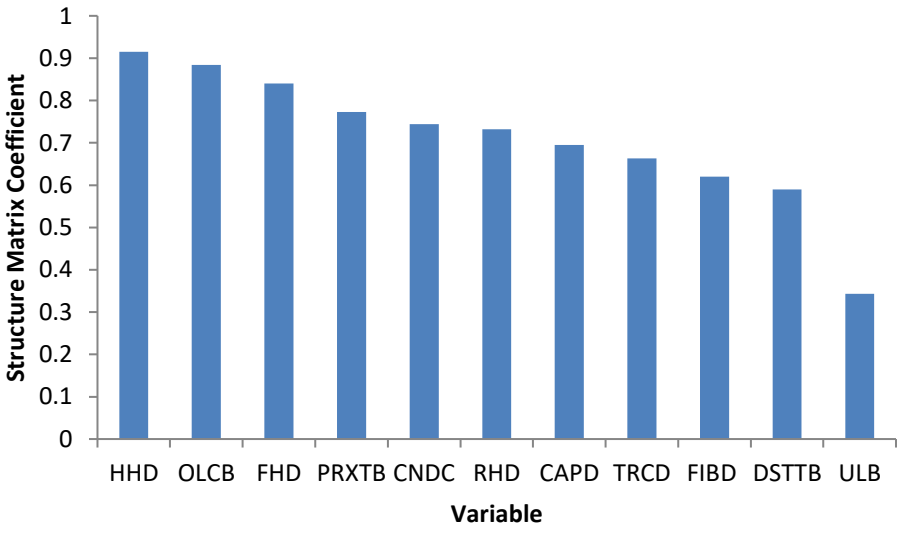

Figure 4.10: Stepwise discriminant function ranking results for *Macaca mulatta,* ranking metric correlation with the stepwise model from highest to lowest.

4.5.2.7: *Pan troglodytes*

OLCB was the best discriminator between sexes of *Pan troglodytes,* with a structure matrix coefficient of 0.710. PRXTB was ranked second with a structure matrix coefficient of 0.684 and CNDC was ranked third with a structure matrix coefficient of 0.659. CAPD was the worst discriminator between sexes with a structure matrix coefficient of 0.207. TRCD was ranked eleventh with a structure matrix coefficient of 0.332 and ULB was ranked tenth with a structure matrix coefficient of 0.344. The classification percentage for this analysis was 92%, with two males incorrectly classified as female and two females incorrectly classified as male.

The stepwise discriminant function analysis provided a ranking of all skeletal metrics. The stepwise discriminant model used two metrics as predictors, with OLCB added in the first step, as the best discriminator. CNDC was added in the second step to make the best model of discrimination. The structure matrix rankings provided OLCB with a structure matrix coefficient of 0.841. CNDC was ranked second with a structure matrix coefficient of 0.780 and PRXTB was ranked third with a structure matrix coefficient of 0.675. TAL was the worst discriminator between sexes with a structure matrix coefficient of 0.178. CAPD was ranked eleventh with a structure matrix coefficient of 0.240 and ULB was still ranked tenth with a structure matrix coefficient of 0.264. The classification percentage for the stepwise discriminant function analysis was 87.9%, with two males incorrectly classified as female and five females incorrectly classified as male.

Table 4.11: Discriminant function analysis results for *Pan troglodytes.*

	Pan troglodytes	
	Discriminant Function Ranking	Structure Matrix Coefficients
HHD	4	0.658
OLCB	1	0.710
CAPD	12	0.207
RHD	5	0.620
ULB	10	0.344
FHD	7	0.495
TRCD	11	0.332
CNDC	3	0.659
PRXTB	2	0.684
DSTTB	6	0.515
FIBD	8	0.393
TAL	9	0.370
Classification Percentage (%)	92	

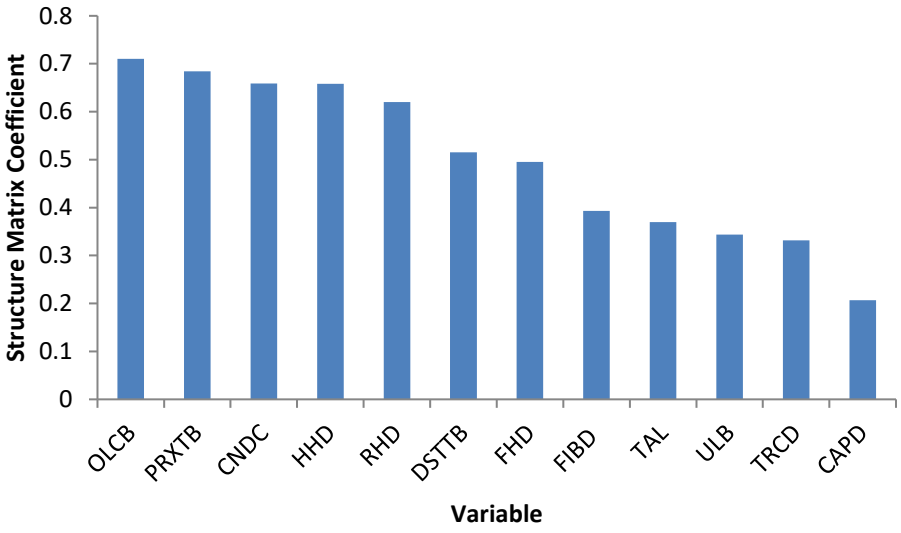

Figure 4.11: Discriminant function ranking results for *Pan troglodytes,* ranked from highest to lowest discriminatory power.

Table 4.12: Stepwise discriminant function analysis results for *Pan troglodytes.*

	Pan troglodytes	
	Discriminant Function Stepwise Ranking	Structure Matrix Coefficients
HHD	4	0.662
OLCB	1	0.841
CAPD	11	0.240
RHD	6	0.525
ULB	10	0.264
FHD	5	0.588
TRCD	7	0.498
CNDC	2	0.780
PRXTB	3	0.675
DSTTB	9	0.376
FIBD	8	0.454
TAL	12	0.178
Classification Percentage (%)	87.9	

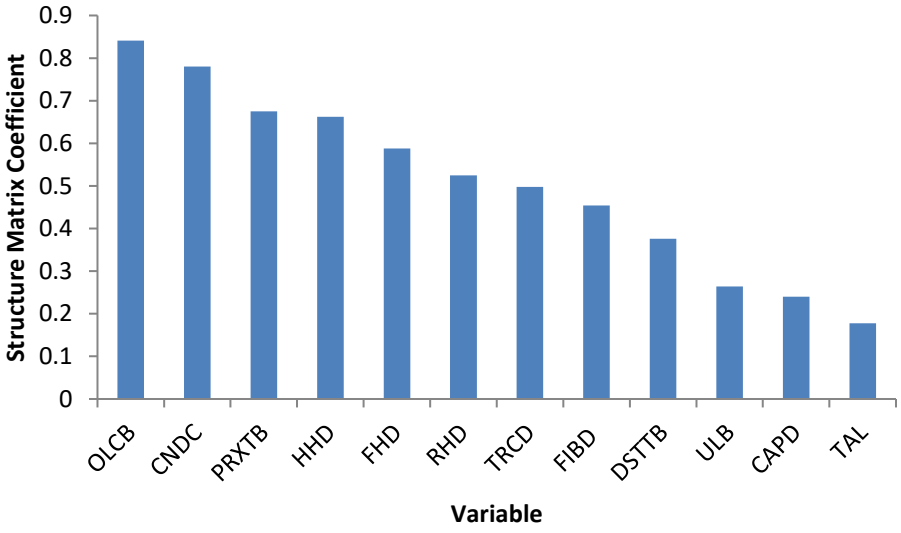

Figure 4.12: Stepwise discriminant function ranking results for *Pan troglodytes,* ranking metric correlation with the stepwise model from highest to lowest.

4.5.2.8: *Gorilla gorilla*

HHD was the best discriminator between sexes of *Gorilla gorilla* with a structure matrix coefficient of 0.703. OLCB was ranked second with a structure matrix coefficient of 0.695 and DSTTB was ranked third with a structure matrix coefficient of 0.647. TRCD was the worst discriminator between sexes with a structure matrix coefficient of 0.335. ULB was ranked eleventh with a structure matrix coefficient of 0.404 and CNDC was ranked tenth with a structure matrix coefficient of 0.459. The classification percentage for this analysis was 100%.

The stepwise discriminant function analysis provided a ranking of all skeletal metrics. The stepwise discriminant model used four metrics as predictors, in five steps, with HHD added to the model in the first step, as the best discriminator. The model was improved by adding DSTTB in the second step, adding FIBD in the third step, adding OLCB in the fourth step and then adding DSTTB, FIBD and OLCB together with HHD removed in the fifth step. The structure matrix rankings still found OLCB to be the best discriminator between sexes with a structure matrix coefficient of 0.738. HHD, which was highest in the unstandardised ranking and therefore the single best predictor, was ranked fifth in the stepwise ranking, due to being highly correlated with one of the other four metrics. This means that the four metrics together provided better discrimination without HHD. DSTTB was ranked second with a structure matrix coefficient of 0.688 and FIBD was ranked third with a structure matrix coefficient of 0.684. TRCD was still the worst discriminator between sexes with a structure matrix coefficient of 0.285. ULB was still ranked eleventh with a structure matrix coefficient of 0.400 and FHD was ranked tenth with a structure matrix coefficient of 0.499. The classification percentage for the stepwise discriminant function analysis was 98.3%, with one female incorrectly classified as male.

Table 4.13: Discriminant function analysis results for *Gorilla gorilla*.

	Gorilla gorilla	
	Discriminant Function Ranking	Structure Matrix Coefficients
HHD	1	0.703
OLCB	2	0.695
CAPD	8	0.540
RHD	5	0.606
ULB	11	0.404
FHD	6	0.572
TRCD	12	0.335
CNDC	10	0.459
PRXTB	7	0.565
DSTTB	3	0.647
FIBD	4	0.644
TAL	9	0.513
Classification Percentage (%)	100	

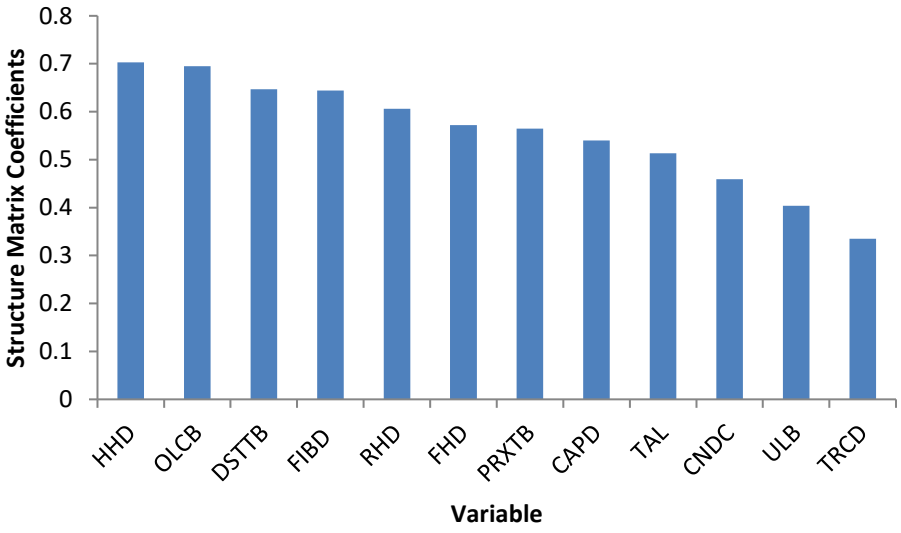

Figure 4.13: Discriminant function ranking results *for Gorilla gorilla,* ranked from highest to lowest discriminatory power.

Table 4.14: Stepwise discriminant function analysis results for *Gorilla gorilla.*

	Gorilla gorilla	
	Discriminant Function Stepwise Ranking	Structure Matrix Coefficients
HHD	5	0.583
OLCB	1	0.738
CAPD	9	0.547
RHD	7	0.576
ULB	11	0.400
FHD	10	0.499
TRCD	12	0.285
CNDC	6	0.577
PRXTB	4	0.635
DSTTB	2	0.688
FIBD	3	0.684
TAL	8	0.571
Classification Percentage (%)	98.3	

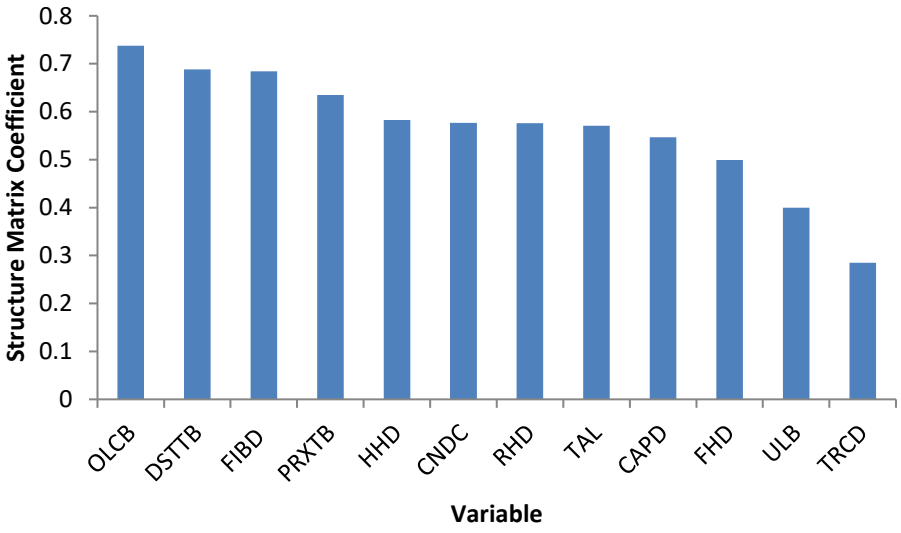

Figure 4.14: Stepwise discriminant function ranking results for *Gorilla gorilla*, ranking metric correlation with the stepwise model from highest to lowest.

4.5.2.9: *Homo sapiens*

ULB was the best discriminator between sexes of *Homo sapiens* with a structure matrix coefficient of 0.722. OLCB was ranked second with a structure matrix coefficient of 0.697 and FHD was ranked third with a structure matrix coefficient of 0.620. TRCD was the worst discriminator between sexes with a structure matrix coefficient of 0.337. FIBD was ranked eleventh with a structure matrix coefficient of 0.341 and DSTTB was ranked tenth with a structure matrix coefficient of 0.357. The classification percentage for this analysis was 98.3%, with one male incorrectly classified as female.

The stepwise discriminant function analysis provided a ranking of all skeletal metrics. The stepwise discriminant model used three metrics as predictors with ULB added to the model in the first step, as the best discriminator. FHD was added in the second step and TAL was added in the third step, to form the best model of discrimination. The structure matrix rankings still found ULB to be the best discriminator between sexes with a structure matrix coefficient of 0.789. HHD was ranked second with a structure matrix coefficient of 0.699 and FHD was still ranked third with a structure matrix coefficient of 0.677. FIBD was the worst discriminator between sexes with a structure matrix coefficient of 0.404. DSTTB was ranked eleventh with a structure matrix coefficient of 0.412 and TRCD was ranked tenth with a structure matrix coefficient of 0.525. The classification percentage for the stepwise discriminant function analysis was 98.3%, with one male incorrectly classified as female.

Table 4.15: Discriminant function analysis results for *Homo sapiens.*

	Homo sapiens	
	Discriminant Function Ranking	Structure Matrix Coefficients
HHD	5	0.578
OLCB	2	0.697
CAPD	7	0.518
RHD	6	0.576
ULB	1	0.722
FHD	3	0.620
TRCD	12	0.337
CNDC	8	0.507
PRXTB	4	0.609
DSTTB	10	0.357
FIBD	11	0.341
TAL	9	0.492
Classification Percentage (%)	98.3	

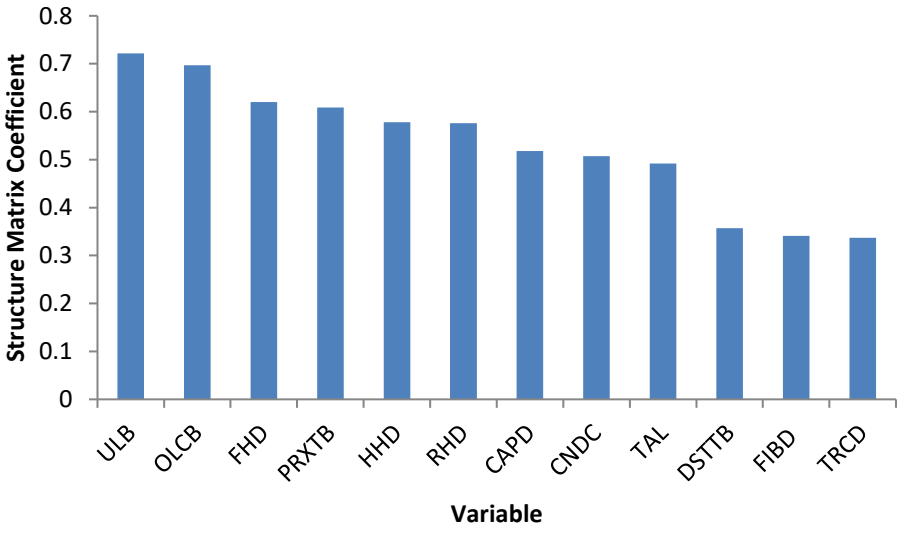

Figure 4.15: Discriminant function ranking results for *Homo sapiens,* ranked from highest to lowest discriminatory power.

Table 4.16: Stepwise discriminant function analysis results for *Homo sapiens*.

	Homo sapiens	
	Discriminant Function Stepwise Ranking	Structure Matrix Coefficients
HHD	2	0.699
OLCB	6	0.574
CAPD	7	0.544
RHD	9	0.535
ULB	1	0.789
FHD	3	0.677
TRCD	10	0.525
CNDC	5	0.612
PRXTB	4	0.669
DSTTB	11	0.412
FIBD	12	0.404
TAL	8	0.538
Classification Percentage (%)	98.3	

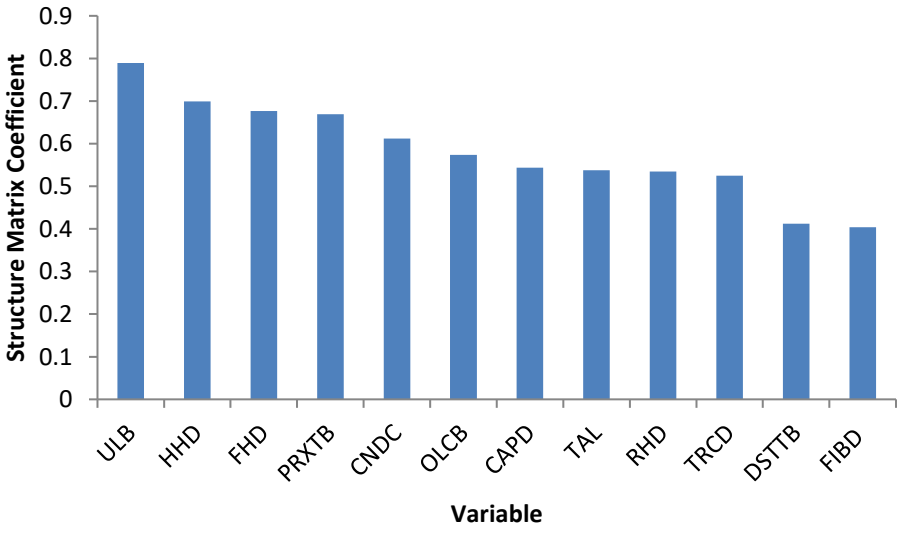

Figure 4.16: Stepwise discriminant function ranking results for *Homo sapiens,* ranking metric correlation with the stepwise model from highest to lowest.

4.5.3: Summary of intraspecies analysis results

This intraspecies analysis answers the question of which skeletal metrics are the best and worst discriminators of sexual dimorphism. HHD was the best discriminator for three of the species and the second-best discriminator for a further two species in the unstandardised discrimination function analysis. OLCB was the best discriminator for three species and the second-best discriminator for a further species in the stepwise discrimination function analysis. Generally, the best skeletal metrics as discriminators of sex were ranked the same by both the unstandardised and stepwise discriminant function analyses (although no comparison between analyses for *Euoticus elegantulus* and *Aotus trivirgatus* were possible as no stepwise discriminant function analysis structure matrices were produced). Negative coefficients occurred in monomorphic species indicating skeletal measurements that are on average larger in females than males.

The highest ranking skeletal metric for *Gorilla gorilla* differed between the two analyses, with HHD the highest ranked from the unstandardised structure matrix and OLCB the highest ranked from the stepwise structure matrix. It should be noted, however, that OLCB was ranked second in the unstandardised structure matrix. There is less consistency between analyses for the worst skeletal metrics as discriminators of sex. For *Chlorocebus pygerythrus*, TAL was the second highest ranked metric from the unstandardised structure matrix, but the lowest ranked metric from the stepwise structure matrix. This may be due to the smaller TAL sample size in comparison to the rest of the *Chlorocebus pygerythrus* sample. For *Saimiri sciureus,* FHD was the lowest ranked metric from the stepwise structure matrix, but ranked seventh in the unstandardised structure matrix. For *Pan troglodytes*, TAL was the lowest ranked metric from the stepwise structure matrix and was ranked ninth from the unstandardised structure matrix. For *Homo sapiens*, FIBD was the lowest ranked metric from the stepwise structure matrix, but was ranked eleventh from the unstandardised structure matrix.

The stepwise discriminant function analyses highlight the complexity of sexual dimorphism within the skeleton. The *Gorilla gorilla* sample required four metrics to produce a stepwise model of discrimination and the *Homo sapiens* sample required three skeletal metrics. The necessity of two or more metrics for the best model of discrimination in most species reflects the dimensionality required to define the best way of distinguishing sex in a skeleton with varied levels of sexual dimorphism.

Kovarovic et al (2011) noted the importance of standardising the discriminant function analysis classification percentage in relation to chance. For all cases, the discriminant function analysis produced classification percentages greater than chance at 50%. The discriminant function analysis provided a surprisingly high classification percentage for species that are known to be monomorphic and therefore not expected to be successfully discriminated into male and female groups any better than by chance. For the unstandardised discriminant function analysis, *Euoticus elegantulus* had a classification percentage of 74.5%, *Aotus trivirgatus* had a classification percentage of 74% *and Saguinus oedipus* had a classification percentage of 81%. For *Euoticus elegantulus* and *Saguinus oedipus* the contribution of both positive and negative structure matrix coefficients (the latter occurring when females are found to be larger than males for a given skeletal metric) suggests that the high classification percentage was produced by the analyses maximising the difference between positive and negative metrics to discriminate sex. The data for *Euoticus elegantulus* and *Aotus trivirgatus* was unable to produce a structure matrix ranking through the stepwise discriminant function analysis and the classification percentage for *Saguinus oedipus* was reduced to 60.7%, far lower than the other species in the sample. The Wilks' Lambda multivariate statistic of fitness was not significant for *Euoticus elegantulus* and *Aotus trivirgatus* and too high to qualify for stepwise analysis. The Wilks' Lambda multivariate statistic of fitness was also not significant for *Saguinus oedipus*, although small enough for a stepwise analysis to be completed. The discriminant function analysis model for *Saguinus oedipus* should therefore be treated with caution, as expected for a known monomorphic species.

The question of what is the structure of sexual dimorphism within the primate order (in terms of the similarities between skeletal metrics within the same species) is also explored in this analysis when metrics are grouped into the areas of the body they are derived from (eg. lower limb). Upper limb metrics (HHD and OLCB) were generally found to be better discriminators of sexual dimorphism. The question of whether the structure of sexual dimorphism in humans differs greatly in comparison to other primate species is partly answered with upper limb metrics found to be the best discriminators in *Homo sapiens*, but differed from other primate species by having ULB as the highest ranked discriminator. The following interspecies analysis provides more detail on the differences between *Homo sapiens* and other primate species. The overall finding from this set of analyses is that sexual dimorphism varies in the skeleton. Skeletal metrics within one species were not

found to have the same level of sexual dimorphism, indicating a non-isometric structure to sexual dimorphism in the primate order.

4.6: Interspecies analysis

The discriminant function analysis rankings for each species can be compared in order to examine whether there is a pattern within the primate order for best and worst discriminators of sexual dimorphism. By comparing between species, the structure of sexual dimorphism within the primate order can be further evaluated and any differences between *Homo sapiens* and the rest of the primate order can be explored. Tables of all the discriminant function analysis rankings and correlation coefficients are provided in Appendix 6. Averaging the skeletal metric rankings for all species is a simple indicator of the overall best and worst discriminators within the data set. Using the unstandardised discriminant function analysis, HHD was found to be the best discriminator with the lowest ranking average, followed by OLCB, which ranked second and FHD, which ranked third. The worst discriminator for all species was FIBD with the highest ranking average of twelfth, followed by TRCD, which ranked eleventh and ULB, which ranked tenth.

There are great differences in discriminant function analysis rankings between monomorphic and dimorphic species (see *Chapter 3: Materials and methodology* for a description of how monomorphic and dimorphic species were defined). *Euoticus elegantulus, Aotus trivirgatus* and *Saguinus oedipus* were grouped together as they are monomorphic species. The average rankings for monomorphic species found that FHD was the best discriminator with the lowest ranking average, followed by TRCD, which ranked second and ULB, which ranked third. The worst discriminator for monomorphic species was CAPD with the highest ranking average of tenth, followed by RHD, which ranked ninth and CNDC, which ranked eighth. *Chlorocebus pygerythrus*, *Saimiri sciureus, Macaca mulatta, Pan troglodytes*, *Gorilla gorilla* and *Homo sapiens* were grouped together as they are dimorphic species. The average rankings for dimorphic species found that HHD was the best discriminator with the lowest ranking average, followed by OLCB, which ranked second and PRXTB, which ranked third. The worst discriminator for dimorphic species was TRCD with the highest ranking average of tenth, followed by ULB, which ranked ninth and FIBD, which ranked eighth. The stepwise discriminant function analyses found the best discriminator for dimorphic species to still be HHD with the lowest ranking average,

followed by OLCB, which ranked second and PRXTB, which ranked third. The worst discriminator for dimorphic species was TAL with the highest ranking average of eleventh, followed by ULB, which ranked tenth and TRCD, which ranked ninth.

Therefore, there is a general trend for upper limb skeletal metrics being better discriminators of sexual dimorphism in dimorphic species. Using the stepwise discriminant function analysis rankings, HHD was the best discriminator for *Chlorocebus pygerythrus* and *Macaca mulatta* and OLCB was the best discriminator for *Saimiri sciureus*, *Pan troglodytes* and *Gorilla gorilla*. *Homo sapiens* differed with ULB being the best discriminator, a skeletal metric that was far lower in the rankings of the other dimorphic species. *Homo sapiens* also differed from the other dimorphic species as FHD was ranked third in both the unstandardised discriminant function analysis and the stepwise discriminant function analysis. The other dimorphic species ranked FHD higher, apart from *Macaca mulatta,* which ranked FHD third in the stepwise discriminant function analysis, but fifth in the unstandardised discriminant function analysis.

Table 4.17: Discriminant function analysis rankings and stepwise discriminant function analysis rankings of upper limb metrics divided by monomorphic and dimorphic species.

Discriminant Function Analysis Rankings

		HHD	OLCB	CAPD	RHD	ULB
Monomorphic species	*E. elegantulus*	6	5	10	7	3
	A. trivirgatus	6	9	7	10	5
	S.oedipus	2	10	12	9	3
Dimorphic species	*C. pygerythrus*	1	9	3	7	11
	S. sciureus	2	1	3	9	11
	M. mulatta	1	2	3	6	11
	P. troglodytes	4	1	12	5	10
	G. gorilla	1	2	8	5	11
	H. sapiens	5	2	7	6	1

Stepwise Discriminant Function Analysis Rankings

		HHD	OLCB	CAPD	RHD	ULB
Monomorphic species	*E. elegantulus*	x	X	x	x	X
	A. trivirgatus	x	X	x	x	X
	S.oedipus	5	9	12	10	11
Dimorphic species	*C. pygerythrus*	1	6	4	3	11
	S. sciureus	3	1	5	2	9
	M. mulatta	1	2	7	6	11
	P. troglodytes	4	1	11	6	10
	G. gorilla	5	1	9	7	11
	H. sapiens	2	6	7	9	1

Table 4.18: FHD discriminant function ranking within dimorphic species.

Unstandardised and stepwise discriminant function analysis rankings for FHD in dimorphic species

	FHD- Unstandardised	FHD- Stepwise
C. pygerythrus	8	10
S. sciureus	7	12
M. mulatta	5	3
P. troglodytes	7	5
G. gorilla	6	10
H. sapiens	3	3

4.7: Discussion

For this chapter, the aim of the set of analyses chosen was to answer the following questions from the dataset: 1) Are there differences in the level of sexual dimorphism between skeletal metrics for a species and if so which skeletal metrics are the best and worst discriminators of sexual dimorphism? 2) What is the structure of sexual dimorphism within the primate order (in terms of the variation and patterns between primate species as well as differences and similarities between skeletal metrics within the same species)? 3) Does the structure of sexual dimorphism in humans differ greatly in comparison to other primate species?

The overall finding from this set of analyses is that sexual dimorphism within the skeleton is non-isometric, with the level of dimorphism varying between skeletal elements. This finding, through discriminant function analysis rankings, confirms an observation made through simple calculations of the sexual dimorphism index (male average/ female average) for each metric per species and histograms of the skeletal metric data (see Appendix 2 and Appendix 5). The sexual dimorphism index differed between metrics of the same species. This suggested that there are differences in the level of sexual dimorphism throughout the skeleton of known dimorphic species, confirmed in this set of analyses. Discriminant function analysis was able to rank the skeletal metrics as discriminators of sexual dimorphism. Upper limb metrics were generally found to be better discriminators of sexual dimorphism for dimorphic species, confirming that there is variation in the structure of sexual dimorphism within the primate order. For *Homo sapiens*, upper limb metrics were still found to be the best discriminators but differed from the dimorphic average through ULB being the highest ranked discriminator, which ranked much lower for other dimorphic species.

Lower limb articular metrics, particularly FHD, have been used to estimate body mass from the skeleton in a wide range of studies (see Chapter 2: *A review of literature relevant to the study*) as there is a known mechanical relationship between load-bearing skeleton elements and body size. FHD was used to produce biomechanical body mass estimation equations later applied to predict the body mass for fossil hominin species *(*Ruff et al. 1991; McHenry, 1992; Grine et al. 1995). These body mass estimates have then been used to determine the level of sexual dimorphism within a species (Richmond and Jungers, 1995; Lockwood et al. 1996; Reno et al. 2003; 2010). The discriminant function analysis results from this study indicate that for many species, upper limb skeletal metrics are more

dimorphic than lower limb skeletal metrics, which may have implications for choice in metrics during estimation procedures.

4.7.1: Implications of non-isometric structure of sexual dimorphism within the primate skeleton

Studies have previously shown that skeletal metrics scale to body mass differently between taxa. Isometric scaling to body mass is preserved when proportional relationships remain as size changes. However, when a variable is oversized in relation to body mass it has positive allometry and when a variable is undersized in relation to body mass it has negative allometry. Ruff (1988) looked at the scaling of hindlimb articular surface dimensions with body mass for chimpanzees, orangutans, gorillas, macaques and modern humans. Orangutans were found to be close to isometry with their articular dimensions scaling strongly to body mass. Femoral head diameter (FHD) was found to give the best estimates of body mass but there was variation in some dimensions. The medial femoral condyle relates to the amount of bowleggedness in the knee and is prominent in gorillas and declining in orangutans and macaques. Macaques have smaller hindlimbs in relation to their body mass and modern humans have larger FHD in relation to their body mass. It was reasoned as being associated with joint excursion, mode of locomotion and activity level. Orangutan scaling differences are due to greater hindlimb mobility in suspensory behaviour. There are differences in locomotor behaviour between orangutan males and females, with males mechanically loading the lower limb less than females (Cant, 1987). Macaques have relatively small FHD and reduced hip mobility in comparison to orangutans, which is expected for animals with quadrupedal locomotion.

Cercopithecoids in general were found to have high mechanical loading of the forelimb, which may be due to other locomotor behaviours such as leaping and climbing. As expected, human bipedality means there is more loading of the lower limb in comparison to quadrupedal primates and so their lower limb joints are larger. Ruff (1988) also notes differences in scaling relationship between articular dimensions and diaphyseal dimensions with body mass. Activity level and bone remodelling affect diaphyseal dimension more than articular dimensions. So for hominins with higher activity levels, their diaphyseal dimensions will scale differently to body mass in comparison to modern humans. The finding by Ruff (1988) of more loading in the lower limb for bipeds when compared to

quadrupeds may provide a reason for human skeletal metric dimorphism to differ from the primate pattern with FHD being higher ranked as a discriminator of sex.

Weight bearing is known to be a major constraint on primate joint size with Swartz (1989) finding significant positive allometry in most limb joints of brachiating primate species. It was presumed that suspensory species would deviate from the general primate pattern of isometry due to the reduced compressive loads of the limb joints. However, the results of Swartz (1989) indicated that only specific types of locomotor specialisation produce changes in joint design. Locomotor modes that reduce joint stress may not have a selective effect on joint morphology in contrast to the selective pressure for increased joint size when stress is increased. The absence of selection for conserving joint material and the retention of larger joint size has also been explained as an indication of phylogenetic inertia, a constraint on evolution set by previous adaptations (Jungers, 1988; Swartz, 1989). The dimorphic upper limb metrics across primate species may therefore indicate a retained joint size difference between males and females within the primate order or separate adaptations to differences in upper limb loading that can be utilised for sex discrimination.

Later studies also found support for isometric scaling, when analyses controlled types of locomotion in species groups (Jungers, 1991; Ruff and Runstad, 1992). Godfrey et al. (1991) also indicated specific differences in joint surfaces vary in their scaling relationship to body mass; the 'female' or concave facet of a joint correlates with body mass scaling whilst the 'male' or convex facet of the joint correlates with differences in mobility. The study confirmed this as the female articular surface areas were found to scale with body mass and the male articular surface areas scaled non-isometrically with body mass, caused by differences in size-related locomotor style. The differences in the scaling of joints mean that the finding of the non-isometric nature of sexual dimorphism in articular surfaces is not unexpected.

Parr et al. (2011) analysed talus articular surface scaling for hominoid primates. Whilst no generalised rules of scaling were found, talus articular surface scaling is dependent on taxon- and sex-specific differences in locomotion and ontogenetic growth. Isometric scaling or with slight negative allometry across sexes of chimpanzees, orangutans and gorillas was found but gibbons and siamangs have a talus that scales with positive allometry like modern humans. Therefore, for gibbons, siamangs and modern humans the males either have larger tali than expected for their body mass or females have smaller tali than expected for their body mass. Talus growth trajectories in modern humans show that along

with the foot generally, the talus matures relatively early, with epiphyseal fusion occuring earlier in females around the age of nine years (Scheuer and Black, 2000). Scaling is undersized in females when a reduction in sexual dimorphism is cause by increased duration or increased rate of female growth, suggesting that *Homo sapiens* as a whole have larger than expected tali, but the pattern is more subtle in females due to constraints on the pattern of maturation.

The difference in general overscaling in humans compared to underscaling of talus dimensions in orangutans (apart from the trochlea facet) was given as a result of bipedalism and the higher loads required when compared to quadrupedal or brachiating species. The negative allometric scaling in the talus head facet of gorillas may reflect sex specific differences in the level of arboreality, but the positive allometric scaling seen in the talus head facet for chimpanzees does not reflect this. It is also unlikely that the negative allometric scaling of the subtalar joint in humans is a reflection of differences in locomotion between sexes. For humans, ontogenetic differences between sexes are a more likely cause of deviations from isometry in the talus. The finding of variation between species for a metric of the talus and all the other skeletal metrics used as predictor variables of sex in this study confirms the Parr et al. (2011) finding of scaling variation.

Another study compared the scaling of joint size dimorphism in cattarhine primates (Lague, 2003). It was expected that larger males will experience greater amounts of joint stress than females unless the forces are compensated for by positive allometry of the articular joint surface areas. So larger body size requires changes to joint size to maintain an equal joint stress level between sexes. However, larger animals have also been found to reduce joint stress by varying locomotor style. Differences in locomotor style and associated behaviours between sexes have been reported in gorillas, chimpanzees and orangutans (Remis, 1995; Doran, 1993; Cant, 1987).

Cercopithecoids were found to show positive allometry in joint size dimorphism but non-human hominoids have joint size dimorphism closer to isometry. Lague (2003) suggest adjustments to body size dimorphism can be accounted for when female body size during pregnancy is taken into account. Modern humans were found to exhibit high joint size dimorphism in both the knee and elbow joint, although the elbow joint is not associated with weight support in humans. This may be caused by activity related differences between the sexes as bone remodelling is associated with increased activity levels (Maïmoun and Sultan, 2011; Niinimäki et al. 2009; Weiss, 2009). Paine and Godfrey (1997) found that

microstructural long bone scaling amongst the primate order is related to differences in mechanical loading. Both African apes and cercopithecoids are subject to compressive loads of the limb joints due to quadrupedalism. Lague (2003) believes that the large mobile joints in hominoids may reduce joint stress enough that positive allometry of joint size is not needed. So as body size increases an allometric increase in joint size is unnecessary because the joint stresses will be lower than cercopithecoids of equal size. The differences in joint size dimorphism are reflected in the discriminant function structure matrix rankings although for the modern human sample in this study, whilst the elbow joint was one of the most dimorphic skeletal elements, the knee joint was found to be less dimorphic than the hip joint and did not differ dramatically when compared to rankings of other primate species.

Gordon et al. (2008) noted the problem of scaling variation in the primate order for hominin sexual dimorphism studies. Whilst articular surfaces and cross-sectional properties of long bone shafts have been previously shown to scale isometrically with body mass in primates but not in humans, Gordon (2004) found that the geometric mean (GM) of these variables was also scaled isometrically with body mass in primates but not in humans. When studies of hominin sexual dimorphism include a variety of comparative taxa the different scaling relationships will affect the reliability of body mass dimorphism estimates. When the scaling relationship deviates from isometry the level of sexual dimorphism will differ between variables of the same specimen. It is unknown whether the scaling relationship of hominin species reflects the human pattern, the ape pattern or is intermediate between the two and so the consequences of choosing an incorrect comparative sample may dramatically reduce the accuracy of estimation. The finding from this chapter that skeletal dimorphism within the primate order is also non-isometric and varies between species means that a further consideration is required when choosing the most appropriate extant species for hominin body mass estimation studies.

4.8: Comparing discriminant function analysis to bionomical logistic regression

4.8.1: Introduction to binomial logistic regression

A similar method of predicting the probability of categorisation like discriminant function analysis is binomial logistic regression. This section will utilise binomial logistic regression as

an independent test of the discriminant function analysis results. Binomial logistic regression estimates the probability of a variable being categorised as one of two groups. If the probability is greater than or equal to chance, the variable is classified as being from the first group and if the probability is lower than or equal to chance, the variable is classified as being from the second group. Binomial logistic regression has been applied to similar archaeological studies that have utilised discriminant function analysis. Patterns of osteoarthritis have been suggested as indicators of sex differences in lifestyle and activity levels for archaeological populations. Previous studies were hindered by the confounding effects of age on the sample. Baker and Pearson (2006) formed a method of comparing osteoarthritis level between populations with differing age structures through the use of age-adjustment and logistic regression. Sex differences in osteoarthritis at the shoulder and foot from prehistoric populations of the American Great Basin were found.

Porčić (2010) used logistic regression to confirm the relationship between average house floor area pattern and marital residence pattern to test previous ethnographic and anthropological observations that suggest matrilocal societies have larger house floor areas than patrilocal societies. The logistic regression of a pooled sample of marital residence patterns found a significant relationship between marital residence patterns and average house floor area. For matrilocal groups the classification percentage was only 50% and for the patrolocal groups the classification percentage was much higher at 96.3%. This is because the lowest house floor areas were almost always for patrolocal groups whilst there was more variability in house floor area for matrilocal groups.

Logistic regression was also used to assess scalar stress theory in anthropology, where above a certain group size, communication flow becomes unmanageable. In response to this scalar stress it is thought that fissioning into smaller groups reduces the number of decision-making units and so there should be a statistical relationship between group size and scalar stress. Logistic regression was used to build a model based on the presence of colony fissioning in a historic North American group. The model could correctly classify 98% of cases and provided a threshold of maximum group size that could be assessed in archaeological populations (Alberti, 2014).

A study modelling Neanderthal clothing also utilised logistic regression. Predictions were made for the use of clothing on specific body parts based on clothing data from recent hunter-gatherer groups. The logistic regression correctly classified clothing for the head with a percentage of 95.3%, clothing of the hands with a percentage of 89.6% and clothing

of the feet with a percentage of 89.2%. Modelling this information across Pleistocene environmental conditions suggested that Neanderthals covered 80% of their body during the winter and that some populations covered the hands and feet (Wales, 2012).

The use of second to fourth digit ratios in human hands has been explored as a method of estimating sex from the skeleton. Although sexually dimorphic enough to discriminate sex in living individuals, maximum phalanx length was tested through logistic regression to determine whether it also has the same discriminatory power. Digit ratios only classified 59% of cases correctly. The study indicated that second to fourth digit ratios may be population specific and not suitable as a general method of determining sex from the skeleton (Barrett and Case, 2014).

Logistic regression was also used to attempt to form a new method of estimating body mass from the skeleton for forensic cases. Eighteen muscle attachment sites from the lower limb were scored for stress and robusticity and then used to classify body mass through logistic regression. Thirteen of the muscle attachment sites were shown to be statistically different between weight groups, however the classification percentages ranged from 54%-74% meaning some variables were only slightly greater than chance and not strong enough indicators of weight for forensic purposes (Godde and Taylor, 2013).

Some studies have compared the classification percentages provided from both logistic regression and discriminant function analysis. Singh et al. (2012) applied both logistic regression and discriminant function analysis to a sample of sternal widths to test their ability to discriminate sex in a modern human population from India. The logistic regression was found to assign the correct sex for 86.6% of the sternum sample in comparison to the discriminant function analysis, which assigned the correct sex for 84% of the sample. Another attempt at forming a method of sexing juvenile skeletal remains was created through both logistic regression and discriminant function analysis. Morphometric crown traits of the deciduous dentition were analysed in a sample of European modern human juveniles. Using all the morphometric crown traits in the study, discriminate function analysis was found to discriminate sex with an accuracy of 70.2%, with mandibular teeth increasing the accuracy to 74.8%. Logistic regression was found to be less suitable with lower success rates (Adler and Donlon, 2010). A further study analysed permanent and deciduous teeth from both adults and juveniles respectively in the Granada ostoelogical collection. The logistic regression equations formed found that dimensions of the first and second deciduous molars and permanent canines were the most sexually dimorphic with

classification percentages between 78.1% and 93.1%, depending on the teeth and dimensions used (Viciano et al. 2013).

Whilst both discriminant function analysis and logistic regression are multivariate statistical methods used for the analysis of data into categories, there are differences. In terms of output, logistic regression produces probabilities of group membership whilst discriminant function analysis provides continuous functions that can be used for classification. Equations can also be contructed from logistic regression outputs. Logistic regression does not assume normality of data, although discriminant function analysis was developed for normally distributed variables. Efron (1975) compared the statistical power of logistic regression and discriminant function analysis, finding that logistic regression was one half to two thirds as effective as discriminant function analysis. Press and Wilson (1978) found that for non-normally distributed data, logistic regression outperformed discriminant function analysis, although the two methods are unlikely to provide substantially different results. It has been noted that in practice, studies utilising discriminant function analysis nearly always violate the normality assumption, and so a test was designed to compare the performance of both discriminant function analysis and logistic regression for non-normally distributed data (Pohar et al. 2004). Classification error is an inefficient measure for comparison of the two methods so other indices of predictive power were used. As discriminant function analysis assumes normality, the errors in prediction are due to mean and variance estimation error. Therefore, as sample size increases and the sampling distributions become more stable, the discriminant function analysis coefficient estimations become more accurate. Whilst logistic regression should provide better results when the normality assumption is violated, for large sample sizes the results of the two methods becomes indistinguishable.

4.8.2: Comparing the results from the discriminant function analysis with binomial logistic regression

Because binomial logistic regression requires fewer assumptions than discriminant function analysis, it can be used as a test of the discriminant function analysis results. If the results of the discriminant function analysis and binomial logistic regression are similar, then the sample size is large enough to accept the results of the discriminant function analysis. It should be noted that that even if the results of the two methods are the same, discriminant function analysis is more appropriate for use in investigating how best to predict sex

categorisation, as it is designed for the specific prediction of group membership. In order to compare the discriminant function analysis method with the binomial logistic regression method, both techniques were applied to two example samples- all the skeletal metrics for *Homo sapiens* and *Homo sapiens* FHD. *Homo sapiens* were used in this comparison as they are a moderately dimorphic species and considered an appropriate comparative sample in fossil hominin sexual dimorphism studies. The FHD sample is used to compare whether there is any difference in either method for defining sex from one skeletal metric in comparison to multiple metrics.

This analysis used the following methodology:

1. Discriminant function analysis was separately performed on the full *Homo sapiens* sample and *Homo sapiens* FHD sample.
2. The two discriminant functions produced provide a count and a classification percentage of the number of correctly sexed cases from the sample.
3. A binomial logistic regression was then separately performed on the full *Homo sapiens* sample and *Homo sapiens* FHD sample.
4. The two logistic regressions produced provide a count and a classification percentage of the number of correctly sexed cases from the sample.
5. The count and classification percentages of the two methods were then compared for both the full *Homo sapiens* sample and the *Homo sapiens* FHD sample.

4.8.3: Results of the comparison between discriminant function analysis and binomial logistic regression

For all *Homo sapiens* metrics, binomial logistic regression classified the same percentage of cases as the discriminant function analysis. One male was classified as female in both the binomial logistic regression and the discriminant function analysis providing an overall classification percentage of 98.3% for both methods. For *Homo sapiens* FHD, binomial logistic regression classified the same percentage of cases as the discriminant function analysis. The classification percentage was smaller than the percentage classified from the sample based on all metrics. One male was classified as female and one female was classified as male in both the binomial logistic regression and the discriminant function analysis, providing an overall classification percentage of 96.7% for both methods. The

same male and female specimens were misclassified by the binomial logistic regression and the discriminant function analysis.

Table 4.19: Comparison of discriminant function analysis and binomial logistic regression classification results.

		Discriminant function analysis classification results from Homo sapiens FHD			Logistic regression classification results from *Homo sapiens* FHD			
		Male	Female	Total		Male	Female	Total
Count	Male	29	1	30	Male	29	1	30
	Female	1	29	30	Female	1	29	30
Percentage (%)	Male	96.7	3.3	100	Male	96.7	3.3	100
	Female	3.3	96.7	100	Female	3.3	96.7	100
		Percentage of original grouped cases classified (%): 96.7			Percentage of original grouped cases classified (%): 96.7			

		Discriminant function analysis classification results from all *Homo sapiens* skeletal metrics			Logistic regression classification results from all *Homo sapiens* skeletal metrics			
		Male	Female	Total		Male	Female	Total
Count	Male	29	1	30	Male	29	1	30
	Female	0	30	30	Female	0	30	30
Percentage (%)	Male	96.7	3.3	100	Male	96.7	3.3	100
	Female	0	100	100	Female	0	100	100
		Percentage of original grouped cases classified (%): 98.3			Percentage of original grouped cases classified (%): 98.3			

The results show, as expected, that whether using discriminant function analysis or binomial logistic regression, the use of multiple skeletal metrics were found to provide a more accurate method of discriminating sex than discriminating from one skeletal metric or body mass estimation. As binomial logistic regression requires fewer assumptions and is less powerful than discriminant function analysis, the identical classification percentages produced by both methods increases confidence in the discriminant function analysis rankings for the other species, as presented earlier in the chapter.

4.9: Chapter summary

Discriminant function analysis has been successfully applied for classification analyses in the field of archaeology, particularly in studies of ecomorphology, osteoarcheology and geometric morphometrics. Studies evaluating the appropriateness of discriminant function analysis for archaeological research note the importance of sample size. Samples must fit the required number of predictors and be large enough to prevent error introduced by lack of normality or divergence from homoscedasticity. Discriminant function analysis is appropriate for the determination of which skeletal metrics are the best classifiers of sex within the primate order. This because the structure of the data collected is particularly suited to discriminant function analysis, with the skeletal metrics acting as multiple predictor variables for the grouping variable of sex.

The results from the discriminant function analysis found that there are differences in the level of sexual dimorphism between skeletal metrics of a species. The structure of sexual dimorphism within the primate order was therefore determined to be non-isometric. The best and worst discriminators overall were determined, with upper limb metrics HHD and OLCB found to be the best classifiers of sex overall for the dimorphic species within the sample. The worst discriminator varied between species, with low rankings of skeletal metrics from both the upper and lower limb. The structure of sexual dimorphism within humans was found to differ from other primates through the higher ranking of FHD, although an upper limb metric, ULB, was the best discriminator for *Homo sapiens* overall.

The results of this chapter have implications for hominin body mass dimorphism estimation procedures. Current methods of body mass dimorphism estimation rely on body mass prediction from FHD before the determination of sex, and subsequently the level of sexual dimorphism. With upper limb metrics being more dimorphic than lower limb metrics for primates, determining the level of sexual dimorphism through the most dimorphic skeletal elements may be more appropriate than the current methodology. The finding that skeletal dimorphism within the primate skeleton is non-isometric also has implications for body mass dimorphism estimation. When the scaling relationships between skeletal metrics deviate from isometry the levels of sexual dimorphism will differ between skeletal variables within the same species. This affects the choice of comparative sample chosen for studies analysing hominin body mass dimorphism. The non-isometric nature of sexual dimorphism

within the primate order exacerbates this problem, with the variation in skeletal dimorphism between primate species also requiring attention when choosing the best comparative species.

Binomial logistic regression is a classification method that requires fewer assumptions than discriminant function analysis and can therefore be used as an independent test of the discriminant function analysis results. A test of the discriminant function and binomial logistic regression results produced for all metrics from the *Homo sapiens* sample and from a single metric found that the classification percentages were the same for both methods. This provides confidence in the discriminant function analysis rankings supplied for other species within this chapter. Moreover, the comparative test displayed the increased accuracy provided from multiple measurements in both the discriminant function analysis and binomial logistic regression. This highlights the advantage obtained by the utilisation of multiple skeletal metrics, and suggests that a similar approach could be profitably applied to studies of hominin dimorphism.

Chapter 5:

Evaluation of sexual dimorphism estimation methods

The ability to accurately estimate the level of sexual dimorphism within hominin species will allow for the evaluation of multiple aspects of hominin palaeoecology. This is because body mass differences within species act as potential indicators of breeding systems, social dynamics and energetic requirements. Existing methods of estimating sexual dimorphism are insufficient because they are based on a two-step procedure, where body mass is estimated from a skeletal measurement (e.g. FHD) and the level of dimorphism for the whole species sample is then predicted from the body masses of a series of individuals. There is also an uncertainty introduced via the regression equation relating the skeletal measurement to body mass, which is only rarely accounted for in published studies. Therefore, confidence in the inferences produced from the predicted level of dimorphism is reduced. Many of the existing methods for estimating sexual dimorphism based on body masses have been found to greatly overestimate dimorphism for samples with moderate differences between males and females (Godfrey et al. 1993; Plavcan, 1994). If accuracy can be increased for sexual dimorphism estimation procedures, then their application to fossil hominin species and the inferences produced from them will be more secure.

The previous chapter found that discriminant function analysis can be utilised as a method for defining the most dimorphic traits across species in the primate order. The discriminant function equations produced from each sample can also be used as a method for classifying sex from incomplete assemblages. This chapter aims to explore the best way of estimating the level of sexual dimorphism for fossil hominin species by:

1. Evaluating which of the most commonly employed methods of estimating sexual dimorphism has the most accuracy;
2. Comparing the best existing methods of estimating sexual dimorphism with the discriminant function produced in the previous chapter;
3. Testing whether accuracy can be increased by predicting sex and body mass independently before proceeding to analysis of sexual dimorphism;
4. Comparing the discrimination power of femoral head diameter (FHD) with other skeletal metrics;

5. Evaluating how alternative skeletal metric discriminators of sex can be used for dimorphism estimation and whether this is a practicable solution for fossil hominin dimorphism estimation.

The chapter will begin with a brief discussion of how sexual dimorphism is measured for extant species followed by the difficulties of measuring dimorphism in fossil hominin species. Descriptions of existing techniques for estimating sexual dimorphism for fossil hominin species will be given. The results of previous tests of their estimating power will be provided along with a discussion of body mass estimation equations and the procedure for estimating sexual dimorphism from predicted body mass. Three analyses will be used to evaluate the best way of estimating the level of sexual dimorphism for fossil hominin species. The first will test existing methods of estimating sexual dimorphism on the *Homo sapiens* data set. The second will compare the best existing methods highlighted by the first analysis in the chapter with sex classification produced from the *Homo sapiens* discriminant function analysis. The final analysis of the chapter will be a test of individual skeletal metric discriminant functions, particularly evaluating the utilisation of FHD for discriminating sex in relation to alternative skeletal metrics. The results will be used to determine if there is merit to a different procedure for fossil hominin sexual dimorphism estimation, as outlined in the previous chapter.

5.1: Introduction to sexual dimorphism estimation procedures

5.1.1: Measures of sexual dimorphism

Sexual dimorphism is the absolute difference in size and shape between males and females of a species. Body mass dimorphism is therefore the absolute difference in body mass between males and females of a species. There are several methods of determining the level of sexual dimorphism. One method is through the use of a size dimorphism index that can quantify the amount of sexual dimorphism a species displays. The simplest and most widely used is the mean value of one sex divided by the mean value of the opposite sex (Smith, 1999). The simple ratio index scales correctly when the numerator displays the larger sex. When the smaller sex is the numerator, the sexual dimorphism index is less than one, reflecting the inverse of the size superiority of the larger sex. To make comparisons between species where the sexual dimorphism directionality is not the same (particularly when a set of sexual dimorphism indices are used in a regression or correlation analysis) a

'compressed' sexual dimorphism index can be applied. This simply takes the original larger size mean divided by the smaller size mean and adding one if males are larger or subtracting one if females are larger. The resulting index is arbitrarily positive when females are larger and negative when smaller, making easier comparisons between indices, especially when one larger sex does not dominate the data (Lovich and Gibbons, 1992). This method is most appropriate when applying bidirectional sexual dimorphism indices to a regression or correlation analysis as the SDI values become symmetric around zero. It should be noted however, that the value of one has to be added or subtracted to reclaim the correct proportion of sexual dimorphism for analysis. For most studies of sexual dimorphism, where males are larger than females, the sexual dimorphism index is calculated as male/female. Smith (1999) notes that, although studies may use other methods of quantifying sexual dimorphism, they revert back to this ratio when describing the result (e.g. stating that 'males are twice the size of females'). The logarithm of the male/female ratio can be used to transform the ratio into a linear function of the numerator and denominator; regardless of the level of dimorphism, log(male/female)= -log(female/male).

Regression of male against female values and the residuals produced have also been used to quantify sexual dimorphism. Whilst residuals are most often used for regression diagnostics, they can also be applied as data and it is this application that makes them suitable as a measure of sexual dimorphism. Some studies have suggested that the use of residuals is preferable to the use of ratios because ratios are not normally distributed, can result in spurious correlations and do not remove the effects of size (Gingerich, 1995; Abouheif and Fairbairn, 1997; Ranta et al. 1994). Smith (1999) countered these arguments by stating that non-normality is not limited to ratios and the data analysis in his study found no effects of spurious correlation for any of the regressions and ratios tested. Moreover, the ratios reflect an established biological construct rather than just a mathematical construct, so correlations from either ratios or residuals can be classed as 'real'. It is also noted that studies of sexual dimorphism rarely intend to control for size, so the fact that ratios do not scale for size is rarely an issue. There are also limitations to the use of residuals for quantifying sexual dimorphism. Least squares regression assumes there is no error in the x-axis trait and therefore error is introduced to residuals when x is measured with error. This means that residuals require the additional expression of standard errors and confidence intervals (Smith, 1999).

Other regression models were evaluated in Aiello (1992) with reduced major axis found to be the preferred technique for prediction and comparison. The reduced major axis slope is independent of the correlation coefficient whilst least squares regression and major axis are dependent on both the variance ratio and correlation coefficient. Reduced major axis also assumes that there is error in both the x and y variables, in comparison to least squares regression which only assumes there is error in the x variable. For applications where the condition of an unknown specimen is being approximated to the central tendency of a reference sample, the use of reduced major axis regression is preferable because it is unaffected by the correlation coefficient and supplies the best estimate when error variance is unknown.

For comparing the level of sexual dimorphism between populations, the standard t-test can be applied. Bennet (1981) developed a technique by deleting the area of overlap between male and female distributions and then using the percentage of remaining areas to determine the level of difference between males and females. A comparison of sexual dimorphism between populations would then be achieved through a t-test. Chakraborty and Majumder (1982) criticised the method because it assumes that there will not be a large overlap between sexes. Furthermore, there are also problems with obtaining a threshold value where the two distributions intersect by averaging the means of two sex groups when the variances of the sexes differ. Instead, the total area (i.e. the integral) of overlap between males and females was determined to be a better measure of sexual dimorphism. To avoid the need for raw data required to generate the distributions used in the above methods, Relethford and Hodges (1985) developed a t-test for analysing the significance of differences in sexual dimorphism between populations based on the linear regression with sex (as a dummy variable). Greene (1989) derived a more general t-test from this method that was easier to utilise. Rather than producing a t-test from a linear regression of a dummy variable (Relethford and Hodges, 1985), the new method formed a t-test directly from the mathematical considerations of the differences between distributions whilst requiring few additional steps as it is homologous in form to the standard t-test. Empirical testing found the results of both Relethford and Hodges (1985) and Greene (1989) to be the same.

5.1.2: Estimating sexual dimorphism for fossil hominin species

Estimating the level of sexual dimorphism for a species is usually a trivial task when there are enough sexually diagnostic characteristics to sex individuals within the sample. For fossil hominin samples, it is much more difficult to estimate the level of sexual dimorphism within a species because fossil assemblages are often incomplete and lacking the required sexually diagnostic characteristics. For most samples, the body mass of males and females overlap within the sample. This means that methods requiring sex to be determined from the extremes of the sample (with the largest individuals classed as male and the smallest individuals classed as female) tend to overestimate the level of sexual dimorphism within the species (Leutenegger and Kelly, 1977). As fossil hominin species have low sample sizes this exacerbates the problem of distribution overlap (Plavcan, 1994).

Before an estimation of sexual dimorphism is performed on a fossil hominin sample there first needs to be confidence that any dimorphism observed is as a result of the sample consisting of both males and females and that it does not reflect two morphologically similar species or two geographically divided groups of the same species. A simple graphic analysis method has been applied where continuity in a bivariate plot of all specimens is used as an indicator for a single species within the sample, whereas a break in the plot indicates two separate species (Fernandez and Monchot, 2007). A problem with this method, however, is that these patterns may just be the result of sampling error and increased sample variation is not always found within samples of closely related species. High levels of variation may be an indication of two separate species but it can also reflect a single species that is highly dimorphic; low levels of variation cannot confidently indicate that only one species is contained within the sample (Plavcan and Cope, 2001; Cope and Lacy, 1992; 1995). Furthermore, because the likelihood of the sample containing equal numbers of sexes or species is low, non-sexually dimorphic traits are often used to define whether a sample contains taxonomically different specimens.

5.1.3: The mean/median methods of estimating sexual dimorphism for fossil hominin species

The simplest technique for estimating fossil hominin sexual dimorphism is the mean method. Godfrey et al. (1993) noted that because highly dimorphic male and female distributions should not intersect, the combined sample with unknown sex can be divided

at the mean. The subsample made up of larger specimens is considered male and the subsample made up of smaller specimens is considered female. The level of sexual dimorphism is calculated by dividing the larger sample by the smaller sample and the ratio formed represents the level of sexual dimorphism within the sample. The median method is a similar technique, which uses the median to divide the combined sex sample of estimated body masses.

The median method has been found to be less reliable than the mean method. A large problem with both methods is that they assume that the sample will be clearly bimodal in distribution. When the actual dimorphism level is minimal, the overlap in size between the sexes will be ignored and so the mean and median methods tend to overestimate the level of sexual dimorphism (Plavcan, 1994; Josephson et al. 1996). It is also noted that the mean method arbitrarily creates male and female means, even when no sexual dimorphism is present. The advantage of the methods is that they do not assume normality of subsample distributions and can provide the outer limits of dimorphism for fossil species if there is overlap between male and female individuals (Godfrey et al. 1993).

5.1.4: Finite mixture analysis as a method for estimating sexual dimorphism for fossil hominin specimens

Godfrey et al. (1993) developed the method of finite mixture analysis to determine the amount of skull length dimorphism within a unimodal sample of giant extinct lemurs. The amount of sexual dimorphism hidden within a single univariate distribution can be easily calculated when actual standard deviations of male and female distributions are known, along with the percentage of males and females within the sample. To estimate the maximum level of sexual dimorphism when these criteria are not met, the assumption that the sample contains equal numbers of males and females as well as equal variance within both subsamples must be made. Finite mixture analysis relates to the theory that the means of two equally proportioned and dispersed subsamples can be split by about two subsample standard deviations before the sample begins to show bimodality (Titterington et al. 1985). This means that the sum of two normal distributions becomes bimodal in a progression as the separation in subsample means increases. When the subsample means are separated by one unit of subsample standard deviation the sum of two normal distributions will still appear unimodal. However, when the subsample means are

separated by just over two units of subsample standard deviation, then the sample begins to show bimodality (see Figure 5.1). The finite mixture analysis method utilises this finding by treating a unimodal sample as two overlapping subsamples and finds the maximum separation of the subsample means that can occur within the whole sample.

Although the separation between subsample means can be calculated in subsample standard deviation units, for answering whether sexual dimorphism is hidden within a univariate distribution, the maximum amount of separation between subsample means must be calculated from the whole sample. Finite mixture analysis enables this by expressing the theoretical maximum separation of the subsample means as a function of the whole sample range. Therefore, sample size and whole sample range are required to calculate the difference between the theoretical maximally separated subsample means.

Empirical estimates of the number of standard deviations that occur on average within an observed whole population range have been calculated, with Pearson (1932) providing a table of the theoretical number of standard deviations in the observed ranges for samples sizes from 2 to 100 individuals. Godfrey et al. (1993) empirically tested these theoretical expectations for various sample sizes and reproduced the table. From this the maximum number of subsample standard deviations contained within the observed range of the whole sample, although still unimodal, can be calculated. This can then be multiplied with the observed sample range to find the distance of the whole sample mean from the mean of either subsample. The resulting value is added and subtracted from the whole sample mean to calculate the means of the two subsamples. The maximum dimorphism contained within the unimodal sample is determined by the measure of the larger subsample mean divided by the smaller subsample mean.

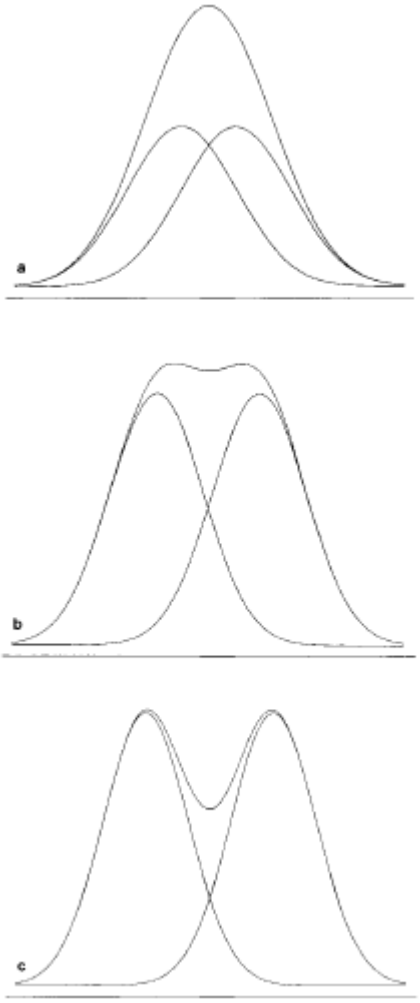

Figure 5.1: from Godfrey et al. (1993) demonstrating how the sum of two normal distributions become more bimodal with the increased separation of their means with (a) showing separation of the means by 1.0 subsample standard deviation units, (b) showing separation of the means by 2.2 subsample standard deviation units and (c) showing separation of the means by 3.0 subsample standard deviation units.

5.1.5: The CV method of estimating sexual dimorphism from fossil hominin specimens

The coefficient of variation (CV) method is also used to estimate the level of dimorphism in a combined sex sample. As the standard deviation increases with the increased distance between the means of the male and female distributions, this can be quantified as the standard deviation divided by the mean, or the coefficient of variation. This was observed in the correlation between mean male and female canine dimension ratios and the

coefficient of variation for Ogliocene anthropoids and Miocene hominoids (Fleagle et al. 1980; Kay, 1982). For CV to be used as a sexual dimorphism estimation method, comparison to the coefficients of variation for extant species and the formation of regression equations must be developed to estimate fossil hominin coefficients of variation. The original method of estimating sexual dimorphism for fossil species was via extrapolation from a linear regression between dimorphism and CVs from a limited number of extant species (Kay, 1982; Leutenegger and Shell, 1987). These results found that natural log transformations of the estimates were required to produce a linear relationship with high correlation between dimorphism and the CV. However, intrasexual variability and unbalanced sex ratios have been found to affect the relationship between dimorphism and the CV and unbalanced sex ratios yield different slopes between the CV and natural log-transformed dimorphism (Plavcan, 1994).

Producing an accurate estimation equation from the extrapolation between dimorphism and the CV requires knowledge of the amount of intrasexual variability and the exact sex ratio within the sample. For fossil hominin samples the amount of intrasexual variability and the exact ratio are unknown. Plavcan (1994) developed an equation that assumes low levels of intrasexual variability and an unbiased sex ratio. The coefficient of variation equation used a sample of extant primates to determine the average amount of variability from postcanine primate teeth to be 5.5%. From these assumptions the regression between CV and natural log –transformed dimorphism produced the following formula to predict the sexual dimorphism level for a combined sex coefficient of variation sample:

$$Sexual\ dimorphism = \mathrm{Exp}(0.0214 \times CV - 0.047)$$

The method is contingent upon forming an equation that best accounts for unbalanced sex ratios and intrasexual variability. Finding a limit to intrasexual variability in extant primates could provide confidence intervals, but as the correlation between the CV and dimorphism is reduced when intrasexual variability increases, this procedure would have limited use. This is because the total sample variation from the separation of males and female means is overwhelmed by the intrasexual variability and so any method utilising sample variation (including the CV method) will be unable to accurately estimate low to moderate levels of dimorphism. Furthermore, there is still the overall problem of choosing the best comparative species to reflect fossil hominin intrasexual variability within the estimation equation formulated, as there are differences in the coefficient of variation between species.

5.1.6: Comparisons of sexual dimorphism estimation methods

Godfrey et al. (1993) measured the skull lengths of adult males and females from monomorphic species (e.g. gibbons and bushbabies), moderately dimorphic species (e.g. langurs and colobus monkeys) and strongly dimorphic species (e.g. macaques and orangutans) from single geographic regions. This extant sample was used to test the finite mixture analysis method, along with the mean and median methods, before being applied to a fossil lemur sample. No single estimation method was found to perform best for all species. There was no statistically significant difference between finite mixture analysis, the mean method and the median method and they were all found to overestimate true dimorphism for extant species placed in the lowest dimorphism category (less than 3.5% difference between males and females). Finite mixture analysis was found to be less reliable for species in the moderate dimorphism category (3.5-10.5% difference between males and females), underestimating true dimorphism. The mean method was the best at estimating dimorphism for species within the strong dimorphism category (greater than 10.5% difference between males and females), with finite mixture analysis underestimating subpopulation mean separation for all species within this category.

Godfrey et al. (1993) suggests applying all three methods to fossil species cases and comparing the estimates produced. When the estimates indicate low amounts of dimorphism, the true sample dimorphism will also be low. Finite mixture analysis is shown to be the most mathematically justifiable estimate when true dimorphism is low. For cases when the true sample dimorphism is high, consistency between the three method estimates is unlikely and the assumptions underpinning the finite mixture analysis are probably violated. This is because high sample dimorphism is underestimated by the two standard deviation unit rule, which is a foundation of finite mixture analysis. Greater levels of dimorphism are more likely to reflect subsamples that are not equally proportioned and dispersed. This is a requirement of the rule stating that subsamples can be split by two subsample standard deviations before showing bimodality. As the assumptions are violated, finite mixture analysis underestimates the level of dimorphism within the whole sample. The mean and median methods are therefore more appropriate for highly dimorphic samples. For three of the 21 extant test species, the observed sample dimorphism exceeded the estimations of all three methods. This means that simply

choosing the method with the highest dimorphism estimation does not guarantee an accurate reflection of the true sample dimorphism level.

Plavcan (1994) tested the mean and median methods, finite mixture analysis and the CV method on simulated data. The comparison attempted to determine the best method of estimating sexual dimorphism on data that reflects the type expected from the fossil record. For each experiment, 100 samples were generated by computer modelling from 10 levels of dimorphism with a range between 1.0-1.9, representing the ratio of males to females. Although the higher end of the dimorphism range, closer to 1.9, will usually reflect bimodal distributions, it was felt necessary to have such a large range of dimorphism ratios to characterise all four methods accurately. The actual sexual dimorphism was calculated from the simulated data before the sexual dimorphism level was estimated by the four methods. Experiments analysed the effects of different sample sizes, sex ratios and intrasexual variation.

Basic comparisons of the four methods, where sex ratios were balanced and there was low intrasexual variability, found the mean and median methods to be most accurate. When intrasexual variability is low (less than 1.2) all four methods overestimate the level of sexual dimorphism. The CV method was found to overestimate sexual dimorphism when true dimorphism was greater than 1.2, whilst finite mixture analysis substantially underestimated sexual dimorphism when the dimorphism level was greater than 1.1. When true sexual dimorphism is low, the standard deviations from mean, median and finite mixture analysis methods are lower than the standard deviation found in the true level of dimorphism. The CV method estimates the standard deviation as slightly higher than the true level of dimorphism unless true dimorphism is lower than 1.1.

Increased sample size was found to have no obvious effect on the accuracy of any of the methods. The standard deviation for all method estimates was found to decrease with increased sample size, meaning that precision improves with greater sample size, even if there is no increase in accuracy. Intrasexual variability was found to be a critical factor in terms of accuracy for all methods tested. Mean and median methods are least affected by high intrasexual variability, but all methods overestimate the level of dimorphism when true dimorphism is low. The CV method consistently overestimated the level of dimorphism for all levels of true dimorphism when there was increased intrasexual variability. Finite mixture analysis was found to overestimate dimorphism the least when intrasexual variability was high. However, finite mixture analysis underestimates the level of

dimorphism when true dimorphism exceeds the level of 1.3. In comparison to the test with low intrasexual variability, this suggests that as the amount of intrasexual variability lowers, finite mixture analysis underestimates the level of sexual dimorphism for progressively decreasing true sexual dimorphism.

A non-balanced sex ratio also affects the accuracy of estimation methods. The mean method was the least affected but the median method, CV method and finite mixture analysis overestimated the level of dimorphism when true dimorphism is low. The level of dimorphism was underestimated as the true level of dimorphism increased. The CV method was found to be more accurate when the sex ratio was skewed towards females. This is because the CV method overestimates dimorphism at all levels of true dimorphism, but estimations for samples with more females display deviations from true dimorphism that are smaller than samples with more males. A further experiment with random fluctuation in sex ratio again demonstrated that the mean method provided the best estimates of sexual dimorphism. Therefore, Plavcan (1994) concluded that for fossil samples where sex of the individuals was unknown, the mean method was both the simplest to apply and provides the most consistent results when intrasexual variability is high and there are non-balanced sex ratios.

Gordon et al. (2008) compared methods of estimating sexual dimorphism on a comparative, extant, all-hominoid sample. The mean method was able to accurately estimate the sexual dimorphism level for the highly dimorphic species *Gorilla gorilla* and *Pongo pygmaeus*, but overestimated dimorphism level for *Homo sapiens*. The coefficient of variation shared the estimation accuracy pattern of the mean method. The results of this study confirmed that methods where a combined sex sample is split by the largest value divided by the smallest value have a tendency to overestimate the sexual dimorphism level when male and female values overlap in terms of distribution. This has important implications for estimating the sexual dimorphism level of hominin fossil species as the restricted accuracy of these methods on moderately dimorphic species will be exacerbated by the small sample sizes that limit fossil hominin studies.

5.1.7: Body mass and sexual dimorphism

Current procedures for estimating body mass dimorphism first involve the prediction of body mass for a specimen and then the estimation of the sexual dimorphism level for the

whole sample. For skeletal specimens, body mass has to be estimated from the assemblage. When a skeletal assemblage is incomplete, body mass has to be estimated from metrics of the skeleton rather than a simple calculation of length plus breadth that can be used with a complete skeleton. Current procedures for estimating body mass in such scenarios involve utilising the mechanical relationship between a load-bearing skeletal element and body size. An estimation equation is formed by the regression of body mass on a skeletal metric and this is then used to predict body mass for other specimens. Trinkaus et al. (1994) and Lieberman et al. (2001) found that articular skeletal metrics had a stronger relationship with body mass than cross sectional dimensions and diaphyseal breadths. The skeletal metric, femoral head diameter (FHD), is often chosen as it is a large articulation that is found frequently in assemblages and because it is easily measured. Cranial variables have also been employed for estimating body mass, particularly orbital breadths, avoiding the problematic influence of loading that occurs with postcranial variables (Aiello and Wood, 1994; Spoctor and Manger, 2007). However, a comparative test of cranial variables for estimating body mass found the equations performed poorly on computed tomography scans from a large sample of modern humans with known body mass (Elliot et al. 2014).

In previous work, three sets of estimation equations that required a human comparative sample for their formation were created and applied to fossil hominin samples. Ruff et al. (1991) used a modern human sample with an average body mass of 77kg, higher than in preindustrial Holocene samples, although the range of the sample corresponded to all modern human body masses except the smallest populations of Pygmy and Andaman females. The McHenry (1992) formula was formed from four sample means for modern humans and included African Pygmies and the small bodied Khoisan populations; the modern human sample had a range between 30.4kg and 64.9kg. As the formula was created with the intention of estimating fossil hominin body mass it was compared to an equivalent estimation equation formed from an all-hominoid sample. The formula from the human comparative sample was expected to provide more accurate estimations for fossil hominin samples. Grine et al. (1995) created an estimation equation from ten sex-specific sample means from modern human populations that included larger bodied humans. The prediction formula was developed to estimate body mass from the large Berg Aukas proximal femora. Tests comparing the prediction power of all three estimation equations found that at the smallest and lowest extremes of the range, the Ruff et al. (1991) formula performed less well, the McHenry (1992) equation was more suitable for estimating the

body mass of smaller bodied samples and the Grine et al. (1995) equation was more suitable for estimating the body mass of larger bodied samples (Auerbach and Ruff, 2004; Pomeroy and Stock, 2012). A further study explored the accuracy of these estimation equations when tested on a southern African Holocene population, noted to have smaller than average statures and pelves. The McHenry (1992) formula had the greatest accuracy in estimating the smaller females in the population and the Ruff et al. (1991) formula was found to overestimate body mass for this population (Kurki et al. 2010).

Table 5.1: Equations utilised for hominin body mass estimation.

Body mass estimation equations	
Ruff et al. (1991)	BM= (2.160 x FHD - 24.8) x 0.90
McHenry (1992)	BM= 2.239 x FHD - 39.9
Grine et al. (1995)	BM= 2.268 x FHD - 36.5

These methods of estimating body mass and the corresponding level of body mass dimorphism have been applied to studies of fossil hominin species. The McHenry (1992) equation was used to provide an estimation of average female *Australopithecus afarensis* having a body mass of 29kg and an average male body mass of 45kg. The *Australopithecus afarensis* specimen, A.L. 288-1 or 'Lucy' was estimated to have a body mass of 27.9kg. The far larger specimen- A.L. 333 was estimated to have a body mass of 50kg. However, it has been noted that the smaller femoral head diameters of *Australopithecus afarensis*, in comparison to modern humans, may mean a non-human hominoid reference sample or an all hominoid reference sample would be more appropriate to form estimation equations for australopithecines (Holliday, 2012). This is especially problematic for larger specimens as the estimation of A.L. 333 was far larger having been developed from hominoid reference samples, with McHenry (1992) providing another estimation of 68.6kg and Jungers (1990b) providing an estimation of 81.9kg. Reno et al. (2003) used a novel approach to estimating the level of sexual dimorphism for *Australopithecus afarensis*, by using A.L. 288-1 as a template specimen from which to estimate FHD for other specimens.

The results found the level of sexual dimorphism for *Australopithecus afarensis* to be closer to modern humans rather than the high dimorphism level closer to *Gorilla gorilla* or *Pongo pygmaeus* that had previously been suggested.

Further studies using the discussed estimation procedures have been applied to specimens from the genus *Homo*. Pontzer (2012) attempted to analyse ecological correlates of *Homo* body size using body mass estimation data from McHenry (1992) for Plio-Pleistocene fossil hominin specimens. The study found an increase in body mass from australopithecines averaging at 36.8kg to *Homo* averaging at 48.8kg, which fit with many predicted models of ecological change. The McHenry (1992) equation was also used by Holliday (2012) to predict the body mass of a wide range of fossil hominin species including *Australopithecus afarensis, Australopithecus africanus, Paranthropus robustus* and *Paranthropus boisei*. Early *Homo* specimens were found to have an estimated mean body mass that was less heavy than Neanderthals, late Pleistocene humans and modern humans from high latitudes, although with a greater average body mass than australopithecines.

These few examples show that these estimation procedures are producing results that are being used to make a range of palaeoecological inferences. A problem occurs if these estimation procedures are not accurate. Smith (1996) highlighted how the analysis of ecological inferences is restricted by the uncertainty caused by multiplication of regressions when applying these estimation procedures. This, alongside the difficult choice of the best comparative sample for certain fossil hominin species, means that predictions often have only moderate value. Elliot et al. (2016a) noted that the accuracy of body mass estimation equations is uncertain as the tests of accuracy discussed earlier in this chapter are based on the comparison of the equations to each other. While this is the case, the BIB-stature method is also used as a gold standard (Pomeroy and Stock, 2012). The Elliot et al. (2016) study tested the accuracy of the equations on a modern human sample with known body mass. The results found that whilst the equations reliably estimated male specimens (50% or more of the specimens fell within 20% of their known mass), the accuracy was reduced for females and the equations did not perform consistently. A further study formed new regression equations from this sample of modern humans with known body mass and found that whilst they were more accurate than the equations provided in the literature, there were only modest improvements and the accuracy rates were still low (Elliot et al. 2016b). For studies of fossil hominin body mass and body mass dimorphism, these results suggest that the accuracy of previous estimations is called into question.

5.2: Test of estimation procedures

From the results of the previous chapter FHD was not found to be the most sexually dimorphic skeletal metric for any of the primate species in the sample. This suggests that as there are more dimorphic skeletal metrics than FHD, accuracy may be improved by estimating sex and body mass independently, rather than calculating sex *from* body mass, as is effectively done in most of the methods detailed above.

Current methods of estimation work via a two-step process where body mass is first predicted from FHD and then the sexual dimorphism level for the whole species is estimated. Other possible methods of estimation may separate the prediction of body mass and the estimation of sex for each specimen, with the level of dimorphism then given for the whole sample:

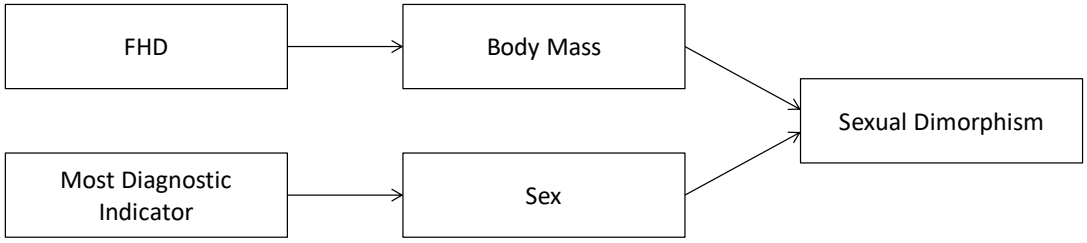

Figure 5.2: The current procedure of FHD used to estimate body mass before sexual dimorphism is predicted from the estimated body mass values and the alternative procedure of using the most diagnostic indicator to predict sex independent of body mass before calculating the level of sexual dimorphism.

To understand the differences between males and females in terms of body mass, and to therefore use this knowledge to infer various palaeoecological implications, body mass has to be predicted and the sex of specimens has to be derived. To predict the level of sexual dimorphism, sex has to be determined either for each individual specimen in the sample or by splitting the whole sample into males and females. Using the most dimorphic traits in the skeleton to determine sex independently of body mass should reduce the multiplication of estimation error. More accurate sex determination plus strong body mass estimation can therefore lead to better predictions of sexual dimorphism in hominin species.

5.2.1: A test to compare sexual dimorphism estimation methods

The introduction of this chapter detailed the most common methods used to estimate the level of dimorphism in fossil hominin specimens, and examined some prior applications of those methods. By applying these methods to the *Homo sapiens* sample in this study with known sex classification, the accuracy of these methods can be tested. To reflect the current methodology for determining sexual dimorphism in fossil hominin species, body mass was estimated from FHD using the McHenry (1992) equation. The estimation equation was produced from a generalized regression based on a human reference sample (US European, US African, African Pygmy and Khoisan populations), making it the most accurate for smaller bodied specimens, with predictions that are more comparable to smaller bodied hominins and the smaller bodied extant primates in this study. The actual sexual dimorphism index for the sample was calculated as the average male value divided by the average female value.

The sexual dimorphism index estimated by the mean method was calculated by splitting the whole sample at the mean and dividing the larger subsample average by the smaller subsample average. The sexual dimorphism index estimated by the median method was calculated by splitting the whole sample by the median point and dividing the larger subsample average by the smaller subsample average.

Steps for applying the mean method to the sample of *Homo sapiens* estimated body mass:

1. Calculate the mean for the whole sample by dividing the sum total by the number of specimens.
2. Divide the sample according to the mean value. Specimens that have an estimated body mass lower than the mean value are classed as ‘female’ and specimens that have an estimated body mass higher than the mean value are classed as ‘male’.
3. The level of sexual dimorphism is calculated by dividing the mean value from the ‘male’ subsample by the mean value from the ‘female’ subsample.

The steps for applying the median method to the sample of *Homo sapiens* are the same but with the median replacing the mean.

Finite mixture analysis provides an index of sexual dimorphism by treating the unimodal *Homo sapiens* estimated body mass sample as two overlapping subsamples and then finding the maximum separation of the subsample means that can occur within the whole

sample. The maximum dimorphism contained within the unimodal sample is determined by the measure of the larger subsample mean divided by the smaller subsample mean.

Steps for applying finite mixture analysis to the sample of *Homo sapiens* estimated body mass (as produced in Godfrey et al. (1993)):

1. For a sample of 60 specimens, the mean number of standard deviations as provided by Godfrey et al. (1993) is 4.64. This is the k value.

$$Observed\ range = k\ \sigma_{tot}$$

2. The expected number of subpopulation standard deviations in the total population's observed range is calculated.

$$Observed\ range = \ k\ \sigma_{tot} = k\sqrt{2}\sigma_{sub}$$

3. The percentage of the observed range containing $2\sigma_{sub}$ is obtained by dividing 2 by $k\sqrt{2}$

$$2\sigma_{sub} \leq 2\left(\frac{observed\ range}{k\sqrt{2}}\right) \leq \left[\frac{2}{k\sqrt{2}}\right] observed\ range$$

4. The percentage of the observed range between the mean of the whole population and either of the subpopulation means is calculated by dividing the result of step 3 by step 2.
5. Obtain the distance from the mean of the whole population to either of the subpopulation means by multiplying the step 4 result by the total observed range.
6. Add and subtract the distance from step 5 to the whole population mean to obtain the values for the two subpopulation means. The distance between these values is the maximum separation of means of two equally variant normal distributions embedded in a single unimodal normal distribution.
7. The means of these subpopulations can then be used to calculate the maximum sexual dimorphism in the sample.

The sexual dimorphism index estimated by the coefficient of variation (CV) method was calculated through the equation provided by Plavcan (1994):

$$Sexual\ dimorphism = \mathrm{Exp}(0.0214 \times CV - 0.047)$$

Whilst other reference samples with difference amounts of intrasexual variability can be used for this method, in studies of fossil hominin sexual dimorphism estimation the best extant comparative sample is unknown and so the primate average amount of intrasexual variability is appropriate for this test.

Steps for applying the CV method to the sample of *Homo sapiens* estimated body mass:

1. Calculate the standard deviation of the whole *Homo sapiens* estimated body mass sample.
2. Divide the standard deviation by the mean of the whole *Homo sapiens* estimated body mass sample and multiply by 100 to calculate the coefficient of variation (CV).
3. Use the formula provided by Plavcan (1994) to estimate sexual dimorphism for the sample.

5.2.2: Results of the test comparing sexual dimorphism estimation methods

The actual sexual dimorphism index (average male/average female) was 1.290, based on the estimated body masses from FHD. The mean and median methods of sexual dimorphism estimation overestimated the level of dimorphism and both provided an index of 1.297. It should be noted that the mean and median methods will always produce the same result if the data are symmetrically distributed. Finite mixture analysis underestimated the level of sexual dimorphism with an index of 1.064. The coefficient of variation method overestimated the level of dimorphism further and provided an index of 1.324.

The results reflect the conclusions of previous literature where the mean, median and coefficient of variation methods were all found to overestimate the level of dimorphism for moderately dimorphic species. Plavcan (1994) indicated that the mean method of estimating sexual dimorphism was the most reliable and the results from the estimated *Homo sapiens* body mass sample provide a dimorphism index that is close to the actual index of sexual dimorphism within the sample. The same study also found the CV method overestimated sexual dimorphism when true dimorphism was greater than 1.2. As the actual index of sexual dimorphism within the estimated *Homo sapiens* body mass sample was over the 1.2 minimum, the overestimation of the CV method was expected. For finite mixture analysis, Godfrey et al. (1993) found that the method was less reliable for species with moderate dimorphism as it underestimated true dimorphism. Plavcan (1994) found finite mixture analysis substantially underestimated sexual dimorphism when the dimorphism level was greater than 1.1. As the actual index of sexual dimorphism within the estimated *Homo sapiens* body mass sample was over 1.1, the underestimation by finite mixture analysis was expected.

Table 5.2: The resulting sexual dimorphism indices estimated from sexual dimorphism estimation methods for *Homo sapiens*.

Comparison of sexual dimorphism indices produced by Mean, Median, Finite Mixture Analysis and CV methods to the actual index of estimated *Homo sapiens* body mass from FHD				
Actual Index	Mean Method	Median Method	Finite Mixture Analysis Method	CV Method
1.290	1.297	1.297	1.064	1.324

5.3: A comparison of mean/median methods of estimating sex to the sex classifications determined by discriminant function analysis

To further explore the accuracy of methods where the largest value is divided by the smallest value and to compare to the discriminant function analysis performed in the previous chapter, *Homo sapiens* FHD and body mass were sex classified by both the mean method, median method and via discriminant function analysis. As the most reliable methods of sexual dimorphism estimation in the previous test were based on splitting the sample by the mean or median, the *Homo sapiens* sample with known males and females can be used to test whether the discriminant function analysis equation was better or worse than methods that split at the mean or median, noting that the use of multiple predictor variables within the discriminant function analysis should provide a better result. The comparison of methods will investigate specific sex classifications for each specimen in the group rather than just providing the level of dimorphism as a whole. The methods are being tested on a moderately dimorphic species meaning that any problems with the methods defining sex for overlapping specimens in the male and female distributions will be highlighted.

FHD was used to directly classify individuals within the sample as either male or female by splitting the sample at the mean and median respectively. The number of correctly classified individuals was produced as a percentage, with individual classifications highlighted in a table. The estimated body mass of the *Homo sapiens* sample via the McHenry (1992) equation was also used to classify individuals within the sample as either male or female through the mean and median methods respectively. The classifications of sex from FHD and body mass estimated from the McHenry (1992) equations will always be the same because the McHenry (1992) equation is a linear transformation of FHD.

Nonetheless, estimating body mass from FHD better reflects the current methodology and other body mass estimation methods may not produce the same linear transformation of FHD. A classification percentage and table of individual classifications were also produced. The discriminant function analysis from the *Homo sapiens* sample produced in the previous chapter provides a percentage classification and the number of correctly classified cases, which are highlighted in comparative tables.

5.3.1: Results from the comparison of mean/median methods of estimating sex to the sex classifications determined by the discriminant function analysis

The results from the comparison of mean/median methods of estimating sex to the sex classifications produced by the discriminant function analysis can be found in Table 5.3. and Table 5.4.

Table 5.3: The results from the mean and median methods for estimating sexual dimorphism from FHD and body mass.

Estimated *Homo sapiens* sex using the mean and median methods of sexual dimorphism determination			
Individuals estimated as female		Individuals estimated as male	
FHD (mm)	Body Mass (Kg)	FHD (mm)	Body Mass (Kg)
36.84	42.58	45.43	61.82
37.39	43.82	45.55	62.09
37.59	44.26	45.79	62.62
38.27	45.79	46.44	64.08
39.50	48.54	46.55	64.33
40.04	49.75	46.79	64.86
40.74	51.32	47.19	65.76
40.86	51.59	47.27	65.94
40.94	51.76	47.29	65.98
41.00	51.90	47.50	66.45
41.08	52.08	47.58	66.63
41.10	52.12	47.73	66.97
41.42	52.84	47.87	67.28
41.53	53.09	47.92	67.39
41.63	53.31	47.92	67.39
42.07	54.29	48.11	67.82
42.28	54.76	48.37	68.40
42.59	55.46	48.57	68.85
42.61	55.50	48.59	68.89
42.61	55.50	48.91	69.61
42.81	55.95	49.43	70.77
42.81	55.95	49.46	70.84
42.87	56.09	49.55	71.04
43.29	57.03	50.33	72.79
43.32	57.09	50.54	73.26
43.73	58.01	50.88	74.02
43.82	58.21	51.75	75.97
43.92	58.44	52.34	77.29
43.94	58.48	53.38	79.62
44.54	59.83	55.09	83.45
Classification percentage (%): 96.7			

Key	
Actual Female	Actual Male

Table 5.4: The results from the discriminant function analysis for estimating sexual dimorphism from FHD and body mass.

Estimated *Homo sapiens* sex using discriminant function analysis			
Individuals estimated as female		Individuals estimated as male	
FHD (mm)	Body Mass (Kg)	FHD (mm)	Body Mass (Kg)
36.84	42.58	45.43	61.82
37.39	43.82	45.79	62.62
37.59	44.26	46.44	64.08
38.27	45.79	46.55	64.33
39.50	48.54	46.79	64.86
40.04	49.75	47.19	65.76
40.74	51.32	47.27	65.94
40.86	51.59	47.29	65.98
40.94	51.76	47.50	66.45
41.00	51.90	47.58	66.63
41.08	52.09	47.73	66.97
41.10	52.12	47.87	67.28
41.42	52.84	47.92	67.39
41.53	53.09	47.92	67.39
41.63	53.31	48.11	67.82
42.07	54.29	48.37	68.40
42.28	54.76	48.57	68.85
42.59	55.46	48.59	68.89
42.61	55.50	48.91	69.61
42.61	55.50	49.43	70.77
42.81	55.95	49.46	70.84
42.81	55.95	49.55	71.04
42.87	56.09	50.33	72.79
43.29	57.03	50.54	73.26
43.32	57.09	50.88	74.02
43.73	58.01	51.75	75.97
43.82	58.21	52.34	77.29
43.92	58.44	53.38	79.62
43.94	58.48	55.09	83.45
44.54	59.83		
45.55	62.09		
Classification percentage (%): 98.3			

Key	
Actual Female	Actual Male

Both the mean and median methods of determining sex have a classification percentage of 96.7% of the *Homo sapiens* sample. One female was incorrectly classified as male and one male was incorrectly classified as female. The table for the sex classifications produced from the mean and median methods of sexual dimorphism determination place the FHD and body mass estimations in order of size. This means that the overlap in male and female distributions through the misclassified male and female specimens can be observed. The male misclassified as female has a body mass estimation that is only 4.81% higher than the average for the female subsample. The female misclassified as a male has a body mass estimation that is only 9.85% lower than the average for the male subsample. In contrast, the discriminant function analysis for *Homo sapiens* was able to correctly classify 98.3% of the sample. The same male that was incorrectly classified as female by the mean and median methods of dimorphism was incorrectly classified by the discriminant function analysis.

For both the mean/median methods and the discriminant function analysis method, the estimated body mass made no difference to the sex classification as both the FHD metric and body mass estimation classified the same. This was expected as FHD and body mass are closely related to each other via the McHenry (1992) equation. For this *Homo sapiens* sample, the mean and median methods were able to classify sex with accuracy, having only two specimens that were incorrectly classified. As humans are known to be moderately dimorphic some overlap between individual male and female body mass is to be expected. It is also known that methods of estimating sexual dimorphism are most accurate at classifying sex for highly dimorphic species. For potential use in estimating hominin sexual dimorphism, this result again highlights the fact that there will be some sex estimation error if the hominin species in question is moderately dimorphic like *Homo sapiens* and *Pan troglodytes*.

The *Homo sapiens* discriminant function analysis equation from all skeletal metrics estimated sex with more accuracy than the mean/median methods, with only one male incorrectly classified as female. Whilst the difference between the sexual dimorphism estimations is only small, the use of a discrimination equation formed from the most dimorphic skeletal metrics did have an increase in accuracy. The discriminant function analysis equation differs from the previous methods of estimating sexual dimorphism as it directly classifies sex for each individual. The mean and median methods work by dividing body mass that has been estimated from a single skeletal metric into two subsamples. The

results of this test confirm those of previous studies that show estimating the level of dimorphism by mean and median methods tend to introduce error especially for moderately dimorphic species. Although the use of multiple predictor variables in the discriminant function analysis was expected to have increased accuracy, and was found to do so, the amount of skeletal variables required is unlikely to be reflected in a fossil hominin assemblage. However, the most dimorphic skeletal elements could potentially be used to classify sex separately from the estimation of body mass. As the most dimorphic elements of hominin skeletons are unknown, the use of a comparative sample will be needed to identify the best skeletal metrics to be utilised in estimation procedures. The level of sexual dimorphism found from FHD in this modern human sample was greater than expected. This indicates that the sample may not be representative of the sexual dimorphism level found in a typical sample or population of modern humans. To thoroughly examine the applicability of these results, a larger study with modern human specimens from a wider range of populations is required.

The mean method has been suggested to provide the most consistent result whilst being the simplest to apply but it still has problems. It assumes that the sample will be clearly bimodal in distribution. When the actual dimorphism level is minimal, the overlap in size between the sexes will be ignored and so the mean and median methods tend to overestimate the level of sexual dimorphism. This is particularly problematic for monomorphic samples as the method arbitrarily creates male and female subsamples even when no dimorphism is present. Whilst the mean method may be suitable for some hominin fossil species, as the level of dimorphism is unknown, the suitability cannot be inferred and the accuracy of the estimation cannot be tested. If fossil hominin species reflect a moderate level of body mass dimorphism like the sample in this test, then there will be overestimation. More accurate sex classification techniques for fossil remains would reduce the need for inaccurate dimorphism estimation methods.

5.4: An evaluation of skeletal metrics as appropriate measures of sexual dimorphism, for potential use in fossil hominin sexual dimorphism estimation

A potentially more accurate dimorphism estimation procedure would be to classify sex directly for a specimen and then calculate the level of dimorphism within the whole sample. The best existing methods of estimating dimorphism work by splitting body mass

estimations into male and female groupings from a calculated cut-off point. Discriminant function analysis, as a method of sex determination, works by directly classifying the sex of a specimen via an equation. This method removes the susceptibility towards inaccuracies when splitting a moderately dimorphic sample, as found in the previous analysis. However, the discriminant function analysis was expected to perform better than existing sexual dimorphism estimation methods because of the number of independent variables (predictors) within the model. It is unlikely that all the elements required would be found in a fossil assemblage. For fossil hominin species the estimation procedure is split into two steps, with the first step requiring the prediction of body mass from FHD and then the second step of pooling the body mass predictions for dimorphism level estimation. As FHD is measured for estimating body mass, the further utilisation as a discriminator of sex would not require any additional measurements. Other skeletal metrics have been found to be better discriminators of sex for the primate order in the previous chapter. It is important to test the power of each skeletal metric as a discriminator of sex, to infer whether a simpler discriminant function equation, with a smaller number of metric inputs, can be utilised for fossil hominin sexual dimorphism estimation. This section will consider the practicalities of discriminant functions as a way of classifying sex, including the best choice of metric for fossil hominins as well as exploring the appropriate choice for a comparative sample.

The following question will be answered:

4. For *Homo sapiens* samples, is there a distinct advantage to selecting skeletal metrics other than FHD as discriminators of sex?
5. Can choosing the most dimorphic skeletal metrics be applicable to fossil hominin cases as a way of estimating sexual dimorphism?

This section will begin with a brief overview of FHD employed in body mass estimation techniques. The results from a comparison of individual skeletal metric discriminating power from the *Homo sapiens* dataset will be evaluated. This will include FHD along with the skeletal metrics highlighted as being the best discriminators of sex through the *Homo sapiens* discriminant function analysis. The results of this test will be used to determine if there is merit in selecting skeletal metrics other than FHD as discriminators of sex and if choosing the most dimorphic skeletal metrics can be applicable to fossil hominin cases.

5.4.1: Femoral head diameter (FHD) and body mass estimation techniques

Femoral head diameter (FHD) is the most commonly chosen skeletal metric for body mass estimation procedures as it is frequently found in skeletal assemblages and can be easily measured. The mechanical relationship between body mass and the proximal femoral articulation was the basis for the body mass estimation equations produced by Ruff et al. (1991) and McHenry (1992). Kurki et al. (2010) tested the limitations of body mass estimation equations via a sample of Later Stone Age humans from South Africa, noted for their small stature and narrow bodies. In comparison to the bi-iliac breath method of estimating body mass and the Ruff et al. (1991) equation, the McHenry (1992) equation produced body mass estimates for Later Stone Age humans that best reflected the sexual dimorphism level within living groups.

The Kurki et al. (2010) study also noted that as there is positive allometry of femoral head diameter relative to body mass within the species, the use of one formula for both sexes tends to overestimate body mass in males as they generally have larger femoral head diameters than females. The greater level of sexual dimorphism predicted by the McHenry (1992) equation, in comparison to the estimates from the Ruff et al. (1991) formulae, may have been caused by the use of one equation for both sexes overestimating male body mass. The application of the Ruff et al. (1991) combined-sex equation confirmed this, presenting a result closer to the level of dimorphism shown from estimates made by the McHenry equation. The Kurki et al. (2010) result has important implications for the estimation of sexual dimorphism. If overestimation of sexual dimorphism is being produced in the estimation of body mass then the accumulated error produced by both body mass and sexual dimorphism estimation procedures reduces confidence in the result. Predicting the level of sexual dimorphism directly from the fossil assemblage will reduce this problem.

Studies have shown that skeletal metrics scale to body mass differently between taxa. Utilising a sample including *Pan troglodytes, Gorilla gorilla, Pongo pygmaeus, Macaca fascicularis* and *Homo sapiens*, Ruff (1988) found a general trend of overall isometry or slightly positive allometry between joint size and body mass, with *Macaca fascicularis* and *Homo sapiens* being outliers. *Macaca fascicularis* display smaller hindlimb articulations in relation to body mass whilst *Homo sapiens* have larger femoral heads relative to body mass. In comparison, femoral head size scales almost isometrically with body mass for *Pongo pygmaeus*. However, the 95% confidence intervals for the slope of regression lines

relating femoral head diameter to body mass had only slight overlap with humans. This means that humans show a different scaling relationship between femoral head diameter and body mass than nonhuman primates, with humans presenting a positively allometric relationship between body mass and FHD.

The femoral head was found to have the strongest relationship to weight in comparison to other articular dimensions. Jungers (1988) also showed that modern humans are positive outliers in terms of the correlation between lower limbs and body mass for primate species, although this is not the case for the upper limb. The study also indicates that the sample used by Ruff (1988) would not be significantly affected in terms of the scaling relationships found for non-human primates if lesser ape species were added to the sample.

Femoral head reflects size reached at adulthood and does not respond to increased body mass and associated mechanical loading, in comparison to femoral diaphyseal dimensions that correspond to current body weight (Ruff et al. 1991). Femoral neck dimensions show an intermediate pattern between the two. There are constraints on articular remodelling that limit the expected response of increasing femoral head size with increasing body mass during a lifetime. Therefore, this limitation obscures the underlying mechanical relationship between femoral head and body mass, particularly in older, larger individuals. This has implications for species that vary in body mass throughout adulthood (Swartz, 1989)

There is a general pattern of increasing joint surface area, which is positively allometric with body size. The reasoning behind this finding was presumed to be because of the necessity to counterbalance the otherwise disproportionate increase in joint stress that occurs with increasing body size. Swartz (1989) used brachiating primate species that display altered forelimb loading to test the assumption that joint size is mainly controlled by the demands of weight support. The results found that there was no significant reduction of joint size, even in brachiating primate species that have reduced compressive loading in the limb joints. Therefore, joint size is a complex result of both the retained past history of a species and biomechanical demands. Whilst a reduction in limb loading seems to have little effect on joint morphology, an increase in limb loading will select for a change in size away from the ancestral morphology. Jungers (1988) suggests that modern human bipedalism is an example of locomotor behaviour altering to the point of greatly increased limb loading. Holliday (2012) highlighted the problem of estimating australopithecine body mass as femoral head diameters are smaller than humans so it is reasonable to ask

whether a non-human hominoid reference or an all hominoid reference sample is more appropriate for developing estimation equations.

5.4.2: A test of femoral head diameter (FHD) for estimating sexual dimorphism in a comparative human sample.

As FHD is the best predictor of body mass, can it also be utilised for defining sex directly from the skeleton? The multiplication of error caused by the process of estimating body mass and then predicting the level of sexual dimorphism means a more direct way of estimating sexual dimorphism from the fossil assemblage will be valuable. However, considering the fact that FHD was not the best discriminator of sex for other dimorphic primate species, is FHD a valid choice for sexing or is there an advantage to choosing another skeletal element that is likely to be found in a fossil assemblage?

In the literature, the estimation procedure in two steps (FHD to predict body mass and then the estimation of sexual dimorphism for the whole species from the predicted body mass), requires *Homo sapiens* as a comparative sample. Evidence for more accurate *Homo sapiens* sexual dimorphism estimation will have implications for its use as a comparative sample and therefore for fossil hominin estimation procedures. Discriminant function analysis provides the ability to classify sex for individuals without the need for common sexually diagnostic characteristics in the skeleton, through the use of skeletal elements that are likely to be found in fossil assemblages and which are already used for body mass estimation. However, the method also requires the use of a valid comparative sample. As most body mass estimation methods utilise *Homo sapiens* as a comparative sample, this species can be used to test the validity of individual skeletal metric discriminant functions and compare them to other potential comparative samples from the primate order. This section attempts to answer the following questions: 1) For *Homo sapiens* samples, is there a distinct advantage to selecting skeletal metrics other than FHD? and 2) can choosing the most dimorphic skeletal metrics be applicable to fossil hominin cases?

As the *Homo sapiens* discriminant function analysis did not find FHD to be the most dimorphic skeletal metric, this indicates that other skeletal metrics may be more appropriate. To explore this further the *Homo sapiens* sample was analysed by comparing the discriminant function analysis equations formed from the best skeletal metric discriminators of sex for the species. The classification percentages and the correct

classification counts show how different the discrimination power is for each equation produced. The skeletal metrics chosen were based on the three best ranked discriminators from the unstandardised discriminant function analysis structure matrix (ULB, HHD, and FHD) and the stepwise discriminant function analysis structure matrix (ULB, OLCB and FHD). The stepwise procedure produced the best model of *Homo sapiens* sex discrimination with ULB, FHD and TAL applied to the model at separate steps. Whilst the individual discriminant function analysis classification results for each of these skeletal metrics were compared, various combinations of these skeletal metrics were also analysed to see if they compare to the best stepwise model.

Discriminant functions were produced from individual skeletal metrics and combined skeletal metric models (see Table 5.5). The counts and percentages of correctly classified cases for each discriminant function analysis were then compared. The *Homo sapiens* sample consists of 30 males and 30 females, each provided with a number from 1 to 60 for simple identification. Any misclassified specimens can therefore be noted from each model of discrimination.

Table 5.5: The discriminant function models compared, split into models from individual skeletal metrics and models from a combination of skeletal metrics.

Models from individual skeletal metrics	Models from combined skeletal metrics
ULB	ULB, FHD & TAL
FHD	ULB & FHD
TAL	ULB & OLCB
OLCB	ULB, OLCB & FHD
HHD	ULB & HHD
	ULB, HHD & FHD

5.4.3: Results of the discriminant function classifications comparison

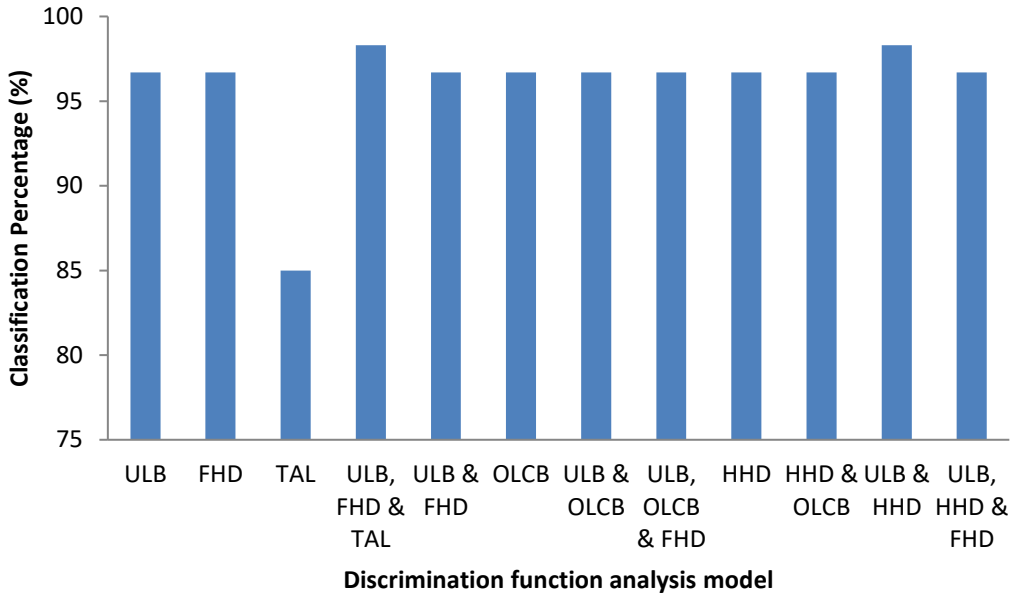

Figure 5.3: The classification percentages of *Homo sapiens* discriminant function analysis models.

5.4.3.1: ULB

ULB was found to be the best discriminator for *Homo sapiens* from the discriminant function analysis. It was the highest ranked skeletal metric for *Homo sapiens* in the structure matrix and was the first step used to discriminate in the stepwise model. On its own, the discrimination model produced from ULB significantly distinguished between males and females of the *Homo sapiens* sample (Wilks Lambda= .242, Chi square= 81.583, $p<0.001$). Discrimination from ULB provided a classification percentage of 96.7%, with one male incorrectly classified as a female and one female incorrectly classified as a male. The male incorrectly classified as a female, specimen numbered 24, has a ULB metric of 15.88mm, closer to the female average of 15.54mm. The female incorrectly classified as a male, specimen numbered 54, has a ULB metric of 17.60mm, closer to the male average of 18.99mm.

Table 5.6: Classification count and percentage for the *Homo sapiens* ULB discriminant function analysis.

Discriminant function analysis classification results for *Homo sapiens* ULB				
		Male	Female	Total
Count	Male	29	1	30
	Female	1	29	30
Percentage (%)	Male	96.7	3.3	100
	Female	3.3	96.7	100
Percentage of original grouped cases classified (%): 96.7				
Wilks Lambda		Chi Square		Sig
.242		81.583		p<0.001

5.4.3.2: FHD

FHD was ranked third in the *Homo sapiens* discriminant function analysis structure matrix and was introduced into the stepwise model during the second step. On its own, the discrimination model produced from FHD significantly distinguished between males and females of the *Homo sapiens* sample (Wilks Lambda= .302, Chi square= 68.757, p<0.001). Discrimination from FHD provided a classification percentage of 96.7%, with one male incorrectly classified as a female and one female incorrectly classified as a male. This is the same as ULB, the skeletal metric that was found to be the most dimorphic for *Homo sapiens*. The male incorrectly classified as a female was the same specimen 24, which was also misclassified by the ULB model. Specimen 24 has an FHD metric of 42.81mm, closer to the female average of 41.66mm. The female incorrectly classified as a male, specimen numbered 48, was not the same as the female misclassified by the ULB model. Specimen 48 has an FHD metric of 45.55, closer to the male average of 48.58mm.

Table 5.7: Classification count and percentage for the *Homo sapiens* FHD discriminant function analysis.

Discriminant function analysis classification results for *Homo sapiens* FHD				
		Male	Female	Total
Count	Male	29	1	30
	Female	1	29	30
Percentage (%)	Male	96.7	3.3	100
	Female	3.3	96.7	100
Percentage of original grouped cases classified (%): 96.7				

Wilks Lambda	Chi Square	Sig
.302	68.757	p<0.001

5.4.3.3: TAL

TAL, whilst only ranked ninth and eighth in the discriminant function analysis structure matrix rankings, was introduced into the stepwise model during the third step. On its own, the discrimination model produced from TAL significantly distinguished between males and females of the *Homo sapiens* sample (Wilks Lambda= .407, Chi square= 51.646, p<0.001). Discrimination from TAL provided a classification percentage of 85.0% with five males being incorrectly classified as female and four females being incorrectly classified as male. The specimen numbered 24, misclassified by both the ULB and FHD models respectively, was also one of the males incorrectly classified as a female by the TAL model. The five males incorrectly classified as females have TAL metrics that are closer to the female average of 48.82mm. The four females incorrectly classified as males do not include the females misclassified as male by the ULB and FHD models respectively. All four misclassified females have TAL metrics that are closer to the male average of 55.71mm.

Table 5.8: Classification count and percentage for the *Homo sapiens* TAL discriminant function analysis.

Discriminant function analysis classification results for *Homo sapiens* TAL				
		Male	Female	Total
Count	Male	25	5	30
	Female	4	26	30
Percentage (%)	Male	83.3	16.7	100
	Female	13.3	86.7	100
Percentage of original grouped cases classified (%): 85.0				

Wilks Lambda	Chi Square	Sig
.407	51.646	p<0.001

5.4.3.4: ULB, FHD and TAL

ULB, FHD and TAL were added to the stepwise discriminant function analysis to provide the best model of discrimination for *Homo sapiens* with ULB added in the first step, FHD added in the second step and TAL added in the third step. The combined model from ULB, FHD and TAL significantly distinguished between males and females of the *Homo sapiens* sample (Wilks Lambda= .166, Chi square= 101.532, p<0.001). In comparison to the separate discriminations for each skeletal metric above, this combined model improved the classification percentage to 98.3%, with only one male incorrectly classified as a female. The misclassified male was the same male misclassified by the specimen ULB, FHD and TAL models, the specimen numbered 24.

Table 5.9: Classification count and percentage for the *Homo sapiens* ULB, FHD and TAL discriminant function analysis.

Discriminant function analysis classification results for *Homo sapiens* ULB, FHD and TAL				
		Male	Female	Total
Count	Male	29	1	30
	Female	0	30	30
Percentage (%)	Male	96.7	3.3	100
	Female	0	100	100
Percentage of original grouped cases classified (%): 98.3				
Wilks Lambda		Chi Square		Sig
.166		101.532		p<0.001

5.4.3.5: ULB and FHD

The combined model from ULB and FHD significantly distinguished between males and females of the *Homo sapiens* sample (Wilks Lambda= .178, Chi square= 98.493, p<0.001). Without TAL, the combined discrimination function analysis from ULB and FHD has a classification percentage reduced to 96.7% with one male incorrectly classified as female and one female incorrectly classified as male. This is the same classification percentage and count provided by the specimen discriminant function analysis for ULB and FHD. The misclassified male and female were the same incorrectly classified specimens from the ULB model, specimens 24 and 54.

Table 5.10: Classification count and percentage for the *Homo sapiens* ULB and FHD discriminant function analysis.

Discriminant function analysis classification results for *Homo sapiens* ULB and FHD				
		Male	Female	Total
Count	Male	29	1	30
	Female	1	29	30
Percentage (%)	Male	96.7	3.3	100
	Female	3.3	96.7	100
Percentage of original grouped cases classified (%): 96.7				
Wilks Lambda		Chi Square		Sig
.178		98.493		p<0.001

5.4.3.6: OLCB

For the unstandardised discriminant function analysis structure matrix for *Homo sapiens*, ULB was ranked first, OLCB was ranked second and FHD was ranked third. On its own, the discrimination model produced from OLCB significantly distinguished between males and females of the *Homo sapiens* sample (Wilks Lambda= .255, Chi square= 78.512, p<0.001). Discrimination from OLCB produced a classification percentage of 96.7% with one male incorrectly classified as female and one female incorrectly classified as male. This is the same as the individual discrimination function analysis for ULB and FHD. However, the specimens misclassified by the OLCB model were different. The male incorrectly classified as a female, the specimen numbered 14, has an OLCB metric of 36.09mm closer to the female average of 33.75mm. The female incorrectly classified as a male, the specimen numbered 50, has an OLCB metric of 38.12mm, closer to the male average of 41.90mm.

Table 5.11: Classification count and percentage for the *Homo sapiens* OLCB discriminant function analysis.

Discriminant function analysis classification results for *Homo sapiens* OLCB				
		Male	Female	Total
Count	Male	29	1	30
	Female	1	29	30
Percentage (%)	Male	96.7	3.3	100
	Female	3.3	96.7	100
Percentage of original grouped cases classified (%): 96.7				
Wilks Lambda		Chi Square		Sig
.255		78.512		p<0.001

5.4.3.7: ULB and OLCB

The combined model from ULB and OLCB significantly distinguished between males and females of the *Homo sapiens* sample (Wilks Lambda= .203, Chi square= 90.800, p<0.001). Combining ULB and OLCB, the first and second ranked skeletal metrics from the unstandardised discriminant function analysis structure matrix, provided the same classification percentage as the individual discriminant function analysis for ULB and OLCB. The discriminant function analysis for the model containing ULB and OLCB, has a classification percentage of 96.7% with one male incorrectly classified as a female and one female incorrectly classified as a male. The misclassified male and female were the same incorrectly classified specimens from the ULB model, 24 and 54.

Table 5.12: Classification count and percentage for the *Homo sapiens* ULB and OLCB discriminant function analysis.

Discriminant function analysis classification results for *Homo sapiens* ULB and OLCB				
		Male	Female	Total
Count	Male	29	1	30
	Female	1	29	30
Percentage (%)	Male	96.7	3.3	100
	Female	3.3	96.7	100
Percentage of original grouped cases classified (%): 96.7				
Wilks Lambda		Chi Square		Sig
.203		90.800		p<0.001

5.4.3.8: ULB, OLCB and FHD

The combined model from ULB, OLCB and FHD significantly distinguished between males and females of the *Homo sapiens* sample (Wilks Lambda= .170, Chi square= 100.211, p<0.001). The three best ranked skeletal metrics from the unstandardised discriminant function analysis structure matrix for *Homo sapiens,* ULB, OLCB and FHD, has the same individual classification percentages as the combined discriminant function analysis. The combined discriminant function analysis has a classification percentage of 96.7% with one male incorrectly classified as female and one female incorrectly classified as male. The misclassified male and female were the same incorrectly classified specimens from the ULB model, 24 and 54.

Table 5.13: Classification count and percentage for the *Homo sapiens* ULB, OLCB and FHD discriminant function analysis.

Discriminant function analysis classification results for *Homo sapiens* ULB, OLCB and FHD				
		Male	Female	Total
Count	Male	29	1	30
	Female	1	29	30
Percentage (%)	Male	96.7	3.3	100
	Female	3.3	96.7	100
Percentage of original grouped cases classified (%): 96.7				

Wilks Lambda	Chi Square	Sig
.170	100.211	p<0.001

5.4.3.9: HHD

For the stepwise discriminant function analysis structure matrix for *Homo sapiens*, ULB was ranked first, HHD was ranked second and FHD was ranked third. On its own, the discrimination model produced from HHD significantly distinguished between males and females of the *Homo sapiens* sample (Wilks Lambda= .333, Chi square= 63.291, p<0.001). Discrimination from HHD provided a classification percentage of 96.7% with two males incorrectly classified as female. Whilst the classification percentage is the same as the individual discriminant function analysis for ULB, FHD and OLCB respectively, it differs in the specimens incorrectly classified, with two males incorrectly classified rather than a male and a female, as was produced from the discriminant function analysis for the other skeletal metrics. The misclassified males were specimens numbered 14 and 24. The incorrectly classified male 14 was also misclassified by the OLCB model. It has a HHD metric of 41.68mm, closer to the female average of 40.32mm. The other incorrectly classified male 24, was also misclassified by the other models accept the model produced from OLCB and had a HHD metric of 40.91mm, closer to the female average of 40.32mm.

Table 5.14: Classification count and percentage for the *Homo sapiens* HHD discriminant function analysis.

Discriminant function analysis classification results for *Homo sapiens* HHD				
		Male	Female	Total
Count	Male	28	2	30
	Female	0	30	30
Percentage (%)	Male	93.3	6.7	100
	Female	0	100	100
Percentage of original grouped cases classified (%): 96.7				
Wilks Lambda		Chi Square		Sig
.333		63.291		p<0.001

5.4.3.10: HHD and OLCB

The combined model from HHD and OLCB significantly distinguished between males and females of the *Homo sapiens* sample (Wilks Lambda= .214, Chi square= 97.903, p<0.001). HHD and OLCB were both ranked second best discriminators from the unstandardised and stepwise discriminant function analysis structure matrix respectively. Combined in a separate discriminant function analysis the classification percentage was still 96.7% with two males incorrectly classified as female, the same as the individual HHD discriminant function analysis. The misclassified males were the same incorrectly classified specimens produced from the HHD model, 24 and 54.

Table 5.15: Classification count and percentage for the *Homo sapiens* HHD and OLCB discriminant function analysis.

Discriminant function analysis classification results for *Homo sapiens* HHD and OLCB				
		Male	Female	Total
Count	Male	28	2	30
	Female	0	30	30
Percentage (%)	Male	93.3	6.7	100
	Female	0	100	100
Percentage of original grouped cases classified (%): 96.7				

Wilks Lambda	Chi Square	Sig
.214	97.903	p<0.001

5.4.3.11: ULB and HHD

The combined model from ULB and HHD significantly distinguished between males and females of the *Homo sapiens* sample (Wilks Lambda= .196, Chi square= 92.979, p<0.001). Combining ULB and HHD, the first and second ranked skeletal metrics from the stepwise discriminant function analysis structure matrix, provided a higher classification matrix of 98.3% with one male incorrectly classified as a female. This classification percentage is equivalent to the best model of discrimination formed through the stepwise discriminant function analysis using ULB, FHD and TAL. The misclassified male specimen 24 was incorrectly classified by all the models apart from the OLCB model.

Table 5.16: Classification count and percentage for the *Homo sapiens* ULB and HHD discriminant function analysis.

Discriminant function analysis classification results for *Homo sapien* ULB and HHD				
		Male	Female	Total
Count	Male	29	1	30
	Female	0	30	30
Percentage (%)	Male	96.7	3.3	100
	Female	0	100	100
Percentage of original grouped cases classified (%): 98.3				
Wilks Lambda		Chi Square		Sig
.196		92.979		p<0.001

5.4.3.12: ULB, HHD and FHD

The combined model from ULB, HHD and FHD significantly distinguished between males and females of the *Homo sapiens* sample (Wilks Lambda= .177, Chi square= 97.937, p<0.001).The three best ranked skeletal metrics from the stepwise discriminant function analysis structure matrix for *Homo sapiens,* ULB, HHD and FHD, had a lower classification percentage than combined with the first and second ranked skeletal metrics, ULB and HHD. The classification percentage is 96.7% with one male incorrectly classified as female and one female incorrectly classified as male. The misclassified male and female were the same specimens, 24 and 54, incorrectly classified by four other models (ULB, ULB & FHD, ULB & OLCB and ULB, OLCB & FHD).

Table 5.17: Classification count and percentage for the *Homo sapiens* ULB, HHD and FHD discriminant function analysis.

Discriminant function analysis classification results for *Homo sapien* ULB, HHD and FHD				
		Male	Female	Total
Count	Male	29	1	30
	Female	1	29	30
Percentage (%)	Male	96.7	3.3	100
	Female	3.3	96.7	100
Percentage of original grouped cases classified (%): 96.7				

Wilks Lambda	Chi Square	Sig
.177	97.937	p<0.001

5.4.3.13: Analysis of misclassifications

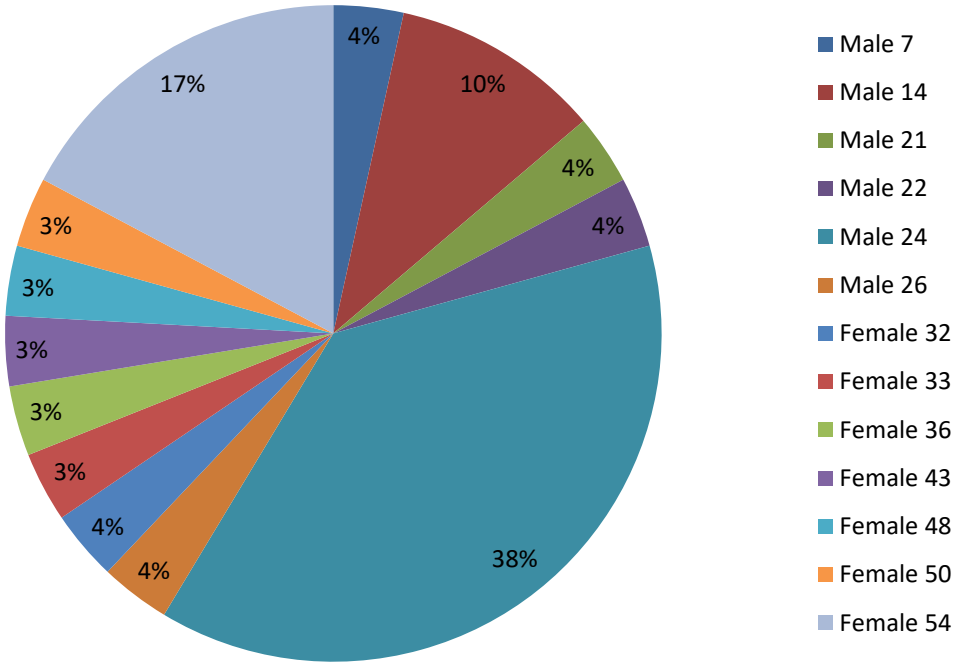

Figure 5.4: Individual case misclassification percentages for all the *Homo sapiens* discriminant function analysis models tested.

Of the 30 males and 30 females within the *Homo sapiens* sample, six males and seven females were classified with the incorrect sex by at least one of the discrimination models compared. The number of misclassifications made by all the discriminant models was higher for males than females with 18 misclassifications of males as females and 11 misclassifications of females as males. The male numbered 24 was incorrectly classified as a female by 11 of the discriminant function models compared, supplying a percentage misclassification of 38% from the whole number of misclassifications produced. In comparison, the most misclassified of the female cases was the female numbered 54, which was incorrectly classified as a male by five of the discriminant function models. This provides a percentage misclassification of 17% from the whole number of misclassifications produced. There is a consistency of misclassifications for specimens that have skeletal metrics closer to the average of the opposite sex, with larger females classified as male and smaller males classified as female. The results highlight the importance of model choice, particularly for moderately dimorphic species where some specimens will not be easily classified as male or female. With 11 of the 12 discriminant function models producing classification percentages greater than 90%, there is choice in the model employed to provide the best possible accuracy level.

5.4.4: Discussion

FHD was found to have the same individual discrimination power as the most dimorphic skeletal metric for *Homo sapiens*, ULB, with classification percentages of 96.7%. The other skeletal metric added to the stepwise model of discrimination, TAL, had a lower classification percentage of 85% than ULB and FHD, but it is only with the addition of TAL that the stepwise procedure creates the best model of discrimination with the highest classification percentage of 98.3%. The second best ranked skeletal metric from the unstandardised discriminant function analysis structure matrix, OLCB and the second best ranked skeletal metric from the stepwise discriminant function analysis structure matrix, HHD, both have classification percentages of 96.7%. These individual classification percentages were the same as the highest ranked skeletal metric, ULB, and the third ranked, FHD. HHD, however, differed in the exact count of individuals correctly classified. Combining second ranked OLCB and HHD did not increase the discriminant function analysis above individual percentages. The top three ranked from both the unstandardised structure matrix (ULB, OLCB and FHD) and the stepwise structure matrix (ULB, HHD and FHD) did not have an increased combined percentage. Interestingly, combining ULB and

HHD formed the equally highest classification percentage of 98.3%, along with the stepwise model.

Nearly all the models of discrimination misclassified the same male as a female, male numbered 24. This indicates a specimen with a body size closer to the female average for most metrics. The best two models of discrimination, ULB, FHD & TAL and ULB & FHD, were unable to correctly classify the sex of this individual case. Only the OLCB model correctly classified the specimen. When models were formed from OLCB and other metrics such as ULB and FHD, the male numbered 24 was again incorrectly classified. Other misclassified cases were only incorrectly classified by certain models utilising different metrics. This is because sexual dimorphism is not isometric throughout the skeleton. The consistency of misclassifications for specimens that have skeletal metrics closer to the average of the opposite sex highlight the importance of model choice, particularly for moderately dimorphic species where some specimens will not be easily classified as male or female. With 11 of the 12 discriminant function models producing classification percentages greater than 90%, there is choice in the model employed to provide the best possible accuracy level.

This exploration of the *Homo sapiens* sample was provided in order to answer the earlier set of questions: 1) For *Homo sapiens* samples, is there a distinct advantage to selecting skeletal metrics other than FHD? and 2) can choosing the most dimorphic skeletal metrics be applicable to fossil hominin cases? In answer to the first question as to whether there is a distinct advantage to selecting skeletal metrics other than FHD, the comparison of individual discriminant function analysis does not show great differences between FHD and the best upper limb metrics. In a case where there is only the choice of one skeletal metric and its corresponding discriminant function equation for a *Homo sapiens* individual, choosing either FHD or an upper limb metric like ULB, HHD or OLCB would provide the same classification power. It is when certain groupings are formed that the percentage is higher. The previous section of this chapter indicated that discriminant function analysis is better at classifying sex than mean/median methods of sexual dimorphism estimation for *Homo sapiens*.

The applicability of these findings for studying fossil hominin sexual dimorphism varies depending on the species being evaluated and whether there are enough specimens to form a reference sample. For early, pre-*Homo* hominins, with specimens that do not have a sample of sexed individuals to form a reference sample, discriminant function analysis can

be used to investigate a range of possible analogue species, and to test whether the range of analogue species produce consistent estimates of sexual dimorphism. For example, if a specimen is consistently classified as a male from equations developed from individual samples of *Pan troglodytes* and *Homo sapiens* then there is an increased likelihood that the sex classification is correct. Discriminant function analysis can be applied to fossil hominin species whenever there exist enough specimens to form a reference sample. For *Homo* species such as *Homo erectus* and *Homo neanderthalensis*, discriminant function equations developed from a modern human sample or a generic *Homo* sample may be used, with the proviso that a species-specific reference sample will always be preferable.

In cases where the assemblage is incomplete, individual discriminant function analysis, which reduces essentially to a simple binomial logistic regression, has an equal classification percentage for the most dimorphic traits, whichever one is available. The fact that the combined ULB and HHD discriminant function analysis has an equally high classification as the stepwise ULB, FHD and TAL discriminant function analysis, suggests a simpler requirement of just two metrics from the upper limb.

In answer to the second question as to whether choosing the most dimorphic skeletal metrics can be applicable to fossil hominin cases, whilst FHD is an acceptable choice for *Homo sapiens* samples it may not be the best choice for fossil hominin species. The previous chapter found FHD was not as dimorphic for *Pan troglodytes* and other primates and choosing FHD equates to an assumption that hominin FHD shows a pattern of dimorphism similar to *Homo sapiens* rather than to other primates. It is therefore potentially safer to estimate sex from other metrics such as HHD and OLCB that are highly dimorphic throughout the primate order, especially when examining dimorphism in more distantly related species such as the gracile australopithecines. The sustained level of accuracy for discriminant function analysis models with minimal required skeletal elements indicates that the methodology is practical and can be applied to skeletal assemblages that are not complete.

This corresponds with the findings of Ruff (1988), Jungers (1988) and Holliday (2012), which noted the scaling differences between modern humans and non-human primates. For the primate order, a general trend of isometry or slightly positive allometry has been noted with humans as outliers displaying a positively allometric relationship between body mass and femoral head diameter (Ruff, 1988). Modern humans are also positive outliers in the general relationship between lower limbs and body mass, but share the same correlation

between upper limbs and body mass as the rest of the primate order (Jungers, 1988). As the best skeletal metric discriminators of sex across the primate order have been found to be from the upper limb, and the upper limb reflects general scaling trends for the primate order, sexing from elements of the upper limb for fossil hominin species may be more appropriate when analysing body mass dimorphism.

Separating the estimation of body mass and the level of dimorphism is important because the current methodology for estimating body mass from femoral head diameter and predicting the level of sexual dimorphism from these estimations causes uncertainty prior to the estimation of dimorphism. Kurki et al. (2010) noted that error in sexual dimorphism estimation is being introduced through the use of estimation equations for predicting body mass from femoral head diameter. Combined sex formulae tend to overestimate sexual dimorphism as body mass is overestimated from the larger male femoral heads. For fossil hominin body mass estimation procedures, there is the issue of which comparative sample is most appropriate for producing estimation equations. Holliday (2012) highlighted the problem of estimating australopithecine body mass from estimation equations produced from modern humans as their femoral head diameters are smaller than those of modern humans. Sexing directly from the skeleton, potentially using elements other that femoral head diameter, does not change the error introduced by body mass estimation techniques. However, the multiplication of error that is produced through estimating body mass from femoral head diameter and then dividing the predicted sample into males and females can be averted by direct methods of classifying sex in fossil hominin species.

5.5: Chapter summary

Body mass differences within species have an important role in determining multiple aspects of hominin palaeoecology. Existing methods of estimating the level of sexual dimorphism within hominin species are insufficient as they are prone to overestimating moderately dimorphic species. Furthermore, the two-step procedure, first estimating body mass from FHD and then predicting the level of dimorphism for the whole sample introduced a multiplication of error problem. In this chapter, existing methods of estimating sexual dimorphism were tested on *Homo sapiens* data. As previous literature indicated, simple methods that split the sample into males and females from a cut-off point were found to be the most accurate.

The best methods were compared to the *Homo sapiens* discriminant function analysis, with results from both FHD and predicted body mass of each individual. As expected, the discriminant function analysis was better than the existing methods for estimating the level of dimorphism. Overlap between males and female distributions provide a greater vulnerability for methods that split the sample from a cut-off point, as compared to the discriminant function analysis. Methods that split the sample from a cut-off point are more susceptible to overlaps between male and female distribution and so have limited power for estimating the amount of dimorphism in moderately dimorphic species. Classifying the sex of individuals would remove the limitations that have been found for moderately dimorphic species, especially the inaccuracy of estimation for specimens around the cut-off point.

The discriminant function analysis used in the estimation procedure comparison requires too many variables to be practical for fossil hominin sex estimation. Therefore, different skeletal metrics were evaluated as appropriate measures of sexual dimorphism with the aim of finding the best discrimination equations with a small number of required measurements. FHD is already utilised for body mass estimation, but it is not the most dimorphic element in the primate order, with upper limb metrics having been found to be consistently better discriminators of sex from the analysis in the previous chapter. The results of the discriminant function comparison found that discrimination from FHD has a classification percentage equal to the best single upper limb metrics, although higher classifications percentages are produced from certain combinations of a small number of skeletal metrics. The combination of two upper limb metrics produced the most parsimonious equation, achieving the highest accuracy with the fewest parameters. In terms of using *Homo sapiens* as comparative sample for fossil hominins, the different scaling of FHD and its lesser level of dimorphism in comparison to other primates mean that it is not the safest choice of discriminator. Nonetheless, the more direct method of classifying sex is advantageous as the error introduced through estimating body mass from femoral head diameter and then dividing the predicted sample into males and females would be avoided.

Chapter 6:

Scaling of sexual dimorphism in the primate skeleton

Previous research highlighted in the literature review has focused on the scaling of skeletal metrics and body mass, with implications for the choice of comparative sample when estimating body mass dimorphism in fossil hominin species. Analysis of how postcranial skeletal elements scale with each other in males and females can provide greater understanding of how the broader pattern of sexual dimorphism occurs in primate species. The difference in scaling between metrics for males and females can be used to examine whether males are just larger females in terms of postcranial metric proportions or if there are more complex scaling patterns underpinning sexual dimorphism. Variation between species can also be inferred including detailed comparisons between *Homo sapiens* and other species. The dimorphic scaling patterns within different primate species can potentially provide another aspect for interpreting sexual dimorphism within fossil hominin species.

This chapter aims to explore the similarities and differences between species in terms of how skeletal metric scaling varies between males and females by:

1. Determining the variability of sexual dimorphic scaling between metrics within the skeleton of primate species.
2. Analysing whether the difference in scaling between males and females varies depending on the area of the skeleton.
3. Comparing humans to other species in the primate order in terms of the difference in scaling between skeletal metrics for males and females.

This chapter begins by highlighting previous studies of the scaling between skeletal metrics and body mass as well as joint size dimorphism. The first analysis compares the difference in skeletal metric scaling within the skeleton of males and females for each species through simple regressions. The difference in skeletal metric correlation coefficients between males and females is then analysed further through clustergrams to determine variation in different areas of the skeleton. The third analysis utilises hierarchical clustering to determine which species are most similar in terms of correlation coefficient differences between skeletal metrics of males and females. The final analysis in this chapter compares the difference in skeletal metric scaling between males and females of *Pan troglodytes* and *Homo sapiens.*

6.1: Introduction to body mass scaling in primates

Previous research has focused on the scaling pattern between metrics of the skeleton and body mass. The primate order does not display a universal scaling pattern with studies highlighting the fact that skeletal metrics scale to body mass differently between taxa. Ruff (1988) employed a sample including *Pan troglodytes, Gorilla gorilla, Pongo pygmaeus, Macaca fascicularis* and *Homo sapiens* to compare scaling relationships between joint size and body mass. Overall isometry or slightly positive allometry was found in the species tested but *Macaca fascicularis* and *Homo sapiens* differ from this trend. The smaller hindlimb articulations in relation to body mass of *Macaca fascicularis* are contrasted with the larger femoral heads relative to body mass displayed in *Homo sapiens.* This variation in scaling pattern in the primate order is emphasised by the contrasting femoral head size of *Pongo pygmaeus,* which scales almost isometrically with body mass.

The results of body mass scaling comparison studies are dependent on the species chosen as a sample. For studies combining samples of hominoids and non-hominoids, articular scaling to body mass has been found to be positively allometric. The greater joint size observed in larger bodied hominoids is thought to influence this result (Ruff, 1988; Jungers, 1990b; Godfrey et al. 1991). For samples of non-human hominoids, slight positive allometry or isometry is reported (Jungers, 1990b; Burgess et al. 2018). This indicates that there are grade shifts between different primate clades.

The most frequently studied scaling relationship is between the femoral head and body mass. This is because the femoral head was found to have the strongest relationship to weight in comparison to other articular dimensions. Humans show a different scaling relationship between femoral head size and body mass than non-human primates, with humans presenting a positively allometric relationship between body mass and FHD. Although modern humans are positive outliers in terms of the correlation between lower limbs and body mass for primate species, with *Homo sapiens* lower limbs being of greater size than expected for their body size, this is not the case for the upper limb (Jungers, 1988).

Although there have been many investigations into the scaling of limb joints in anthropoids, there is no consensus on scaling patterns and the expected biomechanics underpinning findings. The relative scaling of joint size has only been measured in a select number of primate species. Perry et al. (2018) attempted to rectify this with the inclusion

of platyrrhines. Measurements were taken from the proximal and distal ends of the femur and humerus and paired with individual body mass measurements. The results of the study found that cercopithecoids display significantly smaller humeral and distal femoral joint articulations relative to body mass than platyrrhines and hominoids. Platyrrhines also have smaller femoral heads that hominoids, but other articulations show no significant relative size difference. Therefore, platyrrhine joint proportion is more similar to hominoids than cercopithecoids. This is further evidence of possible grade shifts suggesting that clades should be analysed separately.

The finding corresponds with other studies showing that both cercopithecoids and platyrrhines display positive allometric scaling in all joint articulations tested (Ruff, 1988; Jungers; 1990b; Burgess et al. 2018). The larger hominoid femoral head probably relates to greater hip joint excursion employed during vertical climbing or greater hindlimb loading during terrestrial locomotion (Demes et al. 1994; Hammond, 2014). The humeral head has similar scaling to body mass in hominoids and platyrrhines (across the parvorder rather than being specific to larger bodied species). Humeral head is smaller relative to body mass in cercopithecoids. This suggests that there is more uniformity in posture and less upper limb mobility in Old World monkeys.

The Perry et al. (2018) findings for the distal humerus are more complex. Hominoids were found to have relatively larger distal humeri than cercopithecoids. Platyrrhines are not significantly different from hominoids, but display strong positive allometry of the distal humerus. This is caused by the contrast between the large distal humeral dimensions in *Cebus* species and Atelids. Most of the smaller platyrrhines in the study (*Aotus, Saguinus, Saimiri*) have smaller distal humerus articular breadth proportions, similar to those of cercopithecoids.

The findings also noted that the observed scaling slopes are lower than expected, in order to produce proportionate joint surface area to body mass for biomechanical equivalence. The authors suggest that this might be caused by measurements not reflecting true surface area in the study and that most postures do not require full loading of the joint. The results are also consistent with Ruff (2003), which indicates that isometric scaling may be produced through the balance of maintaining equivalent joint surface areas and total joint volume to body mass. Differences in positioning behaviour have also been investigated as a potential factor in scaling discrepancies (see below).

A recent study evaluated a new method for estimating body mass in juvenile non-human primates (Burgess et al. 2018). The scaling of skeletal dimensions with body mass was compared between adults and an ontogenetic sample. The joint dimensions tested, including the proximal and distal femur, distal humerus, and tibial plateau, were found to produce estimation equations of body mass for both adult and juvenile hominoids with percentage prediction errors of 10-20%. There is no evidence of larger joints scaling relative to body mass in juveniles.

Scaling differences between taxa limits body mass estimation accuracy. The Burgess et al. (2018) study found adult scaling patterns to be generally consistent with those presented in Jungers (1991). The similarity of relative proximal joint size between taxonomic groups was greater than the similarity found in distal joints. Proximal joints are expected to produce more reliable body mass estimates in hominoid samples as variation in humeral and femoral heads will be restricted, being directly related to joint excursion.

However, greater variability in the knee and elbow joints was not found in Ruff (2003) and Payseur et al. (1999). Ruff (2003) performed comparisons of cross-sectional diaphyseal and articular surface dimensions for hominoid and cercopithecoid body mass estimation. Knee breadth was found to be the least variable in proportion between hominoids and cercopithecoids, with proximal measurements of the humerus and femur presenting differences in scaling between the two groups. Payseur et al. (1999) estimated the body mass of the middle Eocene primate *Omomys carteri* from comparative samples of extant small-bodied haplorhines and strepsirrhines. Of the postcranial measurements utilised in forming estimation equations, relative tibial plateau width was one of the least variable across taxonomic groups. Proximal joints may not be a suitable choice for body mass estimates in cases where taxonomic affiliation is uncertain, as seen in some Miocene primate fossils; distal measurements with consistent scaling relationships will be more appropriate when taxonomy is unclear. Therefore, along with locomotor effects, phylogeny must also be considered when selecting comparative samples.

The test of body mass estimation equations formed from extant platyrrhines, cercopithecoids and hominoids highlights how variation in phylogeny affects prediction accuracy (Perry et al. 2018). Body mass estimations for extinct platyrrhines and Fayum anthropoids produced from distal femoral articulations yield the most reliable predictions because the scaling between the distal femur and body mass was most consistent in the taxa chosen. Other estimation equations derived from the proximal femur, proximal

humerus and distal humerus were not as accurate, as a consequence of the variation in scaling relationship between taxa. Extant reference samples must therefore be chosen that best match the joint proportionality of fossil taxa where possible.

6.1.1: Joint size dimorphism in relation to body size dimorphism

Joint size dimorphism has important implications for hominin dimorphism estimation methods because there is a potential relationship between a certain degree of joint size dimorphism and body mass dimorphism. The consequence of the relationship must be understood before a reliable choice can be made in terms of the taxon selected as a comparative sample and the joint employed in estimation. It is expected that a species with high body mass dimorphism should also display joint size dimorphism in order to maintain geometric similarity between males and females. This is because the extra forces encountered by limb joints in larger males will require an increase in joint surface area to avoid greater joint stress than females.

Nonetheless, other factors can compensate for increased stress on joints without increasing joint size. Studies have found that larger animals reduce stress on joints through the adjustment of locomotor attributes. Reynolds (1985) demonstrated variation in the primate order in terms of the force applied to forelimbs during different locomotion modes. The ranking of forelimb vertical stress in primate species is roughly parallel to the ranking of brachiation and suspension incidence. Correlation between joint stress and body mass may not occur consistently when there is variation in locomotion mode.

The theory that larger males can reduce stress caused by mechanical loading on joints through the adjustment of locomotor attributes is not supported by evidence of significant locomotor differences between males and females of a species (Ruff, 1988). Sex differences have been observed, however, in the positional behavior of some hominoid species. Western lowland gorillas display a relationship between body size and the amount of arboreal activity, with females utilising smaller arboreal substrates through suspensory postures more than males (Remis, 1995). Similar intraspecies differences in positional behavior have also been reported for mountain gorillas (Schaller, 1976). Male chimpanzees employ more climbing, scrambling and aided bipedalism than female chimpanzees during feeding locomotion with a general reduction in quadrupedalism within arboreal settings (Doran, 1993). Sumatran orangutans also display positional behavior that reflects the

effects of body size dimorphism with males requiring larger branches than females, along with postures limited to above branch sitting and standing. Females employed suspensory locomotor behavior when feeding more frequently (Cant, 1987). Joint size dimorphism may therefore reflect differences in positional behavior between males and females of a species.

The amount of joint size dimorphism is also associated with the magnitude of peak stresses associated with any joint (Lague, 2003). Joints that are not regularly put under high mechanical stress may not require joint size allometry. Therefore, an increase in male body size does not always necessitate an allometric joint size increase, although larger male bodies will operate at lower mechanical stress safety factors than females. Swartz (1989) found that weight bearing is a major constraint on primate joint design with significant positive allometry in most limb joints of brachiating primate species. Suspensory species were expected to deviate from the general primate pattern of isometry due to the reduced compressive loads of the limb joints. The results, however, indicate that only specific types of locomotor specialisation cause changes in joint design. Whilst locomotor modes that produce an increase in limb loading provide selection for increased joint size, locomotor modes that reduce joint stress may not have a selective effect on joint morphology. Human bipedalism is an example of locomotor behaviour altering to the point of greatly increased limb loading. The finding that human hindlimbs are significantly larger than predicted by body size is an indication that there has been no reduction in size to conserve joint material, which may be an example of the lack of selection on joints where loading is reduced. The absence of selection for conserving joint material and the retention of larger joint size is an indication of phylogenetic inertia, a constraint on evolution set by previous adaptations (Jungers, 1988; Swartz, 1989).

6.1.2: Implications for estimating hominin body mass dimorphism

To understand the implications for estimating hominin body mass dimorphism it is important to note that skeletal dimorphism is not the same as body mass dimorphism. Richmond and Jungers (1995) found that modern human sexual dimorphism is greater than chimpanzee dimorphism in most postcranial dimensions but body mass tends to show the reverse trend between the species. Lague (2003) also highlighted the relatively high level of human joint size dimorphism of the knee and elbow that is not reflected in greater body

mass dimorphism relative to chimpanzees. Nonetheless, the relationship between two variables (the most frequent example being body mass and FHD) directly relates to their scaling relationship. Sexual dimorphism is equivalent in variables of the same dimension that scale isometrically. Scaling relationships that differ from isometry will present different levels of sexual dimorphism between variables (Gordon et al. 2008). For body mass estimation, when postcranial variables do not scale isometrically with body mass for all taxa and metrics, the estimates produced will not be reliable enough for comparing differences in body mass dimorphism.

An important example that highlights the implications of this scaling variation is attempts to estimate the level of sexual dimorphism in *Australopithecus afarensis.* Whilst many studies have found that *Australopithecus afarensis* body mass dimorphism level falls between that of chimpanzees and gorillas (McHenry, 1992; Lockwood et al. 1996), a more modest degree of dimorphism has also been inferred closer to the level observed in modern humans (Reno et al. 2003; 2010). The discrepancy in results is dependent on the use of *Homo sapiens* as a comparative model (Plavcan et al. 2005). If *Australopithecus afarensis* FHD does not scale to body mass with positive allometry then a larger amount of body mass dimorphism in comparison to modern humans should be concluded.

Because skeletal dimorphism is not the same as body mass dimorphism it can be employed as a separate tool for understanding how sexual dimorphism varies between species and whether there is a change in the pattern of dimorphism within the skeleton over time. This can be achieved by analysing the difference in scaling between metrics of the male and female skeleton. The best choice of comparative sample for estimating body mass dimorphism in fossil hominin species, such as *Australopithecus afarensis,* is currently unknown. The analysis of dimorphism in the scaling of metrics to each other within the primate skeleton may potentially supply a different way of investigating the similarities and differences between extant and fossil species in the primate order. Any variation in pattern between primates can be inferred making the study a further tool for highlighting the best comparative sample for fossil hominin body mass dimorphism studies.

6.2: Scaling of sexual dimorphism in the primate skeleton aims

Scaling in this context is a description of the extent to which a change in one area of the skeleton explains a change in another. The analyses in this study will look at the scaling

relationship between skeletal metric pairs and then compare the difference in scaling relationship between males and females of a species. It provides a novel way of exploring dimorphism in the primate skeleton. Although many studies have explored the variation in primate body mass scaling, the difference between males and females in terms of scaling within the primate skeleton has not been defined. The data can be split into metrics of the upper and lower limb as a way of evaluating how scaling varies in areas of the skeleton and how this contributes to differences between males and females. Hierarchical clustering can be used to determine which species have the most similarity in terms of skeletal scaling dimorphism. This means that the species most similar to *Homo sapiens* can also be evaluated. The difference in correlation coefficient values between individual metrics for males and females of a species is utilised in this chapter for interpreting skeletal scaling dimorphism because the correlation coefficient provides a measure of how two variables vary together.

The difference in correlation coefficient between males and females was utilised in a clustergram analysis for all species before being separated into upper and lower limb metric data. Both correlation coefficient difference values and actual correlation coefficients for males and females were used for hierarchical clustering to find similarities between species. The hierarchical clustering analysis allows for an exploration into the structure of sexual dimorphism within the primate order. A comparison of *Homo sapiens* and *Pan troglodytes* skeletal scaling dimorphism was also defined through the use of the correlation coefficient difference values.

The analyses in this chapter go beyond assessing basic size dimorphism to evaluate shape dimorphism. By standardising the data through conversion to z scores, size is removed to concentrate on the proportional change in each variable. This means that larger variables do not have a disproportionate effect. Furthermore, through the analysis of the relationship between variables, monomorphic and dimorphic species can be shown to be similar in the structure of dimorphism even when there is no similarity in relation to wholesale size differences.

The chapter have been separated into four analyses:

1. The first addresses scaling differences between species through simple regressions. The change in size of each metric produced by a 1mm increase in each other can be compared between the sexes. Because of the amount of data produced, scaling

between FHD and other skeletal metrics is used as an example to present the level of detail each regression comparison provides.

2. The second examines the correlation coefficient difference (the female correlation coefficient value between skeletal metric pairs subtracted from the male correlation coefficient value between skeletal metric pairs) produced from males and females of each species. The correlation coefficient difference between the sexes is split into upper limb, lower limb and upper/lower limb metric pairs.
3. The third utilises hierarchical clustering to group together species based on the spacing of correlation coefficient difference datapoints. Three dendrograms were produced displaying hierarchical clustering on upper limb metric pairs, lower limb metric pairs and all data.
4. The fourth compares the results from *Pan troglodytes* and *Homo sapiens* to define the differences in skeletal dimorphism scaling.

6.3: Analysis of scaling differences between the sexes through regression slopes

Scaling between metrics was explored for ten metrics, upper limb HHD, OLCB, CAPD, RHD and ULB and lower limb FHD, TRCD, CNDC, PRXTB and DSTTB. The lower limb metrics TAL and FIBD were removed for this analysis due to the low sample numbers for some species. Outliers were removed prior to the analysis based on data points outside the 2.5th and 97.5th percentiles. All nine species were used in the analysis. Before analysing the difference in correlation coefficient values between males and females, it is important to look at the simple scaling between skeletal metric pairs that can be separated into male and female regressions for each species. The unstandardised data produces regression slopes and constants that can be used to compare scaling between all metrics, although the scaling of FHD to other skeletal metrics will be provided as an example. Pairwise least squares regressions were performed of each metric on every other metric. The regression slopes and constants were outputted as a separate 10x10 matrix for males and females of each species. A table of all the regression slopes and constants produced in this analysis and output for all regressions are provided in Appendix 7 and 8.

Least squares regression was chosen as it was used in a previous study for the analysis of primate shape dimorphism, using skeletal metrics (Wood, 1976). The study noted that in situations of low correlation, the regression slopes will move further apart, in contrast to major axis and reduced major axis. Nonetheless, least squares regression is an appropriate

choice as long as the independent variable is the same in the two plots being compared. This is because the regression slope is no less characteristic of the relationship between the two variables than the major axis or reduced major axis (Kidwell & Chase, 1967).

It has been suggested in the literature that alpha levels should be adjusted to account for multiple testing, using methods such as the Bonferroni adjustment (Bland and Altman, 1995). Nonetheless, there is no consensus on the necessity of the adjustment. Perneger (1998) and Feise (2002) note that p-value adjustments are calculated based on the number of tests, which is a number that is chosen arbitrability and variably depending on the study. Moreover, although p-value adjustments reduce the chance of making type I errors, they increase the chance of making type II errors. Rothman (1990) states that adjusting for multiple comparisons is not preferable for data based on actual observations as it can lead to more errors of interpretation. Because of these considerations it was decided that alpha levels should not be adjusted to account for multiple testing in this study.

By comparing male and female slopes, the change in size produced by a 1mm increase in a skeletal metric can be examined for similarities and differences. Although regressions were produced comparing all metrics, FHD is an appropriate example displaying scaling changes produced for an increase in the lower limb femoroacetabular joint. Moreover, FHD is utilised in body mass estimation so differences in scaling between males and females can be studied for potential implications for predicting hominin body mass dimorphism. Bar graphs of male and female differences in slope provide a useful visual comparison of the change in size for each skeletal metric produced from a 1mm increase in FHD.

6.3.1: Results of the regression analysis

6.3.1.1: *Euoticus elegantulus*

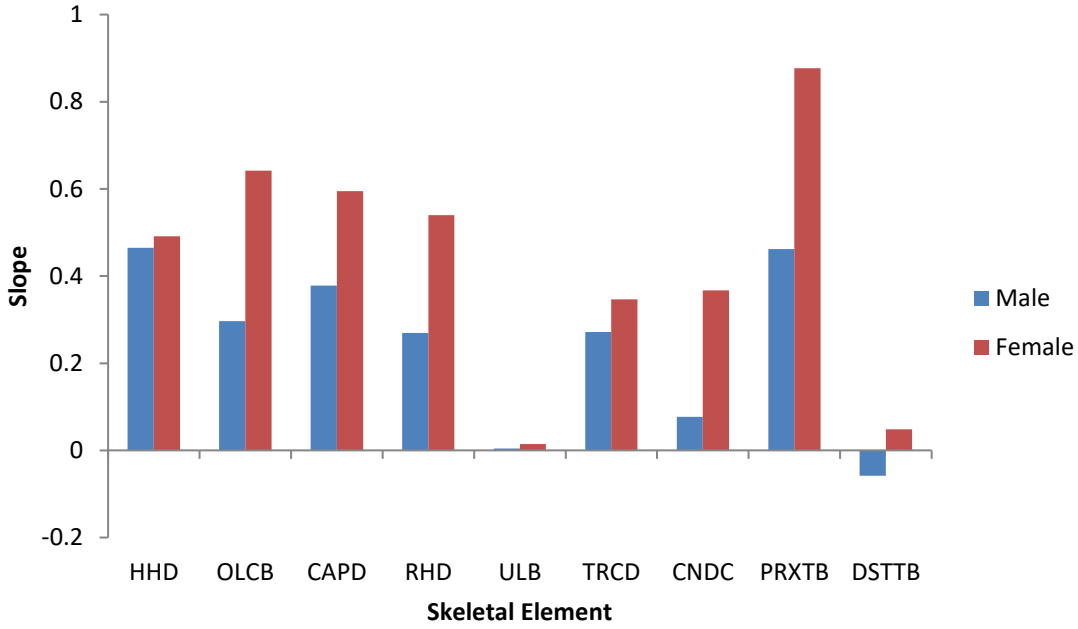

Figure 6.1: The regression slopes produced from *Euoticus elegantulus* FHD and other skeletal metrics.

There were distinct differences in skeletal metric scaling between males and females of *Euoticus elegantulus* for a 1mm increase in FHD. The regression slopes for males ranged between -0.058 and 0.465. The regression slopes for females have a larger range between 0.015 and 0.878. The smallest scaling difference was between FHD and ULB, the pairing that also displays the least difference in male and female regression slopes. For males, the regression slope for FHD and ULB is 0.004 and 0.015 in females. The largest male regression slope was formed for FHD and HHD at 0.465. The largest female regression slope was formed for FHD and PRXTB at 0.878, which also provides the greatest regression slope difference between the sexes with the male slope at 0.462. A further difference between males and females was found from the regressions between FHD and DSTTB. A 1mm increase in FHD for males was found to produce a decrease in DSTTB by 0.058. In contrast, a 1mm increase in average FHD for females was found to produce an increase in DSTTB by 0.048.

6.3.1.2: *Aotus trivirgatus*

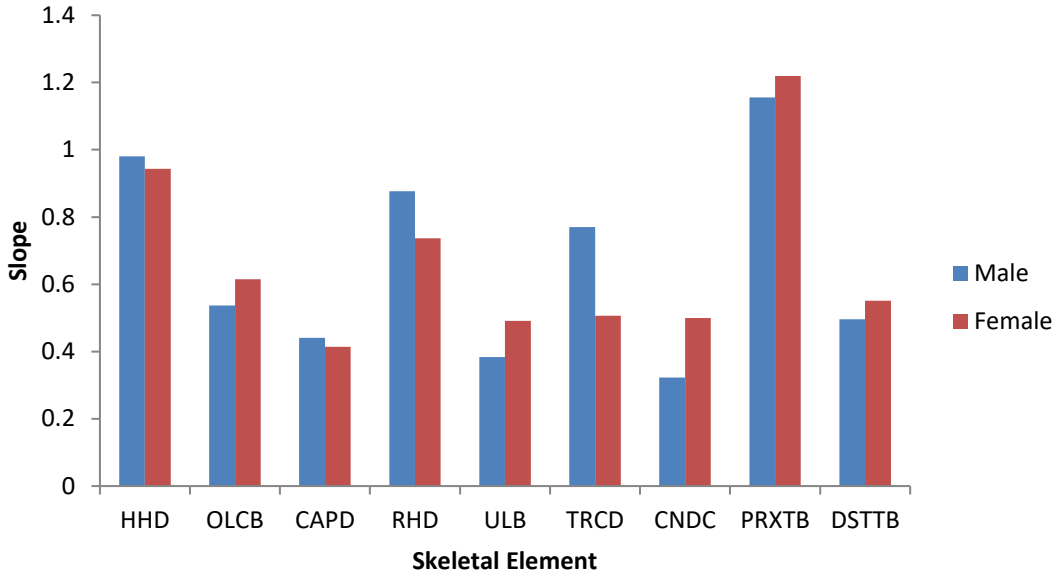

Figure 6.2: The regression slopes produced from *Aotus trivirgatus* FHD and other skeletal metrics.

There are only small differences in skeletal metric scaling between males and females of *Aotus trivirgatus* for a 1mm increase in FHD. The regression slopes for males had a slightly larger range than females between 0.323 and 1.156. The regression slopes for females had a range between 0.414 and 1.219. The smallest slope difference between the sexes was formed from FHD and CAPD with the male regression slope at 0.441 and the female regression slope at 0.414. The smallest skeletal metric scaling increase for males was between FHD and CNDC at 0.323. For females, the smallest metric scaling increase was between FHD and CAPD at 0.414. The largest scaling increase for both males and females was found between FHD and PRXTB, with a male slope of 1.156 and a female slope of 1.219. The largest difference in male and female slopes was produced by FHD and TRCD with the male slope of 0.770 in comparison to the female slope of 0.507.

6.3.1.3: *Saguinus oedipus*

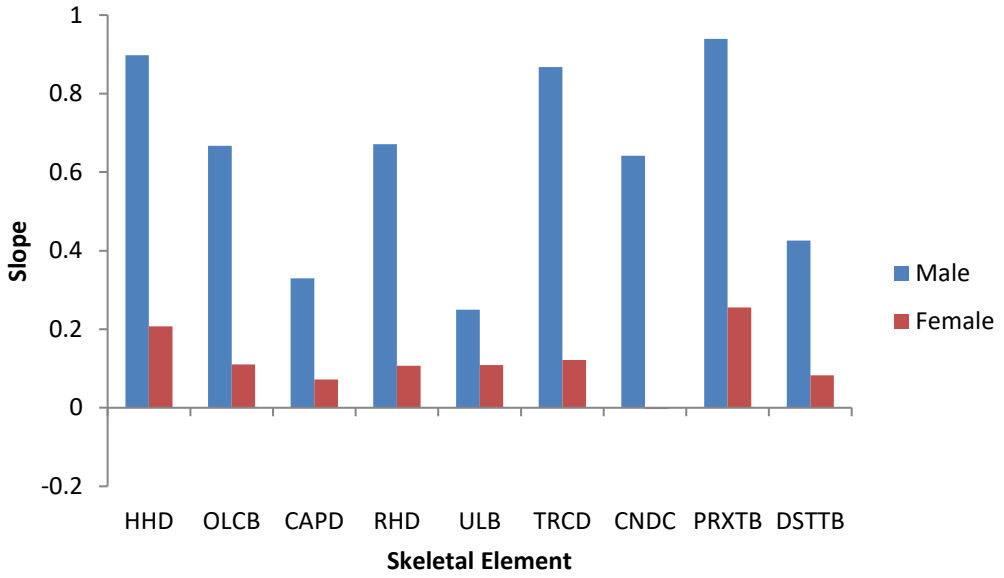

Figure 6.3: The regression slopes produced from *Saguinus oedipus* FHD and other skeletal metrics.

There are large differences in skeletal metric scaling between males and females of *Saguinus oedipus* for a 1mm increase in FHD. The regression slopes for males have a far larger range than females between 0.250 and 0.939. The female regression slope range is between -0.003 and 0.256. The smallest slope difference between the sexes was formed from FHD and PRXTB with the male regression slope at 0.939 and the female regression slope at 0.256. The smallest skeletal metric scaling increase for males was between FHD and ULB with a regression slope of 0.245. The smallest skeletal metric scaling for females was between FHD and CNDC where a 1mm increase in average FHD was found to produce a decrease in CNDC of only 0.003. The largest scaling increase for both males and females was found between FHD and PRXTB with the male regression slope at 0.939 and the female regression slope at 0.256. The largest difference in regression slope between males and females was formed from FHD and CNDC with a 1mm increase in FHD producing an increase in male CNDC of 0.642 in comparison to the increase of 0.003 in female CNDC.

6.3.1.4: *Saimiri sciureus*

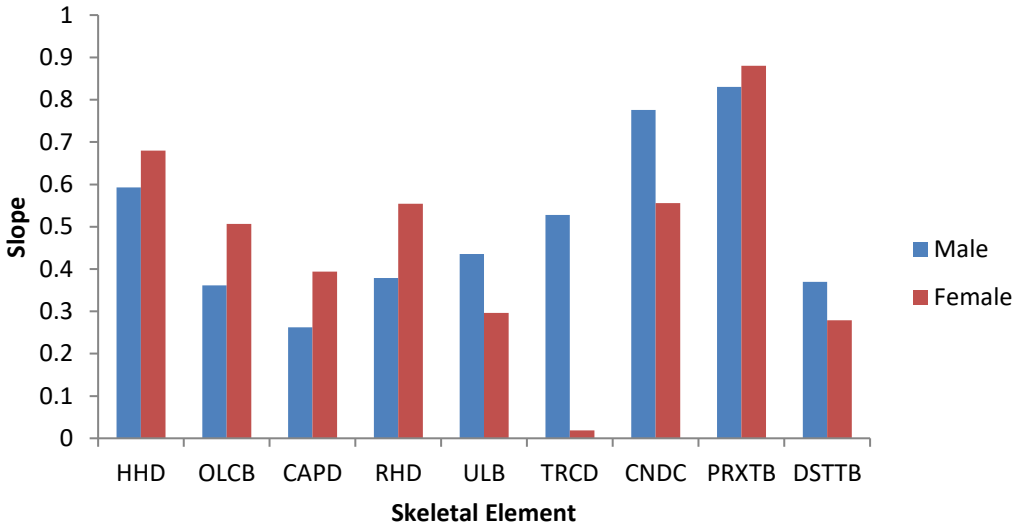

Figure 6.4: The regression slopes produced from *Saimiri sciureus* FHD and other skeletal metrics.

There were moderate differences in metric scaling between males and females of *Saimiri sciureus* for a 1mm increase in FHD. A general trend for larger female regression slopes in upper limb pairings with FHD is contrasted with the general trend for larger male regression slopes in lower limb pairings with FHD. The regression slope range for males is small, between 0.263 and 0.830. Female regression slopes have a larger range between -0.313 and 0.880. The smallest regression slope difference between the sexes was formed from FHD and PRXTB with the male slope at 0.880 and the female slope at 0.830. Although the difference between males and females was small, the regression slopes formed from FHD and PRXTB displayed the greatest scaling increase for males and females. The largest regression slope difference between the sexes was for FHD and TRCD. For a 1mm increase in FHD, a regression slope of male TRCD at 0.528 was produced for a 1mm increase in FHD in contrast to the 0.019 increase in female TRCD. The smallest scaling increase for males was produced from FHD and CAPD at 0.263. The regression slope for FHD and DSTTB produced the smallest female scaling increase at 0.279.

6.3.1.5: *Chlorocebus pygerythrus*

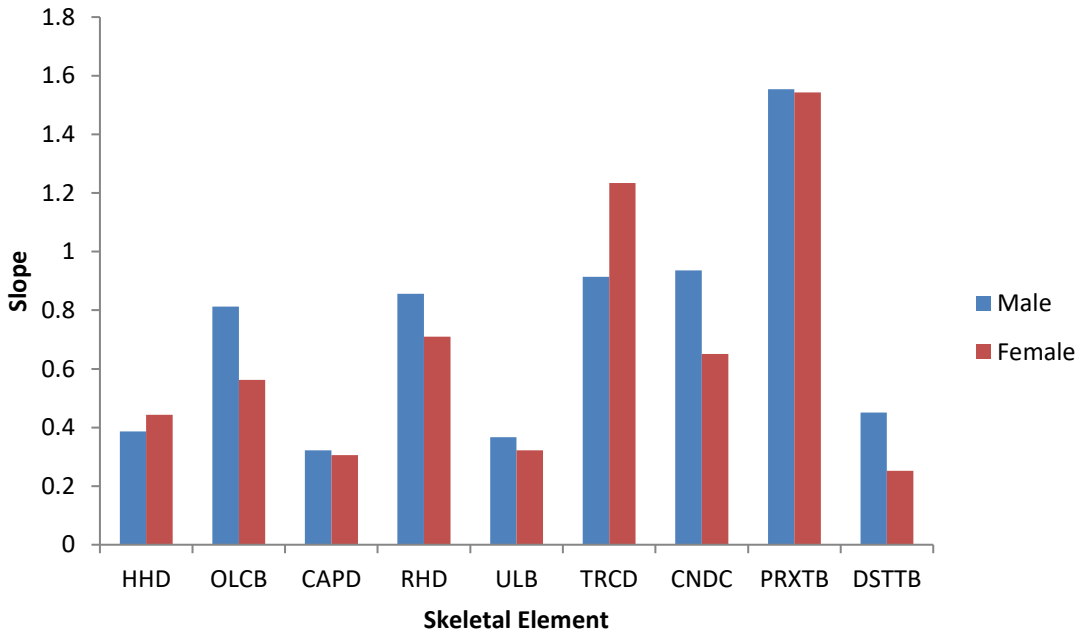

Figure 6.5: The regression slopes produced from *Chlorocebus pygerythrus* FHD and other skeletal metrics.

There were moderate differences in metric scaling between males and females of *Chlorocebus pygerythrus* for a 1mm increase in FHD. The regression slopes for males ranged between 0.322 and 1.553. The regression slopes for females have a slightly larger range between 0.253 and 1.543. The smallest regression slope difference between the sexes was formed from FHD and PRXTB with the male slope at 1.553 and the female slope at 1.543. Although the difference between males and females was small, the regression slopes formed from FHD and PRXTB displayed the greatest scaling increase for both males and females. The largest regression slope difference between the sexes was for FHD and TRCD with the male slope at 0.914 and the female slope at 1.234. The smallest scaling increase for males was produced from FHD and CAPD with the male slope at 0.322.The smallest scaling increase for females was produced from FHD and DSTTB with the female slope at 0.253.

6.3.1.6: *Macaca mulatta*

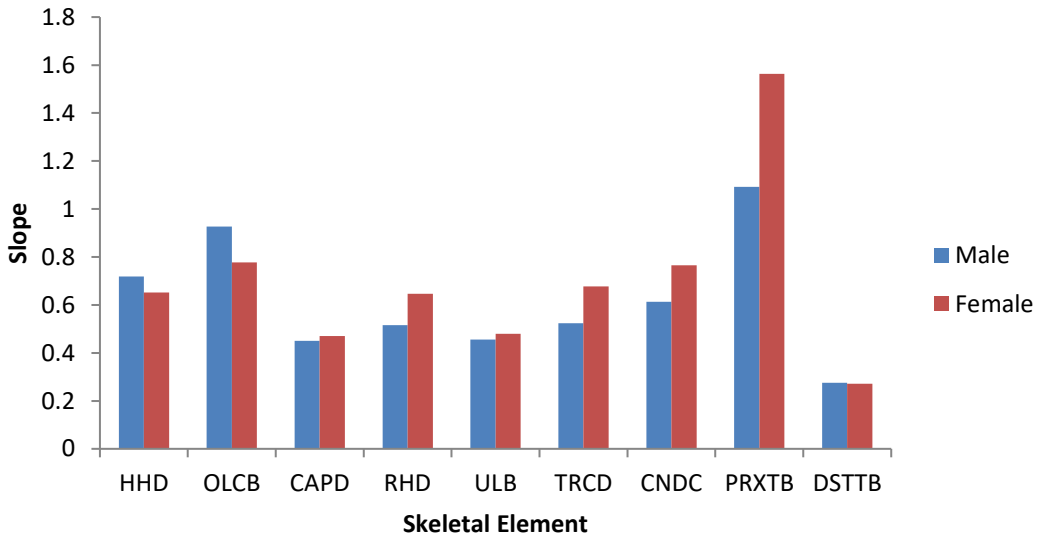

Figure 6.6: The regression slopes produced from *Macaca mulatta* FHD and other skeletal metrics.

There were only small differences in metric scaling between males and females of *Macaca mulatta* for a 1mm increase in FHD. The regression slopes for males ranged between 0.275 and 1.093. The regression slopes for females have a larger range between 0.271 and 1.563. The smallest regression slope difference between the sexes was formed from FHD and DSTTB with the male slope at 0.275 and the female slope at 0.271. The regression slopes for FHD and DSTTB also display the smallest scaling increase between metrics for *Macaca mulatta.* The largest regression slope difference between the sexes was for FHD and PRXTB with the male slope at 1.093 and the female slope at 1.563. The regression slopes for FHD and PRXTB also display the largest scaling increase between metrics for both males and females.

6.3.1.7: *Pan troglodytes*

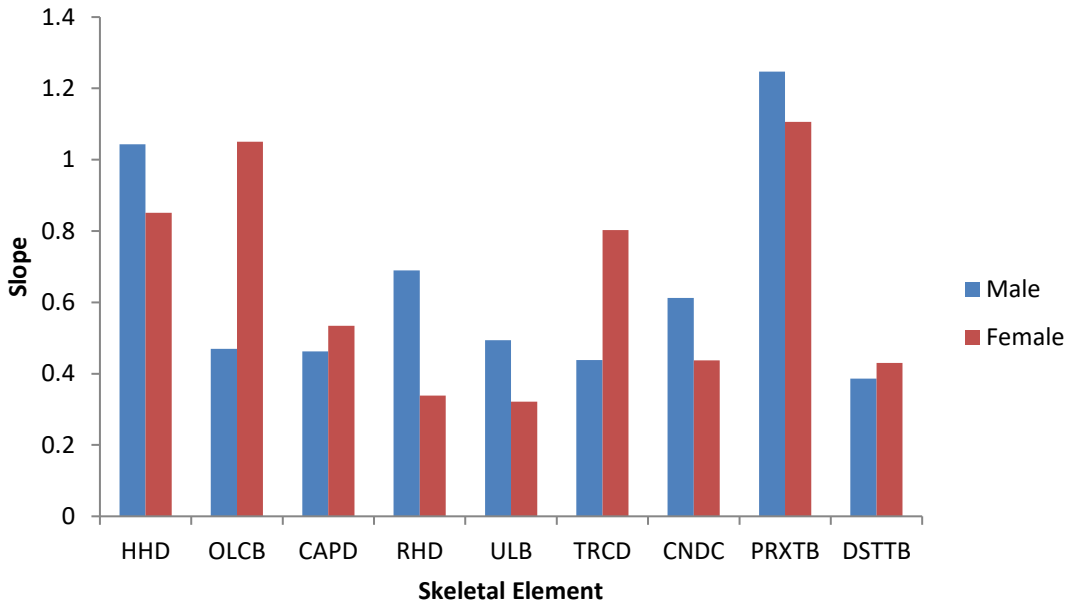

Figure 6.7: The regression slopes produced from *Pan troglodytes* FHD and other skeletal metrics.

There were distinct differences in skeletal metric scaling between males and females of *Pan troglodytes* for a 1mm increase in FHD. The regression slopes for males ranged between 0.386 and 1.247. The regression slopes for females have a smaller range between 0.322 and 1.107. The smallest regression slope difference between the sexes was formed from FHD and DSTTB with the male slope at 0.386 and the female slope at 0.430. FHD and DSTTB also formed the smallest scaling increase between metrics of male *Pan troglodytes.* The smallest scaling difference for females was the FHD and ULB regression slope at 0.322. The largest regression slope difference between the sexes was formed from FHD and OLCB with the male slope at 0.470 and the female slope at 1.051. The largest scaling increase for both males and females was formed between FHD and PRXTB with the male slope at 1.247 and the female slope at 1.107.

6.3.1.8: *Gorilla gorilla*

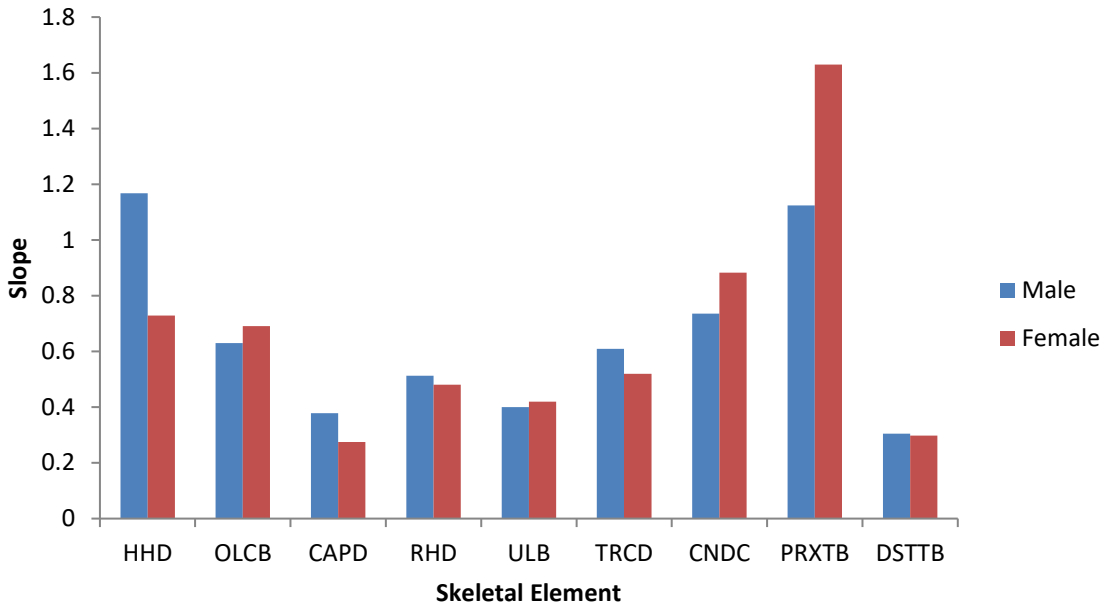

Figure 6.8: The regression slopes produced from *Gorilla gorilla* FHD and other skeletal metrics.

There were only small differences in metric scaling between males and females of *Gorilla gorilla* for a 1mm increase in FHD. The regression slopes for males ranged between 0.305 and 1.168. The regression slopes for females have a larger range between 0.275 and 1.630. The smallest regression slope difference between the sexes was formed from FHD and DSTTB with the male slope at 0.305 and the female slope at 0.298. The regression slope formed from FHD and DSTTB also provided the smallest scaling increase for male metrics of *Gorilla gorilla.* The smallest scaling difference for females was produced from FHD and CAPD with a slope of 0.275. The largest regression slope difference between the sexes was formed from FHD and PRXTB with the male slope at 1.124 and the female slope at 1.630. FHD and PRXTB also provided the largest scaling increase for females. The largest scaling increase for males was formed between FHD and HHD with a slope at 1.168.

6.3.1.9: *Homo sapiens*

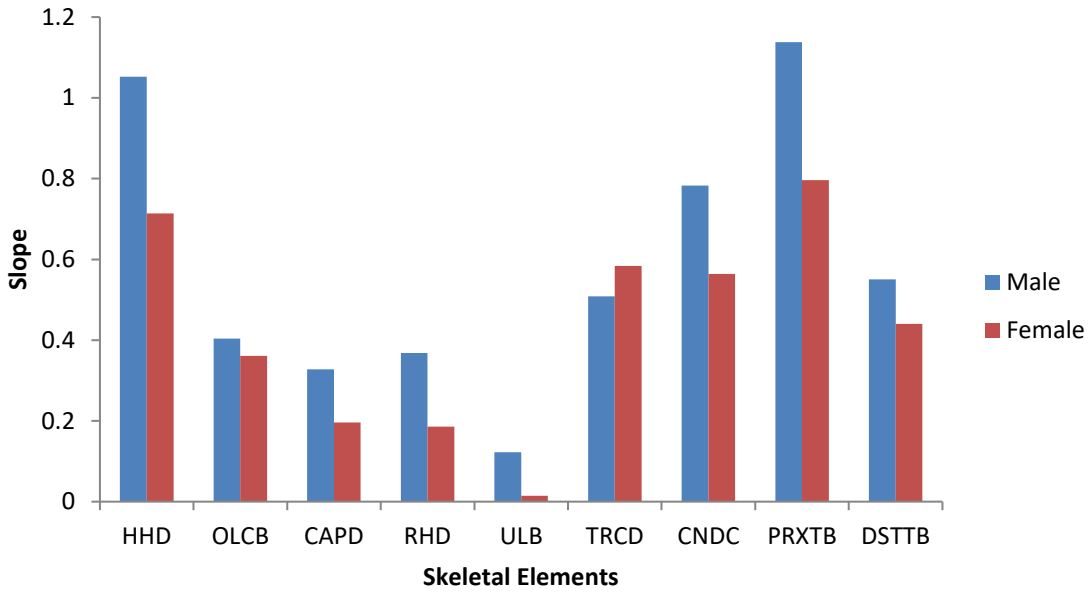

Figure 6.9: The regression slopes produced from *Homo sapiens* FHD and other skeletal metrics.

There were distinct differences in skeletal metric scaling between males and females of *Homo sapiens* for a 1mm increase in FHD. The regression slopes for males ranged between 0.122 and 1.138. The regression slopes for females have a smaller range between 0.015 and 0.796. The smallest regression slope difference between the sexes was formed from FHD and OLCB with the male slope at 0.404 and the female slope at 0.361. The smallest scaling increase for both males and females was produced between FHD and ULB with a male slope at 0.122 and a female slope at 0.015. The largest regression slope difference between the sexes was formed from FHD and PRXTB with the male slope at 1.138 and the female slope at 0.796. FHD and PRXTB also produced regressions with the largest scaling increase for both male and female *Homo sapiens.*

6.3.2: Interspecies scaling differences

The results of this analysis found that scaling differs between males and females in the primate order but there is no standard pattern. By evaluating the scaling relationships produced from one skeletal metric, FHD, with the rest of the sample, the variability can be observed in detail. For some species the scaling relationship between FHD and other metrics express a general pattern of difference between males and females, but for others

there are stark differences between skeletal metrics. There are small differences in scaling between males and females for *Aotus trivirgatus, Macaca mulatta, Gorilla gorilla.* Moderate differences were found for *Saimiri sciureus* and *Chlorocebus pygerythrus*. There are distinct differences in scaling between males and females for *Euoticus elegantulus, Saguinus oedipus, Pan troglodytes* and *Homo sapiens.*

The results of these example regression analyses for metric pairs containing FHD show an unexpected pattern in dimorphism. This is because for some metric pairs the regression slopes for males are greater than females whilst the reverse is true for others. From the three species with small difference in scaling between males and females, *Aotus trivirgatus* and *Macaca mulatta* display slightly more female metrics with a greater change produced from a 1mm increase in FHD. *Gorilla gorilla* has one more male metric with a greater change produced from a 1mm increase in FHD. From the five species with distinct differences in scaling between males and females, *Euoticus elegantulus* and *Saguinus oedipus* display contrasting results. *Euoticus elegantulus* has all nine metrics with a greater female change produced by a 1mm increase in FHD. For *Saguinus oedipus,* all nine metrics have a greater male change produced by a 1mm increase in FHD. *Pan troglodytes* was found to have a near equal split with one more metric displaying a greater male change in the sample. *Homo sapiens*, in contrast, have eight out of nine metrics with a greater male change produced from a 1mm increase in FHD.

The final two species with moderate differences in scaling between males and females, *Saimiri sciureus* and *Chlorocebus pygerythrus* highlight two differences compared to the rest of the sample. *Saimiri sciureus* has generally more female metrics with greater scaling differences, but one metric stands out with a much smaller increase in female TRCD for a 1mm increase in FHD. *Chlorocebus pygerythrus* has a near even split but some metrics show greater differences than others, with the highest slopes of all the regressions produced.

The covariance between FHD and PRXTB produced regression slopes greater than 1 for *Aotus trivirgatus*, *Chlorocebus pygerythrus*, *Macaca mulatta*, *Pan troglodytes*, *Gorilla gorilla* and *Homo sapiens*. This means that for a 1mm increase in FHD there is an increase of PRXTB by over 1mm for these species. This is not unexpected for associated metrics of the lower limb, but provides an example of an allometric relationship that is shared between primate species but displays a varied pattern in dimorphism. The female slope for some of these species is under 1 whilst for others, the male and female slopes are very similar. This

indicates that the scaling relationship between FHD and PRXTB has a general pattern across primate species but not in terms of dimorphism. Plots of the FHDxPRXTB regressions for male and female *Aotus trivirgatus*, *Chlorocebus pygerythrus*, *Macaca mulatta*, *Pan troglodytes*, *Gorilla gorilla* and *Homo sapiens* can be found in Appendix 9.

The negative slope for male *Euoticus elegantulus* FHDxDSTTB is caused by a specimen with a smaller than average DSTTB, though within the interquartile range. When the specimen is removed the regression slope becomes positive at 0.013 and the R^2 value is reduced to 0.0003, suggesting low goodness of fit. Low goodness of fit indicates that the expected values for the regression are far from the actual values. This should be noted when comparing the male and female regression slopes as not all the variability in data is explained through the regression line. For the new positive male *Euoticus elegantulus* slope, the difference between the male and female slopes becomes much smaller, but is a similar amount of variation between the sexes as seen for two other regression slope comparisons in the *Euoticus elegantulus* analysis (FHDxHHD and FHDxULB). Plots of the FHDxDSTTB regressions for *Euoticus elegantulus* males, males without the outlier specimen and females can be found in Appendix 10.

6.4: Analysis of correlation coefficient value difference between males and females of primate species

The correlation coefficient provides a measure of how strong a relationship is between data. A correlation coefficient of 1 suggests a strong positive relationship. A correlation coefficient of -1 indicates a strong negative relationship. Zero suggests no relationship at all. The correlation coefficient is calculated as:

$$r = \frac{n(\Sigma xy) - (\Sigma x)(\Sigma y)}{\sqrt{[n\Sigma x^2 - (\Sigma x)^2] - [n\Sigma y^2 - (\Sigma y)^2]}}$$

Where:
n is the number of pairs of scores

Σxy is the sum of the products of paired scores

Σx is the sum of x scores

Σy is the sum of y scores

Σx^2 is the sum of squared x scores

Σy^2 is the sum of squared y scores

The difference between male and female correlation coefficients provides the strength of coupling between pairs of variables found between the sexes. For the correlation coefficient analysis, male and female data for each species were first converted into seperate z scores. The z score is a measurement showing the relationship between a value and the mean of all values. A z score of 0 means it is the same as the mean. Positive and negative z scores reflect the standard deviations above or below the mean for that value. It removes size to concentrate on proportional change in each value, meaning that large variables do not have a disproportionate effect.

The z score is calculated as:

$$z = \frac{x_i - \bar{x}}{s}$$

Where:

$\bar{x}$ is each value in the data set

x_i is the mean of all values in the data set

s is the standard deviation of a sample

Other studies have analysed the relative scaling of one variable to another to define differences in shape between males and females. Wood (1976) examined whether shape differences between males and females are due to different growth patterns or an allometric relationship between variables, by comparing regression slopes. The study employed five primate species (*Gorilla gorilla, Pan troglodytes, Papio anubis, Papio cynocephalus* and *Colobus guereza*) and utilised teeth, cranial and postcranial measurements. The postcranial metrics were derived from the humerus, femur and pelvis. This study expands on the work of Wood (1976) with an increased number of primate species and a wider range of postcranial metrics using all the long bones.

For these data, the correlation coefficient for all metrics from male specimens was first determined for all 45 standardised metric combinations, per each of the nine species. The correlation coefficient for all metrics from female specimens was then calculated. The difference between the two sexes was explored by subtracting female correlation coefficient values from male correlation coefficient values; negative values therefore indicate instances in which the correlation coefficient between metrics in females was higher than that among males. A clustergram was produced of the output (see Figure 6.10.). Two other clustergrams were produced dividing the upper limb and lower limb data for simpler visualisation (see Figure 6.11. and Figure 6.12.). The differences produced by male and female correlation coefficient values for each metric pairing can be placed onto a scale between -0.700 and 0.800.

6.4.1: Results of the correlation coefficient difference cluster analysis

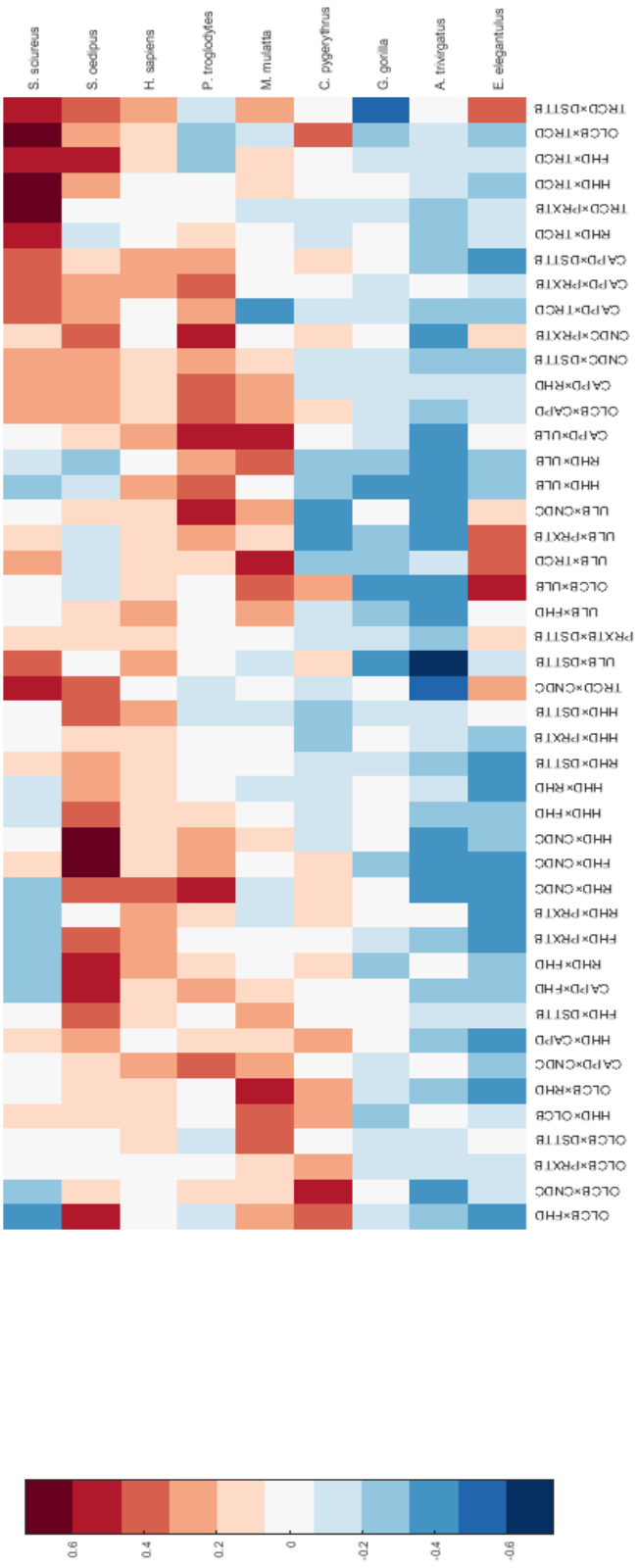

Figure 6.10: Clustergram showing the correlation coefficient difference between males and females for all metric pairs.

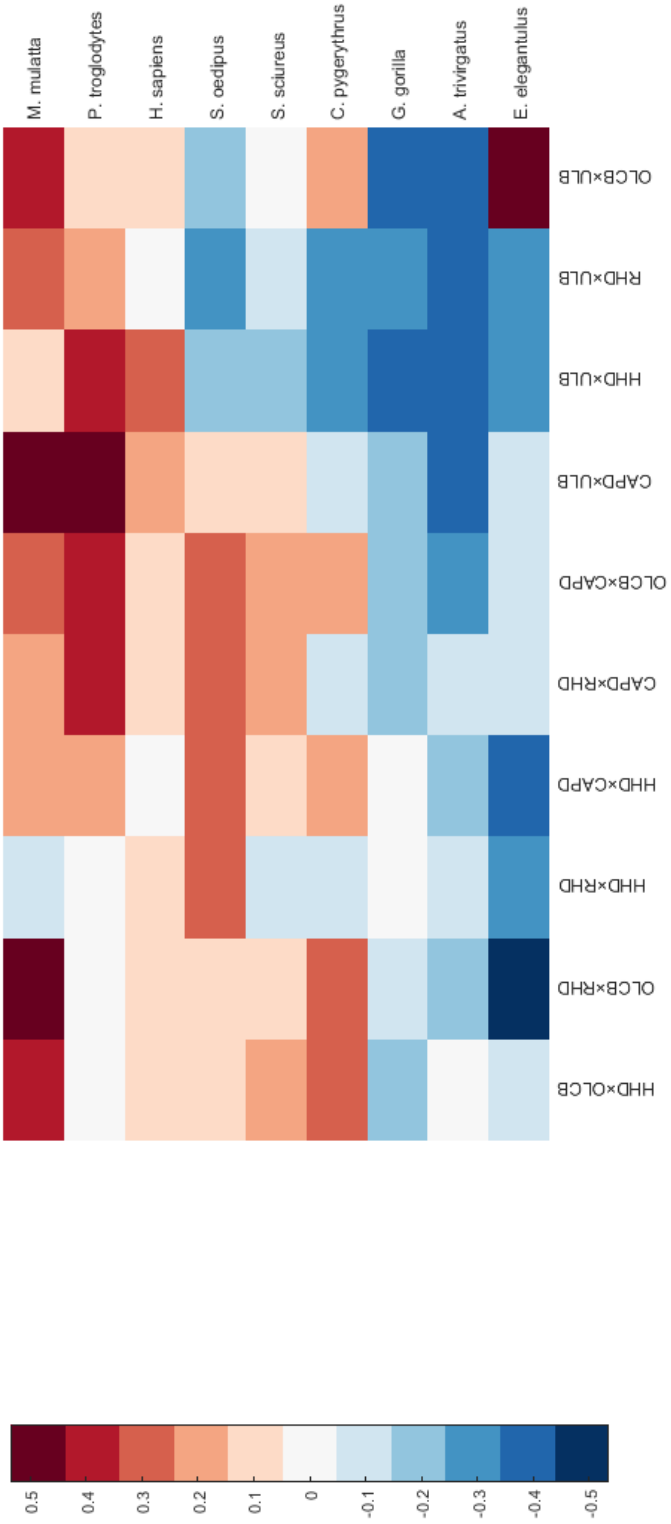

Figure 6.11: Clustergram showing the correlation coefficient difference produced from upper limb metric pairings for all species.

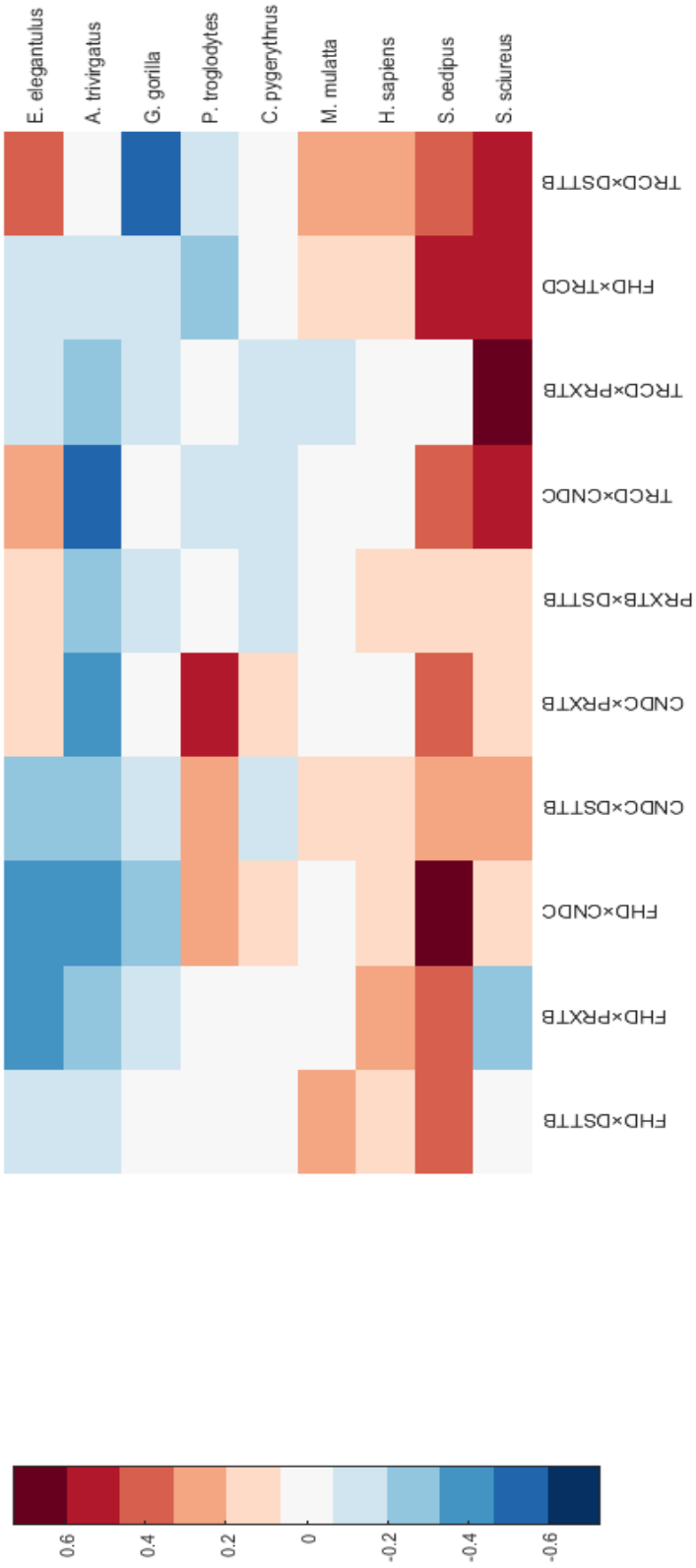

Figure 6.12: Clustergram showing showing the correlation coefficient difference produced from lower limb metric pairings for all species.

6.4.1.1: *Euoticus elegantulus*

Euoticus elegantulus was found to have a mixture of positive and negative differences between male and female correlation coefficients, although the majority of differences were negative. Only four metric pairings have correlation coefficients closer to 0. There were five metric pairings found to have differences between males and females lower than –0.4, OLCBxULB, OLCBxRHD, CAPDxDSTTB, RHDxCNDC, FHDxCNDC and FHDxPRXTB.

The greatest difference between males and females was found in the upper limb correlation coefficient produced from OLCB and ULB at 0.536, with a positive male correlation coefficient at 0.253 and a negative female correlation coefficient at -0.283. When plotted, the negative correlation coefficient value of female *Euoticus elegantulus* OLCBxULB is produced from a general trend for ULB values to decrease as OLCB increases, without an outlier causing the negative slope value. This is in contrast to the pattern for male *Euoticus elegantulus* where there is a general trend for ULB to increase as OLCB increases. *Euoticus elegantulus* is a monomorphic species and whilst the results do suggest a difference between males and females, the actual OLCB and ULB values overlap between the sexes and the R^2 values are low (0.064 and 0.080) indicating a low goodness of fit (see Appendix 11).

Of five correlation coefficient differences lower than -0.4, the greatest difference was produced from an upper limb pairing, OLCBxRHD at -0.459 with a positive male correlation coefficient at 0.270 and a positive female correlation coefficient at 0.729. For lower limb correlation coefficient differences between the sexes, FHDxCNDC was found to have the greatest difference at -0.420, with a positive male correlation coefficient at 0.071 and a positive female correlation coefficient at 0.491. This is closely followed by the correlation coefficient from FHDxPRXTB at -0.407, with a positive male correlation coefficient of 0.359 and positive female correlation coefficient of 0.766.

6.4.1.2: *Aotus trivirgatus*

Aotus trivirgatus was found to have only negative differences between male and female correlation coefficients. Six of the metric pairings have correlation coefficient differences closer to 0. The greatest difference between males and females was found in the correlation coefficient between upper limb metric ULB and lower limb metric DSTTB at -0.652, with a positive male correlation coefficient at 0.031 and a positive female

correlation coefficient at 0.684. Seven metric pairs were found to have correlation coefficient differences between males and females lower than -0.4, TRCDxCNDC, HHDxCNDC, OLCBxCNDC, CAPDxULB, RHDxCNDC, ULBxPRXTB and CNDCxPRXTB.

For upper limb metric pairings, the greatest correlation coefficient difference was found for CAPDxULB at -0.413, with a positive male correlation coefficient at 0.198 and a positive female correlation coefficient at 0.611. The second greatest difference between males and females was produced from the lower limb metrics TRCDxCNDC at -0.584, with a negative male correlation coefficient at -0.041 and a positive female correlation coefficient at 0.543.

6.4.1.3: *Saguinus oedipus*

Saguinus oedipus was found to have a mixture of positive and negative differences between male and female correlation coefficients although the majority of differences are positive. Only five of the metric parings have correlation coefficient differences closer to 0.

The greatest difference between males and females was found in the correlation coefficient between upper limb metric HHD and lower limb metric CNDC at 0.632, with a positive male correlation coefficient at 0.568 and a negative female correlation coefficient at -0.064. This is closely followed by the lower limb pairing FHDxCNDC with a difference between males and females of 0.612, with a positive male correlation coefficient at 0.605 and a negative female correlation coefficient at -0.007. Three other metric pairs were found to have correlation coefficient differences between males and females higher than 0.5, OLCBxFHD, CAPDxFHD and RHDxFHD. For upper limb metrics, the difference between the sexes was far smaller with the greatest variation produced from RHDxULB at -0.323 with a positive male correlation coefficient at 0.423 and a positive female correlation coefficient at 0.746.

6.4.1.4: *Saimiri sciureus*

Saimiri sciureus was found to have a mixture of positive and negative differences between male and female correlation coefficients. Twelve of the metric parings have correlation coefficient differences closer to 0. The greatest difference between males and females was found TRCDxPRXTB correlation coefficient at 0.729. This is because a positive correlation

coefficient at 0.546 was displayed for male TRCDxPRXTB whilst a negative correlation coefficient of -0.182 was displayed for female TRCDxPRXTB.

The next metric pairs with high difference in correlation coefficients between males and females were HHDxTRCD, OLCBxTRCD and OLCBxFHD. For HHDxTRCD, the difference between sexes was 0.664 with a positive male correlation coefficient of 0.537 and a negative female correlation coefficient of -0.127. For OLCBxTRCD, the difference between sexes was 0.656 with a positive male correlation coefficient of 0.441 and a negative female correlation coefficient of -0.214. OLCBxFHD had the greatest negative difference between males and females at -0.336, with a positive male correlation coefficient at 0.170 and a positive female correlation coefficient at 0.505.

6.4.1.5: *Chlorocebus pygerythrus*

Chlorocebus pygerythrus was found to have a mixture of positive and negative differences between male and female correlation coefficients. Although the majority of metric pairs display negative differences, some of the greatest differences are positive. Ten of the metric parings have correlation coefficient differences closer to 0. The greatest difference between males and females was found in the correlation coefficient between upper limb OLCB and lower limb CNDC at 0.465, with a positive male correlation coefficient of 0.609 and a positive female correlation coefficient of 0.144. The next two metric pairs with the greatest positive differences between sexes are upper and lower limb pairings, OLCBxTRCD and OLCBxFHD. For OLCBxTRCD, the difference between sexes was 0.399, with a positive correlation coefficient at 0.590 and a positive female correlation coefficient at 0.191. For OLCBxFHD, the difference between sexes was 0.394, with a positive male correlation coefficient at 0.695 and a positive female correlation coefficient at 0.301.

The metric pair with the greatest negative difference between male and female correlation coefficients was upper and lower limb pairing, ULBxPRXTB at -0.455, with a positive male correlation coefficient at 0.132 and a positive female correlation coefficient at 0.588. The upper limb pairing ULBxCNDC has the next greatest negative difference between male and females at -0.430, with a positive male correlation coefficient at 0.252 and a positive female correlation coefficient at 0.682. For lower limb metrics, the correlation coefficient difference between the sexes was far smaller with the greatest difference produced by

PRXTBxDSTTB at -0.136 with a positive male correlation coefficient at 0.501 and a positive female correlation coefficient at 0.636.

6.4.1.6: *Macaca mulatta*

Macaca mulatta was found to have a mixture of positive and negative differences between male and female correlation coefficients, although the majority of differences are positive. Thirteen of the metric parings have correlation coefficient differences closer to 0. The greatest difference between males and females was found for upper limb OLCBxRHD at 0.497, with a positive male correlation coefficient of 0.825 and a positive female correlation coefficient of 0.328. The upper limb pairing CAPDxULB had the next greatest difference between males and females at 0.469, with a positive male correlation coefficient of 0.520 and a positive female correlation coefficient of 0.052. The upper and lower limb pairing CAPDxTRCD has the greatest negative difference between male and female correlation coefficienta at -0.344, with a positive male correlation coefficient of 0.297 and a positive female correlation coefficient of 0.642. For lower limb metrics, the correlation coefficient difference between the sexes was far smaller with the greatest difference produced by FHDxDSTTB at 0.248 with a positive male correlation coefficient at 0.691 and a positive female correlation coefficient at 0.442.

6.4.1.7: *Pan troglodytes*

Pan troglodytes was found to have generally positive differences between male and female correlation coefficients. Fourteen of the metric parings have correlation coefficient differences closer to 0. The greatest difference between males and females was found in the correlation coefficient between upper limb metric ULB and lower limb metric CNDC at 0.530. This is because the positive correlation coefficient of 0.656 was displayed for male ULBxCNDC and the positive correlation coefficient of 0.126 was displayed for female ULBxCNDC.

The next metric pair with a high difference in correlation coefficients between males and females was upper limb CAPDxULB at 0.522 with a positive male correlation coefficient at 0.170 and a negative female correlation coefficient at -0.352. The upper and lower limb pairing RHDxCNDC correlation coefficient difference was also high for *Pan troglodytes* at

0.468, with a positive male correlation coefficient of 0.673 and positive female correlation coefficient of 0.205. For lower limb metrics, CNDCxPRXTB produced a high correlation coefficient difference of 0.522 with a positive male correlation coefficient of 0.836 and a positive female correlation coefficient of 0.314.

6.4.1.8: *Gorilla gorilla*

Gorilla gorilla was found to have generally negative differences between male and female correlation coefficients. Sixteen of the metric pairings have correlation coefficient differences closer to 0. The greatest difference between males and females was found in the correlation coefficient between lower limb TRCD and DSTTB at -0.563. This is because the negative correlation coefficient of -0.020 was displayed for male TRCDxDSTTB whilst the positive correlation coefficient of 0.544 was displayed for female TRCDxDSTTB.

The next metric pairs with high difference in correlation coefficients between males and females were OLCBxULB, HHDxULB and ULBxDSTTB. For upper limb OLCBxULB, the difference between sexes was -0.438, with a positive male correlation coefficient of 0.183 and a positive female correlation coefficient of 0.621. For upper limb HHDxULB, the difference between sexes was -0.345, with positive male covariance correlation coefficient of 0.378 and positive female correlation coefficient of 0.723. For upper and lower limb pairing ULBxDSTTB, the difference between the sexes was -0.340, with a positive male correlation coefficient of 0.085 and a positive female correlation coefficient of 0.425.

6.4.1.9: *Homo sapiens*

Homo sapiens was found to have generally positive differences between male and female correlation coefficients. Eleven of the metric pairings have correlation coefficient differences closer to 0. Only one metric pair had a correlation coefficient difference greater than 0.4. This metric pair was upper limb RHD and lower limb CNDC, with the difference between sexes at 0.458, with a positive male correlation coefficient at 0.567 and a positive female correlation coefficient at 0.109. For the majority of metric pairs the difference between male and female correlation coefficients was between 0.1 and 0.2. For upper limb metrics, the greatest correlation coefficient difference between the sexes was produced by HHDxULB at 0.289, with a positive male correlation coefficient at 0.368 and a positive

female correlation coefficient at 0.078. For lower limb metrics, the greatest correlation coefficient difference between the sexes was produced by TRCDxDSTTB at 0.288 with a positive male correlation coefficient at 0.657 and a positive female correlation coefficient at 0.473.

6.4.2: Summary for correlation coefficient difference cluster analysis

This analysis was able to answer the first question of how complex is the scaling of sexual dimorphism in the primate skeleton. The results show there is a great amount of variation in skeletal scaling differences between males and females of each species. The monomorphic species, *Euoticus elegantulus*, *Aotus trivirgatus* and *Saguinus oedipus* have smaller numbers of metric pairings with correlation coefficient differences between males and females closer to 0. This means that they have the smallest number of metric pairs with either positive male correlation coefficients equal to positive female correlation coefficients or negative male correlation coefficients equal to negative female correlation coefficients. Generally metric pairings where one metric is derived from the upper limb whilst the other metric is derived from the lower limb were more frequently found to have greater differences in correlation coefficients between males and females for all species.

Metric pairings containing the upper limb measurement ULB were commonly found to have greater variation between male and female correlation coefficients. OLCBxULB had the greatest difference between sexes for *Euoticus elegantulus* with males displaying positive correlation coefficients and females displaying negative correlation coefficients. This means that for males, the two metrics change in the same direction whilst for females the two metrics are inversely related. For *Aotus trivirgatus*, the large negative difference value produced for ULBxDSTB was due to a greater positive female correlation coefficient. For *Chlorocebus pygerythrus*, the metric pairing ULBxPRXTB was also found to have a distinct difference with the positive female correlation coefficient found to be higher than the male correlation coefficient. For *Pan troglodytes*, ULBxCNDC was found to have the greatest difference between male and females with a positive male correlation coefficient much greater than the females. CAPDxULB also showed a large amount of difference for *Pan troglodytes*, produced by males displaying a positive correlation coefficient and females displaying a negative correlation coefficient. For *Gorilla gorilla*, three metric pairs with high differences between the sexes were OLCBxULB, HHDxULB and ULBxDSTTB. The

three metric pairings displayed large differences because the positive correlation coefficients are greater in females than males.

Metric pairings containing the upper limb measurement OLCB were also found to frequently display large differences between male and female correlation coefficients. For *Euoticus elegantulus*, OLCBxULB correlation coefficient difference was produced by a positive male correlation coefficient against a negative female correlation coefficient. The metric pairing FHDxOLCB displayed a large correlation coefficient difference for *Saguinus oedipus* with a higher positive male correlation coefficient than female. For *Saimiri sciureus,* two metric pairings containing OLCB were found to produce large correlation coefficient differences between the sexes. The result of the metric pairing OLCBxFHD was formed from positive correlation being greater in females than males. The other OLCB metric pairing noted as providing a high difference for *Saimiri sciureus*, OLCBxTRCD, has a greater negative male correlation coefficient than a positive female correlation coefficient. For *Chlorocebus pygerythrus*, three metric pairs containing OLCB gave large differences, OLCBxCNDC, OLCBxTRCD and OLCBxFHD. All three metrics have male positive correlation coefficients far greater than female correlation coefficients. For *Macaca mulatta*, OLCBxRHD has the largest difference with the positive male correlation coefficient greater than the female correlation coefficient. For *Gorilla gorilla*, OLCBxULB was one of the metric pairs found to have a distinct difference in correlation coefficients between males and females, with the positive correlation coefficient greater in females.

The lower limb metric CNDC is also common in metric pairings with high differences between males and females. For *Saguinus oedipus*, HHDxCNDC and FHDxCNDC, produced greater positive male correlation coefficients. For *Chlorocebus pygerythrus* OLCBxCNDC, a large difference between the sexes was produced by the positive male correlation coefficient being greater than the positive female correlation coefficient. For *Pan troglodytes*, the metric pairing ULBxCNDC, was also found to have a greater male correlation coefficient than female correlation coefficient. The metric pairing RHDxCNDC had the greatest difference for *Homo sapiens*, with the positive male correlation coefficient also greater than the positive female correlation coefficient. Overall, the results of this analysis were also able to answer the question of whether the difference in scaling between males and females varies depending on the area of the skeleton. The correlation coefficient difference between the sexes varied greatly depending on whether the scaling was between upper or lower limb metrics.

6.5: Hierarchical clustering analysis of skeletal scaling dimorphism

Hierarchical clustering was employed to evaluate similarity and differences between scaling sexual dimorphism within the primate order and to answer the question of how similar are humans to other species in the primate order in terms of sexual dimorphism scaling. The dendrogram is an output of hierarchical clustering that presents which species have the most distance or dissimilarity between clusters. Ward's method was chosen as the linkage method for the hierarchical clustering analysis. It employs the incremental sum of squares to form a linkage between clusters. The total within-cluster sum of squares is formed when two clusters are joined and is calculated as the sum of the squares of the distances between data points in the cluster and the centroid. The initial cluster distances are defined as the Euclidean distance between points. The advantage of performing Ward's method with criterion values that are first inputted as Euclidean distance, rather than squared Euclidean distance, is that a direct comparison can be made between the ultrametric distance produced on the dendrogram and the input distances (Murtagh, 2014). The method is also particularly suitable for continuous variables. The distance metric for this hierarchical clustering analysis is given as:

$$d(r,s) = \sqrt{\frac{2n_r n_s}{(n_r+n_{s)}}}\,\|\bar{x}_r - \bar{x_s}\|_{2,}$$

Where:

$\|_2$ is the Euclidean distance

$\bar{x}_r$ and $\bar{x}_s$ are the centroids of clusters r and s

n_r and n_s are the number of elements in clusters r and s

After standardisation (see section 6.4: *Analysis of correlation coefficient value difference between males and females of primate species*) a 10x10 matrix of correlations between metrics was produced for males and females of each species. The 10x10 matrix was then reduced to 45 unique values (removing repeats of correlation coefficients from the matrix). This data was then used to perform the hierarchical clustering for female and male data respectively. Correlation coefficient difference was calculated by subtracting female correlation coefficients from the male correlation coefficients. The 10x10 matrix of

correlation coefficient difference values between males and females was produced for each species. The matrix was then reduced to the 45 unique correlation coefficient difference values before hierarchical clustering was performed. The same procedure was employed for the hierarchical clustering of upper and lower limb data respectively.

Dendrograms were used for displaying the hierarchical clustering analysis of male correlation coefficients, female correlation coefficients and the difference in correlation coefficients between the sexes. The difference in correlation coefficients between males and females was further divided into two separate hierarchical clustering analyses for the upper limb and lower limb data points respectively. This provides an evaluation of the difference in upper and lower limb clustering and how metrics from separate areas of the skeleton influence the overall clustering for correlation coefficient differences between the sexes.

A further hierarchical clustering analysis, only utilising the statistically significant regression slope differences was also performed, based on statistical significance defined through an ANCOVA analysis. ANCOVA can be used to compare two or more regression lines, by testing the effect of a categorical factor on a dependent variable, whilst controlling for continuous co-variates. The results of the ANCOVA for all species can be found in Appendix 12. No statistically significant differences between male and female slopes were found for the monomorphic species, *Euoticus elegantalus, Aotus trivirgatus* and *Saguinus oedipus*. Statistically significant differences were found for 21 metric pairings across the dimorphic species (see Table 6.1.). The hierarchical clustering analyses were therefore performed using the slopes with statistically significant differences between males and females for *Chlorocebus pygerythrus, Saimiri sciureus, Macaca mulatta, Gorilla gorilla, Pan troglodytes* and *Homo sapiens*. Dendrograms were produced of male slopes, female slopes and the difference between the two.

Table 6.1: Metric pairings with statistically significant differences between regression slopes for males and females (*Chlorocebus pygerythrus, Saimiri sciureus, Macaca mulatta, Gorilla gorilla, Pan troglodytes* and *Homo sapiens*).

Upper limb pairing	Upper limb & lower limb pairing
OLCBxHHD	ULBxFHD
CAPDxHHD	ULBxCNDC
RHDxHHD	ULBxPRXTB
RHDxOLCB	ULBxDSTTB
ULBxHHD	FHDxCAPD
ULBxOLCB	TRCDxHHD
ULBxCAPD	TRCDxOLCB
ULBxRHD	TRCDxCAPD
	CNDCxHHD
	CNDCxCAPD
	DSTTBxHHD
	DSTTBxOLCB
	DSTTBxCAPD

The results of the ANCOVA corroborate the finding that scaling differences are greater between metric pairings where one is from the upper limb and the other is from the lower limb. This suggests that there is a greater difference between males and females in terms of the scaling relationship between the upper and lower body. No statistically significant difference between male and female regression slopes was found for lower limb metric pairings. This indicates that the scaling between lower limb metrics is more similar between the sexes than scaling in other areas of the skeleton.

The output of these analyses was used to answer the following questions:

1. Which species are most similar in terms of the correlation coefficient difference between the sexes?

2. Is there a distinct difference in clustering when utilising data from the upper limb compared to data from the lower limb?
3. Which species are humans most similar to in terms of correlation coefficient difference between the sexes?

Hierarchical clustering can define which species are most similar in terms of distance between clusters. This means that it is suitable for defining which species are most similar in terms of the correlation coefficient difference between the sexes. By evaluating clusters and similarity, patterns of scaling dimorphism in the primate order can be determined. Splitting the upper and lower limb into separate hierarchical clustering analyses supplies greater detail for determining how dimorphism patterns in the primate order are distributed within the skeleton. Understanding which species are most similar to humans will be useful for evaluating how scaling dimorphism can affect studies of hominin dimorphism. The analysis can also define whether dimorphism in the upper and lower limb is similar to the same species, meaning the species that can provide the best comparative sample for upper and lower limb metrics are highlighted.

6.5.1: Results of the hierarchical clustering analyses

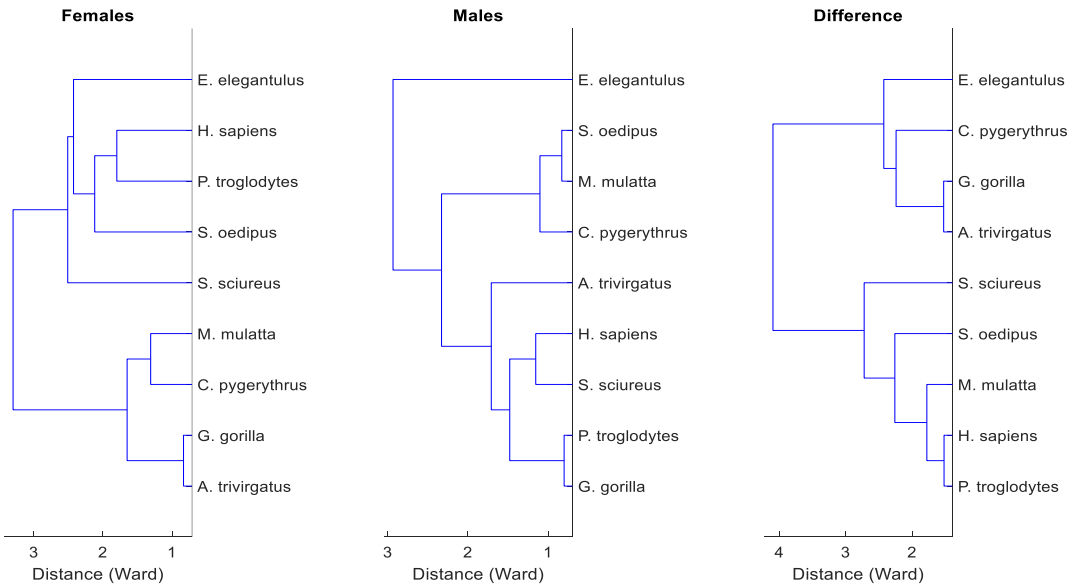

Figure 6.13: Dendrograms of female correlation coefficients, male correlation coefficients and the difference between the two.

6.5.1.1: Results of the hierarchical clustering analysis for all female correlation coefficient data

The hierarchical clustering of regression data for all females divides into two main clusters at a distance of 3 (the unit defined in the Ward's method distance metric formula above). Greater distances indicate greater dissimilarity between species. *Saimiri sciureus* is added to the first cluster at the greatest distance of 2.6. *Euoticus elegantulus* is added at the slightly shorter distance of 2.5. *Saguinus oedipus* is added next at a distance of 2.3 before the pairing of *Homo sapiens* and *Pan troglodytes* is added at a distance of 1.8. The second cluster divides into two pairings at a distance of 1.7. The *Macaca mulatta* and *Chlorocebus pygerythrus* pairing is added first at a distance of 1.4 and the pairing of *Gorilla gorilla* and *Aotus trivirgatus* is added at the shortest distance of 0.8.

6.5.1.2: Results of the hierarchical clustering analysis for all male correlation coefficient data

The hierarchical clustering of regression data for all males divided into two main clusters with the first consisting of *Euoticus elegantulus* as an outlier added at the greatest distance of 2.9. The rest of the species are added in the second main cluster that divides into two subclusters. The first subcluster adds *Aotus trivirgatus* at a distance of 1.8. The *Homo sapiens* and *Saimiri sciureus* pairing is then added at 1.3 before *Pan troglodytes* and *Gorilla gorilla* are added at the shortest distance of 0.8. The second subcluster adds *Chlorocebus pygerythrus* at a distance of 1.2 before adding the *Saguinus oedipus* and *Macaca mulatta* at the shorter distance of 0.9.

6.5.1.3: Results of the hierarchical clustering analysis for correlation coefficient difference between males and females

Hierarchical clustering also formed groups from the skeletal metric correlation coefficient differences between males and females of each species. Figure 6.13. shows two clusters at a distance of 3, which then divides into three clusters at a distance of 2.5. The first of the two main clusters adds *Saimiri sciureus* at the highest distance of 2.7, with *Saguinus oedipus* added after. *Macaca mulatta* is added to the cluster next before the pairing of

Homo sapiens and *Pan troglodytes* at the shortest distance of 1.6. The second main cluster fuses at 2.5 with the addition of *Euoticus elegantulus*. *Chlorocebus pygerythrus* is added to the cluster at a distance of 2.3 before the pairing of *Gorilla gorilla* and *Aotus trivirgatus* at the shortest distance of 1.6, shared with the pairing of *Homo sapiens* and *Pan troglodytes* in the first cluster.

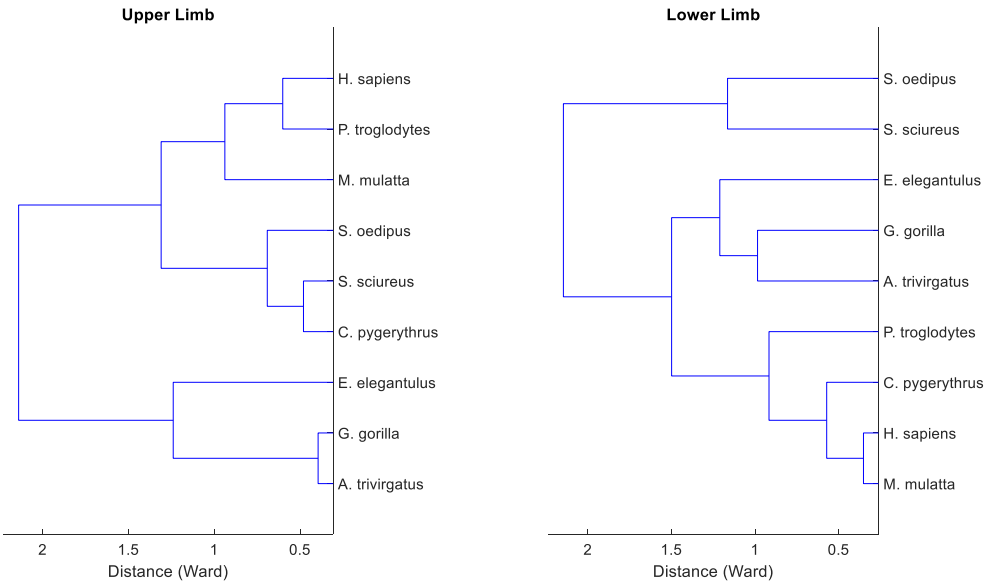

Figure 6.14: Dendrograms of upper and lower limb correlation coefficient difference between males and females.

6.5.1.4: Results of the hierarchical clustering analysis for upper limb correlation coefficient difference between males and females

The hierarchical clustering formed groups from the upper limb skeletal metric correlation coefficient differences between males and females of each species. Figure 6.14. shows two main clusters at a distance of 1.5, which divides into four clusters at a distance of 1.3. For the first main cluster, *Euoticus elegantulus* is added at the highest distance of 1.3 with the *Gorilla gorilla* and *Aotus trivirgatus* pairing added to the cluster at the shortest distance of 0.4. The second main cluster splits into two subclusters with *Macaca mulatta* added at the greatest distance of 1.0., with the *Homo sapiens* and *Pan troglodytes* pairing added at 0.7. *Saguinus oedipus* is added to the second subcluster at 0.8 with the *Saimiri sciureus* and *Chlorocebus pygerythrus* pairing added at the shorter distance of 0.6.

6.5.1.5: Results of the hierarchical clustering analysis for lower limb correlation coefficient difference between males and females

The hierarchical clustering formed groups from the lower limb skeletal metric correlation coefficient differences between males and females of each species. Figure 6.14. shows two clusters at a distance of 2.0. The first main cluster is divided into two subclusters at a distance of 1.5 with *Euoticus elegantulus* added first at the greatest distance of 1.2. *Gorilla gorilla* and *Aotus trivirgatus* are then added to the cluster at the shorter distance of 1.0. The secondary subcluster adds *Pan troglodytes* at the shorter distance of 0.9 with *Chlorocebus pygerythrus* then added at 0.6 before the *Homo sapiens* and *Macaca mulatta* pairing added at the shortest distance of 0.3. The second main cluster pairs *Saguinus oedipus* and *Saimiri sciureus* at a distance of 1.1.

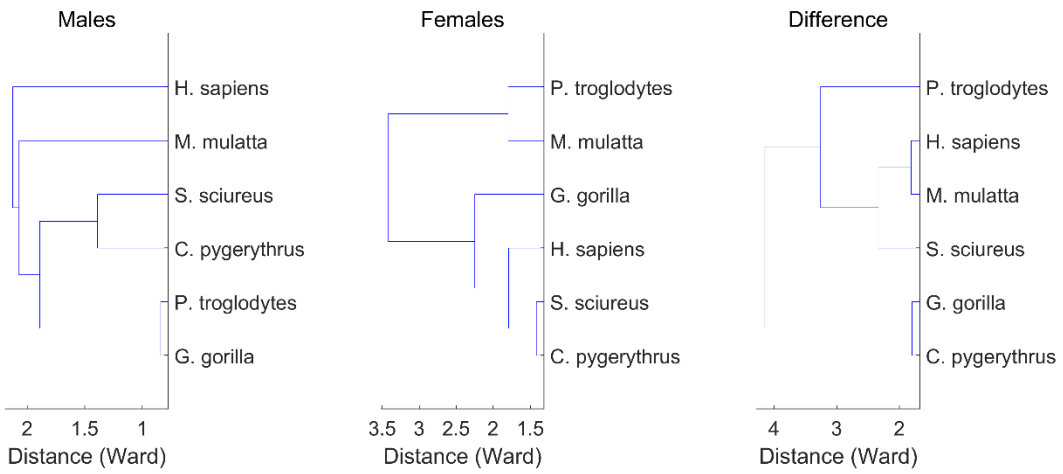

Figure 6.15: Dendrograms of male slopes, female slopes and the difference between males and females for slopes with statistically significant differences between males and females.

6.5.1.6: Results of the hierarchical clustering analysis for female regression slopes.

The hierarchical clustering of regression slope data for all females divides into two main clusters at a distance of 3.4. *Gorilla gorilla* is added to the first cluster at a distance of 2.3.

Homo sapiens is added at the shorter distance of 1.8. The *Saimiri sciureus* and *Chlorocebus pygerythrus* pairing is finally added to the first cluster at a distance of 1.4. The *Pan troglodytes* and *Macaca mulatta* pairing is added to the second cluster at a distance of 1.9.

6.5.1.7: Results of the hierarchical clustering analysis for male regression slopes.

The hierarchical clustering of regression slope data for all males divides into four clusters at a distance of 1.8. *Homo sapiens* is added first at the greatest distance of 2.2. *Macaca mulatta* is added at a distance of 2.1. The *Saimiri sciureus* and *Chlorocebus pygeyrthrus* pairing is added next at a distance of 1.4. The *Pan troglodytes* and *Gorilla gorilla* pairing is added at the shortest distance of 0.3.

6.5.1.8: Results of the hierarchical clustering analysis based on the differences between male and female slopes.

The hierarchical clustering based on the differences between male and female regression slopes divides into two clusters at a distance of 4.2. *Pan troglodytes* is added to the first cluster at a distance of 3.3. *Saimiri sciureus* is added to the cluster at a distance of 2.3. The pairing of *Homo sapiens* and *Macaca mulatta* is finally added to the cluster at a distance of 1.8. The second cluster is made up of the *Gorilla gorilla* and *Chlorocebus pygerythrus* pairing at 1.7.

6.5.2: Summary of the hierarchical clustering analyses

In answer to the question of which species are most similar in terms of correlation coefficient difference between the sexes, the hierarchical clustering of correlation coefficient difference found the closest similarity in data points was between two pairs of species, *Gorilla gorilla* and *Aotus trivirgatus* and *Homo sapiens* and *Pan troglodytes*. This compares to the female clustering where *Gorilla gorilla* and *Aotus trivirgatus* are closest, but contrasts with the male hierarchical clustering, which found *Gorilla gorilla* and *Pan troglodytes* closest in similarity. As members of the family hominidae, *Gorilla gorilla, Pan troglodytes* and *Homo sapiens* share a relatively close evolutionary relationship and so the

correlation coefficients between skeletal metrics for both males and females was expected to be similar between these species. The similar pattern of female correlation coefficients and the correlation coefficient difference between male and female *Gorilla gorilla* and *Aotus trivirgatus* does not reflect phylogeny and indicates a female pattern caused by other factors.

Saimiri sciureus shows the most dissimilarity between species in terms of the correlation coefficient difference between males and females. *Saimiri sciureus* was added to the hierarchical clustering at a greater distance in females than males. Therefore, the dissimilarity to other data points found for correlation coefficient differences between males and females reflects the female data pattern more than the male data pattern. *Euoticus elegantulus* is one of the first species to be added to all the dendrograms indicating dissimilarity of data points to the other species for both male correlation coefficients, female correlation coefficients and the difference between them. The *Euoticus elegantulus* result reflects the expected phylogenetic difference between a strepsirrhine and the rest of the primate species. The dissimilarity of *Saimiri sciureus* in terms of correlation coefficient difference values between the sexes is more surprising and suggests a pattern of dimorphism that differs greatly from other primate species, regardless of evolutionary relationship.

Overall, the results do not represent traditional explanations and suggest unusual comparator species. The pattern of correlation coefficient difference between the sexes is not always the same for closely related species, indicating that factors other than phylogeny are influencing dimorphism within primate skeleton. These findings mean that a more nuanced view of primate sexual dimorphism is required that reflects the varied pattern of correlation coefficient difference between taxa.

In answer to the question of which species are humans most similar to, female *Homo sapiens* were closest to female *Pan troglodytes* whilst male *Homo sapiens* were more similar to *Saimiri sciureus*. The female pairing of *Homo sapiens* and *Pan troglodytes* was added at a greater distance than the male pairing of *Homo sapiens* and *Saimiri sciureus* indicating the close similarity of the male data points. The hierarchical clustering representing the correlation coefficient difference between males and females shows that *Homo sapiens* are more similar *Pan troglodytes*, with *Saimiri sciureus* added at a greater distance.

The hierarchical clustering of correlation coefficient differences divided into the upper and lower limb is able to answer the question of whether there are distinct differences in clustering when utilising data from the upper limb compared to data from the lower limb. For upper limb data points, the correlation coefficient difference between males and females was most similar in *Gorilla gorilla* and *Aotus trivirgatus*. For lower limb data points, the correlation coefficient difference between males and females was most similar in *Homo sapiens* and *Macaca mulatta*. *Euoticus elegantulus* has the most dissimilarity to other species being added at the greatest distance for both the upper and lower limb hierarchical clustering. *Homo sapiens* were found to be more similar to *Pan troglodytes* in terms of upper limb correlation coefficient differences between the sexes. The results of the upper limb analysis suggest an example of phylogenetic inertia with the similar pattern between *Pan troglodytes* and *Homo sapiens* representing a constraint on the evolution of the upper limb.

The separated upper and lower limb clustering can be compared to the combined hierarchical clustering for correlation coefficient difference between males and females. *Macaca mulatta* was added to the overall dendrogram of correlation coefficient difference at a greater distance than the *Homo sapiens* and *Pan troglodytes* pairing, which is similar to the pattern found from upper limb data points. This indicates that the correlation coefficient difference between males and female upper limb metrics are contributing more to the overall pattern of hierarchical clustering, an influence from the greater level of dimorphism found in the primate upper limb as defined in previous chapters. The structure of sexual dimorphism in the *Homo sapiens* upper limb is closest to that of *Pan troglodytes*, whereas the structure of sexual dimorphism in the lower limb is closest to that of *Macaca mulatta*.

The hierarchical clustering analyses based on slopes that displayed statistically significant differences between males and females, also found variation from phylogeny. For male slopes, *Homo sapiens* was added to the hierarchical clustering at the furthest distance from *Pan troglodytes. Homo sapiens* female data points were closest to the *Saimiri sciureus* and *Chlorocebus pygeyrthrus* pairing. For the hierarchical clustering based on the difference between male and female slopes, *Homo sapiens* were found to be most similar to *Macaca mulatta,* a pairing also produced in the the lower limb clustering analysis from all data.

Gorilla gorilla slope difference data points were most similar to *Chlorocebus pygerythrus,* which contrasts with the hierarchical clustering analyses using all data. This is because of

the removal of *Aotus trivirgatus,* which though without statistically significant differences between male and female regressions, was found to show the most similarity with *Gorilla gorilla. Chlorocebus pygerythrus* was the next closest species to *Gorilla gorilla* after *Aotus trivirgatus* in the hierarchical clustering analysis based on correlation coefficient data, indicating similarities using both statistically significant and non-statistically significant data for these species. This suggests that although some of the slopes in the original analyses were not significant, they still contribute some explanation of the variation between species when considered in the multi-dimensional space implied by these analyses.

6.6: A comparison of *Pan troglodytes* and *Homo sapiens* skeletal scaling dimorphism

The hierarchical clustering analysis highlighted the closeness between data points of *Pan troglodytes* and *Homo sapiens*. The difference between male and female correlation coefficients for skeletal metric pairs can be compared between *Pan troglodytes* and *Homo sapiens* to determine similarities and differences. This can be displayed visually as a bar graph. For ease of analysis, the bar graphs can be split into metric pairings with both upper limb metrics, pairings with both lower limb metrics and pairings with an upper and lower limb metrics.

6.6.1: Difference in upper limb correlation coefficients found between males and females for *Pan troglodytes* and *Homo sapiens*

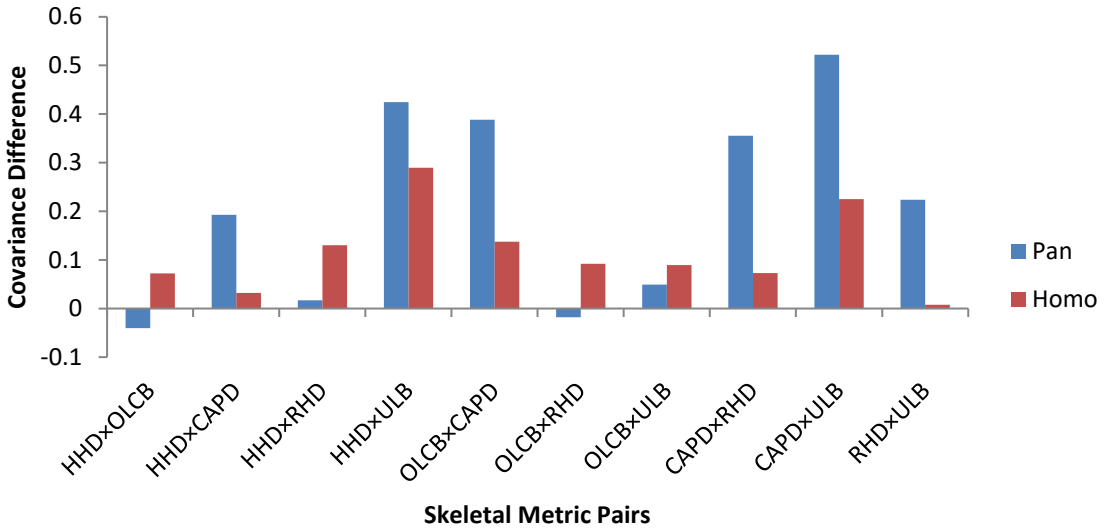

Figure 6.16: Graph comparing upper limb correlation coefficient difference between sexes of *Pan troglodytes* and *Homo sapiens*.

There is a slight trend for upper limb correlation coefficient differences between sexes to be greater in metric pairings from *Pan troglodytes* than *Homo sapiens*, with six of the metric pairings for *Pan troglodytes* showing greater differences in comparison to the four *Homo sapiens* metric pairs. All *Homo sapiens* metric pairing correlation coefficient differences between males and females were under 0.3. For four of the upper limb metric pairings, *Pan troglodytes* displayed correlation coefficient differences that are much higher. The greatest correlation coefficient difference was found in *Pan troglodytes* CAPDxULB at 0.522, in comparison to *Homo sapiens* CAPDxULB at 0.225. CAPDxRHD, OLCBxCAPD and HHDxULB all displayed correlation coefficient differences for *Pan troglodytes* that are higher than 0.3. RHDxULB also displayed a distinct difference between the two species with *Homo sapiens* correlation coefficient difference between the sexes closer to 0 at 0.008. This is in comparison to RHDxULB for *Pan troglodytes* which has a correlation coefficient difference of 0.224.

Two upper limb metric pairs displayed variation between *Pan troglodytes* and *Homo sapiens* where one species has a positive difference between the sexes whilst the other was found to have a negative difference between the sexes. For the metric pairing HHDxCAPD, the difference for *Pan troglodytes* was -0.041 whilst for *Homo sapiens* it was 0.072. This is

because there was greater positive female correlation coefficient at 0.709 than positive male correlation coefficient at 0.669 for *Pan troglodytes*. For *Homo sapiens*, the positive male correlation coefficient was greater at 0.382 than the positive female correlation coefficient at 0.310. The second metric pairing to display this type of difference between the two species was OLCBxRHD. *Pan troglodytes* was found to have a negative difference between males and females at -0.018, whilst *Homo sapiens* was found to have a positive difference at 0.092. A greater female correlation coefficient was displayed for *Pan troglodytes* at 0.516 than males at 0.498. For *Homo sapiens*, the male correlation coefficient was greater at 0.339 than the female correlation coefficient at 0.247.

OLCBxULB was the most similar in terms of correlation coefficient differences when comparing *Pan troglodytes* and *Homo sapiens*. For this metric pairing, the correlation coefficient difference between males and females for *Pan troglodytes* was 0.049 whilst the correlation coefficient difference between males and females for *Homo sapiens* was 0.089. A comparison of male and female plots of OLCB and ULB for *Pan troglodytes* and *Homo sapiens* shows more overlap between male and female metric variables for *Pan troglodytes* than *Homo sapiens* (see Figure 6.16. and Figure 6.17.) The scaling of OLCB and ULB is therefore more dimorphic in *Homo sapiens* than *Pan troglodytes.* This means that even when the correlation coefficient difference values are similar, distinct variation between the species can be observed in the data.

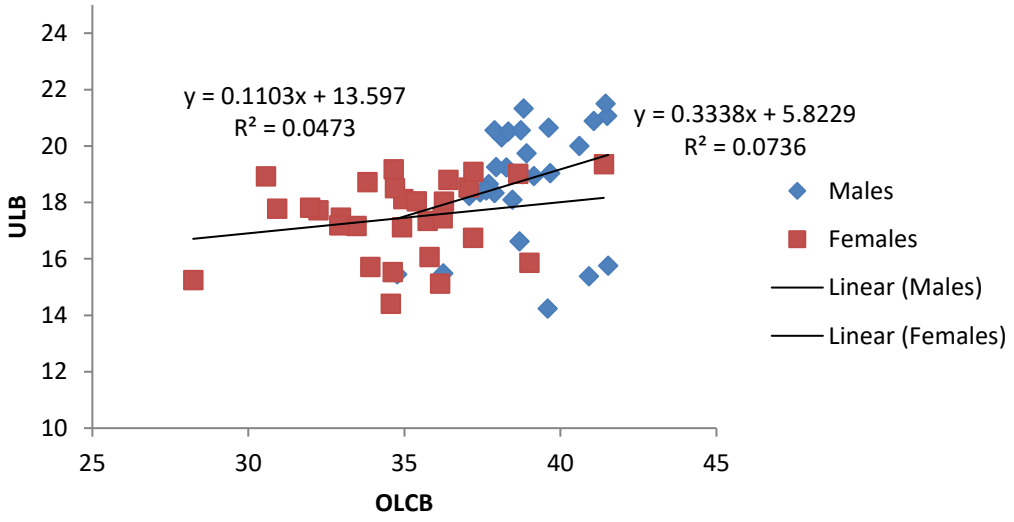

Figure 6.17: Graph showing male and female OLCB and ULB data for *Pan troglodytes*.

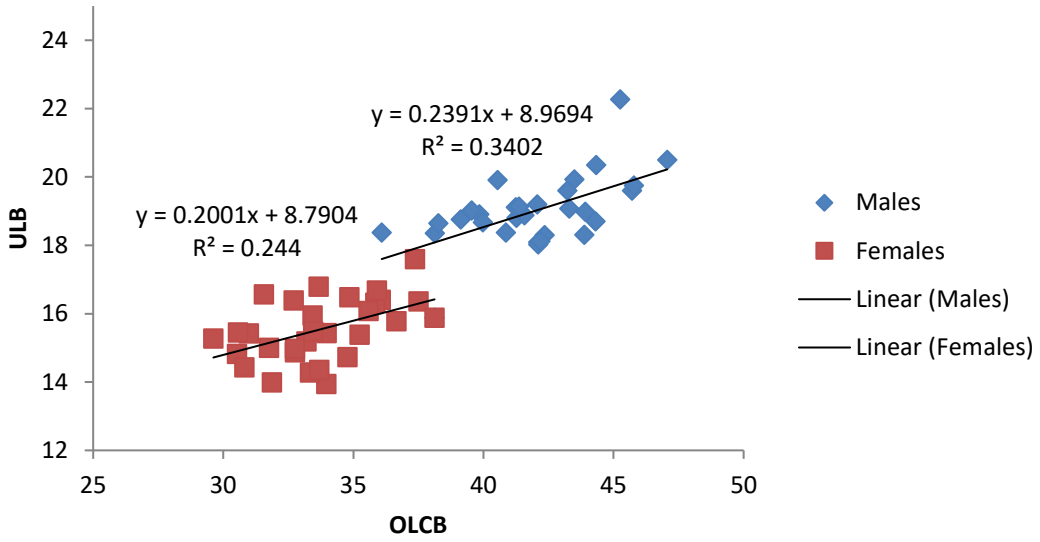

Figure 6.18: Graph showing male and female OLCB and ULB data for *Homo sapiens*.

6.6.2: Difference in lower limb correlation coefficients found between males and females for *Pan troglodytes* and *Homo sapiens*

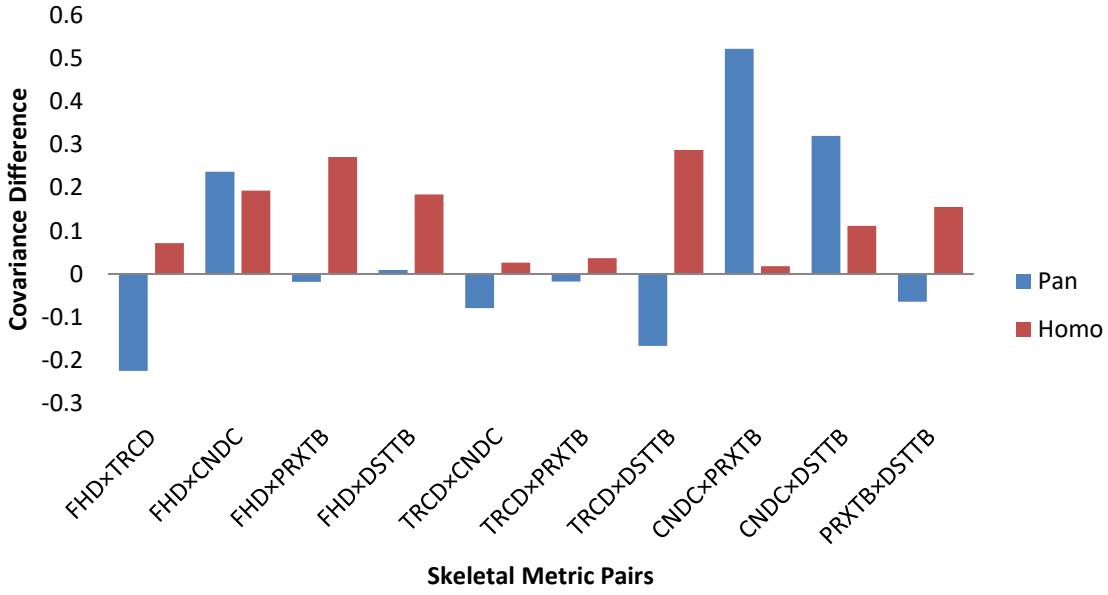

Figure 6.19: Graph comparing lower limb correlation coefficient difference between sexes of *Pan troglodytes* and *Homo sapiens*.

There is not a clear trend for correlation coefficient differences between the sexes for *Pan troglodytes* and *Homo sapiens*, with equal numbers of metric pairings presenting greater differences than the other species. Only two lower limb metric pairings produced correlation coefficient differences between males and females higher than 0.3 for *Pan troglodytes*, CNDCxPRXTB at 0.522 and CNDCxDSTTB at 0.320. No *Homo sapiens* lower limb metric pairings produced differences greater than 0.3. The largest difference between the species was also found in CNDCxPRXTB, with the *Pan troglodytes* correlation coefficient difference of 0.522 compared to the *Homo sapiens* CNDCxPRXTB correlation coefficient difference of only 0.018.

Six of the lower limb metric pairings displayed variation between the species where one species displayed a positive difference and the other displayed a negative difference. The metric pairings, FHDxTRCD, FHDxPRXTB, TRCDxCNDC, TRCDxPRXTB, TRCDxDSTTB and PRXTBxDSTTB all showed *Pan troglodytes* to have a negative difference between male and female correlation coefficients, whilst for *Homo sapiens* the difference between male and female correlation coefficients was positive. All six of the metric pairings for *Pan troglodytes* display positive female correlation coefficients that are greater than male positive correlation coefficients, which is in contrast to *Homo sapiens* where male correlation coefficient are greater.

The metric pairing with the least difference between *Pan troglodytes* and *Homo sapiens* was FHDxCNDC. For this metric pairing the correlation coefficient difference between males and females for *Pan troglodytes* was 0.237 whilst the correlation coefficient difference between males and females for *Homo sapiens* was 0.193.

6.6.3: Difference in upper and lower limb correlation coefficient found between males and females for *Pan troglodytes* and *Homo sapiens*

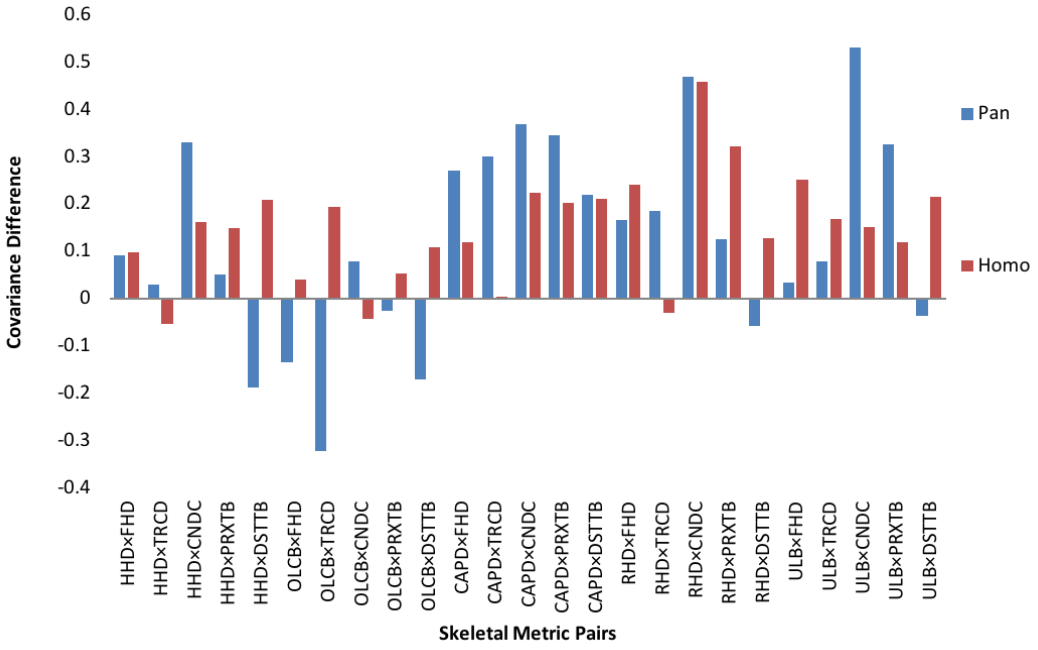

Figure 6.20: Graph comparing upper and lower limb correlation coefficient difference between sexes of *Pan troglodytes* and *Homo sapiens*.

There is a general trend for upper and lower limb correlation coefficient differences between sexes to be greater in metric pairings from *Pan troglodytes* than *Homo sapiens.* Of the 25 upper and lower limb metric pairings, 14 had a greater difference between sexes in *Pan troglodytes* whilst 11 displayed a greater difference in *Homo sapiens.* Two metric pairings produced correlation coefficient differences between the sexes greater than 0.4 for *Pan troglodytes* and one metric pairing for *Homo sapiens.* The largest difference between the two species was found in the metric pairing ULBxCNDC with the *Pan troglodytes* correlation coefficient difference of 0.530 compared to the *Homo sapiens* CNDCxPRXTB correlation coefficient difference of only 0.152. For RHDxCNDC, the correlation coefficient difference between the sexes for both species was similar, at 0.468 for *Pan troglodytes* and 0.458 for *Homo sapiens*.

Ten of the upper and lower limb metric pairings displayed variation between the species where one species displayed a positive difference and the other displayed a negative

difference. For HHDxTRCD, OLCBxCNDC and RHDxTRCD, there was negative correlation coefficient difference between males and females for *Homo sapiens* but positive correlation coefficient difference between males and females for *Pan troglodytes*. This is because these metric pairings for *Homo sapiens* display positive female correlation coefficients that are greater than male positive correlation coefficients. HHDxDSTTB, OLCBxFHD, OLCBxTRCD, OLCBxPRXTB, OLCBxDSTTB, RHDxDSTTB and ULBxDSTTB all have negative correlation coefficient differences between the sexes for *Pan troglodytes* as a consequence of greater positive female correlation coefficients.

The metric pairings with the smallest difference between *Pan troglodytes* and *Homo sapiens* are HHDxFHD and CAPDxDSTTB. For HHDxFHD, the correlation coefficient difference between the sexes for *Pan troglodytes* is 0.090 and for *Homo sapiens* it is 0.098. For CAPDxDSTTB, the correlation coefficient difference between the sexes for *Pan troglodytes* is 0.219 and for *Homo sapiens* it is 0.210.

6.7: Discussion

For this chapter, the aim of the set of analyses chosen was to answer the following questions from the dataset: 1) How complex is the scaling of sexual dimorphism in the primate skeleton? 2) Does the difference in scaling between males and females vary depending on the area of the skeleton? 3) How similar are humans to other species in the primate order in terms of sexual dimorphism scaling?

The overall finding of this chapter is of considerable complexity in the scaling of dimorphism within the primate skeleton. Although many studies have evaluated the effects of body *size* scaling, the large amount of shape variation within the primate skeleton between males and females is also worth defining. Therefore, the analyses in this chapter provide a novel approach through the comparison of *shape* rather than size dimorphism. The regression slopes for metrics scaling with FHD and the correlation coefficient differences between males and females did not produce a standard pattern for the primate order or one explained exclusively by phylogeny, although the differences between males and females indicate separate restrictions on the growth of certain joints. The correlation coefficient difference clustering analysis also found variation in scaling depending on whether the metrics derived from the upper or lower limb of the skeleton. The hierarchical clustering of male correlation coefficients, female correlation coefficients and the

difference between the two found that *Homo sapiens* skeletal scaling dimorphism was closest to *Pan troglodytes* generally, but was more similar to other primate species when defined by the correlation coefficients in one sex or the lower limb. *Homo sapiens* was most similar to *Saimiri sciureus* in terms of male correlation coefficient data points and *Macaca mulatta* in terms of lower limb correlation coefficient difference data between the sexes. The comparison of *Pan troglodytes* and *Homo sapiens* found that variation occurred even in closely related species with upper limb covariance differences between the sexes greater in metric pairings from *Pan troglodytes* than *Homo sapiens.* For this section, each analysis will be discussed in terms of the implications the findings have for understanding primate sexual dimorphism and for hominin dimorphism studies.

6.7.1: Interspecies FHD scaling differences

The large data sample means that scaling dimorphism can be examined for all skeletal metrics. FHD provides an appropriate example for determining any difference in scaling within the male and female skeleton for an increase in the femoroacetabular joint. Moreover, differences in scaling between males and females can be studied for potential implications when predicting hominin body mass dimorphism. Comparisons of regression slopes found that scaling differs between males and females in the primate order but there is no standard pattern.

How FHD scales with body mass is important for body mass estimation, with scaling pattern variation between taxa affecting comparative sample choice. Differences between males and females in terms of how FHD scaled with other skeletal metrics can define variation in skeletal size dimorphism. Lague (2003) notes that dimorphism of a certain skeletal joint has implications for hominin dimorphism level estimation techniques because a certain degree of joint size dimorphism may be related to body mass dimorphism, depending on the species chosen as a comparative sample and the skeletal metric used for prediction.

6.7.2: Interspecies scaling differences for the primate upper and lower limb

Differences between the two areas of prediction (scaling between FHD and body mass for body mass estimation and the dimorphism in scaling between metrics for estimating sexual dimorphism level) also has important implications for how body mass dimorphism is

estimated in fossil hominins, by providing greater detail about the structure of dimorphism. Correlation coefficient differences between males and females reflect the dimorphism of scaling within the skeleton for all metric parings. The results can be split into the scaling of metric pairs from the upper limb, lower limb and pairs with both upper and lower limb metrics. This output provides a simple way of expressing how variables change together, whether this differs between males and females of the same species and if a standard dimorphism scaling pattern can be defined for the primate upper and lower limb.

The species with the smallest number of metric parings with correlation coefficient differences between males and females close to 0 were *Euoticus elegantulus*, *Aotus trivirgatus* and *Saguinus oedipus*. This means that they have the smallest number of metric pairs with either positive male correlation coefficients equal to positive female correlation coefficients or negative male correlation coefficients equal to negative female correlation coefficients. The three species are known to be monomorphic and this result therefore indicates that when size as a factor is removed, monomorphic species do not display the same skeletal metric correlation coefficients between males and females. Though many monomorphic species have monogamous breeding systems that are not associated with male-male competition and sexual selection, competition for other resources, such as food supply or territories, may influence the scaling differences found between males and females. Skewed sex ratios are associated with increased competition for resources in prosimian species (Clark, 1978), and this may be a factor in the scaling dimorphism found within monogamous species that do not display differences in size.

Across the primate order, metric parings with the greatest correlation coefficient difference between sexes varied greatly between taxa. However, metric pairings where one metric is derived from the upper limb whilst the other metric is derived from the lower limb were more frequently found to have greater differences in correlation coefficients between males and females. Single metrics such as upper limb ULB, upper limb OLCB and lower limb CNDC were common in metric pairings with high correlation coefficient difference. The scaling of the primate skeleton varies between males and females in certain skeletal metrics. This indicates that certain areas of the skeleton are restricted in terms of scaling within males or females of a species.

Previous research has noted that the expected scaling of the skeleton to body mass differs for animals of varying size (Biewener, 1982; 1991). Area to volume scaling predicts that stresses will increase with size and so larger animals utilise different limb postures to limit

the stress to joints. Nonetheless, it appears that certain joints are constrained by their function in locomotion, for example the angle of the ankle is constrained in arboreal species (Polk, 2002). The finding in this chapter of scaling between metric pairs varying between the sexes may reflect differences in the level of size restriction for larger-bodied males and smaller-bodied females. This is because functional constraints limit the adaption of limb posture for maintaining safety factors – the strength required for an expected load – and so larger-bodied males are still required to restrict the scaling of joints.

Wood (1976) examined whether shape differences between males and females are due to different growth patterns or an allometric relationship between variables, by comparing regression slopes. The study employed five primate species (*Gorilla gorilla, Pan troglodytes, Papio anubis, Papio cynocephalus* and *Colobus guereza*) and utilised teeth, cranial and post cranial measurements. The post cranial metrics were derived from the humerus, femur and pelvis. This study expands on the work of Wood (1976) with an increased number of primate species and a wider range of postcranial metrics using all the long bones.

Wood (1976) found that males differ in both shape and size to females but only the ischial length of the pelvis was found to have statistically significant dimorphic slopes in more than one species. This indicates that there are varying degrees of shape between sexes in primates and that shape change is associated with size differences between males and females. This study corroborates the results of Wood (1976) by indicating that dimorphism within the body includes differences in the relative scaling of various joints. The greater number of post cranial metrics and wider variety of primate species found more statistically significant dimorphic regression slopes across species. The results of this study have clarified that dimorphism is greater between relative scaling of skeletal elements from the upper and lower limb.

6.7.3: Hierarchical clustering of correlation coefficients and correlation coefficient difference between males and females

The hierarchical clustering analysis defined which species are most similar in terms of correlation coefficients and the correlation coefficient difference between males and females. For female correlation coefficient clustering, *Gorilla gorilla* and *Aotus trivirgatus* were found to be the most similar. For male correlation coefficient clustering, *Pan troglodytes* and *Gorilla gorilla* were found to be the most similar. The similarity between

male correlation coefficient data points of *Pan troglodytes* and *Gorilla gorilla* may be expected as both are hominids. Moreover, the species share similar limitations in male arboreal substrate use in comparison to females, which is linked to their larger body size (Doran, 1993; Remis, 1995). The connection underpinning female *Gorilla gorilla* and female *Aotus trivirgatus* correlation coefficient clustering is less clear. The clustergram data in Figure 5.12. shows that both *Gorilla gorilla* and *Aotus trivirgatus* have correlation coefficient differences between males and females limited to a range between 0 and -0.7. The results were produced because female correlation coefficients were generally larger than male correlation coefficients for both species creating a negative difference. Therefore, although *Gorilla gorilla* and *Aotus trivirgatus* differ in general levels of body mass dimorphism, there is similarity in terms of skeletal scaling dimorphism because females have greater correlation coefficients.

For *Gorilla gorilla,* a large male size gives a clear reproductive advantage but restrictions in scaling would be expected due to constraints in maintaining safety factors. *Aotus trivirgatus* are monomorphic and so the greater female correlation coefficients are not related to restrictions from a larger male body size. There is, however, evidence for sexual selection operating primarily to increase female size in owl monkeys with increased female size developing as a response to competition for reproductive positions between resident and solitary females (Fernandez-Duque et al. 2009). Greater female correlation coefficients may be a reflection of the freedom of scaling required for an increased body size. Alternatively, sexually-selected stabilizing selection has been found to be a potential contributor to male size in monomorphic primate species (Lawler, 2009). Stabilizing selection reduces sexual dimorphism by working on male size. A constraint on male body size may therefore result in the lower skeletal metric correlation coefficients in *Aotus trivirgatus* males.

The hierarchical clustering analysis was also used to determine the closest species to *Homo sapiens* in terms of female correlation coefficients, male correlation coefficients and the difference between the two. The results for the correlation coefficient difference clustering found *Homo sapiens* to be more similar to *Pan troglodytes,* which was also found in the female correlation coefficient clustering. For male correlation coefficient data points, *Homo sapiens* was found to be more similar to *Saimiri sciureus.* The correlation coefficient matrices provided in the appendix supply the number of metric pairings with similar male correlation coefficient values for *Homo sapiens* and *Saimiri sciureus.* The correlation

coefficients for male *Homo sapiens* upper limb metrics, both pairings between upper limb metrics and pairings with a lower limb metric, showed the most similarity to male *Saimiri sciureus* correlation coefficient values. Male metric pairs containing upper limb measurements show the most similarity in correlation coefficient data between the two species (see Appendix 12).

Male *Saimiri sciureus* display weight gain of the upper arms, shoulders and torso prior to and during the mating season, gaining an advantage in male-male competition and female preference. Fatter males are found to spend more time with females than less robust males (Stone, 2014). Female choice is indicated by a lack of aggression with observations of attacks on unwanted males. Although there is selective pressure for fattening in the upper limb and torso, there may be some restriction on larger upper limb size and scaling that means a long-term increase in these areas of the skeleton are not found. This may include a limitation for maintaining arboreal locomotor behaviour. Female preference for male upper body strength has also been observed in *Homo sapiens* (Franzoi and Herzog, 1987; Sell et al. 2017) and sexual selection may also account for the similar pattern in male correlation coefficient data found for *Homo sapiens* and *Saimiri sciureus*.

The correlation coefficient difference hierarchical clustering analysis was further split into upper and lower limb data to evaluate any difference in clustering. *Homo sapiens* lower limb correlation coefficient difference between the sexes was found to be most similar (in terms of cluster data) to *Macaca mulatta*. For the upper limb, the *Homo sapiens* correlation coefficient difference between the sexes was most similar to *Pan troglodytes*. The correlation coefficient matrices provided in Appendix 13 supply the number of lower limb metric pairings with similar correlation coefficient difference values. The correlation coefficient difference for *Homo sapiens* metric pairings including TRCD and DSTTB showed the most numerical similarity (<0.1 difference) to *Macaca mulatta* correlation coefficient difference values. This indicates that there is a similar level of scaling dimorphism between lower limb metrics of *Homo sapiens* and *Macaca mulatta,* particularly in metrics of the tibia. The results corroborate the previous finding that the tibial bending regime, characterised by compression on the concave side of the tibial curvature and tension on the convex side, was shared between female *Macaca mulatta* and *Homo sapiens* during the stance phase of walking (Demes et al. 2001). The Demes et al. 2001 study identified this unique similarity in tibial bending regime by comparing the patterns of bone loading between multiple primates and non-primate mammals. The consistency in loading regimes

may account for the similarity in skeletal metric covarance difference, particularly within the tibia, for both species.

The results of the hierarchical clustering analyses indicate that skeletal sexual dimorphism is complex and *Pan troglodytes* is not always the best comparative species to *Homo sapiens* for all factors of scaling dimorphism. The upper limb correlation coefficient difference clustering is closest to the correlation coefficient difference for all metrics showing the influence of the higher level of dimorphism found in the primate upper limb, as defined in previous chapters.

6.7.4: A comparison of skeletal scaling dimorphism differences between *Pan troglodytes* and *Homo sapiens*

Differences in terms of scaling can provide greater detail of sexual dimorphism for each species and how male and female scaling compares between closely related species. The dendrogram produced from all the metric pairing data highlights the closeness between data points of *Pan troglodytes* and *Homo sapiens.* Nonetheless, correlation coefficient differences between the two species can be defined between scaling of upper or lower limb metrics. Upper limb correlation coefficient differences between the sexes are greater in metric pairings from *Pan troglodytes* than *Homo sapiens.* There is not a clear trend for lower limb correlation coefficient difference between males and females of *Pan troglodytes* and *Homo sapiens*, with equal numbers of metric pairings presenting greater differences than the other species. The scaling difference between male and female upper/lower limb metric pairs was greater in *Pan troglodytes* than *Homo sapiens*.

Comparing the variation in scaling correlation coefficients between the sexes of *Pan troglodytes* and *Homo sapiens* is important because of their evolutionary relationship. Whilst larger trends in scaling are useful for understanding sexual dimorphism throughout the primate order, the differences in scaling patterns between *Pan troglodytes* and *Homo sapiens* has important implications for hominin studies. Previous research has highlighted the difference in scaling patterns between joint size and body mass for *Pan troglodytes* and *Homo sapiens*. The results from the comparison of correlation coefficient difference between sexes indicate that the pattern of scaling dimorphism between *Pan troglodytes* and *Homo sapiens* also differs. Plavcan et al. (2005) and Gordon et al. (2008) note that differences in scaling will affect the accuracy of body mass dimorphism for hominin species

such as *Australopithecus afarensis*, which possess an unknown scaling pattern. Current methods of estimation require a choice of comparative sample that may cause a reduction in accuracy when scaling patterns vary between the hominin and comparative species. With some hominin species requiring a comparative sample choice between *Pan troglodytes* and *Homo sapiens,* an increased understanding of the scaling differences that underline skeletal dimorphism emphasise the importance of that choice. Although the hierarchical clustering indicates the closeness of data points, the scaling dimorphism displayed in *Pan troglodytes* and *Homo sapiens* is not the same. Therefore, the factors influencing and restricting skeletal joint size and body mass will vary between the two species, meaning assumptions about the hominin species in question are being formed when a comparative sample is chosen. Comparing the scaling pattern of skeletal dimorphism in fossil hominin species to those analysed in this study may provide more information on the underlying restrictions in skeletal metric size that differ between males and females. This means that the correlation coefficient difference of metric pairs between the sexes can also be used as another indicator of sexual dimorphism, providing more evidence of how skeletal variation between males and females has changed over time.

6.8: Chapter summary

Studies have previously focused on the scaling between a restricted number of skeletal metrics and body mass. The results suggest different scaling relationships between areas of the skeleton and body mass for species within the primate order. This provides an indication of grade shifts and that clades should be analysed separately. Variation in body mass scaling has implications for fossil hominin body mass dimorphism estimation because accurate predictions are dependent on a comparative sample being chosen with the same scaling relationship between metrics and body mass to the fossil hominin species. This leads to problems as the fossil hominin scaling relationship is unknown and will vary between species.

Because skeletal dimorphism is not the same as body mass dimorphism it can be employed as a separate tool for understanding how sexual dimorphism varies between species and whether there is a change in the pattern of dimorphism within the skeleton over time. This chapter aimed to explore the similarities and differences between species in terms of how

skeletal metric scaling varies between males and females. Regressions for all metrics were produced to display the variation in scaling relationship between two skeletal metrics found in males and females of a species. Correlation coefficients were calculated as a value for comparison between males and females. The difference in covariance correlation coefficients between skeletal metrics for males and females was found to be complex and variable between species.

Metric pairings where one metric is derived from the upper limb whilst the other metric is derived from the lower limb were more frequently found to have greater differences in correlation coefficient between males and females. This may indicate that certain areas of the skeleton are restricted in terms of scaling within males or females of a species, due to the necessary constraint of maintaining safety factors. The greater difference in correlation coefficient difference may also be providing evidence for other contrasting pressures, such as differences in locomotor and positional behaviour or the composition of body mass (Doran, 1993; McFarland, 1996; Wells, 2007). The hierarchical clustering analysis shows that the structure of dimorphism in the primate skeleton is variable. Hierarchical clustering generally found that the correlation coefficients and correlation coefficient difference data points were most similar in *Homo sapiens* and *Pan troglodytes,* although *Saimiri sciureus* and *Macaca mulatta* were most similar to *Homo sapiens* in terms of male correlation coefficient data and lower limb correlation coefficient difference data respectively. Although the hierarchical clustering indicates the closeness of data points, the scaling dimorphism displayed in *Pan troglodytes* and *Homo sapiens* is not the same.

Overall, the chapter shows that variation in the scaling between metrics of the male and female skeleton can be used as a valid assessment of the structure of sexual dimorphism in the primate order. Analysis through correlation coefficient difference provides a potential way of comparing early hominins to *Pan troglodytes* and *Homo sapiens.* Any species with a large enough sample can be compared to the species within this study in terms of the scaling difference within the skeleton of males and females. Comparing the scaling pattern of skeletal dimorphism in *Australopithecus afarensis* specimens for example may provide more information on the underlying restrictions in skeletal metric size that differ between males and females of the species. This can then be used for investigating which extant species shared a pattern of skeletal scaling dimorphism most similar to *Australopithecus afarensis* and would therefore make the best comparative sample. A future comparison of correlation coefficient differences between the sexes could also be applied to other

hominin species to produce greater understanding of the skeletal variation between males and females and reflect how this has changed over time.

Chapter 7:

Discussion

7.1: Major conclusions of the results chapters

7.1.1: Skeletal dimorphism within the primate order is non-isometric and upper limb metrics are generally better discriminators of sex for dimorphic primates

The discriminant function analysis results found that skeletal dimorphism within the primate order is not isometric and variable between species. The classification procedure also indicates that upper limb metrics are generally better discriminators of sexual dimorphism for dimorphic species. Humeral head diameter (HHD) was the most dimorphic skeletal metric overall, having the highest discriminant function ranking average across species. The mediolateral width of the ulna immediately distal to the radial facet (ULB), was found to be the best discriminator of sex for *Homo sapiens,* but *Homo sapiens* differed from the dimorphic primate average through femoral head diameter (FHD) also having a high discrimination ranking (as opposed to the lower ranking displayed in other primate species).

The non-isometric nature of skeletal dimorphism within the primate order can be compared to studies of primate body mass scaling. Articular scaling to body mass has been found to be positively allometric in studies with a combined sample of hominoids and non-hominoids, because of the relatively greater joint size observed in larger-bodied hominoids (Ruff, 1988; Jungers, 1990a; Godfrey et al. 1991). Non-human hominoid samples are found to have slight positive allometry or isometry (Jungers, 1990a; Burgess et al. 2018). Studies evaluating the scaling relationship between femoral head and body mass have found a difference in human samples with a positively allometric relationship between body mass and FHD. Although modern humans are positive outliers in terms of the correlation between lower limbs and body mass for primate species, this is not the case for the upper limb (Jungers, 1988).

Ruff (1988) found more loading in the lower limb for bipeds in comparison to quadrupeds that may reflect why human skeletal metric dimorphism differs from the general primate pattern, with FHD being higher ranked as a discriminator of sex. Weight bearing is known to be a major determinant on primate joint design. Swartz (1989) found significant positive

allometry in most limb joints of brachiating primate species. Suspensory species were expected to deviate from the general primate pattern of isometry due to the reduced compressive loads of the limb joints. The results instead indicated that only specific types of locomotor specialisation cause changes in joint design. Although there is a selective pressure for increased joint size by locomotor modes that produce an increase in limb loading (e.g. brachiators with greater sized upper limb joints), locomotor modes that reduce joint stress may not have a selective effect on joint morphology. Human bipedalism is an example of locomotor behaviour altering to the point of greatly increased limb loading. The fact that human hindlimbs are often significantly larger than predicted by body size may also be an example of selection acting to increase the capacity of joints to support weight, in comparison to the lack of selection on joints where loading is reduced. Whilst articulations of the human hindlimb have increased in size relative to body mass, there has been no corresponding change to the size of forelimb articulations, although forelimb length has reduced relative to earlier hominins (Jungers. 1988). This means that joints of the forelimb have remained relatively unchanged due to a lack of selection for reducing articular areas even when they are not under stress. The absence of selection for conserving joint material and the retention of larger joint size is an indication of phylogenetic inertia, a constraint on evolution set by previous adaptations (Jungers, 1988; Swartz, 1989).

Lague (2003) noted that the similarity in joint size dimorphism between catarrhine species may indicate a developmental constraint where these limb joints maintain proportional similarity even when there is differential loading to the upper and lower limb. Ruff (2000b) found that the mechanical scaling of long bone bending/torsional strength in modern human upper and lower limb bones remained similar when body size varied. Upper limb strength analysed from cross-sectional properties was also found to be less correlated with body mass than lower limb strength. This suggests that modern human upper limbs experience loads that are comparable to those of the lower limb but scaling is not associated with growth factors affecting both limbs (Lague, 2003). The dimorphic upper limb metrics across primate species as found in the discriminant function analysis may therefore indicate a retained joint size difference between males and females within the primate order or separate adaptations to differences in upper limb loading that can be utilised for sex discrimination. Upper limb dimorphism and the greater flexibility in scaling relationship between the upper limb and body mass in modern humans may be caused by

various stresses produced in activities unrelated to weight bearing, as will be discussed in Section 7.1.2: *Homo sapiens upper limb metrics are also good discriminators of sex*.

The discriminant function analysis results also corroborated previous research on primate joint size dimorphism. *Homo sapiens* have been found to exhibit high joint size dimorphism in both the knee and elbow joint, although the elbow joint is not associated with weight support in humans. Activity related differences are thought to cause this variation as bone remodelling is associated with increased activity levels (Niinimäki et al. 2009; Maïmoun and Sultan, 2011). Sex specific activities associated with bone remodelling include the unimanual actions of spear hunting in California Amerind males and the processing of grains causing upper limb bilateral symmetry in females compared to male directional asymmetry from maritime transportation activities in pre-Hispanic coastal Maya populations (Wanner et al. 2007; Weiss, 2009).

Long bone scaling amongst the primate order is also related to differences in mechanical loading (Paine and Godfrey, 1997). Quadrupedalism is known to cause compressive loads of the limb joints in African apes and cercopithecoids. Joint stress during locomotion may not require an allometric increase in joint size as body size increases because of the large mobile joints found in hominoids (Lague, 2003). This is because as body size increase, the joint stresses will still be lower than for cercopithecoids of equal size. Nonetheless, although an increase in male hominoid size does not necessitate an allometric joint size increase, there will be a difference between males and females in terms of the lower mechanical stress safety factors operating on male bodies. These differences in joint size dimorphism are reflected in the discriminant function structure matrix rankings. For *Homo sapiens*, the elbow joint was one of the most dimorphic skeletal elements. The knee joint was also found to be less dimorphic than the hip joint and did not differ dramatically when compared to rankings of other primate species.

Higher sex classification percentages have been found for arm bone circumference than leg bone circumference in archaeological samples. Safont et al. (2000) evaluated long bone circumference in a late Roman sample and found that humeral circumference produced a sex classification percentage of 92.6% with ulnar circumference having a slightly smaller percentage accuracy at 91.1%. Previous studies have also found that epiphyseal dimensions are better discriminators of sex than diaphyseal dimensions in upper limb bones, as was found in the discriminant function analysis (Holman et al. 1991; Charisi et al. 2011). A similar pattern has also been shown for metrics of the femur and tibia (Işcan et al. 1994;

King et al. 1998). Ruff (1987) compared human lower limb bone structure and the relationship to the sexual division of labour in the Middle and Upper Palaeolithic. The study also found epiphyses to be more dimorphic, which was attributed to higher mechanical stress on the epiphyses during loading causing a size increase.

7.1.2: *Homo sapiens* upper limb joint metrics are also good discriminators of sex

The discriminant function analysis results for *Homo sapiens* also found upper limb joint metrics to be the best discriminators but differed from the dimorphic primate average through the proximal ulna metric ULB being the highest ranked discriminator, which ranked much lower for other dimorphic species. The ulna has been evaluated for sex determination in archaeological and forensic cases. Although the os coxae provide sex classifications with the greatest percentage of accuracy, they may be damaged or absent in an assemblage. Steel (1962) formed a method of assessing sex through metrics of the complete ulna. Although reasonable percentage accuracies were produced, the requirement for complete bone made the method impractical for use in archaeological and forensic cases with fragmented remains. This study demonstrates that sex determination may not require the complete bone to produce high classification percentage accuracy.

High accuracy percentages have been produced through methods utilising the proximal end of the ulna (Purkait, 2001). Cowal et al. (2013) tested the method on a sample from Spitalfields, UK and found a smaller percentage accuracy than previously reported, indicating that dimorphism in the ulna varies within human populations. Srivastava et al. (2013) evaluated the ulnae of a north Indian population as a method of sex classification. The discriminant function analysis produced highlighted maximum ulna length as the best discriminator of sex, followed by radial notch width. Kwak et al. (2015) evaluated the use of bone volume and surface area for determining sex from 3D models. The ulnae of the Korean sample were found to have the highest percentage accuracy of 94% from volume and surface area. The authors of the study suggested that the highly dimorphic upper limb bone volume and surface area found for that particular population was caused by arm bones in men being more stimulated during movement and increased loads than women.

The highly dimorphic proximal ulna metric for *Homo sapiens*, determined by the discriminant function analyses in this study, may be as a result of environment factors such as mechanical stress or the division of physical labour. Nutritional stress can also cause a

differential response in the sexes; long-term protein deficiency can reduce the growth rate of the male skeleton more than the female skeleton, meaning that sexual dimorphism is reduced (Stinson, 1985). Moreover, populations with intermediate levels of protein consumption are noted to have generally higher levels of sexual dimorphism (Gray and Wolfe, 1980).

Human sexual dimorphism is also dependent on activity patterns and the division of labour between the sexes (Ruff 1987; Stock and Pfeiffer, 2001; Weiss, 2003; Stock and Pfieffer, 2004; Carlson et al. 2007). Shaw and Stock (2009) defined certain relationships between behavioural differences and bone structure, including the structure of the ulna. Humeral and ulnar robusticity were found to be greater in the dominant arm of cricketers and bilaterally in swimmers. This was contrasted with the more gracile bones in controls and the non-dominant arms of cricketers. The results clearly indicate that mechanically loaded upper limb elements result in greater robusticity than less mechanically loaded skeletal elements. Comparison between the two bones tested indicated that mechanical loading has a more significant effect on proximal limb segments.

Other studies analysing loading intensity differences between activites have suggested that the division of labour could substantially affect the ability to discriminate between the sexes via skeletal metrics (Macintosh et al. 2017). Nonetheless, Pearson and Lieberman (2004) promote caution when investigating sexual dimorphism, particularly the inference of different activities. The variation in hormones between males and females may mediate the remodelling response to mechanical loading. Males also have a greater ability to respond to loading than females because of sex differences in growth trajectory. Furthermore, there is a potentially limiting effect to osseous changes as a response to loading in females from the elevated estrogen secretion in puberty, which supports the storage of calcium (Järvinen et al. 2003). The difference between the sexes may also occur later in adulthood when females lose bone mass at a faster rate than males.

Plasticity can cloud phylogenetic signals and is an important factor to consider when evaluating the potential implications of behavioural differences to the upper and lower limb. Adaptability to changes in environment was originally considered an example of the environment interfering with the selection of a trait. It is now known that there is genetic variation in plastic responses (Pigliucci, 2005). Studies have previously found greater plasticity in human diaphyseal breadths relative to lengths and articular breadths (Lieberman et al. 2001). Auerbach and Ruff (2004) also found larger amounts of variation in

diaphyseal breadth asymmetry between individuals and populations from a geographically and temporally diverse Holocene adult sample. The known effects of mechanical loading on the asymmetry of diaphyseal breadths indicate that the results are caused by variation in behavioural patterns. It is expected that more plastic areas of the upper and lower limb will reflect adaption to behaviour, in comparison to canalised regions with consistent phenotypes that are connected to phylogeny.

Nadell and Shaw (2016) analysed site-specific long bone plasticity to clarify the relationship between diaphyseal structure and habitual loading. Plasticity was found to vary between limb elements and specific areas of the diaphyses in response to known activity patterns. The humeral midshaft displayed the most plasticity in the upper limb indicating that the upper arm is more plastic than the forearm. Midshafts in general seem more adaptable to changes in structure as a result of habitual loading in comparison to proximal and distal bone segments. Trinkaus et al. (1994) found right-bias in humeral diaphyseal breadth in a small sample of five Neanderthal humeri. This is evidence of a high degree of diaphyseal plasticity within the genus *Homo* as a result of changing biomechanical loading conditions.

Plasticity of long bone diaphyses in response to mechanical loading has also been evaluated as evidence of population-level handedness in *Pan troglodytes.* Sarringhaus et al. (2005) reported left upper arm dominance in the skeletons of wild-caught *Pan troglodytes,* reflected in greater total subperiosteal area of the left humeral diaphysis. The finding implies behavioural laterality in upper limb function and was interpreted as an effect caused by behaviour where the left upper limb supports a larger portion of body weight for prolonged periods of time, whilst leaving the right hand free to manipulate objects. Captive-chimpanzees have also shown a population-level bias in the left upper arm, with the asymmetry more pronounced in males than females (Hopkins, 2008). This suggests that plasticity and loading regimes may be a factor in the level of skeletal dimorphism for species other than humans, particularly as there are differences between male and female *Pan troglodytes* in terms of asymmetry, indicating differences in loading behaviour.

A more recent study evaluated patterns of asymmetry in a non-hominoid primate (Reeves et al. 2016). *Saguinus oedipus* was found to have a similar pattern of long bone asymmetry to humans in terms of their diaphyseal breadths displaying the most asymmetry. The species differs to humans and *Pan troglodytes* in asymmetry being greater in lower limb bones than upper limb bones. Differential loading to one side of the lower limb has been demonstrated during leaping behaviours and may influence the level of asymmetry found

in *Saguinus oedipus* (Hook and Rogers, 2002). The similar asymmetry in humans, *Pan troglodytes* and *Saguinus oedipus* may indicate a general pattern of developmental instability in primate limbs. Diaphyseal breadths are less constrained than lengths or articular breadths. The skeletal metrics chosen for this study do not include breadths at the midshaft so the results are less likely to reflect environmental plasticity and separate loading regimes for males and females. Nonetheless, for studies analysing the consequences of different loading behaviour between males and females it is important to consider the effects of plasticity as well as the actual activity influencing the skeleton.

Metric methods of estimating sex are known to be population specific. Differing environmental factors may account for much of the variation but sexual dimorphism is also dependent on genetics. For example, bone size variation in human populations has been linked to several genomic regions (Deng et al. 2003). It should be noted that the samples within this study are derived from certain geographic areas, meaning that the full variation within each species may not be represented. The large amount of variation in human sexual dimorphism must be taken into account when considering the application of modern human samples to hominin sexual dimorphism estimation studies. Defining sexually dimorphic traits that are found across dimorphic primate species may reduce adverse effects relating to comparative sample choice. The *Homo sapiens* sample in this study was produced from modern humans and a wider range of populations are required to produce specific discriminant functions suitable for classifying the sex of human specimens.

7.1.3: Discriminant function analysis achieves greater accuracy in estimating sexual dimorphism than previous methods

Body mass dimorphism methods are dependent on the estimation of body mass from regression equations and then splitting the pooled species sample into male and females. Previous studies have found the most accurate method of predicting sexual dimorphism from pooled body mass is to split the sample at the mean (Godfrey et al. 1993; Plavcan, 1994). The analysis in Chapter 5 corroborated previous results with the mean and median method being the most accurate in terms of estimating *Homo sapiens* body mass estimated through McHenry's (1992) equations. The comparison between discriminant function analysis and the mean/median method found that the *Homo sapiens* discriminant function analysis achieves greater accuracy in estimating sexual dimorphism.

Although the mean method is often utilised because it provides consistency with a simple application, problems occur because it assumes that the sample will be clearly bimodal in distribution. When the actual dimorphism level is minimal, the overlap in size between the sexes is ignored and so the method tends to overestimate the level of sexual dimorphism. In comparison to the current best method of splitting the sample into male and female groupings from a calculated cut-off point, discriminant function analysis works by directly classifying the sex of a specimen via an equation. The Chapter 5 test on the moderately dimorphic *Homo sapiens* data found that the discriminant function analysis result produced higher percentage accuracy than the mean/median method. Discriminant function analysis is more accurate because it provides a weighted mean across skeletal elements. The advantage over the mean method is therefore due to the use of multiple skeletal elements, along with discrimination between the elements that are more or less useful for determining sex.

Although discriminant function analysis was found to be more accurate than the mean method, the technique cannot be applied to all cases in the fossil record. The applicability of these findings for studying fossil hominin sexual dimorphism varies depending on the species being evaluated and whether there are enough specimens to form a reference sample. For early hominins with specimens that do not have a sample of sexed individuals to form a reference sample, discriminant function analysis can still be used to investigate possibilities. The sex of individual specimens can be evaluated by utilising discriminant function equations formed from different species and populations (e.g. *Pan troglodytes* and *Homo sapiens*). If a specimen is consistently classified as one sex using all discriminant function equations then there is an increased likelihood that the sex classification is correct.

7.1.4: Accuracy levels are maintained by the best choice of individual skeletal metrics

For the discriminant function analysis to have practical use as a sex classification method it needs to be shown to work with a smaller number of skeletal metrics. Stepwise discriminant function analysis employs the most diagnostic variables to provide the strongest discrimination model. The *Homo sapiens* data was used to understand how the accuracy of discrimination models varied depending on the type and number of metrics added. Individual skeletal metrics could be tested to infer whether a simpler discriminant

function equation, with a smaller number of metric inputs, could be utilised for sexual dimorphism estimation on incomplete assemblages. The results found that the same high level of classification accuracy (98%), found from the addition of all twelve variables, could be produced from discriminant function equations requiring only two upper limb skeletal metrics. Discrimination from the most dimorphic individual skeletal metrics maintained an accuracy percentage of 96.7%. This indicates that discriminant function, combined with the knowledge of best metric choice, is a valid potential method of discrimination for incomplete assemblages. Discriminant function analysis has the ability to provide enhanced accuracy in defining the level of sexual dimorphism by maximising the differences between the sexes. The application of the discriminant function equation forces the data into a situation in which it is bimodal, meaning the differences between the sexes are magnified.

7.1.5: Discrimination from FHD provides good accuracy but there are superior metric choices

Upper limb skeletal metrics have been found to be generally better discriminators of sex across the primate order in Chapter 4. Nonetheless, current methods of estimating fossil hominin sexual dimorphism rely on the estimation of body mass from FHD before the sexual dimorphism level is predicted. The results of the discriminant function comparison found that discrimination from FHD has a classification percentage equal to the best single upper limb metrics, although higher classifications percentages are produced from certain combinations of a small number of skeletal metrics. In terms of using *Homo sapiens* as comparative sample for fossil hominins, the different scaling of FHD and its lesser level of dimorphism in comparison to other primates mean that it is not the safest choice of discriminator and that upper limb metrics have a high level of dimorphism throughout the primate order. Nonetheless, a more direct method of classifying sex is advantageous as the increased uncertainty introduced through estimating body mass from femoral head diameter and then dividing the predicted sample into males and females would be avoided.

As FHD is employed for estimating body mass, the further utilisation as a discriminator of sex would not require any additional measurements. Other skeletal metrics have been found to be better discriminators of sex for the primate order in Chapter 4. It was important to test the power of each skeletal metric as a discriminator of sex, to infer whether a simpler discriminant function equation, with a smaller number of metric inputs, can be utilised for fossil hominin sexual dimorphism estimation. Although FHD has good

levels of accuracy for discriminating sex in *Homo sapiens* samples it may not be the best choice for fossil hominin species. The discriminant function analysis found FHD was not as dimorphic for *Pan troglodytes* and other primates, and by choosing FHD there is a presumption of hominin FHD being similar in dimorphism to *Homo sapiens* rather than to other primates. So it is therefore potentially safer to estimate sex from other metrics such as HHD and OLCB that are highly dimorphic throughout the primate order. The sustained level of accuracy for discriminant function analysis models with minimal required skeletal elements indicates that the methodology is practical and can be applied to skeletal assemblages that are not complete.

Femoral head diameter is frequently chosen for body mass estimation procedures because it is often found in skeletal assemblages and can be easily measured. The mechanical relationship between body mass and the proximal femoral articulation was the basis for the body mass estimation equations produced by Ruff et al. (1991) and McHenry (1992). It has previously been noted that techniques for estimating body mass are less accurate when body proportions differ from the reference sample, as has also been described for sexual dimorphism estimation methods. The use of one formula for both sexes was also found to overestimate body mass in males as they generally have larger femoral head diameters than females because of the positive allometry of femoral head diameter relative to body mass (Kurki et al. 2010). This was found when the Ruff et al. (1991) equation was applied to small-bodied Later Stone Age Southern Africans, which supplied a result closer to the level of dimorphism shown from estimates made by the McHenry (1992) equation. Kurki et al (2010) has important implications for the estimation of sexual dimorphism because the uncertainty introduced prior to the prediction of sexual dimorphism from the overestimation of male and female difference in body mass regression equations reduces confidence in the result. The influence of combined-sex body mass estimation equations on sexual dimorphism level prediction has also been reported in Ruff et al. (2012) and Sládek et al. (2018). The ability to classify sex directly from an incomplete assemblage through discriminant function analysis will help reduce this problem.

Studies have shown that skeletal metrics scale to body mass differently between taxa. Ruff (1988) found a general trend of overall isometry or slightly positive allometry between joint size and body mass, with *Macaca fascicularis* and *Homo sapiens* being outliers. *Macaca fascicularis* display smaller hindlimb articulations in relation to body mass whilst *Homo*

sapiens have larger femoral heads relative to body mass. *Homo sapiens* display a different scaling relationship between femoral head size and body mass than non-human primates, with a positively allometric relationship between body mass and FHD. The femoral head was found to have the strongest relationship to weight in comparison to other articular dimensions. Jungers (1988) also showed that modern humans are positive outliers in terms of the correlation between lower limbs and body mass for primate species, although this is not the case for the upper limb. Therefore, alongside evidence for more dimorphic upper limb skeletal elements in the primate order found from the discriminant function analysis, FHD is not the best choice for studies evaluating body mass dimorphism.

Separating the estimation of body mass and sex is important because the current methodology for estimating body mass from femoral head diameter creates uncertainty prior to the prediction of sexual dimorphism level. For fossil hominin body mass estimation procedures, there is the issue of which comparative sample is most appropriate for producing estimation equations. Holliday (2012) highlighted the problem of estimating australopithecine body mass from estimation equations produced from modern humans as their femoral head diameters are smaller than those of modern humans. This means that there is extrapolation beyond the range of the prediction equation, which will negatively affect the accuracy of estimation. Sexing directly from the skeleton, potentially using elements other that femoral head diameter, does not change the error introduced by body mass estimation techniques. However, the uncertainty that is produced through estimating body mass from femoral head diameter and then dividing the predicted sample into males and females can be averted by direct methods of classifying sex in fossil hominin species.

7.1.6: Scaling of sexual dimorphism in the primate skeleton

The analysis of sexual dimorphism scaling within the primate skeleton found that skeletal dimorphism is complex and an important factor in itself, rather than simply being used as a proxy for body mass dimorphism. The difference in male and female skeletal metric scaling was used to explore variation in shape between the sexes. This is in contrast to previous studies that have concentrated on size difference. The investigation of shape means that the relationship between variables of monomorphic and dimorphic species can be compared in terms of similarities in structure, even when there is no similarity in relation to wholesale size differences.

There is no standard pattern for the primate order, with the amount of scaling difference between the sexes varying across taxa. The differences between males and females indicate separate restrictions on the growth of certain joints. Metric pairings where one metric is derived from the upper limb whilst the other metric is derived from the lower limb were more frequently found to have greater differences in correlation coefficients between males and females. This indicates that certain areas of the skeleton are restricted in terms of scaling within males or females of a species.

Hierarchical clustering of the correlation coefficient results found surprising similarity between pairs of species. *Gorilla gorilla* and *Aotus trivirgatus* differ in general levels of body mass dimorphism but there is similarity in terms of skeletal scaling dimorphism as females have greater correlation coefficients. Difference between males and females can be explained as restricted scaling for males in comparison to non-restricted females. For *Gorilla gorilla,* a large male size gives a clear reproductive advantage but restrictions in scaling would be expected due to constraints in maintaining safety factors.

Biewener (1982; 1991) noted that the expected scaling pattern differs for animals of varying size. Peak locomotory stresses are much greater in larger animals but there is no significant difference in failure stress for bones of various sized animals. Therefore, other aspects of locomotion are required to reduce peak locomotory stresses in larger animals. To avoid bone breakage, areas of the body exposed to force during locomotion require sufficient factors of safety to avoid failure. The safety factor of a structure can be calculated as ratio of failure stress to its peak operating stress. Yield stress can also be calculated as fracture relative to energy absorption and is a more relevant measure of safety factors during locomotion. Repeated loading causes fatigue damage and eventual failure that also results in lower safety factors. Although area to volume scaling predicts that stresses will increase with size, there is no significant difference in failure stress for bones of various sized animals. Instead, larger animals change posture when running, becoming more erect and using more extended limb postures than smaller animals to increase the extensor muscle mechanical advantage (Biewener, 2005). Maintaining safety factors and reducing the risk of bone breakage comes with the cost of decreased agility and speed in the large species (Rubin and Lanyon, 1982).

Other functional constraints appear to limit the adaption of limb posture for maintaining safety factors. Polk (2002) found that the angles of weight bearing joints did not change with increasing body mass for primates. This indicates that certain joints are constrained by

their function in locomotion, for example the angle of the ankle may be constrained in arboreal species. Polk et al. (2009) compared joint postures for different sized primates; the results found that larger primates utilised more extended knee postures but variation exists, particularly within smaller primate species. Smaller species therefore appear to be less constrained by their body size and display a wide variety of knee postures.

Although the smaller correlation coefficient values for male *Gorilla gorilla* may be a result of their larger body size, *Aotus trivirgatus* are monomorphic. There is, however, evidence for sexual selection operating primarily to increase female size in owl monkeys. Increased female size may have developed as a response to competition for reproductive positions between resident and solitary females. Competition between the two is noted to be of similar intensity and frequency as between males (Fernandez-Duque et al. 2009). Gordon et al. (2006a) evaluated the scaling of size and sexual dimorphism in moustached tamarins (*Saguinus mystax*), with the negative scaling indicating primary selection on female size. Fernandez-Duque (2011) notes the similarity in social systems between owl monkey species and *Saguinus mystax*. The social system of *Saguinus mystax* involves one female monopolising breeding in the group and males participating in infant care. This means there is potential competition between females for males that will aid the care of offspring. Owl monkeys also live in socially monogamous groups with large amounts of paternal care. Nonetheless, the results of Chapter 6 found no greater female correlation coefficients in *Saguinus oedipus* to indicate a similarity in skeletal metric scaling linked to their shared monogamous social system.

Lawler (2009) analysed alternative sociecological mechanisms underpinning the relationship between sexual dimorphism, male-male competition and mating systems. One alternative mechanism tested was sexually-selected stabilizing selection, which was found to be a potential contributor to male size in the monomorphic primate species Verreaux's sifakas (*Propithecus verreauxi*). This is because directional selection was found to act on traits such as leg shape rather than body mass or canine size. This indicates that behaviors related to locomotion may be more connected to male reproductive success than advantages through male-male competition. *Propithecus verreauxi* males of intermediate size are noted to have more reproductive success; larger males have reduced reproductive success because they are less agile and smaller males are outcompeted. Stabilizing selection will reduce sexual dimorphism by working on male size. Constraints on male body

size may therefore result in the lower correlation coefficients in *Aotus trivirgatus* males as a restriction to their scaling pattern.

For male correlation coefficient data points, *Homo sapiens* were found to be more similar to *Saimiri sciureus.* This is surprising because of the phylogenetic separation between the two species in comparison to the similarity between female *Homo sapiens* and *Pan troglodytes* correlation coefficient data points. *Saimiri sciureus* live in large multi-male multi-female groups, have seasonal breeding with concealed ovulation and female dominance (di Bietti and Janson, 2000; Izar et al. 2008). Direct comparison of correlation coefficient data for the two species found that male scaling pairs containing upper limb metrics have the most similarity.

Male *Saimiri sciureus* display weight gain of the upper arms, shoulders and torso prior to and during the mating season. Weight gain of between 85 and 222g occurs during a two to eight week mating season through fat deposition and water retention in the arms, torso and shoulders (Stone, 2014). Studies have found the fattening response to be controlled by a seasonal increase in testosterone converted into estrogen and increased levels of thyroid hormones (Coe et al. 1985). An associated increase in cortisol indicates that there is a physiological cost to the process (Schiml et al. 1999). Seasonal fattening has also been noted in captive *Macaca mulatta* allowing males to engage in mate guarding and sociosexual behaviour without the cost of a reduced feeding time (Bercovitch, 1992).

Stone (2014) determined the evolutionary costs and benefits of this seasonal fattening in *Saimiri sciureus*. Weight gain in the upper arms, shoulder and torso provides an advantage in gaining female preference and during male-male competition. Fatter males were found to spend more time with females than less robust males. Increased time engaged in sociosexual behaviour and less time foraging/feeding was also recorded for males with the greatest amount of fattening. Male-male aggression is frequent with increased injury risk during the breeding season. Attacks from juveniles and late infants also occur, reducing the number of successful copulations with their mothers in an example of sexual interference.

Fattening probably provides an advantage during male-male competition through a competitive signal as a way of assessing rivals (Clutton-Brock, 2007). Fattening has also been observed in providing physical protection during male antagonism in *Saimiri boliviensis* (Mitchell, 1990). Sexual selection is a more likely mechanism behind male

fattening than compensation for reduced feeding time (as in *Macaca mulatta*) because male *Saimiri sciureus* do not lose weight as the mating season progresses, although there is a trade off as reduced time for foraging/feeding is reported.

It should be noted that the selective pressure for fattening, whether through female preference or as an advantage during male-male competition, is occurring in the upper limb and torso only. There may be some restriction on larger upper limb size and scaling that means a long term increase in these areas of the skeleton are not found, perhaps constrained by arboreality. Fattening in *Saimiri sciureus* is a plastic response and may not leave a phylogenetic signal. A constraint on upper limb skeletal scaling may also be occurring in male *Homo sapiens* reflecting the need for long hindlimbs and short forelimbs in bipedal locomotion.

Lower limb correlation coefficient difference between the sexes was most similar between *Homo sapiens* and *Macaca mulatta.* The correlation coefficient difference between males and females for metric pairings containing tibial TRCD and DSTTB displayed the most similarity. This indicates that there is a similar level of scaling dimorphism between lower limb metrics of *Homo sapiens* and *Macaca mulatta,* particularly in metrics of the tibia. Demes et al. (2001) evaluated the tibial midshaft strain environment for female *Macaca mulatta* through *in vivo* bone strain experiments. Bending was found to be the major loading regime for the *Macaca mulatta* tibia, consistent with the long bones of other mammals. The bending regime was characterised by compression on the concave side of the tibial curvature and tension on the convex side. Muscle forces affect the overall bending pattern in *Macaca mulatta* as the substrate reaction force during terrestrial quadrupedalism had previously been found to incline medially. This means muscle forces are an additional source of bending on the medial side of the leg.

The bending regime of the *Homo sapiens* tibia was found to be similar to that of *Macaca mulatta* during the stance phase of walking (Peterman et al. 2001). Strain was measured in the human distal tibia through a gait simulator. The ground force reactions associated with the stance phase of walking displayed a bending regime consistent with the *Macaca mulatta* tibia, through compression at the posterolateral cortex and tension of the anteromedial cortex. The pair of muscles that make up the triceps surae, the two-headed gastrocnemius and the soleus, are associated with strains on the anterior and posterior cortex of the tibia (Demes et al. 2001). For humans, the triceps surae are not responsible for propulsion but instead support the body during walking and prevent the body from

falling (Honeine et al. 2013). The gastrocnemius muscle was also found to be moderately active in *Macaca mulatta* during terrestrial locomotion. Although the soleus activity is greater for both species, the soleus does not originate from the tibia in *Macaca mulatta* (Jouffroy et al. 1999). Nonetheless, there is a consistency in loading regimes that is not evident in locomotor kinematics alone and may account for the similarity in skeletal metric scaling difference, particularly within the tibia, for both species.

The hierarchical clustering also found that *Pan troglodytes* and *Homo sapiens* are closest in similarity for female correlation coefficient, the overall correlation coefficient difference between sexes and the difference for upper limb metrics. Nonetheless, by directly comparing the correlation coefficient data for both species, upper limb correlation coefficient differences between the sexes are greater in metric pairings from *Pan troglodytes* than *Homo sapiens.* The scaling difference between male and female upper/lower limb metric pairs was also greater in *Pan troglodytes* than *Homo sapiens*. Richmond and Jungers (1995) found that modern human sexual dimorphism is greater than chimpanzee dimorphism in most postcranial dimensions but body mass tends to show the reverse trend between the species. Lague (2003) also highlighted the relatively high level of human joint size dimorphism of the knee and elbow that is not reflected in greater body mass relative to chimpanzees. The results of the skeletal dimorphism scaling analysis indicate that although there is generally greater dimorphism in postcranial dimensions for *Homo sapiens*, the differences in scaling between males and females is greater for *Pan troglodytes.*

7.2: Implications for studying hominin body mass dimorphism

7.2.1: Discriminant functions have potential application for fossil hominin dimorphism estimation

Although the mean method has been found to provide a high level of accuracy, the arbitrary creation of subsamples means that the method may not be suitable for all fossil species. If there is a moderate level of body mass dimorphism then an overestimation will occur. Therefore, the mean method is not a suitable technique for fossil hominin body mass dimorphism estimation because the level of dimorphism is unknown and the accuracy of the method cannot be tested. Discriminant function analysis provides an alternate method of estimating sexual dimorphism by directly classifying the sex of a specimen. A test of accuracy found that the greater power provided by multiple skeletal elements and

the employment of a weighted average across skeletal elements in the discriminant function analysis produced higher percentage accuracy than the mean method.

The discriminant function analysis results were compared to logistic binomial regression, which requires fewer assumptions. The test found the same classification percentages for both methods indicating that the results are robust and that discriminant function analysis is a valid method of classifying sex. For discriminant function analysis to be a practicable method for incomplete skeletal assemblages, including many fossil hominin specimens, then a discriminant function requiring a smaller number of elements must be developed that maintains a high level of accuracy. The results from the comparison of individual skeletal metric discrimination power found that the same percentage accuracy can be supplied from models with only two skeletal elements.

Discriminant function analysis provides increased accuracy through the utilisation of multiple measurements. This means that the data collected for the six dimorphic species can be employed in forming new discriminant functions based on the skeletal elements available from another specimen with unknown sex. For example, a new *Pan troglodytes* case with only a distal humerus and proximal tibia could be sexed through a discriminant function derived from the *Pan troglodytes* data with the same level of accuracy as the discriminant function with all twelve metrics, because the most dimorphic traits are known. The testing of discrimination power for new cases is a potential area of future research.

The creation of discriminant functions for classifying sex in fossil hominin cases is more limited as the sample required to develop the equation limits the number of current species it can be applied to. Nonetheless, another study could form and test discriminant functions created from samples of *Homo erectus* and *Homo neanderthalensis* or any species where there are enough valid specimens with sufficient skeletal elements. By creating discriminant functions from a reference sample with sex determined securely by other methods (e.g. pelvic sex indicators as used in Ruff, 2010 and Simpson et al. 2014 or DNA shotgun sequencing as used in Skoglund et al. 2013), discriminant function analysis can be used as a quick method for classifying the sex of new specimens with incomplete skeletal representation.

For early hominins that do not have a sample of confidently sexed individuals to form a reference sample, discriminant function analysis can still be used to investigate possibilities. Discriminant functions from different populations of humans or hominoids can

be used to evaluate the sex of individual fossil hominin specimens. If a specimen is consistently classified as one sex from all reasonable analogue species then there is an increased likelihood that the sex classification is correct.

The existing modern human sample can also be expanded to provide a more general reference for *Homo sapiens*. By including data from a variety of groups, including Upper Palaeolithic populations, a discriminant function equation can be developed utilising whatever skeletal elements are found.

7.2.2: The implications of male and female scaling differences within the skeleton for fossil hominin sexual dimorphism studies

With some hominin species requiring a comparative sample choice between *Pan troglodytes* and *Homo sapiens,* an increased understanding of the scaling differences that underline skeletal dimorphism between these species is valuable. Although the hierarchical clustering indicates the closeness of data points, the scaling dimorphism displayed in *Pan troglodytes* and *Homo sapiens* is not the same. The difference between the two species means that there is a difficulty in choosing one as a comparative sample for fossil hominin estimation, because the pattern of variation between males and females that is most similar is unknown. A potential way of comparing early hominins to *Pan troglodytes* and *Homo sapiens* is through correlation coefficient difference between the sexes. Any species with a large enough sample can be compared in terms of the scaling difference within the skeleton of males and females.

This means that a comparison can be made in terms of the difference between males and females in how a change in one skeletal metric can affect another. This provides a detailed exploration of sexual dimorphism within the skeleton that can be employed for comparative analysis through skeletal metrics in hominin assemblages. For species that are closely related, the correlation coefficient difference still displays detailed differences in the male and female skeleton. These differences can be used to infer restrictions in areas of the skeleton that are limited to one sex. This means that the correlation coefficient difference from skeletal metric pairs between males and females can highlight factors such as how locomotion limits size in some males or a general female size increase that may be associated with a change in diet.

A future examination of correlation coefficient differences in males and females could be applied to studying the last common ancestor (LCA) between *Homo sapiens* and *Pan troglodytes*. Prior to the discovery of *Ardipithecus ramidus*, the prevalent model of the LCA was human characteristics derived from modified features displayed in the closest extant ape relatives. The *Ardipithecus ramidus* skeleton supports a last common ancestor that was not chimpanzee-like. It refutes previous models of the LCA that assumed a species anatomically intermediate between living apes and humans (Lovejoy, 2009; Lovejoy et al. 2009).

Sexual dimorphism for *Ardipithecus ramidus* was inferred from the ARA-VP-6/500 skeleton. The upper and lower canines of ARA-VP-6/500 are small relative to other specimens yet the postcrania provides an estimated relatively large weight of ~50 kg, indicating that it is either a large female or a male with small canines. It should be noted that body mass was estimated from metrics of the capitate and talus and their relationship with body mass in extant primates. The accuracy of the estimation therefore depends on the validity of the reference sample chosen. The authors note that though the actual body mass of the specimen may vary from this estimate, the skeleton still indicates a large female. Suwa et al. (2009) analysed the canine teeth suggesting that *Ardipithecus ramidus* was slightly more dimorphic than modern humans, with an expected range of 10 to 15% dimorphism in mean crown diameter. The probability of ARA-VP-6/500 being male was calculated as low meaning the large-bodied female specimen provides evidence for slight body mass dimorphism that is within the range of *Pan*. The results of the study were used to infer a LCA with relatively low levels of canine and body size dimorphism. This study of hominin sexual dimorphism estimation is an important example of prediction being used to infer potential social behaviours. *Ardipithecus ramidus* is described as having weak amounts of male-male competition that is potentially associated with male philopatry and male-female codominance.

The estimation of sexual dimorphism is an important tool for inferring various socieoecological implications, but requires an enhanced understanding of sexual dimorphism and improved methods of estimation. The discriminant function analysis method has been shown to be a valid method for defining the sex of specimens and has potential as a method for classifying sex in certain fossil hominin samples. The analysis of correlation coefficient differences between males and females of different species can also be used to examine the transition from the LCA by providing evidence into the scaling

patterns of fossil hominin species and whether they are more similar to *Homo sapiens* or *Pan troglodytes*.

Ardipithecus ramidus is also connected to studies evaluating the level of sexual dimorphism within *Australopithecus afarensis*. The large, female *Ardipithecus ramidus* specimen with small canines indicates skeletal size overlap between the sexes. *Australopithecus afarensis* has reduced canine dimorphism in comparison to *Ardipithecus ramidus* but the level of body mass dimorphism is contentious (Kimbel and Delzene, 2009). Studies utilising resampling procedures have found high levels of body mass dimorphism within *Australopithecus afarensis* (Richmond and Jungers, 1995; Lockwood et al. 1996). Gordon et al. (2008) employed the geometric mean method to reduce a multivariate dataset to univariate data before measuring sexual dimorphism. The results indicate that the level of sexual dimorphism within *Australopithecus afarensis* is potentially greater than displayed in *Gorilla gorilla* and *Pongo pygmaeus.*

Reno et al. (2003; 2010) found contrasting evidence for a level of dimorphism within the range of modern humans by the use of the template method. Reno and Lovejoy (2015) compared the results of the template method with the geometric mean method for resampling, along with adding the large partial skeleton KSD-VP-1/1 “Kadanuumuu” as a template specimen. The geometric mean method was applied to the same sample testing the template method with results still falling within the upper range of *Gorilla gorilla*. This indicated that the difference between the two methods is not as a result of different sample compositions or modelling methods.

Reno and Lovejoy (2015) tested the contribution of multiple metrics from more complete specimens such as small-bodied Lucy and large bodied KSD-VP-1/1 Kadanuumuu to the geometric mean method. By restricting the contribution of Lucy to one skeletal metric the level of sexual dimorphism was reduced in the geometric mean method. The restriction of Lucy and another small bodied specimen, A.L. 128/129 contributing one metric each reduced the geometric mean method result to a sexual dimorphism level within the range of modern humans.

The results of the Reno and Lovejoy (2015) did not clarify the actual level of dimorphism within *Australopithecus afarensis* because the two methods tested provide different results depending on the specimens and skeletal elements chosen. The results will vary depending on underlying assumptions as to whether the body mass extremes found in the fossil

record are representative of those found in standard populations. As this is unknown, the level of sexual dimorphism within *Australopithecus afarensis* has yet to be inferred. It is therefore of value to examine other elements of sexual dimorphism as evidence of the level found in hominins such as *Australopithecus afarensis.* Comparing the scaling pattern of skeletal dimorphism in *Australopithecus afarensis* specimens to species analysed in this study may provide more information on the underlying restrictions in skeletal metric size that differ between males and females of the species. Rather than comparing the broad difference in male and female body size, analysis of correlation coefficient difference between male and female skeletal metric pairs can display a level of detail that presents the level of dimorphism within different areas of the skeleton. Producing a map of differences between areas of the skeleton for male and female *Australopithecus afarensis*, and comparing this to data from extant species, will produce more evidence for the pattern of sexual dimorphism displayed in the fossil hominin species and which extant species it is most similar to. A future comparison of correlation coefficient differences between the sexes could also be applied to other hominin species to produce greater understanding of the skeletal variation between males and females and how this has changed over time.

7.2.3: Implications for hominin palaeoecology

Evaluating fossil hominin sexual dimorphism through body mass is important because sexual dimorphism in body mass is prevalent among the extant primates and related to a range of palaecological correlates. Body mass dimorphism has been used to investigate home range in fossil hominin species. McHenry (1994) suggested that the high level of body mass dimorphism inferred for early hominins is connected to a ranging pattern where females forage in smaller territories than males. The reduction in sexual dimorphism through increased female *Homo* body size may therefore be associated with an expansion in ranging area. Damuth (1980) found a relationship between body mass and population density in mammalian species with population density scaling to body mass through a slope of -0.75 (log-scale). Hominin population density has been previously estimated from body mass by a calculation of home range before conversion into population densities per km^2 (Martin, 1981). Through a comparison of ecological data for extant species, the close relationship between body size, home size range and diet quality has been used to suggest that the change in *Homo* body size and foraging behaviour produced a tenfold increase in home range compared with australopithecines (Antón et al. 2002).

Body mass also has important implications for hominin energetics. Total energy expenditure is strongly correlated with body mass. Expenditure models indicate the increase in energy demands for *Homo erectus* was partially caused by larger body mass in relation to australopithecines (Leonard and Robertson, 1997). Aiello and Key (2002) note the important implications for large-bodied female *Homo erectus*, particularly the significant increase in energetic requirements for reproduction. In comparison to smaller-bodied australopithecines, female *Homo erectus* would have had to invest more energy for each infant if the same reproductive schedule was maintained. This means that shortening the interbirth interval would have reduced the costs per infant, necessitating changes for reducing the energetic load of females, (e.g. alloparental care, the division of labour, changes to locomotor energetics). These examples show the importance of body mass estimation and defining the differences in male and female body size for hominin species.

A main goal of palaeoanthropology is to reconstruct social behavior in extinct hominin species to evaluate the diversity of behaviours in the past and provide clarification on the development of modern human behavior. Inferring behavior from fossils is not without difficulty with Dixson (2009) believing that current estimates of hominin sexual dimorphism are too tentative to be used as evidence for evolution of human behavior. Social behavior does not preserve in the fossil record and must be assessed via proxy through associated anatomical and ecological attributes. Broad classifications of social systems such as single-male or multi-male groups can be inferred along with the determination of mating systems, from monogamous breeding pairs to polygynous groups.

One line of evidence for determining social behaviour is phylogeny. Extinct species have been compared to their closest living relatives based on the assumption that their behaviour will be the most similar. The fossil record has shown that the reality is not as simple. Whilst it is presumed that the level of sexual dimorphism within early hominins will be lower than seen in other primate species, strong body size dimorphism in *Australopithecus afarensis* has been inferred. This means that for evaluating social behaviour the use of extant primate data alone is unreliable (Plavcan, 2013). Phylogenetic reconstructions can also change with the introduction of new evidence, particularly new additions to the fossil record. Plavcan (2013) notes that if *Ardipithecus ramidus* is monomorphic in size then the greater level of sexual dimorphism interpreted in *Australopithecus afarensis* may represent a derived condition rather than an ancestral trait. Nonetheless, phylogeny is still an important tool for testing hypotheses and establishing

the connections and causal relationships between morphology, life history traits and behaviour. Studies that explore sexual dimorphism across taxa are therefore useful in evaluating how the evidence of behaviour links to ancestral lineages. The hierarchical clustering analyses in Chapter 6 found that the pattern of difference between males and females in some areas of the skeleton did correspond to the connection between closely related species, particularly *Homo sapiens* and *Pan troglodytes*. Other areas of the human skeleton display a pattern of sexual dimorphism that is most similar to less closely related species, indicating complex factors affecting the level of dimorphism in the skeleton beyond those that can be inferred through phylogenetic analysis.

The best evidence for interpreting behaviour in fossil species is through direct morphological correlates such as sexual dimorphism. Morphology is commonly used to determine locomotor and feeding behaviour, but it can also be utilised in the interpretation of breeding systems and mating behaviour. Primate sexual dimorphism in body size and canine tooth size is generally thought to be caused by sexual selection. A larger body and canine size provide an advantage to males during male-male competition and through female choice (Plavcan, 2001). Increased success during male-male competition increases reproductive output by providing access to females and excluding other males from reproductive success. The strong selective pressure for large body and canine tooth size should be more evident in social systems where there is male agonistic mate competition. Monogamous and polyandrous species are therefore associated with monomorphism whilst polygynous species display a stronger amount of sexual dimorphism (Leutenegger and Cheverud, 1982; Lindenfors, 2002). In terms of breeding systems, this means that one-male, multi-female groups will be more dimorphic than multi-male, multi-female groups (Clutton-Brock, 1985).

Studies assessing the link between sexual dimorphism and primate species have found that whilst high levels of dimorphism show statistically significant correlation to polygyny, low levels of dimorphism or monomorphism are not consistently correlated with any breeding system (Plavcan, 2004). Furthermore, the inaccuracy of methods predicting the level of body size dimorphism in fossil hominin species weakens the ability to predict mating behaviour. To improve the situation, more rigorous methods of predicting sexual dimorphism must be produced. Evaluating sexual dimorphism within the primate order and producing discriminant functions from multiple skeletal measurements can reduce uncertainty in the estimation of sexual dimorphism. The improvement of methods for

estimating sexual dimorphism is one way of providing greater confidence in the inference of socioecological implications.

The importance of female contributions to the level of sexual dimorphism within a species has been highlighted in previous studies. The level of dimorphism can also be affected by factors selecting for larger female size with advantages in competition for resources and the potential for reduced maternal and infant mortality (Ralls, 1976; Lindenfors, 2002). Selection for a smaller female size may be dependent on the need for early maturity and faster reproduction or to reduce metabolic demand in environments with unreliable resources (Martin et al. 1994; Gordon, 2006b). There is no current consensus on factors affecting either larger or smaller female size or the amount of change in female size required to affect the level of dimorphism.

Nonetheless, analysing the separate change in male and female trait size provides a potential method of identifying fossil hominin behaviour without the limitations of matching the degree of dimorphism to a particular mating system (Plavcan, 2013). Gordon (2006b) noted that changes to female body size over time can also be linked to shifts in diet or a female response to selective pressures caused by changes in the environment. Shifts in male body size relative to female size can be used to infer female grouping patterns and behaviour that affects the amount of female monopolisation by males.

In the fossil record, a reduction in *Homo erectus* body size dimorphism has been interpreted as being caused by an increase in female body size whilst the higher level of dimorphism in earlier hominins was as a consequence of a reduction in female size (McHenry, 1994; White et al. 2009). The analysis of differences in male and female skeleton scaling restrictions within this study provides another way of exploring changes in male and female trait size. If behavioural changes through social dimorphism are connected to factors influencing female size then it is important to explore what these factors might be. The difference in male and female correlation coefficient between skeletal metrics is an indication of restrictions to either male or female size in certain areas of the skeleton. By investigating the restrictions in male and female size for areas in fossil hominin skeletons, with comparison to the data from extant species, this may provide more information on whether an area of the skeleton is restricted in size by the needs of factors such as locomotion and energetics.

Chapter 8:

Conclusions

8.1: Completion of aims

This thesis had three main aims:

1. *To investigate the structure of sexual dimorphism within the primate order through an analysis of postcranial skeletal dimorphism.*

Investigating the structure of sexual dimorphism within the primate order is important to the field of palaeoanthropology because current methods of estimating hominin dimorphism have known limitations in terms of their accuracy. Understanding patterns and differences of sexual dimorphism between humans and other primates in more detail is an important first step for developing enhanced methods of estimating hominin sexual dimorphism. The analysis of postcranial skeletal dimorphism across the primate order through discriminant function analysis achieved this aim and found that skeletal dimorphism within the primate order is non-isometric. The best skeletal metrics of dimorphism varied between species, although there is a general trend for upper limb metrics to be better discriminators of dimorphic species. This includes *Homo sapiens* meaning that upper limb metrics are a convenient choice for discriminating sex across the primate order.

2. *To evaluate how greater understanding of primate sexual dimorphism could be applied to the estimation of sexual dimorphism within fossil hominin species.*

An evaluation of how greater understanding of primate sexual dimorphism could be applied to the estimation of sexual dimorphism within fossil hominin species was achieved through the comparison of discriminant function analysis to current sexual dimorphism estimation procedures. Discriminant function analysis was found to achieve greater accuracy than previous methods. Accuracy levels were maintained by choosing the best skeletal discriminators, allowing the production of discriminant function equations for determining sex through a smaller number of skeletal measurements. FHD is a good discriminator for *Homo sapiens* but does not maintain the same level for other species. There are superior metric choices, particularly as the current procedure for estimating body

mass from FHD has previously been found to produce overestimation of dimorphism. Separating the estimation of body mass and the estimation of sex is important for reducing uncertainty prior to the estimation of dimorphism. The direct classification of sex through discriminant function analysis provides a method for doing so.

3. *To explore the similarities and differences between species in terms of how skeletal metric scaling varies between males and females.*

An exploration into the similarities and differences between species, in terms of how skeletal metric scaling varies between males and females, was achieved through analysis of the correlation coefficient difference for metric pairs between males and females. Overall, this set of analyses showed that variation in the scaling between metrics of the male and female skeleton can be used as a valid assessment of the structure of sexual dimorphism in the primate order. The hierarchical clustering analysis indicated that the structure of dimorphism in the primate skeleton is highly variable and that phylogenetically related species do not always display the most similar patterns of correlation coefficient difference values between males and females. Other factors, such as positional behaviour, are therefore effecting differences between the sexes in how skeletal metrics scale to each other. Metric pairings where one metric is derived from the upper limb whilst the other metric is derived from the lower limb were more frequently found to have greater differences in correlation coefficients between males and females. This indicates that certain areas of the skeleton are restricted in terms of scaling within males or females of a species.

8.2: Implications for hominin body mass dimorphism estimation procedures

These findings have important implications for hominin body mass dimorphism estimation procedures. The fact that upper limb skeletal metrics are better discriminators of sex across dimorphic primate species indicates that they are a better choice than FHD for determining sex in fossil hominin species. Discriminant function analysis can be used to form new sex determination equations depending on the skeletal elements available. Discriminant function analysis is a particularly useful tool for determining the sex of fossil hominin specimens with incomplete assemblages. The comparison of discriminant function analysis (as an initial method of classifying sex before defining the level of sexual dimorphism) and

previous methods of predicting sexual dimorphism level, found that discriminant function analysis has increased accuracy through the power provided by multiple skeletal elements and the employment of a weighted average across skeletal elements. This accuracy was maintained with a smaller number of skeletal metrics, therefore supplying a practicable method for determining sex from a limited number of skeletal elements, as often found in fossil hominin assemblages.

It is important to note that for the sex classification technique to be employed on modern human specimens a larger sample that encompasses the wide variation within *Homo sapiens* is required. This analysis utilised samples from certain geographic areas meaning the full variation within each species may not be represented. The focus of this study was a detailed evaluation of variation within each specific sample rather than analysing temporal and population differences. A novel analysis of shape dimorphism was included in this study meaning that monomorphic species could be used for comparison to understand the structural differences between primate males and females once size is removed. This study also evaluated the implications of the current method for estimating fossil hominin body mass dimorphism and is the first to suggest splitting the current procedure to avoid predictions of sex *from* body mass.

8.3: Recommendations for future studies

Discriminant function equations could be created for fossil hominin species with enough valid specimens. Skeletal metric correlation coefficient difference between the sexes may also be applied to fossil hominin species to produce greater understanding of skeletal variation between males and females and how this has changed over time. The problem of choosing the most appropriate comparative sample for fossil hominin estimation may be overcome through the analysis of shape variation patterning between males and females. A potential way of comparing early hominins to *Pan troglodytes* and *Homo sapiens* is through correlation coefficient difference between the sexes. Any species with a large enough sample can be compared leading to a greater understanding of whether *Pan troglodytes* or *Homo sapiens* share a pattern of shape variation most similar to a given fossil hominin species.

The difference in male and female skeletal metric correlation coefficients is an indication of restrictions to either male or female size in certain areas of the skeleton. A future

investigation into the restrictions in certain areas of fossil hominin male and female skeleton size, with comparison to the data from extant species, may provide more information on the factors influencing size restrictions in the skeleton. The analysis of separate changes in male and female trait size also suggests a potential method for identifying fossil hominin behaviour without the limitations of matching the degree of dimorphism to a particular mating system.

Overall, the aims of the thesis were achieved and the investigation into the structure of primate skeletal dimorphism developed a greater understanding of variation in dimorphism patterns across the primate order and produced new methods that can be used to reconstruct fossil hominin body mass dimorphism. It is hoped that strengthening the procedures involved in estimating sex, body mass and sexual dimorphism, will lead to greater confidence when making inferences regarding various aspects of hominin palaeoecology.

Bibliography

Abouheif, E. and Fairbairn, D.J. (1997) 'A comparative analysis of allometry for sexual size dimorphism: assessing Rensch's rule', *The American Naturalist*, 149(3), pp. 540-562.

Achenbach, G.G. and Snowdon, C.T. (2002) 'Costs of caregiving: weight loss in captive adult male cotton-top tamarins (*Saguinus oedipus*) following the birth of infants', *International Journal of Primatology,* 23(1), pp. 179-189.

Adeyemo, A.I. (1997) 'Diurnal activities of green monkeys *Cercopithecus aethiops* in Old Oyo National Park, Nigeria', *South African Journal of Wildlife Research,* 27(1), pp. 24-26.

Adler, C.J. and Donlon, D. (2010) 'Sexual dimorphism in deciduous crown traits of a European derived Australian sample', *Forensic Science International,* 199(1), pp. 29-37.

Aiello, L.C. (1992) 'Allometry and the analysis of size and shape in human evolution', *Journal of Human Evolution,* 22(2), pp. 127-47.

Aiello, L.C. and Key, C. (2002) 'Energetic consequences of being a *Homo erectus* female', *American Journal of Human Biology*, 14(5), pp. 551-565.

Aiello, L.C. and Wheeler, P. (1995) 'The expensive-tissue hypothesis: the brain and the digestive system in human and primate evolution', *Current Anthropology,* 36(2), pp. 199-221.

Aiello, L.C. and Wood, B.A. (1994) 'Cranial variables as predictors of hominine body mass', *American Journal of Physical Anthropology,* 95(4), pp. 409-26.

Alberti, G. (2014) 'Modeling group size and scalar stress by logistic regression from an archaeological perspective', *PLoS One*, 9(3), e91510.

Allman, J., McLaughlin, T. and Hakeem, A. (1993) 'Brain weight and life-span in primate species', *Proceedings of the National Academy of Sciences of the United States of America*, 90(1), pp. 118-122.

Anapol, F., Turner, T.R., Mott, C.S. and Jolly, C.J. (2005) 'Comparative postcranial body shape and locomotion in *Chlorocebus aethiops* and *Cercopithecus mitis*', *American Journal of Physical Anthropology*, 127(2), pp. 231-239.

Andersson, M. (1994) *Sexual Selection.* Princeton: Princeton University Press.

Antón, S.C. (2012) 'Early Homo who, when, and where', *Current Anthropology,* 53(6), pp. 278-298.

Antón, S.C., Leonard, W.R. and Robertson, M.L. (2002) 'An ecomorphological model of the initial hominid dispersal from Africa', *Journal of Human Evolution*, 43(6), pp. 773-785.

Arroyo, M., Freire, M., Ansotegui, A. and Rocandio, M. (2010) 'Intraobserver error associated with anthropometric measurements made by dieticians', *Nutricion Hospitalaria*, 25(6), pp. 1053-1056.

Arsuaga, J., Lorenzo, C., Carretero, J-M., Gracia, A., Martínez, I., García, N., de Castro, J-M.B. and Carbonell, E. (1999) 'A complete human pelvis from the middle Pleistocene of Spain', *Nature,* 399(6733), pp. 255-258.

Aruguete, M.S. and Mason, W.A. (1996) 'Effect of infants on adult social relations in the squirrel monkey (*Saimiri sciureus*)', *Psychological Reports,* 79(2), pp. 603-611.

Atterton, T., De Groote, I. and Eliopoulos, C. (2016) 'Assessing size and strength of the clavicle for its usefulness for sex estimation in a British medieval sample', *HOMO - Journal of Comparative Human Biology,* 67(5), pp. 409-416.

Auerbach, B.M. and Ruff, C.B. (2004) 'Human body mass estimation: a comparison of "morphometric" and "mechanical" methods', *American Journal of Physical Anthropology,* 125(4), pp. 331-42.

Auerbach, B.M. and Ruff, C.B. (2006) 'Limb bone bilateral asymmetry: variability and commonality among modern humans', *Journal of Human Evolution*, 50(2), pp. 203-218.

Baer, J., Kakoma, I. and Weller, R. (1994) *Aotus: The Owl Monkey*. San Diego, CA: Academic Press.

Baker, J. and Pearson, O.M. (2006) 'Statistical methods for bioarchaeology: applications of age-adjustment and logistic regression to comparisons of skeletal populations with differing age-structures', *Journal of Archaeological Science,* 33(2), pp. 218-226.

Barelli, C., Heistermann, M., Boesch, C. and Reichard, U.H. (2008) 'Mating patterns and sexual swellings in pair-living and multimale groups of wild white-handed gibbons, *Hylobates lar*', *Animal Behaviour,* 75(3), pp. 991-1001.

Barelli, C., Matsudaira, K., Wolf, T., Roos, C., Heisterman, M., Hodges, K., Ishida, T., Malaivijitnond, S. and Reichard, U.H. (2013) 'Extra-pair paternity confirmed in wild white-handed gibbons', *American Journal of Primatology,* 75(12), pp. 1185-95.

Bardi, M., Petto, A.J. and Lee-Parritz, D.E. (2001) 'Parental failure in captive cotton-top tamarins (*Saguinus oedipus*)', *American Journal of Primatology*, 54(3), pp. 159-69.

Barrett, C.K. and Case, D.T. (2014) 'Use of 2D: 4D digit ratios to determine sex', *Journal of Forensic Science*, 59(5), pp. 1315-1320.

Behrensmeyer, A.K. (2008) 'Paleoenvironmental context of the Pliocene AL 333 "First Family" hominin locality, Hadar Formation, Ethiopia', *Geological Society of America Special Papers,* 446(1) pp. 203-14.

Bennett, K.A. (1981) 'On the expression of sex dimorphism', *American Journal of Physical Anthropology,* 56(1), pp. 59-61.

Bercovitch, F.B. (1992) 'Estradiol concentrations, fat deposits, and reproductive strategies in male rhesus macaques', *Hormones and Behavior,* 26(2), pp. 272-282.

Bercovitch, F.B. (1997) ‘Reproductive strategies for rhesus macaques’, *Primates,* 38(3), pp. 247-263.

Berge, C., Penin, X., Buchanan, B., O'Brien, M. and Collard, M. (2014) ‘Ontogenetic allometry, heterochrony, and interspecific differences in the skull of African apes, using tridimensional Procrustes analysis’, *American Journal of Physical Anthropology*, 124(2), pp. 124-138.

Bernstein, I.S., Weed, J.L., Judge, P.G. and Ruehlmann, T.E. (1989) ‘Seasonal weight changes in male rhesus monkeys (*Macaca mulatta*)’, *American Journal of Primatology,* 18(3), pp. 251-257.

Biewener, A.A. (1982) 'Bone strength in small mammals and bipedal birds: do safety factors change with body size?' *Journal of Experimental Biology,* 98(1), pp. 289-301.

Biewener, A.A. (1991) 'Musculoskeletal design in relation to body size', *Journal of Biomechanics,* 24(1), pp. 19-29.

Biewener, A.A. (2005) ‘Biomechanical consequences of scaling’, *Journal of Experimental Biology,* 208(9), pp. 1665-1676.

Bland, J.M. and Altman, D.G. (1995) ‘Multiple significance tests: the Bonferroni method’, *BMJ*, 310(1), pp. 170-171.

Boaz, N. and Almquist, A. (2002) *Biological Anthropology: A Synthetic Approach to Human Evolution.* New Jersey: Prentice Hall.

Boesch, C. (1994) ‘Cooperative hunting in wild chimpanzees’, *Animal Behaviour,* 48(3), pp. 653-667.

Boddy, A.M., McGowen, M.R., Sherwood, C.C., Grossman, L.I., Goodman, M. and Wildman, D.E. (2012) 'Comparative analysis of encephalization in mammals reveals relaxed constraints on anthropoid primate and cetacean brain scaling', *Journal of Evolutionary Biology,* 25(5), pp. 981-994.

Boinski, S., Jack, K., Lamarsh, C. and Coltrane, J.A. (1998) ‘Squirrel monkeys in Costa Rica: drifting to extinction’, *Oryx*, 32(1), pp. 45-58.

Boinski, S., Kauffman, L., Ehmke, E., Schet, S. and Vreedzaam, A. (2005) ‘Dispersal patterns among three species of squirrel monkeys (*Saimiri oerstedii*, *S. boliviensis*, and *S. sciureus*): divergent costs and benefits’, *Behaviour*, 142(5), pp. 525-632.

Boinski, S., Sughrui, K., Selvaggi, L., Quatrone, R., Henry, M. and Cropp, S. (2002) ‘An expanded test of the ecological model of primate social evolution: competitive regimes and female bonding in three species of squirrel monkeys (*Saimiri oerstedii*, *S. boliviensis*, and *S. sciureus*)’, *Behaviour*, 139(2), pp. 227-61.

Bonadonna, G., Torti, V., Randrianarison, R.M., Martinet, N., Gamba, M. and Giacoma, C. (2014) 'Behavioral correlates of extra-pair copulation in *Indri indri'*, *Primates,* 55(1), pp. 119-23.

Bonmati, A., Gomez-Olivencia, A., Arsuaga, J., Carretero, J.M., Gracia, A., Martinez, I., Lorenzo, C., Bérmudez de Castro, J.M. and Carbonell, E. (2010) 'Middle Pleistocene lower back and pelvis from an aged human individual from the Sima de los Huesos site, Spain', *Proceedings of the National Academy of Sciences of the United States of America*, 107(43), pp. 18386-18391.

Borries, C., Gordon, A.D. and Koenig, A. (2013) 'Beware of primate life history data: A plea for data standards and a repository', *PLoS ONE,* 8(6), pp. 1-12.

Borries, C., Lu, A., Ossi-Lupo, K., Larney, E. and Koenig, A. (2011) 'Primate life histories and dietary adaptations: a comparison of asian colobines and macaques', *American Journal of Physical Anthropology*, 144(2), pp. 286-299.

Brassey, C.A., O'Mahoney, T.G., Chamberlain, A.T. and Sellers, W.I. (2018) 'A volumetric technique for fossil body mass estimation applied to *Australopithecus afarensis'*, *Journal of Human Evolution*, 115(1-7), pp. 47-64.

Brown, P.J. and Sundberg, R. (1987) 'Confidence and conflict in multivariate calibration', *Journal of the Royal Statistical Society B,* 49(1), pp. 46-57.

Buchanan, B., Collard, M., Hamilton, M.J. and O'Brien, M. (2011) 'Points and prey: an evaluation of the hypothesis that prey size predicts early Palaeoindian projectile point form', 38(4), pp. 852-864.

Buchanan, B., O'Brien, M. and Collard, M. (2014) 'Continent-wide or region-specific? A geometric morphometrics-based assessment of variation in Clovis point shape', *Archaeological and Anthropological Sciences*, 6(2), pp. 145-162.

Buck, T.J. and Viðarsdóttir, U.S. (2004) 'A proposed method for the identification of race in sub-adult skeletons: a geometric morphometric analysis of mandibular morphology', *Journal of Forensic Sciences,* 49(6), pp. 1150-1164.

Buikstra, J.E. and Ubelaker, D.H. (1994) *Standards for Data Collection from Human Skeletal Remains.* Fayetteville, Arkansas: Arkansas Archaeological Survey Report Number 44.

Burgess, M.L., McFarlin, S.C., Mudakikwa, A., Cranfield, M.R. and Ruff, C.B. (2018) 'Body mass estimation in hominoids: Age and locomotor effects', *Journal of Human Evolution,* 115(1-7), pp. 36-46.

Burkart, J.M., Hrdy, S.B. and van Schaik, C. (2009) 'Cooperative breeding and human cognitive evolution', *Evolutionary Anthropology: Issues, News and Reviews*, 18(5), pp. 175-186.

Caldwell, H.K., Lee, H., Macbeth, A.H. and Young, W.S. (2008) 'Vasopressin: behavioral roles of an "original" neuropeptide', *Progress in Neurobiology,* 84(1), pp. 1-24.

Cant, J.G.H. (1987) 'Effects of sexual dimorphism in body size on feeding postural behavior of Sumatran orangutans (*Pongo pygmaeus*)', *American Journal of Physical Anthropology*, 74(2), pp. 143-148.

Carlson, K.J., Grine, F.E. and Pearson, O.M. (2007) 'Robusticity and sexual dimorphism in the postcranium of modern hunter-gatherers from Australia', *American Journal of Physical Anthropology*, 134(1), pp. 9-23.

Cartmill, M. and Milton, K. (1977) 'The lorisiform wrist joint and the evolution of 'brachiating' adaptations in the hominoidea', *American Journal of Physical Anthropology,* 47(2), pp. 249-272.

Chakraborty, R. and Majumder, P.P. (1982) 'On Bennett's measure of sex dimorphism', *American Journal of Physical Anthropology,* 59(3), pp. 295-298.

Charisi, D., Eliopoulos, C., Vanna, V., Koilias, C.G. and Manolis, S.K. (2011) 'Sexual dimorphism of the arm bones in a modern Green population', *Journal of Forensic Science*, 56(1), pp. 10-18.

Charles-Dominique, P. (1977) *Ecology and Behaviour of Nocturnal Prosimians.* London: Duckworth.

Charles-Dominique, P. and Bearder, S.K. (1979) 'Field studies of lorisid behavior: methodological aspects', in Martin, G. (ed.) *The Study of Prosimian Behavior*. Cambridge: Academic Press, pp. 567-629.

Charnov, E.L. (1993) *Life History Invariants.* Oxford: Oxford University Press.

Charnov, E.L. and Schaffer, W.M. (1973) 'Life-history consequences of natural selection: Cole's result revisited', *The American Naturalist*, 107(958), pp. 791-793.

Cheney, D.L and Seyfarth, R.M. (1983) 'Nonrandom dispersal in free-ranging vervet monkeys: social and genetic consequences', *The American Naturalist*, 122(3), pp. 392-412.

Cheverud, J.M., Dow, M.M. and Leutenegger, W. (1985) 'The quantitative assessment of phylogenetic constraints in comparative analyses: sexual dimorphism in body weight among primates', *Evolution,* 39(6) pp. 1335-1351.

Churchill, S.E. (2012) 'Body size in African Middle Pleistocene *Homo*'. In Reynolds, S. and Gallagher, A. (eds.). *African Genesis: Perspectives on Hominin Evolution.* Cambridge: Cambridge University Press, pp. 319-46.

Clark, A.B. (1978) 'Sex ratio and local resource competition in a prosimian primate', *Science*, 201(4351), pp. 163-165.

Clutton-Brock, T. (1985) 'Size, sexual dimorphism, and polygyny in primate', in Jungers, W.L. (ed.) *Scaling in Primate Biology.* New York: Plenum Press, pp. 51-60.

Clutton-Brock, T. (2007) 'Sexual selection in males and females', *Nature,* 318(5858), pp. 1882-1885.

Coe, C.L., Smith, E.R. and Levine, S. (1985) 'The endocrine system of the squirrel monkey', in Rosenblum, L.A. and Coe, C.L. (eds.) *Handbook of Squirrel Monkey Research,* New York: Plenum Press, pp. 191-218.

Cope, D.A. and Lacy, M.G. (1992) 'Falsification of a single species hypothesis using the coefficient of variation: a simulation approach', *American Journal of Physical Anthropology*, 89(3), pp. 359-378.

Cope, D.A. and Lacy, M.G. (1995) 'Comparative application of the coefficient of variation and range-based statistics for assessing the taxonomic composition of fossil samples', *Journal of Human Evolution*, 29(6), pp. 549-575.

Cowal, L.S., Pastor, R.F., Srivastava, R., Srivastava, R., Saini, V., Rai, R.K., Tripathi, S.K., Pandey, S., Singh, T.B. and Pandey, A.K. (2013) 'Dimensional variation in the proximal ulna: evaluation of a metric method for sex assessment', *American Journal of Physical Anthropology*, 135(4), pp. 469-478.

Cowlishaw, G. and Dunbar, R.I.M. (1991) 'Dominance rank and mating success in male primates', *Animal Behaviour,* 41(6), pp. 1045-1056.

Cowlishaw, G. and Dunbar, R.I.M. (2000) *Primate Conservation Biology.* Chicago: University of Chicago Press.

Dagosto, M., Gebo, D., Ni, X. and Smith, T. (2018) 'Estimating body size in early primates: the case of Archicebus and Teilhardina', *Journal of Human Evolution*, 115(1-7), pp. 8-19

Damuth, J. (1980) 'Population density and body size in mammals', *Nature,* 290(1), pp. 699-700.

Darwin, C. (1871) *The Descent of Man and Selection in Relation to Sex.* J. Murray: London.

Dayal, M.R., Spocter, M.A. and Bidmos, M.A. (2008) 'An assessment of sex using the skull of black South Africans by discriminant function analysis', *HOMO - Journal of Comparative Human Biology,* 59(3), pp. 209-221.

Deaner, R.O., Barton, R.A. and van Schaik, C.P. (2003) 'Primate brains and life histories: renewing the connection', in Kappeler, P.M. and Pereira, M.E. (eds.) *Primate Life Histories and Socioecology*. Chicago: The University of Chicago Press, pp. 233- 265.

DeGusta, D. and Vrba, E. (2003) 'A method for inferring paleohabitats from the functional morphology of bovid astragali', *Journal of Archaeological Science,* 30(8), pp. 1009-1022.

Delson, E., Terranova, C.J., Jungers, W.L., Sargis, E.J., Jablonski, N.G. and Dechow, P.C. (2000). *Body Mass in Cercopithecidae (Primates, Mammalia): Estimation and Scaling in Extinct and Extant Taxa.* New York: American Museum of Natural History- Anthropological Papers of the American Museum of Natural History Number 83.

Dement, M.W. (1983) 'Feeding ecology and the evolution of body size of baboons', *African Journal of Ecology,* 21(4), pp. 219-33.

Demes, B., Larson, S.G., Stern Jr., J.T., Jungers, W.L., Biknevicius, A.R. and Schmitt, D. (1994) 'The kinetics of primate quadrupedalism: "hindlimb drive" reconsidered', *Journal of Human Evolution,* 26(5-6), pp. 353-374.

Demes, B., Qin, Y.-X., Stern, J.T., Larson, S.G. and Rubin, C.T. (2001) 'Patterns of strain in the macaque tibia during functional activity', *American Journal of Physical Anthropology*, 116(4), pp. 257-265.

Deng, H.-W., Shen, H., Xu, F.-H., Deng, H., Conway, T., Liu, Y.-J., Liu, Y.-Z., Huang, Q.-Y., Davies, K.M., Recker, R.R. and Li, J.-L. (2003) 'Several genomic regions potentially containing QTLs for bone size variation were identified in a whole-genome linkage scan', *American Journal of Medical Genetics,* 119(2), pp. 121-131.

DeSilva, J. M. (2011) 'A shift toward birthing relatively large infants early in human evolution', *Proceedings of the National Academy of Sciences of the United States of America,* 108(3), pp. 1022-1027.

de Waal, F.B.M. and Gavrilets, S. (2013) 'Monogamy with a purpose', *Proceedings of the National Academy of Sciences of the United States of America,* 110(38), pp. 15167-15168.

di Bitetti, M.S. and Janson, C.H. (2000) 'When will the stork arrive? Patterns of birth seasonality in neotropical primates', *American Journal of Primatology*, 50(2), pp. 109-130.

di Fiore, A. (2003) 'Molecular genetic approaches to the study of primate behavior, social organization, and reproduction', *American Journal of Physical Anthropology*, 122(37), pp. 62-99.

Dirks, P.H., Roberts, E.M., Hilbert-Wolf, H., Kramers, J.D., Hawks, J., Dosseto, A., Duval, M., Elliott, M., Evans, M., Grün, R., Hellstrom, J., Herries, A.I.R., Joannes-Boyau, R., Makhubela, T.V., Placzek, C.J., Robbins, J., Spandler, C., Wiersma, J., Woodhead, J. and Berger, L.R. (2017) 'The age of *Homo naledi* and associated sediments in the Rising Star Cave, South Africa', *eLife*, 6(1), e24231.

Dixson, A.F. (2009) *Sexual Selection and the Origins of Human Mating Systems*. Oxford: Oxford University Press.

Dixson, A.F. (2012) *Primate Sexuality: Comparative Studies of the Prosimians, Monkeys, Apes, and Humans*. 2nd edn. Oxford: Oxford University Press.

Dixson, A.F. (2013) 'Male infanticide and primate monogamy', *Proceedings of the National Academy of Sciences of the United States of America,* 110(51), pp. 4937-4941.

Doran, D.M. (1993) 'Sex differences in adult chimpanzee positional behavior: the influence of body size on locomotion and posture', *American Journal of Physical Anthropology,* 91(1), pp. 99-115.

Doran, D. (1997) 'Influence of seasonality on activity patterns, feeding behavior, ranging, and grouping patterns in Tai chimpanzees', *International Journal of Primatology,* 18(2), pp. 183-206.

Dunbar, R.I.M. (1998) 'The social brain hypothesis', *Evolutionary Anthropology: Issues, News, and Reviews,* 6(5), pp. 178-190

Dunbar, R.I.M. (2009) 'The social brain hypothesis and its implications for social evolution', *Annals of Human Biology,* 36(5), pp. 562-572.

Dunbar, R.I.M. and Shultz, S. (2007) 'Evolution in the social brain', *Science,* 317(5843), pp. 1344-1347.

Efron, B. (1975) 'The efficiency of logistic regression compared to normal discriminant analysis', *Journal of the American Statistical Association*, 70(352), pp. 892-898.

Eisenberg, J.F., Muckenhirn, N.A. and Rudran, R. (1972) 'The relation between ecology and social structure in primates', *Science*, 176(4037), pp. 863-874.

Elliott, M., Collard, M., Kurki, H. and Weston, D.A. (2014) 'Estimating fossil hominin body mass from cranial variables: an assessment using CT data from modern humans of known body mass', *American Journal of Physical Anthropology,* 154(2), pp. 201-214.

Elliot, M., Kurki, H., Weston, D.A. and Collard, M. (2016a) 'Estimating body mass from postcranial variables: an evaluation of current equations using a large known-mass sample of modern humans', *Archaeological and Anthropological Sciences*, 8(4), pp. 689-704.

Elliot, M., Kurki, H., Weston, D.A. and Collard, M. (2016b) 'Estimating body mass from skeletal material: new predictive equations and methodological insights from analyses of a known-mass sample of humans', *Archaeological and Anthropological Sciences*, 8(4), pp. 731-750.

Elton, S., Jansson, A., Meloro, C., Louys, J., Plummer, T. and Bishop, L.C. (2016) 'Exploring morphological generality in the Old World monkey postcranium using an ecomorphological framework', *Journal of Anatomy,* 228(4), pp. 534-560.

Ely, J. and Kurland, J.A. (1989) 'Spatial autocorrelation, phylogenetic constraints and the causes of sexual dimorphism in primates, *International Journal of Primatology*, 10(1), pp. 151-171.

Ernest, S. (2003) 'Life history characteristics of placental nonvolant mammals', *Ecological Archives*, 84(12), pp. 3402-3402.

Estes, R.D. (1992) *The Behavior Guide to African Mammals.* Oakland: University of California Press.

Fairbanks, L.A. (1990) 'Reciprocal benefits of allomothering for female vervet monkeys', *Animal Behaviour,* 40(3), pp. 553-562.

Feise, R.J. (2002) 'Do multiple outcome measures require p-value adjustment?' *BMC Medical Research Methodology*, 2(8), pp. 1-4.

Fernandez-Duque, E. (2011) ‘Rensch's rule, Bergmann's effect and adult sexual dimorphism in wild monogamous owl monkeys (*Aotus azarai*) of Argentina’, *American Journal of Anthropology*, 146(1), pp. 38-48.

Fernandez-Duque, E., Valeggia, C.R. and Mendoza, S.P. (2009) 'The biology of paternal care in human and nonhuman primates', *Annual Review of Anthropology,* 38(1), pp. 115-130.

Fernandez, H. and Monchot, H. (2007) ‘Sexual dimorphism in limb bones of Ibex (*Capra ibex* L.): mixture analysis applied to modern and fossil data’, *International Journal of Osteoarchaeology*, 17(5), pp. 479-491.

Ford, S.M. (1994) 'Evolution of sexual dimorphism in body weight in platyrrhines', *American Journal of Primatology,* 34(2), pp. 221-244.

Ford, S.M. and Davis, L.C. (1992) ‘Systematics and body size - implications for feeding adaptations in New World Monkeys’, *American Journal of Physical Anthropology*, 88(4), pp. 415-468.

Fleagle, J.G., Kay, R. and Simons, E. (1980) ‘Sexual dimorphism in early anthropoids’, *Nature*, 287(1), pp. 328-330.

Fleagle, J.G. and Mittermeier, R.A. (1980) 'Locomotor behavior, body size, and comparative ecology of seven Surinam monkeys', *American Journal of Physical Anthropology,* 52(3), pp. 301-304.

Franzoi, S.L. and Herzog, M.E. (1987) ‘Judging physical attractiveness: what body aspects do we use?’ Society for Personality and Social Psychology’, 13(1), pp. 19-33.

Fruth, B. and Hohmann, G. (1996) ‘Nest building behaviour in the great apes: the great leap forward?’ in McGrew, W.C., Marchant, L.F. and Nishida, T. (eds.) *Great Ape Societies*. Cambridge: Cambridge University Press, pp. 225-240.

Garber, P.A. (1980) ‘Locomotor behavior and feeding ecology of the panamanian tamarin (*Saguinus oedipus geoffroyi*, Callitrichidae, Primates)’, *International Journal of Primatology,* 1(2), pp. 185-201.

Garber, P.A. (1996) ‘One for all and breeding for one: cooperation and competition as a tamarin reproductive strategy’, *Evolutionary Anthropology,* 5(6), pp. 187-199.

Garvin, H.M., Elliot, M.C., Delezene, L.K. Hawks, J., Churchill, S.E., Berger, L.R. and Holliday, T.W. (2017) ‘Body size, brain size, and sexual dimorphism in *Homo naledi* from the Dinaledi Chamber’, *Journal of Human Evolution*, 111(1), pp. 119-138.

Gingerich, P.D. (1995) 'Statistical power of EDF tests of normality and the sample size required to distinguish geometric-normal (lognormal) from arithmetic-normal distributions of low variability', *Journal of Theoretical Biology,* 173(2), pp. 125-136.

Godde, K. and Taylor, R.W. (2013) 'Distinguishing body mass and activity level from the lower limb: Can entheses diagnose obesity?' *Forensic Science International*, 226(1-3), pp. 1-7.

Godfrey, L.R., Boy, D., Gomberg, N. and Sutherland, M. (1991) 'Scaling of limb joint surface areas in anthropoid primates and other mammals', *Journal of Zoology,* 223(4), pp. 603-625.

Godfrey, L.R., Lyon, S.K. and Sutherland, M.R. (1993) 'Sexual dimorphism in large-bodied primates: The case of the subfossil lemurs', *American Journal Physical Anthropology,* 90(3), pp. 315-334.

Godfrey, L.R., Samonds, K.E., Jungers, W.L., Sutherland, M.R. and Irwin, M.T. (2004) 'Ontogenetic correlates of diet in Malagasy Lemurs', *American Journal of Physical Anthropology,* 123(3), pp. 250-276.

Gonzalez, P.N., Bernal, V. and Perez, S.I. (2009) 'Geometric morphometric approach to sex estimation of human pelvis', *Forensic Science International,* 189(1-3), pp. 68-74.

Gordon, A.D. (2004) *Evolution of body size and sexual size dimorphism in the order primates: Rensch's rule, quantitative genetics, and phylogenetic effects*. PhD thesis. University of Texas.

Gordon, A.D. (2006a) 'Scaling of size and dimorphism in primates I: Microevolution', *International Journal of Primatology,* 27(1), pp. 27-61.

Gordon, A.D. (2006b) 'Scaling of size and dimorphism in primates: II: Macroevolution', *International Journal of Primatology*, 27(1), pp. 63-105.

Gordon, A.D., Green, D.J. and Richmond, B.G. (2008) 'Strong postcranial size dimorphism in *Australopithecus afarensis*: results from two new resampling methods for multivariate data sets with missing data', *American Journal of Physical Anthropology,* 135(3), pp. 311-328.

Grabowski, M., Hatala, K.G., Jungers, W.L. and Richmond, B.G. (2015) 'Body mass estimates of hominin fossils and the evolution of human body size', *Journal of Human Evolution*, 85(1), pp. 75-93.

Gray, J.P. and Wolfe, L.D. (1980) 'Height and sexual dimorphism of stature among human societies', *American Journal of Physical Anthropology,* 53(3), pp. 441-456.

Green, H. and Curnoe, D. (2009) 'Sexual dimorphism in Southeast Asian crania: A geometric morphometric approach', *HOMO - Journal of Comparative Human Biology,* 60(6), pp. 517-534.

Greenacre, M.J. and Vrba, E.S. (1984) 'Graphical display and interpretation of antelope census data in african wildlife areas, using correspondence analysis the Ecological Society of America', *Ecology*, 65(3), pp. 984-997.

Greene, D.L. (1989) 'Comparison of t-tests for differences in sexual dimorphism between populations', *American Journal of Physical Anthropology,* 79(1), pp. 121-125.

Grine, F.E., Jungers, W.L., Tobias, P.V. and Pearson, O.M. (1995) 'Fossil homo femur from Berg Aukas, Northern Namibia', *American Journal of Physical Anthropology,* 97(2), pp. 151-85.

Groves, C. (2001) *Primate Taxonomy (Smithsonian Series in Comparative Evolutionary Biology).* Washington D.C: Smithsonian Institution Press.

Groves, C. (2005) '*Chlorocebus pygerythrus'*, in Wilson, D.E. and Reeder D.M. (eds.) *Mammal Species of the World: A Taxonomic and Geographic Reference*. 3rd edn, Baltimore: Johns Hopkins University Press, pp. 159-159.

Grubb, P., Butynski, T.M., Oates, J.F., Bearder, S.K., Disotell, T.R., Groves, C.P. and Struhsaker, T.T. (2003) 'Assessment of the diversity of African primates', *International Journal of Primatology*, 24(6), pp. 1301-1357.

Grzimek, B. (1990) *Grzimek's Encyclopedia of Mammals.* New York: McGraw-Hill.

Gurven, M. and Kaplan, H. (2007) 'Longevity among hunter-gatherers: a cross-cultural examination', *Population and Development Review*, 33(2), pp. 321-365.

Hakeem, A., Sandoval, R., Jones, M. and Allman, J. (1996) 'Brain and lIfe span in primates', in Birren, J. (ed.) *Handbook of the Psychology of Aging*. New York: Academic Press, pp. 78-104.

Hamada, Y., Urasopon, N., Hadi, I. and Malaivijitnond, S. (2006) 'Body size and proportions and pelage color of free-ranging *Macaca mulatta* from a zone of hybridization in Northeastern Thailand', *International Journal of Primatology,* 27(2), pp. 497-513.

Hamada, Y., Watanabe, T., Chatani, K., Hayakawa, S., and Iwamoto, M. (2005) 'Morphometrical comparison between Indian- and Chinese-derived rhesus macaques (*Macaca mulatta*)', *Anthropological Sciences*, 113(2), pp. 183–188.

Hammond, A. and Hammond, A.S. (2014) 'In vivo baseline measurements of hip joint range of motion in suspensory and nonsuspensory anthropoids', *American Journal of Physical Anthropology*, 153(3), pp. 417-434.

Harcourt, A.H. and Greenberg, J. (2001) 'Do gorilla females join males to avoid infanticide? A quantitative model', *Animal Behaviour,* 62(5), pp. 905-915.

Harmon, E.H. (2006) 'Size and shape variation in *Australopithecus afarensis* proximal femora', *Journal of Human Evolution,* 51(3) pp. 217-227.

Harrison, M.J.S. (1983) 'Patterns of range use by the green monkey, *Cercopithecus sabaeus*, at Mt. Assirik, Senegal', *Folia Primatologica,* 41(3-4), pp. 157-179.

Harvey, P.H. and Clutton-Brock, T. (1985) 'Life history variation in primates society', *Society for the Study of Evolution*, 39(3), pp. 559-581.

Harvey, P.H. and Krebs, J.R. (1990) 'Comparing brains', *Science*, 249(4965), pp. 140-146.

Hawkes, K., O'Connell, J.F., Blurton Jones, N.G., Alvarez, H. and Charnov, E.L. (1998) 'Grandmothering, menopause, and the evolution of human life histories', *Proceedings of the National Academy of Sciences of the United States of America*, 95(3), pp. 1336-1339.

Hector, A.K. and Raleigh, M.J. (1992) 'The effects of temporary removal of the alpha male on the behavior of subordinate male vervet monkeys', *American Journal of Primatology,* 26(2), pp. 77-87.

Hens, S.M., Konigsberg, L.W. and Jungers, W.L. (2000) 'Estimating stature in fossil hominids: which regression model and reference sample to use?' *Journal of Human Evolution,* 38(6), pp. 767-784.

Herculano-Houzel, S., Mota, B. and Lent, R. (2006) 'Cellular scaling rules for rodent brains', *Proceedings of the National Academy of Sciences of the United States of America*, 103(32), pp. 12138-12143.

Higham, J.P., Heistermann, M. and Maestripieri, D. (2011) 'The energetics of male–male endurance rivalry in free-ranging rhesus macaques, *Macaca mulatta*', *Animal Behaviour,* 81(5), pp. 1001-1007.

Holliday, T.W. (2012) 'Body size, body shape, and the circumscription of the genus Homo', *Current Anthropology,* 53(6) pp. 330-345.

Holman, D.J and Bennett, K.A. (1991) 'Determination of sex from arm bone measurements', *American Journal of Physical Anthropology,* 84(4), pp. 421-426.

Holt, B.M. (2003) 'Mobility in upper Paleolithic and Mesolithic Europe: evidence from the lower limb', *American Journal of Physical Anthropology,* 122(3), pp. 200-215.

Honeine, J., Schieppati, M., Gagey, O. and Manh-Cuong, D. (2013) 'The functional role of the triceps surae muscle during human locomotion', *PLoS ONE,* 8(1), pp. 1-12.

Hook, M.A. and Rogers, L.J. (2002) 'Leading-limb preferences in marmosets (*Callithrix jacchus*): walking, leaping and landing', *Laterality*, 7(2), pp. 145-162.

Hopkins, W.D. (2008) 'Brief communication: locomotor limb preferences in captive chimpanzees (*Pan troglodytes*): implications for morphological asymmetries in limb bones', *American Journal of Physical Anthropology,* 137(1), pp. 113-118.

Huberty, C.J. and Hussein, M.H. (2003) 'Some problems in reporting use of discriminant analyses', *The Journal of Experimental Education*, 71(2), pp. 177-192.

Hunt, D.R. and Albanese, J. (2005) 'History and demographic composition of the Robert J. Terry anatomical collection', *American Journal of Physical Anthropology*, 127(4), pp. 406-417.

Isaac, N.J.B., Storch, D. and Carbone, C. (2013) 'The paradox of energy equivalence', *Global Ecology and Biogeography,* 22(1), pp. 1-5.

Isbell, L.A., Cheney, D.L. and Seyfarth, R.M. (1991) 'Group fusions and minimum group sizes in vervet monkeys (*Cercopithecus aethiops*)', *American Journal of Primatology,* 25(1), pp. 57-65.

Isbell, L.A., Cheney, D.L. and Seyfarth, R.M. (2002) 'Why vervet monkeys (*Cercopithecus aethiops*) live in multimale groups', in Glenn, M.E. and Cords, M. (eds.) *The Guenons: Diversity and Adaptation in African Monkeys*. New York: Springer, pp. 173-187.

Isbell, L.A., Pruetz, J.D., Lewis, M. and Young, T.P. (1999) 'Rank differences in ecological behavior: a comparative study of patas monkeys (*Erythrocebus patas*) and vervets (*Cercopithecus aethiops*)', *International Journal of Primatology,* 20(2), pp. 257-272.

Işcan, M.Y., Yoshino, M. and Kato, S. (1994) 'Sex determination from the tibia: standards for contemporary Japan', *Journal of Forensic Sciences,* 39(3), pp. 785-792.

Isler, K. and van Schaik, C.P. (2006) 'Metabolic costs of brain size evolution', *Biology Letters,* 2(4), pp. 557-560.

Isler, K., Christopher Kirk, E., Miller, J.M.A., Albrecht, G.A., Gelvin, B.R. and Martin, R.D. (2008) 'Endocranial volumes of primate species: scaling analyses using a comprehensive and reliable data set', *Journal of Human Evolution,* 55(6), pp. 967-978.

Izar, P., Stone, A., Carnegie, S. and Nakai, E.S. (2008) 'Sexual selection, female choice and mating systems', in Garber, P.A., Estrada, A., Bicca-Marques, J.C., Heymann, E. and Strier, K. (eds.) *South American Primates: Testing New Theories in the Study of Primate Behavior, Ecology and Conservation,* New York: Springer Science+Business Media, pp. 157-198.

Janson, C.H. and Boinski, S. (1992) 'Morphological and behavioral adaptations for foraging in generalist primates - the case of the cebines', *American Journal of Physical Anthropology*, 88(4), pp. 483-98.

Janson, C.H. and van Schaik, C.P. (1993) 'Ecological risk aversion in juvenile primates: slow and steady wins the race', in Pereira, M.E. and Fairbanks, L.A. (eds.) *Juvenile Primates: Life History, Development and Behavior.* Oxford: Oxford University Press, pp. 57-76.

Järvinen, T.L.N., Kannus, P., Pajamäki, I., Vuohelainen, T., Tuukkanen, J., Järvinen, M. and Sievänen, H. (2003) 'Estrogen deposits extra mineral into bones of female rats in puberty, but simultaneously seems to suppress the responsiveness of female skeleton to mechanical loading', *Bone,* 32(6), pp. 642-651.

Jerison, H.J. (1973) *Evolution of the Brain and Intelligence.* New York: Academic Press.

Jetz, W., Carbone, C., Fulford, J. and Brown, J.H. (2004) 'The scaling of animal space use', *Science,* 306(5694), pp. 266-268.

Jiménez-Arenas, J.M. (2013) 'Tooth size and metabolic requirements in primates: the 'equivalence between exponents under discussion', *International Journal of Morphology,* 31(4), pp. 1191-1197.

Jones, C.J., Clyde, C.A., Jones, J.K. and Wilson, D.E. (1996) '*Pan troglodytes'*, *Mammalian Species,* 529(1), pp. 1-9.

Jones, J.H. (2011) 'Primates and the evolution of long, slow life histories', *Current Biology,* 21(18), pp. 708-717.

Josephson, S.C., Juell, K.E. and Rogers, A.R. (1996) 'Estimating sexual dimorphism by method-of-moments', *American Journal of Physical Anthropology,* 100(2), pp. 191-206.

Jouffroy, F.K., Stern, J.T., Medina, M.F. and Larson, S.G. (1999) 'Function and cytochemical characteristics of postural limb muscles of the rhesus monkey: a telemetered EMG and immunofluorescence study', *International Journal of Primatology*, 70(5), pp. 235-253.

Jungers, W.L. (1988) 'Relative joint size and hominoid locomotor adaptations with implications for the evolution of hominid bipedalism', *Journal of Human Evolution*, 17(1-2), pp. 247-265.

Jungers, W.L. (1990a) 'Scaling of postcranial joint size in hominoid primates', in Jouffroy, F.K., Stack, M.H and Niemitz, C. (eds.). *Gravity, Posture and Locomotion in Primates.* Il Sedicesimo: Firenze, pp. 87-95.

Jungers, W.L. (1990b) 'Problems and methods in reconstructing body size in fossil primates', in: Damuth, J. and MacFadden, B.J. (eds.). *Body Size in Mammalian Paleobiology: Estimation and Biological Implications.* Cambridge: Cambridge University Press, pp. 103-18.

Jungers, W.L. (1991) 'Scaling of postcranial joint size in hominoid primates', *Journal of Human Evolution,* 6(5-6), pp. 391-399.

Jungers, W.L., Grabowski, M., Hataka, K.G. and Richmond, B.G. (2016) 'The evolution of body size and shape in the human career', *Philosophical Transactions of the Royal Society B,* 371(1698), e20150247.

Kaplan, H., Hill, K., Lancaster, J. and Hurtado, A.M. (2000) 'A theory of human life history evolution: diet, intelligence, and longevity', *Evolutionary Anthropology,* 9(4), pp. 156-185.

Kappeler, P.M. (2000) *Primate Males: Causes and Consequences of Variation in Group Composition.* Cambridge: Cambridge University Press.

Kappeler, P.M. (2014) 'Lemur behaviour informs the evolution of social monogamy', *Trends in Ecology & Evolution,* 29(11), pp. 591-593.

Kappelman, J. (1996) 'The evolution of body mass and relative brain size in fossil hominids', *Journal of Human Evolution,* 30(3), pp. 243-276.

Kay, R.F. (1982) 'Sexual dimorphism in Ramapithecinae', *Proceedings of the National Academy of Sciences of the United States of America,* 79(2), pp. 209-212.

Kay, R.F., Plavcan, J.M., Glander, K.E. and Wright, P.C. (1988) 'Sexual selection and canine dimorphism in New World monkeys', *American Journal of Physical Anthropology,* 77(3), pp. 385-397.

Kelt, D.A. and van Vuren, D.H. (2001) ‘The ecology and macroecology of mammalian home range area’, *The American Naturalist*, 157(6), pp. 637-645.

Kenyon, M., Roos, C., Vo Thanh Binh and Chivers, D. (2011) 'Extrapair paternity in golden-cheeked gibbons (*Nomascus gabriellae*) in the secondary lowland forest of Cat Tien National Park, Vietnam', *Folia Primatolology,* 82(3), pp. 154-164.

Kidwell, J.F. and Chase, H.B. (1967) ‘Fitting the allometric equation- a comparison of ten methods by computer simulation’, *Growth*, 31(2), pp. 165-179.

Kim, P.S., McQueen, J.S., Coxworth, J.E. and Hawkes, K. (2014) 'Grandmothering drives the evolution of longevity in a probabilistic model', *Journal of Theoretical Biology,* 353(1), pp. 84-94.

Kimbel, W.H. and Delezene, L.K. (2009) ‘'Lucy' redux: A review of research on *Australopithecus afarensis*’, *American Journal of Physical Anthropology*, 140(49), pp. 2-48.

King, C.A., Işcan, M.Y. and Loth, S.R. (1998) 'Metric and comparative analysis of sexual dimorphism in the Thai femur', *Journal of Forensic Sciences,* 43(5), pp. 954-958.

Kinzey, W.G. (1997) *New World Primates: Ecology, Evolution, and Behavior.* New York: Aldine Transaction.

Klopfer, P.H. and Boskoff, K.J. (1979) ‘Maternal behavior in prosimians’ in Martin, G.A.D.D. (ed.) *The Study of Prosimian Behavior*. Cambridge: Academic Press, pp. 123-156.

Konigsberg, L.W., Hens, S.M., Jantz, L.M. and Jungers, W.L. (1998) 'Stature estimation and calibration: bayesian and maximum likelihood perspectives in physical anthropology', *American Journal of Physical Anthropology,* 107(1), pp. 65-92

Kouchi, M., Mochimaru, M., Tsuzuki, K. and Yokoi, T. (1999) ‘Interobserver error in anthropometry’, *Journal of Human Ergology*, 28(1-2), pp. 15-24.

Kovarovic, K., Aiello, L.C., Cardini, A. and Lockwood, C.A. (2011) 'Discriminant function analyses in archaeology: are classification rates too good to be true?' *Journal of Archaeological Science,* 38(11), pp. 3006-3018.

Kurki, H.K., Ginter, J.K., Stock, J.T. and Pfeiffer, S. (2010) 'Body size estimation of small-bodied humans: applicability of current methods', *American Journal of Physical Anthropology,* 141(2), pp. 169-180.

Kuzawa, C.W. and Bragg, J.M. (2012) *Plasticity in Human Life History Strategy: Implications for Contemporary Human Variation and the Evolution of Genus Homo*. Chicago: University of Chicago Press.

Kwak, D., Lee, U., Kim, I. and Kwak, D. (2015) ‘Sex determination using discriminant analysis of upper and lower extremity bones: new approach using the volume and surface area of digital model’, *Forensic Science International*, 253(135), pp. 1-4.

Lacruz, R.S., Dean, M.C., Ramirez-Rozzi, F. and Bromage, T.G. (2008) 'Megadontia, striae periodicity and patterns of enamel secretion in Plio-Pleistocene fossil hominins', *Journal of Anatomy,* 213(2), pp. 148-158.

Lague, M.R. (2003) 'Patterns of joint size dimorphism in the elbow and knee of catarrhine primates', *American Journal of Physical Anthropology*, 120(3), pp. 278-297.

Lande, R. (1980) 'Sexual dimorphism, sexual selection, and adaptation in polygenic characters', *Evolution,* 34(2), pp. 292-305.

Langley, N.R., Meadows Jantz, L., McNulty, S., Maijanen, H., Ousley, S.D. and Jantz, R.L. 2018. 'Error quantification of osteometric data in forensic anthropology', *Forensic Science International*, 287(1), pp. 183-189.

Lawler, R.R. (2009) 'Monomorphism, male-male competition, and mechanisms of sexual dimorphism', *Journal of Human Evolution,* 57(3), pp. 321-325.

Leigh, S.R. (1994) 'Ontoaenetic correlates of diet in anthropoid primates', *American Journal of Physical Anthropology,* 94(4), pp. 499-522.

Leigh, S.R. (2001) 'Evolution of human growth', *Evolutionary Anthropology: Issues, News, and Reviews,* 10(6), pp. 223-236.

Leigh, S.R. (2004) 'Brain growth, life history and cognition in primate and human evolution', *American Journal of Physical Anthropology*, 62(3), pp. 139-164.

Leigh, S.R. and Shea, B.T. (1995) 'Ontogeny and the evolution of adult body size dimorphism in apes', *American Journal of Primatology,* 36(1), pp. 37-60.

Leonard, W.R. and Robertson, M.L. (1997) 'Comparative primate energetics and hominid evolution', *American Journal of Physical Anthropology*, 102(2), pp. 265-281.

Leutenegger, W., and Cheverud, J.M. (1982) 'Correlates of sexual dimorphism in primates: ecological and size variables', *International Journal of Primatology*, 3(1), pp. 387-402.

Leutenegger, W. and Kelly, J.T. (1977) 'Relationship of sexual dimorphism in canine size and body size to social, behavioral, and ecological correlates in anthropoid primates', *Primates,* 18(1), pp. 117-136.

Leutenegger, W. and Shell, B. (1987) 'Variability and sexual dimorphism in canine size of *Australopithecus* and extant hominoids', *Journal of Human Evolution,* 16(4), pp. 359-367.

Libório, R.A. and Martins, M.M. (2013) 'Body size in predator–prey interactions: an investigation of neotropical primates and their predators', *Studies on Neotropical Fauna & Environment,* 48(1), pp. 81-87.

Lieberman, D.E., Devlin, M.J. and Pearson, O.M. (2001) 'Articular area responses to mechanical loading: effects of exercise, age, and skeletal location', *American Journal of Physical Anthropology,* 116(4), pp. 266-77.

Lindberg, D.G. (1971) ‘The rhesus monkey in a north Indian ecological and behavioral study’, in Rosenblum, L.A. (ed.) *Primate Behavior: Developments in Field and Laboratory Research.* New York: Academic Press, pp. 1-106.

Lindenfors, P. (2002) 'Sexually antagonistic selection on primate size', *Journal of Evolutionary Biology,* 15(4), pp. 595-607.

Lockwood, C.A., Richmond, B.G., Jungers, W.L. and Kimbel, W.H. (1996) 'Randomization procedures and sexual dimorphism in *Australopithecus afarensis'*, *Journal of Human Evolution,* 31(6), pp. 537-548.

Lordkipanidze, D., Ponce de Leon, M.S., Margvelashvili, A., Rak, Y., Rightmire, G.P. and Vekua, A. (2013) ‘A complete skull from Dmanisi, Georgia and the evolutionary biology of early Homo’, *Science*, 342(6156), pp. 326-331.

Lovejoy, C.O. (1981) 'The origin of man', *Science,* 211(4480), pp. 341-50.

Lovejoy, C.O. (2009) 'Reexamining human origins in light of *Ardipithecus ramidus* ', *Science,* 326(5949), pp. 74-74.

Lovejoy, C., Suwa, G., Simpson, S.W., Matternes, J.H. and White, T.D. (2009) 'The great divides: *Ardipithecus ramidus* reveals the postcrania of our last common ancestors with African Apes', *Science,* 326(5949), pp. 73-106.

Lovich, J.E. and Gibbons, J.W. (1992) 'A review of techniques for quantifying sexual size dimorphism', *Growth, Development and Aging,* 56(4), pp. 269-281.

Lukas, D. and Clutton-Brock, T.H. (2013) 'The evolution of social monogamy in mammals', *Science,* 341(6145), pp. 526-30.

Lukas, D. and Clutton-Brock, T.H. (2014) 'Evolution of social monogamy in primates is not consistently associated with male infanticide', *Proceedings of the National Academy of Science United States of America,* 111(17), pp. 1674.

Lukas, D. and Huchard, E. (2014) 'The evolution of infanticide by males in mammalian societies', *Science,* 346(6211), pp. 841-844.

MacDonald, D. (2009) *The Encyclopedia of Mammals.* 2nd edn. Oxford: Oxford University Press.

Macintosh, A.A., Pinhasi, R. and Stock, J.T. (2017) 'Prehistoric women's manual labor exceeded that of athletes through the first 5500 years of farming in Central Europe', *Science Advances,* 3(11), pp. 3893-3893.

Maïmoun, L. and Sultan, C. (2011) 'Effects of physical activity on bone remodeling', *Metabolism: Clinical and Experimental,* 60(3), pp. 373-388.

Marino, L. (1998) 'A comparison of encephalization between odontocete cetaceans and anthropoid primates', *Brain, Behavior and Evolution,* 51(4), pp. 230-238.

Martin, R.D. (1981) ‘On extinct hominin population densities’, *Journal of Human Evolution*, 10(5), pp. 427-428.

Martin, R.D. (1996) 'Scaling of the mammalian brain: the maternal energy hypothesis', *News in Physiological Sciences,* 11(4), pp. 149-156.

Martin, R.D., Willner, L.A. and Dettling, A. (1994) 'The evolution of sexual size dimorphism in primates' in Short, R.V. and Balaban, E. (eds.). *The Differences Between the Sexes.* Cambridge: Cambridge University Press, pp. 159-200.

McFarland, R. (1996) ‘Female primates: fat or fit?’, in Morbeck, M.E., Galloway, A. and Zihlman, A.L. (eds.) *The Evolving Female: A Life History Perspective.* Princeton, New Jersey: Princeton University Press, pp. 163-178.

McHenry, H.M. (1984) 'Relative cheek-tooth size in Australopithecus', *American Journal of Physical Anthropology,* 64(3), pp. 297-306.

McHenry, H.M. (1992) 'Body size and proportions in early hominids', *American Journal of Physical Anthropology,* 87(4), pp. 407-31.

McHenry, H.M. (1994) 'Behavioral ecological implications of early hominid body size', *Journal of Human Evolution,* 27(1-3), pp. 77-87.

McKenzie, H.G. and Popov, A.N. (2016) 'A metric assessment of evidence for artificial cranial modification at the Boisman 2 Neolithic cemetery (ca. 5800-5400 14C BP), Primorye, Russian Far East', *Quaternary International,* 405(B) pp. 210-221

Milton, K. and May, M.L. (1976) 'Body weight, diet and home range area in primates', *Nature,* 259(5543), pp. 459-462.

Mitani, J.C., Gros-Louis, J. and Richards, A.F. (1996) 'Sexual dimorphism, the operational sex ratio, and the intensity of male competition in polygynous primates', *American Naturalist,* 147(6), pp. 966-980.

Mitchell, C.L. (1990) *The Ecological Basis of Female Dominance: A Behavioral Study of the Squirrel Monkey (Saimiri sciureus) in the wild.* PhD thesis. Princeton University.

Morino, L. (2009) 'Monogamy in mammals: expanding the perspective on hylobatid mating systems', in Lappan, S. and Whittaker, D. (eds.). *The Gibbons: New Perspectives on Small Ape Socioecology and Population Biology.* New York: Springer, pp. 279-311.

Morris, W.F., Altmanm, J., Broackman, D.K., Cords, M., Fedigan, L., Pusey, A.E., Stoinski, T.S., Bronikowski, A.M., Alberts, S.C. and Strier, K.B. (2011) ‘Low demographic variability in wild primate populations: fitness impacts of variation, covariation, and serial correlation in vital rates’, *American Naturalist*, 177(1), pp. 14-28.

Muller, M.N. and Wrangham, R.W. (2004) ‘Dominance, aggression and testosterone in wild chimpanzees: a test of the ‘challenge hypothesis’’, *Animal Behaviour,* 67(1), pp. 113-123.

Murtagh, F. (2014) ‘Ward’s hierarchical agglomerative clustering method: which algorithms implement Ward’s criterion?’ *Journal of Classification*, 31(3), pp. 274-295.

Nadell, J.A. and Shaw, C.N. (2016) ‘Phenotypic plasticity and constraint along the upper and lower limb diaphyses of *Homo sapiens’*, *American Journal of Physical Anthropology*, 159(3), pp. 410-422.

Napier, J.R. and Walker, A.C. (1967) 'Vertical clinging and leaping– a newly recognized category of locomotor behaviour of primates', *Folia Primatologica,* 6(3-4), pp. 204-219.

Napier, P.H. (1981*) Catalogue of the Primates in the British Museum, Part 2: Family Cercopithecidae, subfamily Cerpcopithecinae*. London: Natural History Museum (London NHM), pp.203-205.

National Research Council (1981) ‘Techniques for sexing and aging’, in National Research Council, *Techniques for the Study of Primate Population Ecology*. Washington D.C.: National Academy Press, pp. 81-83.

Navarrete, A., van Schaik, C.P. and Isler, K. (2011) 'Energetics and the evolution of human brain size', *Nature,* 480(7375), pp. 91-93.

Nelson, E., Rolian, C., Cashmore, L. and Shultz, S. (2011) 'Digit ratios predict polygyny in early apes, Ardipithecus, Neanderthals and early modern humans but not in Australopithecus', *Proceedings of the Royal Society B,* 278(1711), pp. 1556-1563.

Neymann, P.F. (1977) ‘Aspects of the ecology and social organization of free-ranging cotton-top tamarins (*Saguinus oedipus*) and the conservation status of the species’, in Kleiman, D.G. (ed.) *The Biology and Conservation of the Callitrichidae*. Washington D.C.: Smithsonian Institution Press, pp. 39-71.

Niinimäki, S., Söderling, S., Junno, J., Finnilä, M., Niskanen, M. and Weiss, E. (2009) ‘Cortical bone thickness can adapt locally to muscular loading while changing with age’, *HOMO - Journal of Comparative Human Biology*, 64(6), pp. 474-490.

Nowak, R. (1999) *Walker’s Mammals of the World.* 6th edn. Baltimore: John Hopkins University Press.

O'Brien, T. and Stanley, A.M. (2013) ‘Boards and cords: discriminating types of artificial cranial deformation in Prehispanic South Central Andean Populations’, *International Journal of Osteoarchaeology*, 23(4), pp. 459-470.

O’Higgins, P. and Dryden, I.L. (1993) ‘Sexual dimorphism in hominoids – further studies of craniofacial shape differences in Pan, Gorilla and Pongo’, *Journal of Human Evolution*, 24(3), pp. 183-205.

Opie, C., Atkinson, Q.D., Dunbar, R.I.M. and Shultz, S. (2013a) 'Male infanticide leads to social monogamy in primates', *Proceedings of the National Academy of Sciences United States of America,* 110(33), pp. 13328-13332.

Opie, C., Atkinson, Q.D., Dunbar, R.I.M. and Shultz, S. (2013b) 'Reply to Dixson: infanticide triggers primate monogamy', *Proceedings of the National Academy of Sciences United States of America,* 110(51), pp. 4938-4938.

Paine, R.R. and Godfrey, L.R. (1997) 'The scaling of skeletal microanatomy in non-human primates', *Journal of* Zoology, 241(4), pp. 803-821.

Parr, W., Chatterjee, H.J. and Soligo, C. (2011) 'Inter- and intra-specific scaling of articular surface areas in the hominoid talus', *Journal of Anatomy*, 218(4), pp. 386-401.

Patriquin, M.L., Steyn, M. and Loth, S.R. (2005) 'Metric analysis of sex differences in South African black and white pelves', *Forensic Science International,* 147(2-3), pp. 119-127.

Payseur, B.A., Vinyard, C.J., Dagosto, M. and Covert, H.H. (1999) 'New body mass estimates for *Omomys carteri*, a middle Eocene primate from North America', *American Journal of Physical Anthropology,* 109(1), pp. 41-52.

Pearce, F., Carbone, C., Cowlishaw, G. and Isaac, N.J.B. (2013) 'Space-use scaling and home range overlap in primates', *Proceedings of the Royal Society B: Biological Sciences,* 280(1751), pp. 2012-2122.

Pearson, E.S. (1932) 'The percentage limits for the distribution of range in samples from a normal distribution (n<100)', *Biometrika,* 24(3), pp. 404-417.

Pearson, O.M. and Lieberman, D.E. (2004) 'The aging of Wolff's "law": ontogeny and responses to mechanical loading in cortical bone', *American Journal of Physical Anthropology,* 125(39), pp. 63-99.

Perini, T.A., Lameira de Oliveira, G., Santos Ornellas, J. and Palha de Oliveira, F. (2005) 'Technical error of measurement in anthropometry', *Brazilian Journal of Sporting Medicine*, 11(1), pp. 86-90.

Perneger, T.V. (1998) 'What's wrong with Bonferroni adjustments?' *BMJ*, 316(7139), pp. 1236-1238.

Perry, J.M.G., Cooke, S.B., Runestad Connour, J.A., Burgess, M.L. and Ruff, C.B. (2018) 'Articular scaling and body mass estimation in platyrrhines and catarrhines: Modern variation and application to fossil anthropoids', *Journal of Human Evolution,* 115(1-7), pp. 20-35.

Peterman, M.M., Hamel, A.J., Cavanagh, P.R., Piazza, S.J. and Sharkey, N.A. (2001) '*In vitro* modeling of human tibial strains during exercise in micro-gravity', *Journal of Biomechanics*, 34(5), pp. 693-698.

Pigliucci, M. (2005) 'Evolution of phenotypic plasticity: where are we going now?', *Trends in Ecology and Evolution*, 20(9), pp. 481-486.

Plavcan, J.M. (1994) 'Comparison of four simple methods for estimating sexual dimorphism in fossils', *American Journal of Physical Anthropology,* 94(4), pp. 465-76.

Plavcan, J.M. (2001) 'Sexual dimorphism in primate evolution', *American Journal of Physical Anthropology,* 116(S33), pp. 25-53.

Plavcan, J.M. (2003) 'Scaling relationships between craniofacial sexual dimorphism and body mass dimorphism in primates: Implications for the fossil record', *American Journal of Physical Anthropology,* 120(1), pp. 38-60.

Plavcan, J.M. (2004) 'Sexual selection, measures of sexual selection, and dimorphism in primates', in Kappeler, P. and Van Schaik, C. (eds.) *Sexual Selection in Primates: New and Comparative Perspectives.* Cambridge: Cambridge University Press, pp. 230–252.

Plavcan, J.M. (2011) 'Group size, female resource competition, female body size and dimorphism in primates', *American Journal of Physical Anthropology*, 52(1), pp. 240-241.

Plavcan, J.M. (2012a) 'Implications of male and female contributions to sexual size dimorphism for inferring behavior in the hominin fossil record', *International Journal of Primatology,* 33(6), pp. 1364-81.

Plavcan, J.M. (2012b) 'Body size, size variation, and sexual size dimorphism in early Homo', *Current Anthropology*, 53(S6), pp. 409-423.

Plavcan, J.M. (2013) 'Reconstructing social behavior from fossil evidence', in Begun, D.R. (ed.) *A Companion to Palaeoanthropology.* Oxford: Blackwell Publishing Ltd, pp. 226-243.

Plavcan, J.M. and Cope, D.A. (2001) 'Metric variation and species recognition in the fossil record', *Evolutionary Anthropology*, 10(6), pp. 204-222.

Plavcan, J.M. and Van Schaik, C. P. (1997) 'Intrasexual competition and body weight dimorphism in anthropoid primates', *American Journal of Physical Anthropology,* 103(1), pp. 37-68.

Plavcan, J.M., Lockwood, C.A., Kimbel, W.H., Harmon, E.H. and Lague, M.R. (2005) 'Sexual dimorphism in *Australopithecus afarensis* revisited: how strong is the case for a human-like pattern of dimorphism?' *Journal of Human Evolution,* 48(3), pp. 313-20.

Pohar, M., Blas, M. and Turk, S. (2004) ' Comparison of logistic regression and linear discriminant analysis: a simulation study', *Advances in Methodology and Statistics,* 1(1), pp. 143-161.

Polk, J.D. (2002) 'Adaptive and phylogenetic influences on musculoskeletal design in cercopithecine primates', *Journal of Experimental Biology,* 205(21), pp. 3399-3412.

Polk, J.D., Williams, S.A. and Peterson, J.V. (2009) 'Body size and joint posture in primates', *American Journal of Physical Anthropology,* 140(2), pp. 359-367.

Pomeroy, E. and Stock, J.T. (2012) 'Estimation of stature and body mass from the skeleton among coastal and mid-altitude andean populations', *American Journal of Physical Anthropology,* 147(2), pp. 264-279.

Pontzer, H. (2012) 'Ecological energetics in early Homo', *Current Anthropology,* 53(6), pp. 346-358.

Pontzer, H., Raichlen, D.A. and Sockol, M.D. (2009) 'The metabolic cost of walking in humans, chimpanzees, and early hominins', *Journal of Human Evolution,* 56(1), pp. 43-54.

Popovic, Z.B. and Thomas, J.D. (2017) 'Assessing observer variability: a user's guide', *Cardiovascular Diagnosis and Therapy*, 7(3), pp. 317-324.

Population Reference Bureau (2018) *World Population Data Sheet 2018*. Available at: https://www.prb.org/2018-world-population-data-sheet-with-focus-on-changing-age-structures/ (Accessed: 23 July 2018).

Porčić, M. (2010) 'House floor area as a correlate of marital residence pattern: a logistic regression approach', *Cross-Cultural Research,* 44(4), pp. 405-424.

Press, S.J. and Wilson, S. (1978) 'Choosing between logistic regression and discriminant analysis', *Journal of the American Statistical Association*, 73(363), pp. 699-705.

Purkait, R. (2001) 'Measurements of ulna—a new method for determination of sex', *Journal of Forensic Sciences,* 46(4), pp. 924-927.

Pusey, A., Williams, J. and Goodall, J. (1997) 'The influence of dominance rank on the reproductive success of female chimpanzees'*, American Society for the Advancement of Science*, 277(5327), pp. 828-831.

Ralls, K. (1976) 'Mammals in which females are larger than males', *Quarterly Review of Biology,* 51(2), pp. 245-276.

Ranta, E., Laurila, A. and Elmberg, J. (1994) 'Reinventing the wheel: analysis of sexual dimorphism in body size', *Oikos*, 70(30), pp. 313-321.

Reeves, N.M., Auerbach, B.M. and Sylvester, A.D. (2016) 'Fluctuating and directional asymmetry in the long bones of captive cotton-top tamarins (*Saguinus oedipus*)', *American Journal of Physical Anthropology*, 160(1), pp. 41-51.

Regh, J.A. and Leigh, S.R. (1999) 'Estimating sexual dimorphism and size differences in the fossil record: A test of methods', *American Journal of Physical Anthropology,* 110(1), pp. 95-104.

Reichard, U.H., Ganpanakngan, M. and Barelli, C. (2012) 'White-handed gibbons of Khao Yai: social flexibility, complex reproductive strategies, and a slow life history', in Kappeler, P.M. and Watts, D.P. (eds.). *A Long-Term Study of Primates.* Berlin: Springer, pp. 237-258.

Relethford, J.H. and Hodges, D.C. (1985) 'A statistical test for differences in sexual dimorphism between populations', *American Journal of Physical Anthropology,* 66(1), pp. 55-61.

Remis, M. (1995) 'Effects of body size and social context on the arboreal activities of lowland gorillas in the Central African Republic', *American Journal of Physical Anthropology,* 97(4), pp. 413-433

Ren, D., Chin, K.R. and French, J.A. (2014) 'Molecular variation in AVP and AVPR1a in new world monkeys (primates, platyrrhini): evolution and implications for social monogamy', *Plos One,* 9(10), pp. 111638.

Reno, P.L. and Lovejoy, C.O. (2015) 'From Lucy to Kadanuumuu: balanced analyses of *Australopithecus afarensis* assemblages confirm only moderate skeletal dimorphism', *PeerJ,* 28(3), e925.

Reno, P.L., McCollum, M.A., Meindl, R.S. and Lovejoy, C.O. (2010) 'An enlarged postcranial sample confirms *Australopithecus afarensis* dimorphism was similar to modern humans', *Philosophical Transactions - Royal Society of London Biological Sciences,* 365(1556), pp. 3355-3363.

Reno, P.L., Meindl, R.S., McCollum, M.A. and Lovejoy, C.O. (2003) 'Sexual dimorphism in *Australopithecus afarensis* was similar to that of modern humans', *Proceedings of the National Academy of Sciences United States of America,* 100(16), pp.9404-9409.

Reynolds, T.R. (1985) 'Stresses on the limbs of quadrupedal primates', *American Journal of Physical Anthropology,* 67(4), pp. 351-362.

Richmond, B.G. and Jungers, W.L. (1995) 'Size variation and sexual dimorphism in *Australopithecus afarensis* and living hominoids', *Journal of Human Evolution,* 29(3), pp. 229-245.

Robbins, M.M., Bermejo, M., Cipolletta, C., Magliocca, F., Parnell, R.J. and Stokes, E. (2004) 'Social structure and life-history patterns in western gorillas (*Gorilla gorilla gorilla*)', *American Journal of Primatology,* 64(2), pp. 145-159.

Robson, S.L. and Wood, B. (2008) 'Hominin life history: reconstruction and evolution', *Journal of Anatomy,* 212(4), pp. 394-425.

Rogers, M.E., Abernethy, K., Bermejo, M., Cipolletta, C., Doran, D., McFarland, K., Nishihara, T., Remis, M. and Tutin, C. (2004) 'Western gorilla diet: A synthesis from six sites', *American Journal of Primatology*, 64(2), pp. 173-192.

Rohlf, F.J. and Marcus, L.F. (1993) 'A revolution in morphometrics', *Trends in Ecology and Evolution*, 8(4), pp. 129-132.

Rosenberg, K.R., Zune, L. and Ruff, C.B. (2006) 'Body size, body proportions, and encephalization in a middle Pleistocene archaic human from northern China', *Proceedings of the National Academy of Sciences United States of America,* 103(10), pp. 3552-3556.

Ross, C. (1992) 'Basal metabolic rate, body weight and diet in primates: an evaluation of the evidence', *Folia Primatologica,* 58(1), pp. 7-23.

Ross, C. (2003) ‘Life history, infant care strategies and brain size in primates’, in Kappeler, P.M. and Pereira, M.E. (eds.) *Primate Life Histories and Socioecology*. Chicago: The University of Chicago Press, pp. 266-284.

Rothman, K.J. (1990) ‘No adjustments are needed for multiple comparisons’, *Epidemiology*, 1(1), pp. 43-46.

Rowe, N. (1996) *The Pictorial Guide to the Living Primates.* New York: Pogonias Press.

Rubin, C.T. and Lanyon, L.E. (1982) 'Limb mechanics as a function of speed and gait: a study of functional strains in the radius and tibia of horse and dog', *Journal of Experimental Biology,* 101(1), pp. 187-211.

Ruff, C. (1987) 'Sexual dimorphism in human lower limb bone structure: relationship to subsistence strategy and sexual division of labor', *Journal of Human Evolution,* 16(5), pp. 391-416.

Ruff, C.B. (1988) 'Hindlimb articular surface allometry in hominoidea and Macaca, with comparisons to diaphyseal scaling', *Journal of Human Evolution,* 17(7), pp. 687-714

Ruff, C.B. (1998) ‘Evolution of the hominid hip’, in: Strasser, E., Rosenberger, A., McHenry, H., Fleagle, J. (eds.), *Primate Locomotion: Recent Advances*. Davis, California: Plenum Press, pp. 449-469.

Ruff, C.B. (2000a) 'Body mass prediction from skeletal frame size in elite athletes', *American Journal of Physical Anthropology,* 113(4), pp. 507-517.

Ruff, C.B. (2000b) 'Body size, body shape, and long bone strength in modern humans', *Journal of Human Evolution,* 38(2), pp. 269-290.

Ruff, C.B. (2002a) ‘Long bone articular and diaphyseal structure in Old World monkeys and apes. I: locomotor effects’, *American Journal of Physical Anthropology*, 119(4), pp. 305-342.

Ruff, C. (2002b) ‘Variation in human body size and shape’, *Annual Reviews*, 31(1), pp. 211-232.

Ruff, C.B. (2003) 'Long bone articular and diaphyseal structure in Old World monkeys and apes. II: estimation of body mass', *American Journal of Physical Anthropology,* 120(1), pp. 16-37.

Ruff, C.B. (2010) 'Body size and body shape in early hominins – implications of the Gona Pelvis', *Journal of Human Evolution,* 58(2), pp. 166-178.

Ruff, C.B., Burgess, M.L., Squyres, N., Junno, J. and Trinkaus, E. (2018) ‘Lower limb articular scaling and body mass estimation in Pliocene and Pleistocene hominins’, *Journal of Human Evolution*, 115(1), pp. 85-111.

Ruff, C.B. and Higgins, R. (2013) ‘Femoral neck structure and function in early hominins’, *American Journal of Physical Anthropology,* 150(4), pp. 512-525.

Ruff, C.B., Holt, B.M., Niskanen, M., Sládek, V., Berner, M., Garofalo, E., Garvin, H.M., Hora, M., Maijanen, H., Niinimäki, S., Salo, K., Schuplerová, E. and Tomkins, D. (2012) 'Stature and body mass estimation from skeletal remains in the European Holocene', *American Journal of Physical Anthropology*, 148(4), pp. 601-617.

Ruff, C.B., Holt, B.M., Sládek, V., Berner, M., Murphy, W.A. Jr., zur Nedden, D., Seidler, H. and Recheis, W. (2006) 'Body size, body proportions, and mobility in the Tyrolean "Iceman"', *Journal of Human Evolution*, 51(1), pp. 91-101.

Ruff, C. and Niskanen, M. (2018) 'Introduction to special issue: Body mass estimation-methodological issues and fossil applications', *Journal of Human Evolution*, 115(1), pp. 1-7.

Ruff, C., Niskanen, M., Junno, J. and Jamison, P. (2005) 'Body mass prediction from stature and bi-iliac breadth in two high latitude populations, with application to earlier higher latitude humans', *Journal of Human Evolution,* 48(4), pp. 381-92.

Ruff, C.B. and Runestad, J.A. (1992) 'Primate limb bone structural adaptations', *Annual Review of Anthropology*, 21(1) pp. 407-433.

Ruff, C.B., Scott, W.W. and Liu, A.Y. (1991) 'Articular and diaphyseal remodeling of the proximal femur with changes in body mass in adults', *American Journal of Physical Anthropology,* 86(3), pp. 397-413.

Ruff, C.B., Trinkaus, E. and Holliday, T.W. (1997) 'Body mass and encephalization in Pleistocene Homo', *Nature,* 387(6629), pp. 173-6.

Safont, S., Malgosa, A. and Subira, M.E. (2000) 'Sex assessment on the basis of long bone circumference', *American Journal of Physical Anthropology*, 113(3), pp. 317-328.

Sarringhaus, L.A., Stock, J.T., Marchant, L.F. and McGrew, W.C. (2005) 'Bilateral asymmetry in the limb bones of the chimpanzee (*Pan troglodytes*)', *American Journal of Physical Anthropology*, 128(4), pp. 840-845.

Savage, A., Giraldo, L.H., Soto, L.H. and Snowdon, C.T. (1996a) 'Demography, group composition, and dispersal in wild cotton-top tamarin (*Saguinus oedipus*) groups', *American Journal of Primatology,* 38(1), pp. 85-100.

Savage, A., Snowdon, C.T., Giraldo, L.H. and Soto, L.H. (1996b) 'Parental care patterns and vigilance in wild cotton-top tamarins (*Saguinus oedipus*)', in Norconk, M.A., Rosenberger, A.L. and Garber, P.A. (eds.) *Adaptive Radiations of Neotropical Primates*. New York: Plenum Press, pp. 187-199.

Schaller, G.B. (1976) *The Mountain Gorilla: Ecology and Behaviour.* Chicago: University of Chicago Press.

Scheuer, L. and Black, S. (2000) *Developmental Juvenile Osteology*. London: Academic Press Ltd.

Schiml, P.A., Mendoza, S.P., Mason, W.A., Saltzman, W. and Lyons, D.M. (1996) 'Seasonality in squirrel monkeys (*Saimiri sciureus*): social facilitation by females', *Physiology and Behavior,* 60(4), pp. 1105-1113.

Schiml, P.A., Mendoza, S.P., Saltzman, W., Lyons, D.M. and Mason, W.A. (1999) 'Annual physiological changes in individually housed squirrel monkeys (*Saimiri sciureus)'*, *American Journal of Primatology*, 47(2), pp. 93-103.

Schmidt, M. (2005) 'Hind limb proportions and kinematics: are small primates different from other small mammals?' *Journal of Experimental Biology*, 208(17), pp. 3367-3383.

Schmidt, M. (2010) 'Locomotion and postural behaviour', *Advances in Science & Research,* 5(1), pp. 23-39.

Sehrawat, J.S. (2018) Sex estimation from discriminant function analysis of clavicular and sternal measurements: a forensic anthropological study based on examination of two bones of Northwest Indian subjects, *Australian Journal of Forensic Sciences*, 50(1), pp. 20-41.

Sell, A., Lukazsweski, A.W. and Townsley, M. (2017) 'Cues of upper body strength account for most of the variance in men's bodily attractiveness', *Proceedings of the Royal Society Biological Sciences*, 284(1869), e20171819.

Shaw, C.N. and Stock, J.T. (2009) 'Habitual throwing and swimming correspond with upper limb diaphyseal strength and shape in modern human athletes', *American Journal of Physical Anthropology*, 140(1), pp. 160-172.

Simpson, S.W., Quade, J., Levin, N.E. and Semaw, S. (2014) 'The female *Homo* pelvis from Gona: Response to Ruff (2010)', *Journal of Human Evolution*, 68(1), pp. 32-35.

Singh, J., Pathak, R.K. and Singh, D. (2012) 'Morphometric sex determination from various sternal widths of Northwest Indian sternums collected from autopsy cadavers: a comparison of sexing methods', *Egyptian Journal of Forensic Sciences,* 2(1), pp. 18-28.

Skinner, J.D. and Chimimba, C.T. (2005) *The Mammals of the Southern African Subregion.* 3rd edn. Cambridge: Cambridge University Press.

Skinner, M. and Wood, B.A. (2006) 'The evolution of modern human life history- a palaeontological perspective', in Paines, R.L. and Hawkes, K. (eds.) *The Evolution of Human Life History.* Santa Fe: School of American Research Press, pp. 331-364.

Skoglund, P., Storå, J., Götherström, A. and Jacobsson, M. (2013) 'Accurate sex identification of ancient human remains using DNA shotgun sequencing', *Journal of Archaeological Sciences*, 40(12), pp. 4477-4482.

Sládek, V., Macháček, J., Makajevová, E., Přichystalová, R. and Hora, M. (2018) 'Body mass estimation in skeletal samples using the hybrid approach: the effect of population-specific variations and sexual dimorphism', *Archaeological and Anthropological Sciences*, 10(4), pp. 833-847.

Smith, D.G. and McDonough, J. (2005) ‘Mitochondrial DNA variation in Chinese and Indian rhesus macaques (*Macaca mulatta*)’, *American Journal of Primatology,* 65(1), pp. 1-25.

Smith, J.M. and Smith, A.C. (2013) ‘An investigation of ecological correlates with hand and foot morphology in Callitrichid primates’, *American Journal of Physical Anthropology*, 152(4), pp. 447-458.

Smith, R.J. (1996) 'Biology and body size in human evolution - statistical inference misapplied', *Current Anthropology,* 37(3), pp. 451-81.

Smith, R.J. (1999) ‘Statistics of sexual size dimorphism’, *Journal of Human Evolution,* 36(4), pp. 423-458.

Smith, R.J, and Leigh, S. (1998) 'Sexual dimorphism in primate neonatal body mass', *Journal of Human Evolution,* 34(2), pp. 173-201.

Snodgrass, J.J., Leonard, W.R. and Robertson, M.L. (2009) ‘The energetics of encephalization in early hominids’, in Hublin, J.J. and Richard, M.P. (eds.) *The Evolution of Hominin Diets: Integrating Approaches to the Study of Palaeolithic Subsistence*. Dordrecht: Springer Netherlands, pp. 15-29.

Sol, D. (2009) ‘Revisiting the cognitive buffer hypothesis for the evolution of large brains’, *Biology Letters*, 5(1), pp. 130-133.

Sol, D., Bacher, S., Reader, S.M. and Lefebvre, L. (2008) ‘Brain size predicts the success of mammal species introduced into novel environments’, *The American Naturalist*, 172(1), pp. 63-71.

Spocter, M.A. and Manger, P.R. (2007) 'The use of cranial variables for the estimation of body mass in fossil hominins', *American Journal of Physical Anthropology,* 134(1), pp. 92-105.

Squyres, N. and Ruff, C.B. (2015) ‘Body mass estimation from knee breadth, with application to early hominins’, *American Journal of Physical Anthropology*, 158(2), pp. 198-208.

Srivastava, R., Srivastava, R., Saini, V., Rai, R.K., Tripathi, S.K., Pandey, S., Singh, T.B. and Pandey, A.K. (2013) ‘Sexual dimorphism in ulna: An osteometric study from India’, *Journal of Forensic* Science, 58(5), pp. 1251-1256.

Stanford, C.B. (2001) ‘A comparison of social meat-foraging by chimpanzees and human foragers’, in Stanford, C.B. and Bunn, H.T. (eds.) *Meat-Eating & Human Evolution*. Oxford: Oxford University Press, pp. 122-140.

Steel, F.L.D. (1962) 'The sexing of long bones, with reference to the St Bride's series of identified skeletons', *The Journal of the Royal Anthropological Institute of Great Britain and Ireland,* 92(2), pp. 212-222.

Steele, J. (1996) ‘On predicting hominin group size’, in Steele, J. and Shennan, S. (eds.) *The Archaeology of Human Ancestry: Power, Sex and Tradition.* London: Routledge, pp. 207-229.

Stephan, H., Frahm, H. and Baron, G. (1981) ‘New and revised data on volumes of brain structures in insectivores and primates’, *Folia Primatologica,* 35(1), pp. 1-29.

Stephenson, I.R., Bearder, S.K., Donati, G. and Karlsson, J. (2010) ‘A guide to galago diversity: getting a grip on how best to chew gum’, in Burrows, A.M. and Nash, L.T. (eds.) *Evolution of Exudativory in Primates.* New York: Springer, pp. 235-255.

Stewart, F.A., Hansell, M.H. and Pruetz, J.D. (2007) ‘Do chimpanzees build comfortable nests?’ *American Journal of Primatology,* 69(8), pp. 930-939.

Stewart, K.J. (2001) ‘Social relationships of immature gorillas and silverback’, in Robbins, M.M., Sicotte, P. and Stewart, K.J. (eds.) *Mountain Gorillas*. Cambridge: Cambridge University Press, pp. 183-213.

Steyn, M. and Işcan, M.Y. (1998) 'Sexual dimorphism in the crania and mandibles of South African whites', *Forensic Science International,* 98(1-2), pp. 9-16.

Steyn, M. and Işcan, M.Y. (2008) 'Metric sex determination from the pelvis in modern Greeks', *Forensic Science International,* 179(1), pp. 86.e1-86.e6.

Stinson, S. (1985) 'Sex differences in environmental sensitivity during growth and development', *American Journal of Physical Anthropology,* 28(6), pp. 123-147.

Stock, J. and Pfeiffer, S.K. (2001) 'Linking structural variability in long bone diaphyses to habitual behaviors: foragers from the southern African later Stone Age and the Andaman Islands', *American Journal of Physical Anthropology,* 115(4), pp. 337-348.

Stock, J.T. and Pfeiffer, S.K. (2004) ‘Long bone robusticity and subsistence behaviour among Later Stone Age foragers of the forest and fynbos biomes of South Africa’, *Journal of Archaeological Science*, 31(7), pp. 999-1013.

Stokes, E.J., Parnell, R.J. and Olejniczak, C. (2003) ‘Female dispersal and reproductive success in wild western lowland gorillas (*Gorilla gorilla gorilla*)’, *Behavioral Ecology and Sociobiology*, 54(4), pp. 329-339.

Stone, A.I. (2014) ‘Is fatter sexier? Reproductive strategies of male squirrel monkeys (*Saimiri sciureus*)’, *International Journal of Primatology,* 35(3-4), pp. 628-642.

Suwa, G., Kono, R.T., Simpson, S.W., Asfaw, B., Lovejoy, O.C. and White, T.D. (2009) 'Paleobiological implications of the *Ardipithecus ramidus* dentition', *Science,* 326(5949), pp. 94-99.

Swales, D.M. and Nystrom, P. (2015) ‘Recording primate spinal degenerative joint disease using a standardized approach’, in Gerdau-Radonic, K. and McSweeney, K. (eds). *Trends in Biological Anthropology*. Oxford: Oxbow Books, pp. 25-39.

Swartz, S.M. (1989) 'The functional morphology of weight bearing: limb joint surface area allometry in anthropoid primates', *Journal of Zoology,* 218(3), pp. 441-460.

Tabachnick, B.G. and Fidell, L.S. (2006) *Using Multivariate Statistics*. 5th edn. Boston: Allyn & Bacon.

Tardif, S.D. (1994) 'Relative energetic cost of infant care in small-bodied neotropical primates and its relation to infant-care patterns', *American Journal of Primatology,* 34(2), pp. 133-143.

Thompson, J.L., Krovitz, G.E. and Nelson, A.J. (2003) *Patterns of Growth and Development in the Genus Homo.* Cambridge : Cambridge University Press.

Titterington, D.M., Smith, A.F.M. and Makov, V.E. (1985) *Statistical Analysis of Finite Mixture Distributions.* New York: J. Wiley & Sons.

Tomasello, D. (1994) 'The question of chimpanzee culture', in Wrangham, R.W., McGrew, W.C., de Waal, F.B.M. and Heltne, P. (eds.) *Chimpanzee Cultures*. Massachusetts: Harvard University Press, pp. 301-317.

Trinkaus, E., Conroy, G.C. and Ruff, C.B. (1999) 'The anomalous archaic Homo femur from Berg Aukas, Namibia: A biomechanical assessment', *American Journal of Physical Anthropology,* 110(3), pp. 379-991.

Trinkaus, E., Churchill, S.E. and Ruff, C.B. (1994) 'Postcranial robusticity in Homo. II: Humeral bilateral asymmetry and bone plasticity', *American Journal of Physical Anthropology,* 93(1), pp. 1-34.

Tutin, C. (1979) 'Mating patterns and reproductive strategies in a community of wild chimpanzees (*Pan troglodytes schweinfurthii*)', *Behavioral Ecology & Sociobiology,* 6(1), pp. 29-38.

Tutin, C. (1996) 'Ranging and social structure of lowland gorillas in the Lopé Reserve, Gabon' in McGrew, W.C., Marchant, L.F. and Nishida, T. (eds.) *Great Ape Societies*. Cambridge: Cambridge University Press, pp. 58-70.

Uhl, N.M., Konigsberg, L.W. and Rainwater, C.W. (2013) 'Testing for size and allometric differences in fossil hominin body mass estimation', *American Journal of Physical Anthropology,* 151(2), pp. 215-29.

van Schaik, C.P. (1996) 'Social evolution of primates: the role of ecological factors on male behaviour' in Runciman, W., Smith, G. and Dunbar, R.I.M. (eds.) *Evolution of Social Behaviour Patterns in Primates and Man*. Oxford: Oxford University Press, pp. 9-31.

van Schaik, C.P., van Noordwijk, M.A. and Nunn, C.L. (1999) 'Sex and social evolution in primates', in Lee, P.C. (ed.). *Comparative Primate Socioecology.* Cambridge: Cambridge University Press, pp. 204-40.

Viciano, J., Lopez-Lazaro, S. and Aleman, I. (2013) 'Sex estimation based on deciduous and permanent dentition in a contemporary Spanish population', *American Journal of Physical Anthropology*, 152(1), pp. 31-43.

Viðarsdóttir, U.S., O'Higgins, P. and Stringer, C. (2002) 'A geometric morphometric study of regional differences in the ontogeny of the modern human facial skeleton', Journal of Anatomy, 201(3), pp. 211-229.

Wales, N. (2012) 'Modeling Neanderthal clothing using ethnographic analogues', *Journal of Human Evolution,* 63(6), pp. 781-795.

Wang, Z., Heo, M., Lee, R., Kotler, D. and Heymsfield, S. (2000) 'Muscularity in adult humans: proportion of adipose tissue-free body mass as skeletal muscle', *American Journal of Human Biology*, 13(5), pp. 612-619.

Wanner, I.S., Sierra Sosa, T., Alt, K.W. and Tiesler Blos, V. 2007. 'Lifestyle, occupation, and whole bone morphology of the pre-Hispanic Maya coastal population from Xcambó, Yucatan, Mexico', *International Journal of Osteoarchaeology*, 17(3), pp. 253-268.

Washabaugh, K.F., Snowdon, C.T. and Ziegler, T.E. (2002) 'Regular articles: variations in care for cotton-top tamarin, *Saguinus oedipus*, infants as a function of parental experience and group size', *Animal Behaviour,* 63(6), pp. 1163-1174.

Watts, D. (1998) 'Coalitionary mate guarding by male chimpanzees at Ngogo, Kibale National Park, Uganda', *Behavioral Ecology and Sociobiology*, 44(1), pp. 43-55.

Watts, D. (2002) 'Reciprocity and interchange in the social relationships of wild male chimpanzees', *Behaviour*, 139(2), pp. 343-370.

Watts, D. and Pusey, A.E. (1993) 'Behaviour of juvenile and adolescent great apes', in Pereira, M.E. and Fairbanks, L.A. (eds.) *Juvenile Primates.* New York: Oxford University Press, pp. 148-167.

Weiss, E. (2003) 'Effects of rowing on humeral strength, *American Journal of Physical Anthropology*, 121(4), pp. 293-302.

Weiss, E. (2009) 'Sex differences in humeral bilateral asymmetry in two hunter-gatherer populations: California Amerinds and British Columbian Amerinds', *American Journal of Physical Anthropology*, 140(1), pp. 19-24.

Wells, J.C.K. (2007) 'Sexual dimorphism of body composition', *Best Practice & Research Clinical Endocrinology & Metabolism,* 21(3), pp. 415-430.

White, T.D., Asfaw, B., Beyene, Y., Haile-Selassie, Y., Lovejoy, C.O. and Suwa, G. (2009) '*Ardipithecus ramidus* and the paleobiology of early hominids', *Science*, 326(5949), pp. 64-86.

White, J.W. and Ruttenberg, B.I. (2007) 'Discriminant function analysis in marine ecology: some oversights and their solutions', *Marine Ecology Progress Series*, 329(1), pp, 301-305.

Will, M. and Stock, J.T. (2015). ‘Spatial and temporal variation of body size among early Homo’, *Journal of Human Evolution,* 82(1), pp. 15-33.

Will, M., Pablos, A. and Stock, J.T. (2017) ‘Long-term patterns of body mass and stature evolution within the hominin lineage’, *Royal Society Open Science*, 4(11), e171339.

Willemet, R. (2013) ‘Reconsidering the evolution of brain, cognition, and behavior in birds and mammals’, *Frontiers in Psychology*, 4(396), pp. 1-26.

Williams, F.L. and Geissler, E. (2014) 'Reconstructing the diet and paleoecology of Plio-Pleistocene *Cercopithecoides williamsi* from Sterkfontein, South Africa', *Palaios,* 29(9), pp. 483-494.

Williams, F.L. and Patterson, J.W. (2010) 'Reconstructing the paleoecology of Taung, South Africa from low magnification of dental microwear features in fossil Primates', *Palaios,* 25(7), pp. 439-448.

Wilson, D. and Reader, D. (1993) *Mammal Species of the World: A Taxonomic and Geographic Reference.* Washington D.C.: Smithsonian Institution Press.

Wittenberger, J.F. and Tilson, R.L. (1980) 'The evolution of monogamy: hypotheses and evidence', *Annual Review of Ecological Systems,* 11(1), pp. 197-232.

Wolpoff, M.H., Aguirre, E., Becker, M.J., Hajn, V., Kennedy, A., Kennedy, R., Murad, T.A., Rao, V.V., Rosinkski, F., Siegel, M.I., Smith, F.H., Trinkaus, E., Wood, B.A. and Živanović, S. (1976) 'Some aspects of the evolution of early hominid sexual dimorphism [and comments and reply]', *Current Anthropology,* 17(4) pp. 579-606.

Wood, B.A. (1976) ‘The nature and basis of sexual dimorphism in the primate skeleton’, *Journal of Zoology*, 180(1), pp. 15-34.

Wrangham, R.W. (2009) *Catching Fire: How Cooking Made Us Human.* New York: Basic Books.

Wright, P.C. (1978) ‘Home range, activity pattern, and agonistic encounters of a group of night monkeys (*Aotus trivirgatus*) in Peru’, *Folia Primatologica,* 29(1), pp. 43-55.

Wright P.C. (1994) ‘The behavior and ecology of the owl monkey’, in Baer, J.F., Weller, R.E. and Kakoma, I. (eds.) *Aotus*: *The Owl Monkey*. San Diego (CA): Academic Press, pp. 97-112.

Ziegler, T.E., Savage, A., Scheffler, G. and Snowdon, C.T. (1987) ‘The endocrinology of puberty and reproductive functioning in female cotton-top tamarins (*Saguinus oedipus*) under varying social conditions’, *Biology of Reproduction,* 37(3), pp. 618-627.

Appendix 1: All skeletal metric data can be found in the supplementary spreadsheet found on the CD-ROM at the back of the thesis.

Appendix 2: Histograms of postcranial metric data for each species showing probability that is proportional to sample size.

The histograms were calculated through the 'normalization' MATLAB function, which computes the relative frequency (see code below). The relative frequency is calculated by dividing the frequency by the total number in the sample. Expected relative frequency is equal to the probability of the outcome and so the histograms display the probability of each metric for males and females of a species.

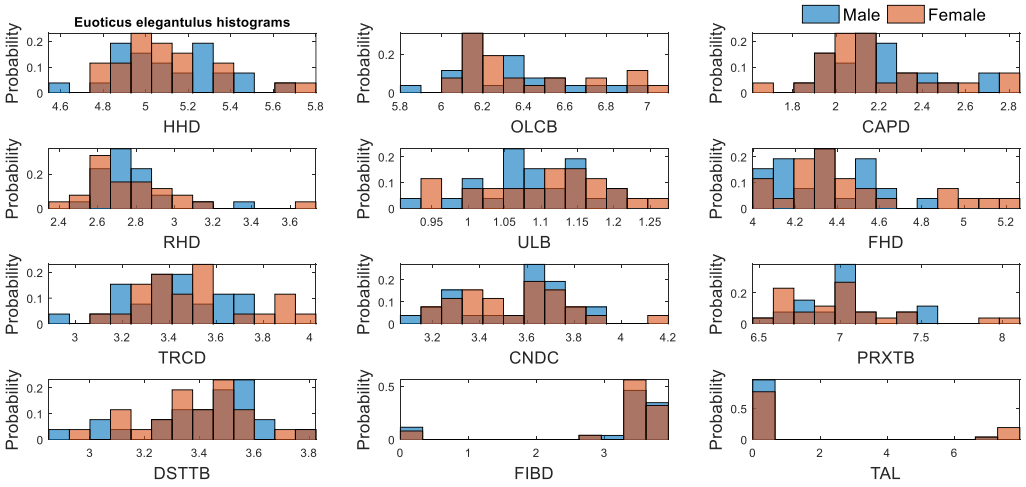

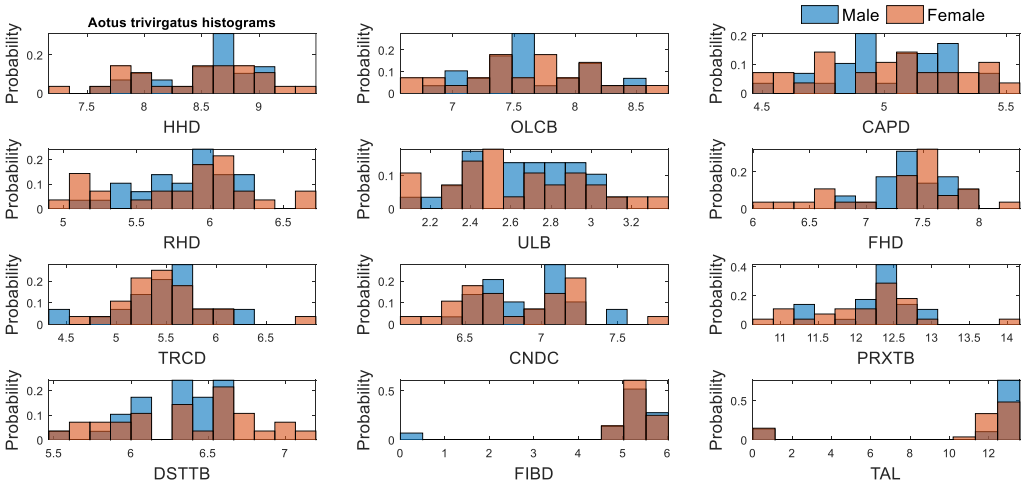

Appendix 2: Histograms of postcranial metric data for each species showing probability that is proportional to sample size continued.

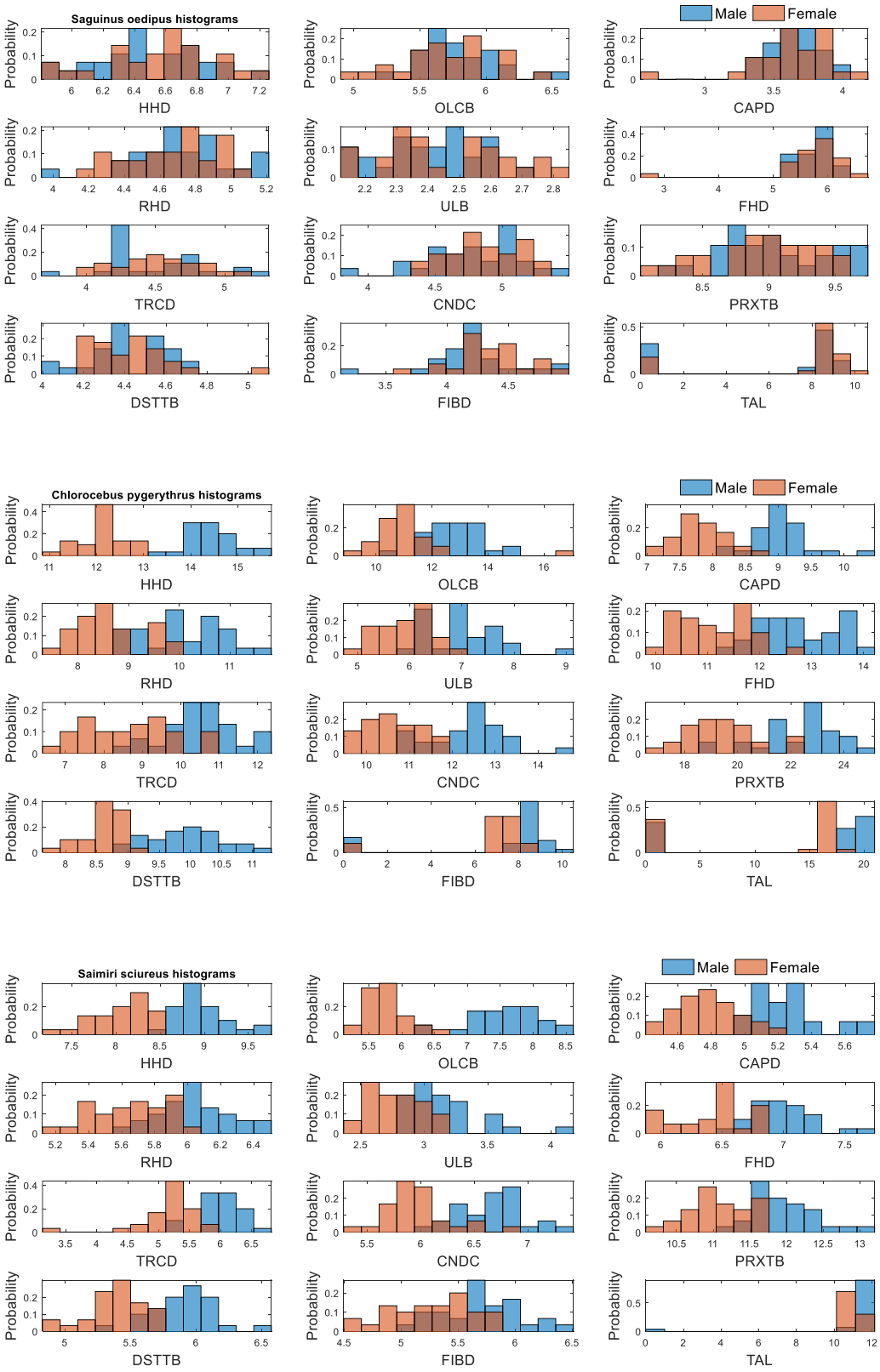

Appendix 2: Histograms of postcranial metric data for each species showing probability that is proportional to sample size continued.

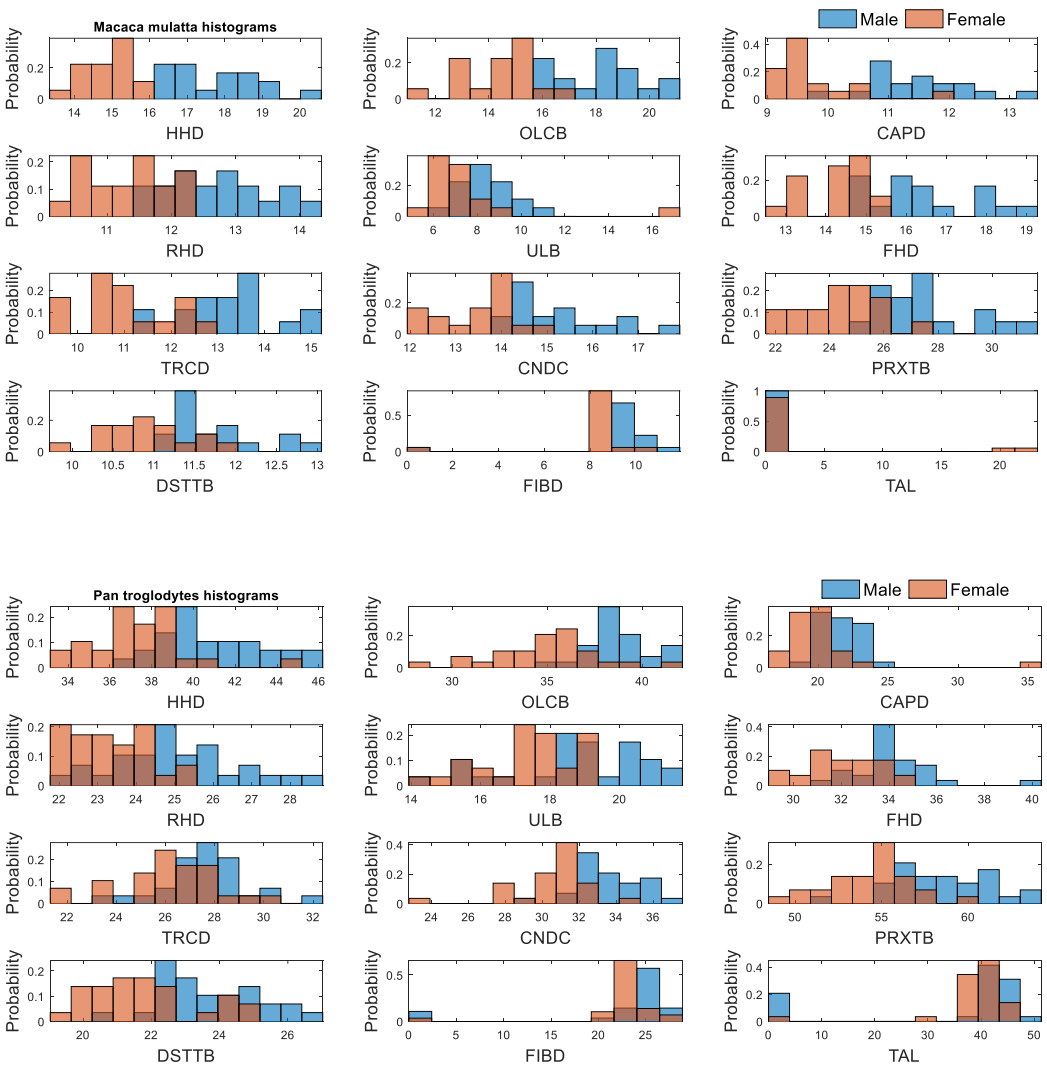

Appendix 2: Histograms of postcranial metric data for each species showing probability that is proportional to sample size continued and code used to produce histograms.

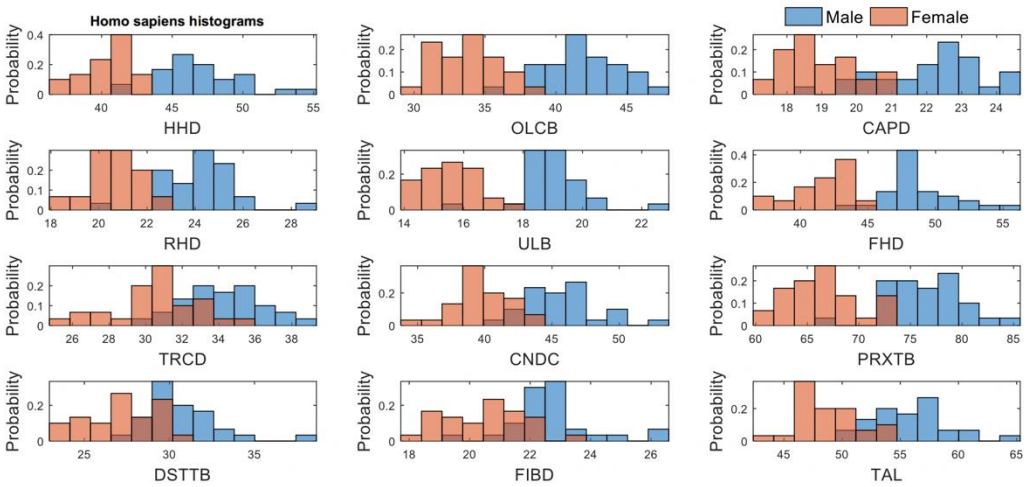


```
%% Descriptive Plots
% Load data for Species 1:
data = zeros(1,1);
labels = cell(1,1);

%% Save data:
z = find(~data); % Replace zeros with NaNs
data(z) = NaN;
save data labels % save data as .mat file

%% Analyses
clear, clc, close all % clear workspace
load data % load saved data
a = find(data(:,1)==1); % find row numbers for M & F data
b = find(data(:,1)==2);

% Draw plots using loop:
for n = 2:13 % number of graphs (col 1 is grouping variable)
    subplot(4,3,n-1) % number and position of subplot
    x = data(a,n); y = data(b,n); % separate male and female
    h1 = histogram(x); hold on % Plot histograms
    h2 = histogram(y);
    % Normalize histograms by sample size:
    h1.Normalization = 'probability'; h2.Normalization = 'probability';
    bw = (1/12)*(max(data(:,n))-min(data(:,n))); % calculate bin widths
    h1.BinWidth = bw; h2.BinWidth = bw;
    axis tight % set axes tight to data
    xlabel(labels(n-1),'FontSize',14) % add x labels from list
    ylabel('Probability','FontSize',14) % add y labels
    if n == 2 % Add legend to first subplot only
        legend({'Male','Female'},'Location','northwest','Orientation',...
            'horizontal','FontSize',14,'Box','off')
    end
end
set(gcf,'color','w') % set background colour to white
```

Appendix 3: MATLAB code for analyses in Chapter 6.

This outputs regression constant and slope, comparing each metric to every other by species using unstandardised data:

```
% Data order: A. trivirgatus, C. pygerythrus, S. sciureus, M. mulatta,
%  S. oedipus, G. gorilla, P. troglodytes, E. elegantulus, H. sapiens

clear, clc, close all
load alldata.mat % load data
% Note that alldata.mat is all data for the 9 species
s = [58 60 60 36 56 60 58 52 60]; % sample sizes for the 9 species
s = cumsum(s); % added together as a cumulative count
t(1) = 1; t(2:9) = s(1:8)+1; % and indices for starting values
% The above says that the data for a given species is in
% alldata(t(i) to s(i)), for example 1 to 58
slopeM = zeros(90,10); % create empty output matrices
slopeF = zeros(90,10);
constM = zeros(90,10);
constF = zeros(90,10);
Ms = zeros(10,10); Fs = zeros(10,10);
Mc = zeros(10,10); Fc = zeros(10,10);
x = 1; y = 10; % indices to loop through the data

for i = 1:9 % (for 9 species)
    SV = alldata(t(i):s(i),:); % pick out data for one species
    b = length(SV); a = 0.5*b; % cut it in half (male and female)
    male = SV(1:a,:);
    female = SV(a+1:b,:);
    for n = 1:10
        for m = 1:10
            pm = polyfit(male(:,n),male(:,m),1); % otherwise, compute the
correlation coefficient matrix
            pf = polyfit(female(:,n),female(:,m),1);
            Ms(n,m) = pm(1); % male slope
            Fs(n,m) = pf(1); % female slope
            Mc(n,m) = pm(2); % male constant
            Fc(n,m) = pf(2); % female constant
        end
    end
    slopeM(x:y,1:10) = Ms; % store the data for this species for males
    slopeF(x:y,1:10) = Fs; % and females
    constM(x:y,1:10) = Mc;
    constF(x:y,1:10) = Fc;
    x = x + 10; y = y + 10; % and move on to the next species
end

% Output files are slopeM, slopeF, constM and constF
```

Appendix 3: MATLAB code for analyses in Chapter 6 continued.

This is the code for the correlation coefficient analysis in Chapter 6.

```
% Data order: A. trivirgatus, C. pygerythrus, S. sciureus, M. mulatta,
%  S. oedipus, G. gorilla, P. troglodytes, E. elegantulus, H. sapiens

clear, clc, close all
load alldata.mat % load data
s = [58 60 60 36 56 60 58 52 60]; % sample sizes for the 9 species
s = cumsum(s); % added together as a cumulative count
t(1) = 1; t(2:9) = s(1:8)+1; % and indices for starting values
% The above says that the data for a given species is in
% alldata(t(i) to s(i)), for example 1 to 58
outM = zeros(90,10); % create empty output matrices
outF = zeros(90,10);
M = zeros(10,10); F = zeros(10,10);
x = 1; y = 10; % indices to loop through the data

for i = 1:9 % (for 9 species)
    SV = alldata(t(i):s(i),:); % pick out data for one species
    b = length(SV); a = 0.5*b; % cut it in half (male and female)
    male = zscore(SV(1:a,:)); % standardise male data (i.e. convert to z-
scores)
    female = zscore(SV(a+1:b,:)); % standardise female data

    for n = 1:10
        for m = 1:10
            if n==m % if the correlation coefficient is the metric with
itself,
                M(n,m) = 0; % just enter a zero
                F(n,m) = 0;
            else
                pm = cov(male(:,n),male(:,m)); % otherwise, compute the
correlation coefficent matrix
                pf = cov(female(:,n),female(:,m));
                M(n,m) = pm(2); % and output the correlation coefficient
                F(n,m) = pf(2);
            end
        end
    end
    outM(x:y,1:10) = M; % store the data for this species for males
    outF(x:y,1:10) = F; % and females
    x = x + 10; y = y + 10; % and move on to the next species
end
```

Appendix 3: MATLAB code for analyses in Chapter 6 continued.

This code produced the hierarchical clustering analysis and dendrograms for female correlation coefficient data, male correlation coefficent data and the difference between the two:

```
 %% Just Females
JF = zeros(9,45); % create empty matrix
x = 1; y = 10; % indices for looping

for n = 1:9
    JF(n,:) = squareform(outF(x:y,1:10));
    x = x + 10; y = y + 10; % move on to next species
end

Zf = linkage(JF,'ward','euclidean');
rowlabels = {'A. trivirgatus','C. pygerythrus','S. sciureus','M.
mulatta',...
    'S. oedipus','G. gorilla','P. troglodytes','E. elegantulus','H.
sapiens'};
dendrogram(Zf,'Orientation','left','Labels',rowlabels)
xlabel('Distance (Ward)')
set(gca,'FontSize',18)
set(gcf,'Color','w')
%% Just Males
JM = zeros(9,45); % create empty matrix
x = 1; y = 10; % indices for looping

for n = 1:9
    JM(n,:) = squareform(outM(x:y,1:10));
    x = x + 10; y = y + 10; % move on to next species
end

Zm = linkage(JM,'ward','euclidean');
rowlabels = {'A. trivirgatus','C. pygerythrus','S. sciureus','M.
mulatta',...
    'S. oedipus','G. gorilla','P. troglodytes','E. elegantulus','H.
sapiens'};
dendrogram(Zm,'Orientation','left','Labels',rowlabels)
xlabel('Distance (Ward)')
set(gca,'FontSize',18)
set(gcf,'Color','w')


 %% Difference
diff = outM - outF;
DIFF = zeros(9,45); % create empty matrix
x = 1; y = 10; % indices for looping

for n = 1:9
    DIFF(n,:) = squareform(diff(x:y,1:10));
    x = x + 10; y = y + 10; % move on to next species
end

Zdiff = linkage(DIFF,'ward','euclidean');
rowlabels = {'A. trivirgatus','C. pygerythrus','S. sciureus','M.
mulatta',...
    'S. oedipus','G. gorilla','P. troglodytes','E. elegantulus','H.
sapiens'};
dendrogram(Zdiff,'Orientation','left','Labels',rowlabels)
xlabel('Distance (Ward)')
set(gca,'FontSize',18)
set(gcf,'Color','w')
```

Appendix 3: MATLAB code for analyses in Chapter 6 continued.

```
%% Plot all three together
subplot(1,3,1)
dendrogram(Zf,'Orientation','left','Labels',rowlabels)
xlabel('Distance (Ward)')
title('Females')
set(gca,'FontSize',18)
subplot(1,3,2)
dendrogram(Zm,'Orientation','left','Labels',rowlabels)
xlabel('Distance (Ward)')
title('Males')
set(gca,'FontSize',18)
subplot(1,3,3)
dendrogram(Zdiff,'Orientation','left','Labels',rowlabels)
xlabel('Distance (Ward)')
title('Difference')
set(gca,'FontSize',18)
set(gcf,'Color','w')
```

This code was used to produce the clustergram of all correlation coefficient difference values:

```
load columnlabels.mat
cgo =
clustergram(DIFF,'RowLabels',rowlabels,'ColumnLabels',columnlabels,.
..
    'Linkage','ward','Colormap',redbluecmap,'Dendrogram','default');
```

Appendix 3: MATLAB code for analyses in Chapter 6 continued.

This code is to produce the hierarchical clustering analyses and dendrograms for the upper limb and lower limb:

Standardise upper limb data and calculate correlation coefficients for male and female metrics:

```
%% Upper limb only

clear, clc, close all
load alldata.mat % load data
s = [58 60 60 36 56 60 58 52 60]; % sample sizes for the 9 species
s = cumsum(s); % added together as a cumulative count
t(1) = 1; t(2:9) = s(1:8)+1; % and indices for starting values
% The above says that the data for a given species is in
% alldata(t(i) to s(i)), for example 1 to 58
UoutM = zeros(45,5); % create empty output matrices
UoutF = zeros(45,5);
M = zeros(5,5); F = zeros(5,5);
x = 1; y = 5; % indices to loop through the data

for i = 1:9 % (for 9 species)
    SV = alldata(t(i):s(i),1:5); % pick out data for one species
    b = length(SV); a = 0.5*b; % cut it in half (male and female)
    male = zscore(SV(1:a,:)); % standardise male data (i.e. convert to z-
scores)
    female = zscore(SV(a+1:b,:)); % standardise female data
    % The above removes size to concentrate on proportional change in each
    % variable - so large metrics don't have disproportionate effect
    for n = 1:5
        for m = 1:5
            if n==m % if the correlation coefficent is the metric with
itself,
                M(n,m) = 0; % just enter a zero
                F(n,m) = 0;
            else
                pm = cov(male(:,n),male(:,m)); % otherwise, compute the
correlation coefficent matrix
                pf = cov(female(:,n),female(:,m));
                M(n,m) = pm(2); % and output the correlation coefficient
                F(n,m) = pf(2);
            end
        end
    end
    UoutM(x:y,1:5) = M; % store the data for this species for males
    UoutF(x:y,1:5) = F; % and females
    x = x + 5; y = y + 5; % and move on to the next species
end
```

Appendix 3: MATLAB code for analyses in Chapter 6 continued.

Calculate hierarchical clustering from upper limb correlation coefficent difference and produce dendrogram:

```
%% Squareforms for hierarchical clustering
Udiff = zeros(9,10); % create empty matrix
diff = UoutM - UoutF; % calculate difference between males and females
using
% the data from above
x = 1; y = 5; % indices for looping

for n = 1:9
    Udiff(n,:) = squareform(diff(x:y,1:5));
    x = x + 5; y = y + 5; % move on to next species
end

ZU = linkage(Udiff,'ward','euclidean'); % create links
rowlabels = {'A. trivirgatus','C. pygerythrus','S. sciureus','M.
mulatta',...
    'S. oedipus','G. gorilla','P. troglodytes','E. elegantulus','H.
sapiens'};
dendrogram(ZU,'Orientation','left','Labels',rowlabels) % draw dendrogram
xlabel('Distance (Ward)') % x axis label
set(gca,'FontSize',18) % increase font size
set(gcf,'Color','w') % set figure background to white
```

This code produces the clustergram of upper limb correlation coefficent difference between the sexes:

```
load newlabels.mat
%cgo =
clustergram(Udiff,'Linkage','ward','Colormap',redbluecmap,'Dendrogra
m','default');

upper =
clustergram(Udiff,'RowLabels',rowlabels,'ColumnLabels',ULlabels,...
    'Linkage','ward','Colormap',redbluecmap,'Dendrogram','default');
```

Appendix 3: MATLAB code for analyses in Chapter 6 continued.

Standardise lower limb data and calculate correlation coefficient for male and female metrics:

```
%% Lower limb only

s = [58 60 60 36 56 60 58 52 60]; % sample sizes for the 9 species
s = cumsum(s); % added together as a cumulative count
t(1) = 1; t(2:9) = s(1:8)+1; % and indices for starting values
% The above says that the data for a given species is in
% alldata(t(i) to s(i)), for example 1 to 58
LoutM = zeros(45,5); % create empty output matrices
LoutF = zeros(45,5);
M = zeros(5,5); F = zeros(5,5);
x = 1; y = 5; % indices to loop through the data

for i = 1:9 % (for 9 species)
    SV = alldata(t(i):s(i),6:10); % pick out data for one species
    b = length(SV); a = 0.5*b; % cut it in half (male and female)
    male = zscore(SV(1:a,:)); % standardise male data (i.e. convert to z-
scores)
    female = zscore(SV(a+1:b,:)); % standardise female data
    % The above removes size to concentrate on proportional change in each
    % variable - so large metrics don't have disproportionate effect
    for n = 1:5
        for m = 1:5
            if n==m % if the correlation coefficient is the metric with
itself,
                M(n,m) = 0; % just enter a zero
                F(n,m) = 0;
            else
                pm = cov(male(:,n),male(:,m)); % otherwise, compute the
correlation coefficient matrix
                pf = cov(female(:,n),female(:,m));
                M(n,m) = pm(2); % and output the correlation coefficient
                F(n,m) = pf(2);
            end
        end
    end
    LoutM(x:y,1:5) = M; % store the data for this species for males
    LoutF(x:y,1:5) = F; % and females
    x = x + 5; y = y + 5; % and move on to the next species
end
```

Appendix 3: MATLAB code for analyses in Chapter 6 continued.

Calculate hierarchical clustering from lower limb correlation coefficient difference and produce dendrogram:

```
%% Squareforms for hierarchical clustering
% The above created a series of 10 * 10 matrices - one for each species
% This rearranges them into rows for the hierarchical clustering
% Note that in the matrices, only n*n-1 values (45) are of use
% This creates a matrix with each species in one row
Ldiff = zeros(9,10); % create empty matrix
diff = LoutM - LoutF; % calculate difference between males and females
using
% the data from above
x = 1; y = 5; % indices for looping

for n = 1:9
    % 'squareform' converts the matrix to a single row, keeping only the 45
    % relevant values
    Ldiff(n,:) = squareform(diff(x:y,1:5));
    x = x + 5; y = y + 5; % move on to next species
end

ZL = linkage(Ldiff,'ward','euclidean'); % create links
% Create cell array with species names
rowlabels = {'A. trivirgatus','C. pygerythrus','S. sciureus','M.
mulatta',...
    'S. oedipus','G. gorilla','P. troglodytes','E. elegantulus','H.
sapiens'};
dendrogram(ZL,'Orientation','left','Labels',rowlabels) % draw dendrogram
xlabel('Distance (Ward)') % x axis label
set(gca,'FontSize',18) % increase font size
set(gcf,'Color','w') % set figure background to white



%% Plot both together

subplot(1,2,1)
dendrogram(ZU,'Orientation','left','Labels',rowlabels) % draw dendrogram
xlabel('Distance (Ward)') % x axis label
title('Upper Limb')
set(gca,'FontSize',18) % increase font size
subplot(1,2,2)
dendrogram(ZL,'Orientation','left','Labels',rowlabels) % draw dendrogram
xlabel('Distance (Ward)') % x axis label
title('Lower Limb')
set(gca,'FontSize',18) % increase font size
set(gcf,'Color','w') % set figure background to white
```

This code produces the clustergram of upper limb correlation coefficient difference between the sexes:

```
load newlabels.mat
%cgo =
clustergram(Ldiff,'Linkage','ward','Colormap',redbluecmap,'Dendrogra
m','default');

lower =
clustergram(Ldiff,'RowLabels',rowlabels,'ColumnLabels',LLlabels,...
    'Linkage','ward','Colormap',redbluecmap,'Dendrogram','default');
```

Appendix 3: MATLAB code for analyses in Chapter 6 continued.

Calculate hierarchical clustering from statistically significant slopes only and produce dendrogram:

```
% Data structure is two columns per species (male, female) * 21 significant
% slopes in rows
clear, clc, close all % empty workspace
load SFA.mat % load data
a = [1 3 5 7 9 11]; % indices for male columns
b = [2 4 6 8 10 12]; % indices for female columns

subplot(1,3,1) % MALES
d = SFA(:,a)'; % males only
Z = linkage(d,'ward','euclidean'); % create links
rowlabels = {'C. pygerythrus','S. sciureus','M. mulatta','G. gorilla',...
    'P. troglodytes','H. sapiens'}; % labels for dendrogram
dendrogram(Z,'Orientation','left','Labels',rowlabels) % draw dendrogram
xlabel('Distance (Ward)') % x axis label
title('Males') % title
set(gca,'FontSize',18) % increase font size in whole figure

subplot(1,3,2) % FEMALES
d = SFA(:,b)'; % females only
Z = linkage(d,'ward','euclidean'); % create links
rowlabels = {'C. pygerythrus','S. sciureus','M. mulatta','G. gorilla',...
    'P. troglodytes','H. sapiens'}; % labels for dendrogram
dendrogram(Z,'Orientation','left','Labels',rowlabels) % draw dendrogram
xlabel('Distance (Ward)') % x axis label
title('Females') % title
set(gca,'FontSize',18) % increase font size

subplot(1,3,3) % DIFFERENCE
c = SFA(:,a)'; % males
d = SFA(:,b)'; % females
e = c-d; % difference as male minus female
Z = linkage(e,'ward','euclidean'); % create links
rowlabels = {'C. pygerythrus','S. sciureus','M. mulatta','G. gorilla',...
    'P. troglodytes','H. sapiens'}; % labels for dendrogram
dendrogram(Z,'Orientation','left','Labels',rowlabels) % draw dendrogram
xlabel('Distance (Ward)') % x axis label
title('Difference') % title
set(gca,'FontSize',18) % increase font size
set(gcf,'Color','w') % set figure background to white
```

Appendix 4: Normality tests for all species.

Tests of Normality

E.elegantulus		Kolmogorov-Smirnov[a]			Shapiro-Wilk		
	Sex	Statistic	Df	Sig.	Statistic	df	Sig.
HHD	Male	0.128	23	.200*	0.982	23	0.941
	Female	0.225	24	0.003	0.882	24	0.009
OLCB	Male	0.177	23	0.060	0.942	23	0.201
	Female	0.212	24	0.006	0.857	24	0.003
CAPD	Male	0.130	23	.200*	0.930	23	0.111
	Female	0.200	24	0.014	0.914	24	0.044
RHD	Male	0.210	23	0.010	0.824	23	0.001
	Female	0.122	24	.200*	0.878	24	0.008
ULB	Male	0.113	23	.200*	0.95	23	0.292
	Female	0.107	24	.200*	0.955	24	0.346
FHD	Male	0.123	23	.200*	0.947	23	0.253
	Female	0.187	24	0.030	0.887	24	0.011
TRCD	Male	0.093	23	.200*	0.978	23	0.866
	Female	0.178	24	0.047	0.935	24	0.124
CNDC	Male	0.226	23	0.004	0.898	23	0.023
	Female	0.089	24	.200*	0.962	24	0.481
PRXTB	Male	0.152	23	0.181	0.963	23	0.528
	Female	0.195	24	0.018	0.875	24	0.007
DSTTB	Male	0.141	23	.200*	0.928	23	0.100
	Female	0.114	24	.200*	0.971	24	0.685
FIBD	Male	0.156	23	0.155	0.899	23	0.024
	Female	0.111	24	.200*	0.934	24	0.121

*. This is a lower bound of the true significance.

a. Lilliefors Significance Correction

Appendix 4: Normality tests for all species continued.

Tests of Normality

A.trivirgatus		Kolmogorov-Smirnov[a]			Shapiro-Wilk		
	Sex	Statistic	Df	Sig.	Statistic	df	Sig.
HHD	Male	0.177	25	0.043	0.929	25	0.083
	Female	0.159	25	0.106	0.942	25	0.164
OLCB	Male	0.164	25	0.080	0.968	25	0.606
	Female	0.107	25	.200*	0.967	25	0.561
CAPD	Male	0.123	25	.200*	0.969	25	0.631
	Female	0.123	25	.200*	0.952	25	0.284
RHD	Male	0.115	25	.200*	0.948	25	0.224
	Female	0.166	25	0.073	0.930	25	0.087
ULB	Male	0.164	25	0.081	0.938	25	0.132
	Female	0.191	25	0.019	0.941	25	0.159
FHD	Male	0.122	25	.200*	0.945	25	0.192
	Female	0.167	25	0.070	0.951	25	0.268
TRCD	Male	0.121	25	.200*	0.960	25	0.414
	Female	0.110	25	.200*	0.945	25	0.195
CNDC	Male	0.105	25	.200*	0.947	25	0.219
	Female	0.135	25	.200*	0.941	25	0.154
PRXTB	Male	0.185	25	0.026	0.865	25	0.004
	Female	0.110	25	.200*	0.967	25	0.576
DSTTB	Male	0.166	25	0.075	0.893	25	0.013
	Female	0.140	25	.200*	0.960	25	0.422
FIBD	Male	0.098	25	.200*	0.963	25	0.488
	Female	0.091	25	.200*	0.989	25	0.992
TAL	Male	0.183	25	0.030	0.932	25	0.098
	Female	0.119	25	.200*	0.961	25	0.430

*. This is a lower bound of the true significance.

a. Lilliefors Significance Correction

Appendix 4: Normality tests for all species continued.

Tests of Normality

S.oedipus		Kolmogorov-Smirnov[a]			Shapiro-Wilk		
	Sex	Statistic	df	Sig.	Statistic	df	Sig.
HHD	Male	0.152	19	.200*	0.980	19	0.938
	Female	0.121	23	.200*	0.973	23	0.749
OLCB	Male	0.090	19	.200*	0.981	19	0.956
	Female	0.136	23	.200*	0.966	23	0.598
CAPD	Male	0.148	19	.200*	0.948	19	0.363
	Female	0.198	23	0.020	0.844	23	0.002
RHD	Male	0.096	19	.200*	0.973	19	0.827
	Female	0.143	23	.200*	0.940	23	0.181
ULB	Male	0.131	19	.200*	0.929	19	0.163
	Female	0.150	23	0.198	0.947	23	0.251
FHD	Male	0.114	19	.200*	0.967	19	0.706
	Female	0.106	23	.200*	0.975	23	0.811
TRCD	Male	0.240	19	0.005	0.901	19	0.050
	Female	0.107	23	.200*	0.974	23	0.786
CNDC	Male	0.159	19	.200*	0.951	19	0.404
	Female	0.122	23	.200*	0.939	23	0.174
PRXTB	Male	0.160	19	.200*	0.930	19	0.172
	Female	0.138	23	.200*	0.949	23	0.284
DSTTB	Male	0.129	19	.200*	0.958	19	0.540
	Female	0.115	23	.200*	0.906	23	0.034
FIBD	Male	0.159	19	.200*	0.903	19	0.055
	Female	0.122	23	.200*	0.972	23	0.736
TAL	Male	0.085	19	.200*	0.981	19	0.954
	Female	0.111	23	.200*	0.963	23	0.532

*. This is a lower bound of the true significance.

a. Lilliefors Significance Correction

Appendix 4: Normality tests for all species continued.

Tests of Normality

C.pygerythrus		Kolmogorov-Smirnov[a]			Shapiro-Wilk		
	Sex	Statistic	Df	Sig.	Statistic	df	Sig.
HHD	Male	0.280	20	0	0.857	20	0.007
	Female	0.186	19	0.083	0.917	19	0.099
OLCB	Male	0.143	20	.200*	0.96	20	0.553
	Female	0.118	19	.200*	0.979	19	0.932
CAPD	Male	0.185	20	0.071	0.849	20	0.005
	Female	0.121	19	.200*	0.969	19	0.747
RHD	Male	0.153	20	.200*	0.959	20	0.527
	Female	0.130	19	.200*	0.953	19	0.449
ULB	Male	0.133	20	.200*	0.934	20	0.185
	Female	0.130	19	.200*	0.937	19	0.235
FHD	Male	0.152	20	.200*	0.952	20	0.391
	Female	0.133	19	.200*	0.959	19	0.561
TRCD	Male	0.142	20	.200*	0.957	20	0.480
	Female	0.119	19	.200*	0.956	19	0.502
CNDC	Male	0.100	20	.200*	0.959	20	0.521
	Female	0.135	19	.200*	0.962	19	0.612
PRXTB	Male	0.115	20	.200*	0.967	20	0.685
	Female	0.140	19	.200*	0.931	19	0.183
DSTTB	Male	0.094	20	.200*	0.95	20	0.369
	Female	0.183	19	0.094	0.833	19	0.004
FIBD	Male	0.182	20	0.080	0.929	20	0.151
	Female	0.133	19	.200*	0.952	19	0.423
TAL	Male	0.112	20	.200*	0.972	20	0.806
	Female	0.145	19	.200*	0.955	19	0.487

*. This is a lower bound of the true significance.

a. Lilliefors Significance Correction

Appendix 4: Normality tests for all species continued.

Tests of Normality

S.sciureus	Sex	Kolmogorov-Smirnov[a]			Shapiro-Wilk		
		Statistic	df	Sig.	Statistic	df	Sig.
HHD	1	0.116	29	.200*	0.962	29	0.360
	2	0.135	30	0.172	0.927	30	0.042
OLCB	1	0.097	29	.200*	0.958	29	0.288
	2	0.143	30	0.119	0.921	30	0.028
CAPD	1	0.129	29	.200*	0.899	29	0.009
	2	0.079	30	.200*	0.979	30	0.785
RHD	1	0.094	29	.200*	0.970	29	0.565
	2	0.092	30	.200*	0.964	30	0.382
ULB	1	0.178	29	0.020	0.863	29	0.001
	2	0.105	30	.200*	0.977	30	0.750
FHD	1	0.115	29	.200*	0.966	29	0.463
	2	0.164	30	0.039	0.924	30	0.034
TRCD	1	0.093	29	.200*	0.954	29	0.235
	2	0.204	30	0.003	0.793	30	0.000
CNDC	1	0.075	29	.200*	0.985	29	0.935
	2	0.157	30	0.058	0.934	30	0.062
PRXTB	1	0.171	29	0.030	0.939	29	0.096
	2	0.118	30	.200*	0.959	30	0.293
DSTTB	1	0.098	29	.200*	0.983	29	0.901
	2	0.122	30	.200*	0.942	30	0.103
FIBD	1	0.113	29	.200*	0.973	29	0.638
	2	0.093	30	.200*	0.968	30	0.482
TAL	1	0.123	29	.200*	0.960	29	0.335
	2	0.136	30	0.161	0.964	30	0.392

*. This is a lower bound of the true significance.

a. Lilliefors Significance Correction

Appendix 4: Normality tests for all species continued.

Tests of Normality

M.mulatta		Kolmogorov-Smirnov[a]			Shapiro-Wilk		
	Sex	Statistic	df	Sig.	Statistic	df	Sig.
HHD	Male	0.150	17	.200*	0.937	17	0.289
	Female	0.140	17	.200*	0.945	17	0.381
OLCB	Male	0.142	17	.200*	0.947	17	0.405
	Female	0.135	17	.200*	0.960	17	0.640
CAPD	Male	0.129	17	.200*	0.960	17	0.628
	Female	0.233	17	0.015	0.781	17	0.001
RHD	Male	0.104	17	.200*	0.957	17	0.582
	Female	0.154	17	.200*	0.925	17	0.179
ULB	Male	0.090	17	.200*	0.987	17	0.995
	Female	0.290	17	0.000	0.550	17	0.000
FHD	Male	0.138	17	.200*	0.938	17	0.294
	Female	0.162	17	.200*	0.903	17	0.077
TRCD	Male	0.134	17	.200*	0.951	17	0.466
	Female	0.134	17	.200*	0.935	17	0.263
CNDC	Male	0.183	17	0.135	0.890	17	0.047
	Female	0.200	17	0.069	0.912	17	0.109
PRXTB	Male	0.167	17	.200*	0.906	17	0.085
	Female	0.146	17	.200*	0.955	17	0.536
DSTTB	Male	0.203	17	0.060	0.849	17	0.010
	Female	0.115	17	.200*	0.972	17	0.860
FIBD	Male	0.218	17	0.031	0.850	17	0.011
	Female	0.222	17	0.025	0.823	17	0.004

*. This is a lower bound of the true significance.

a. Lilliefors Significance Correction

Appendix 4: Normality tests for all species continued.

Tests of Normality

G.gorilla		Kolmogorov-Smirnov[a]			Shapiro-Wilk		
	Sex	Statistic	df	Sig.	Statistic	df	Sig.
HHD	Male	0.080	25	.200*	0.960	25	0.411
	Female	0.067	28	.200*	0.976	28	0.740
OLCB	Male	0.119	25	.200*	0.969	25	0.631
	Female	0.119	28	.200*	0.977	28	0.766
CAPD	Male	0.113	25	.200*	0.956	25	0.333
	Female	0.085	28	.200*	0.971	28	0.605
RHD	Male	0.099	25	.200*	0.967	25	0.564
	Female	0.134	28	.200*	0.947	28	0.163
ULB	Male	0.165	25	0.076	0.941	25	0.159
	Female	0.111	28	.200*	0.946	28	0.158
FHD	Male	0.134	25	.200*	0.967	25	0.560
	Female	0.124	28	.200*	0.951	28	0.209
TRCD	Male	0.150	25	0.148	0.902	25	0.020
	Female	0.113	28	.200*	0.970	28	0.585
CNDC	Male	0.095	25	.200*	0.979	25	0.866
	Female	0.135	28	.200*	0.940	28	0.108
PRXTB	Male	0.085	25	.200*	0.969	25	0.627
	Female	0.117	28	.200*	0.972	28	0.635
DSTTB	Male	0.106	25	.200*	0.972	25	0.693
	Female	0.241	28	0.00	0.877	28	0.003
FIBD	Male	0.086	25	.200*	0.967	25	0.578
	Female	0.110	28	.200*	0.973	28	0.658
TAL	Male	0.077	25	.200*	0.977	25	0.830
	Female	0.094	28	.200*	0.985	28	0.949

*. This is a lower bound of the true significance.

a. Lilliefors Significance Correction

Appendix 4: Normality tests for all species continued.

Tests of Normality

P.troglodytes		Kolmogorov-Smirnov[a]			Shapiro-Wilk		
	Sex	Statistic	df	Sig.	Statistic	df	Sig.
HHD	Male	0.121	23	.200*	0.975	23	0.809
	Female	0.126	27	.200*	0.932	27	0.079
OLCB	Male	0.152	23	0.181	0.945	23	0.226
	Female	0.112	27	.200*	0.978	27	0.826
CAPD	Male	0.122	23	.200*	0.955	23	0.378
	Female	0.281	27	0.000	0.552	27	0.000
RHD	Male	0.115	23	.200*	0.977	23	0.855
	Female	0.129	27	.200*	0.94	27	0.123
ULB	Male	0.162	23	0.121	0.913	23	0.048
	Female	0.154	27	0.099	0.954	27	0.264
FHD	Male	0.203	23	0.015	0.877	23	0.009
	Female	0.096	27	.200*	0.976	27	0.767
TRCD	Male	0.139	23	.200*	0.965	23	0.562
	Female	0.121	27	.200*	0.962	27	0.410
CNDC	Male	0.183	23	0.044	0.922	23	0.075
	Female	0.217	27	0.002	0.869	27	0.003
PRXTB	Male	0.160	23	0.131	0.945	23	0.233
	Female	0.128	27	.200*	0.975	27	0.740
DSTTB	Male	0.162	23	0.121	0.953	23	0.344
	Female	0.125	27	.200*	0.947	27	0.182
FIBD	Male	0.150	23	0.198	0.967	23	0.607
	Female	0.175	27	0.033	0.936	27	0.097
TAL	Male	0.120	23	.200*	0.967	23	0.628
	Female	0.172	27	0.039	0.853	27	0.001

*. This is a lower bound of the true significance.

a. Lilliefors Significance Correction

Appendix 4: Normality tests for all species continued.

Tests of Normality

H.sapiens		Kolmogorov-Smirnov[a]			Shapiro-Wilk		
	Sex	Statistic	df	Sig.	Statistic	df	Sig.
HHD	Male	0.140	30	0.136	0.947	30	0.139
	Female	0.137	30	0.159	0.949	30	0.162
OLCB	Male	0.066	30	.200*	0.989	30	0.986
	Female	0.094	30	.200*	0.977	30	0.738
CAPD	Male	0.124	30	.200*	0.957	30	0.262
	Female	0.144	30	0.112	0.931	30	0.051
RHD	Male	0.096	30	.200*	0.963	30	0.370
	Female	0.119	30	.200*	0.962	30	0.351
ULB	Male	0.154	30	0.067	0.900	30	0.008
	Female	0.103	30	.200*	0.977	30	0.745
FHD	Male	0.132	30	0.196	0.959	30	0.288
	Female	0.134	30	0.179	0.951	30	0.182
TRCD	Male	0.067	30	.200*	0.992	30	0.997
	Female	0.137	30	0.160	0.976	30	0.702
CNDC	Male	0.102	30	.200*	0.972	30	0.583
	Female	0.069	30	.200*	0.986	30	0.953
PRXTB	Male	0.111	30	.200*	0.981	30	0.839
	Female	0.104	30	.200*	0.973	30	0.638
DSTTB	Male	0.169	30	0.028	0.908	30	0.013
	Female	0.109	30	.200*	0.965	30	0.407
FIBD	Male	0.193	30	0.006	0.902	30	0.009
	Female	0.103	30	.200*	0.971	30	0.557
TAL	Male	0.078	30	.200*	0.979	30	0.806
	Female	0.151	30	0.079	0.956	30	0.242

*. This is a lower bound of the true significance.

a. Lilliefors Significance Correction

Appendix 5: Sexual dimorphism index (SDI) for each species calculated from the male and female mean for each metric.

HHD

	Male Mean (mm)	Female Mean (mm)	SDI
A. trivirgatus	8.50	8.44	1.01
C. pygerythrus	14.43	12.15	1.19
S. sciureus	8.97	8.07	1.11
M. mulatta	17.71	14.85	1.19
S. oedipus	6.49	6.56	0.99
E. elegantulus	5.12	5.10	1.00
P. troglodytes	40.96	37.28	1.10
G. gorilla	63.41	48.79	1.30
H. sapiens	46.97	40.32	1.16

OLCB

	Male Mean (mm)	Female Mean (mm)	SDI
A. trivirgatus	7.64	7.57	1.01
C. pygerythrus	12.85	11.13	1.15
S. sciureus	7.59	5.76	1.32
M. mulatta	18.16	14.46	1.26
S. oedipus	5.80	5.70	1.02
E. elegantulus	6.33	6.39	0.99
P. troglodytes	38.75	34.92	1.11
G. gorilla	57.31	43.11	1.33
H. sapiens	41.90	33.75	1.24

CAPD

	Male Mean (mm)	Female Mean (mm)	SDI
A. trivirgatus	5.03	5.00	1.01
C. pygerythrus	9.03	7.81	1.16
S. sciureus	5.26	4.78	1.10
M. mulatta	11.44	9.72	1.18
S. oedipus	3.66	3.63	1.01
E. elegantulus	2.19	2.17	1.01
P. troglodytes	21.53	20.16	1.07
G. gorilla	32.36	24.87	1.30
H. sapiens	22.10	18.96	1.17

Appendix 5: Sexual dimorphism index (SDI) for each species calculated from the male and female mean for each metric continued.

RHD

	Male Mean (mm)	Female Mean (mm)	SDI
A. trivirgatus	5.81	5.81	1.00
C. pygerythrus	10.06	8.65	1.16
S. sciureus	6.04	5.65	1.07
M. mulatta	12.73	11.33	1.12
S. oedipus	4.72	4.66	1.01
E. elegantulus	2.76	2.78	0.99
P. troglodytes	25.01	23.31	1.07
G. gorilla	34.94	27.10	1.29
H. sapiens	24.23	20.65	1.17

ULB

	Male Mean (mm)	Female Mean (mm)	SDI
A. trivirgatus	2.67	2.62	1.02
C. pygerythrus	6.99	5.9	1.18
S. sciureus	3.14	2.77	1.13
M. mulatta	8.51	7.56	1.13
S. oedipus	2.41	2.46	0.98
E. elegantulus	1.08	1.1	0.98
P. troglodytes	18.76	17.41	1.08
G. gorilla	27.14	21.13	1.28
H. sapiens	18.99	15.54	1.22

FHD

	Male Mean (mm)	Female Mean (mm)	SDI
A. trivirgatus	7.43	7.29	1.02
C. pygerythrus	12.74	11.14	1.14
S. sciureus	7.00	6.43	1.09
M. mulatta	16.51	14.30	1.15
S. oedipus	5.79	5.71	1.01
E. elegantulus	4.34	4.45	0.98
P. troglodytes	34.14	32.08	1.06
G. gorilla	50.77	40.80	1.24
H. sapiens	48.58	41.66	1.17

Appendix 5: Sexual dimorphism index (SDI) for each species calculated from the male and female mean for each metric continued.

TRDC

	Male Mean (mm)	Female Mean (mm)	SDI
A. trivirgatus	5.50	5.46	1.01
C. pygerythrus	10.54	8.63	1.22
S. sciureus	6.00	5.17	1.16
M. mulatta	13.23	10.96	1.21
S. oedipus	4.48	4.51	0.99
E. elegantulus	3.40	3.50	0.97
P. troglodytes	27.65	26.15	1.06
G. gorilla	40.09	33.26	1.21
H. sapiens	34.22	30.57	1.12

CNDC

	Male Mean (mm)	Female Mean (mm)	SDI
A. trivirgatus	6.91	6.86	1.01
C. pygerythrus	12.37	10.58	1.17
S. sciureus	6.67	5.97	1.12
M. mulatta	15.23	13.52	1.13
S. oedipus	4.78	4.86	0.98
E. elegantulus	3.56	3.55	1.00
P. troglodytes	33.59	30.59	1.10
G. gorilla	50.46	40.27	1.25
H. sapiens	45.67	39.76	1.15

PRXTB

	Male Mean (mm)	Female Mean (mm)	SDI
A. trivirgatus	12.27	12.14	1.01
C. pygerythrus	22.33	19.36	1.15
S. sciureus	11.97	11.07	1.08
M. mulatta	27.50	24.42	1.13
S. oedipus	9.04	8.95	1.01
E. elegantulus	7.03	7.01	1.00
P. troglodytes	58.54	54.37	1.08
G. gorilla	86.48	69.41	1.25
H. sapiens	76.61	66.42	1.15

Appendix 5: Sexual dimorphism index (SDI) for each species calculated from the male and female mean for each metric continued.

DSTTB

	Male Mean (mm)	Female Mean (mm)	SDI
A. trivirgatus	6.29	6.36	0.99
C. pygerythrus	9.93	8.60	1.15
S. sciureus	5.90	5.39	1.09
M. mulatta	11.74	10.89	1.08
S. oedipus	4.42	4.42	1.00
E. elegantulus	3.41	3.38	1.01
P. troglodytes	23.69	21.84	1.08
G. gorilla	32.88	24.65	1.33
H. sapiens	30.70	27.20	1.13

FIBD

	Male Mean (mm)	Female Mean (mm)	SDI
A. trivirgatus	5.36	5.35	1.00
C. pygerythrus	8.14	6.90	1.18
S. sciureus	5.71	5.27	1.08
M. mulatta	9.87	8.70	1.13
S. oedipus	4.21	4.35	0.97
E. elegantulus	3.53	3.54	1.00
P. troglodytes	25.06	23.25	1.08
G. gorilla	30.76	23.38	1.32
H. sapiens	22.71	20.47	1.11

TAL

	Male Mean (mm)	Female Mean (mm)	SDI
A. trivirgatus	12.70	12.55	1.01
C. pygerythrus	19.41	15.93	1.22
S. sciureus	11.20	10.96	1.02
M. mulatta	N/A	N/A	N/A
S. oedipus	8.71	8.77	0.99
E. elegantulus	N/A	N/A	N/A
P. troglodytes	42.97	40.23	1.07
G. gorilla	61.24	48.95	1.25
H. sapiens	55.71	48.82	1.14

Appendix 6: Discriminant function analysis correlation coefficients and ranking tables.

Appendix 6.1: Table of correlation coefficients from the unstandardised discriminant function analysis.

	HHD	OLCB	CAPD	RHD	ULB	FHD	TRCD	CNDC	PRXTB	DSTTB	FIBD	TAL
E. elegantulus	-0.07	0.14	-0.01	0.06	0.34	0.66	0.42	-0.01	0.01	-0.28	0.02	n/a
A. trivirgatus	0.25	0.17	0.25	0.11	0.27	0.47	0.31	0.19	0.33	0.08	0.01	0.28
S.oedipus	0.36	-0.07	0.01	-0.08	0.27	0.27	0.20	0.10	0.05	0.19	0.49	0.11
C. pygerythrus	0.74	0.34	0.50	0.37	0.27	0.35	0.27	0.46	0.40	0.41	0.31	0.53
S. sciureus	0.54	0.75	0.43	0.31	0.26	0.36	0.33	0.39	0.37	0.39	0.21	0.30
M. mulatta	0.75	0.73	0.69	0.51	0.14	0.51	0.64	0.47	0.47	0.40	0.47	n/a
P. troglodytes	0.66	0.71	0.21	0.62	0.34	0.50	0.33	0.66	0.68	0.52	0.39	0.37
G. gorilla	0.70	0.70	0.54	0.61	0.40	0.57	0.34	0.46	0.57	0.65	0.64	0.51
H. sapiens	0.58	0.70	0.52	0.58	0.72	0.62	0.34	0.51	0.61	0.36	0.34	0.49

Appendix 6.2: Table of correlation coefficients from the stepwise discriminant function analysis.

	HHD	OLCB	CAPD	RHD	ULB	FHD	TRCD	CNDC	PRXTB	DSTTB	FIBD	TAL
E. elegantulus	x	x	x	x	x	x	x	x	x	x	X	x
A. trivirgatus	x	x	x	x	x	x	x	x	x	x	X	x
S.oedipus	0.60	0.46	0.35	0.46	0.41	0.59	0.59	0.70	0.73	0.49	1.00	0.60
C. pygerythrus	1.00	0.51	0.52	0.66	0.43	0.44	0.48	0.51	0.73	0.49	0.45	0.40
S. sciureus	0.50	0.95	0.42	0.59	0.36	0.25	0.42	0.37	0.47	0.32	0.39	0.27
M. mulatta	0.92	0.88	0.70	0.73	0.34	0.84	0.66	0.74	0.77	0.59	0.62	x
P. troglodytes	0.66	0.84	0.24	0.53	0.26	0.59	0.50	0.78	0.68	0.38	0.45	0.18
G. gorilla	0.58	0.74	0.55	0.58	0.40	0.50	0.29	0.58	0.64	0.69	0.68	0.57
H. sapiens	0.70	0.57	0.54	0.54	0.79	0.68	0.53	0.61	0.67	0.41	0.40	0.54

Appendix 6.3: Table of unstandardised discriminant function analysis rankings.

	HHD	OLCB	CAPD	RHD	ULB	FHD	TRCD	CNDC	PRXTB	DSTTB	FIBD	TAL
E. elegantulus	6	5	10	7	3	2	1	9	11	4	8	x
A. trivirgatus	6	9	7	10	5	1	3	8	2	11	12	4
S.oedipus	2	10	12	9	3	4	5	8	11	6	1	7
C. pygerythrus	1	9	3	7	11	8	12	4	6	5	10	2
S. sciureus	2	1	3	9	11	7	8	5	6	4	12	10
M. mulatta	1	2	3	6	11	5	4	7	8	10	9	x
P. troglodytes	4	1	12	5	10	7	11	3	2	6	8	9
G. gorilla	1	2	8	5	11	6	12	10	7	3	4	9
H. sapiens	5	2	7	6	1	3	12	8	4	10	11	9
Average	1	2	9	7	10	3	11	6	4	5	12	8

Appendix 6.4: Table of stepwise discriminant function analysis rankings.

	HHD	OLCB	CAPD	RHD	ULB	FHD	TRCD	CNDC	PRXTB	DSTTB	FIBD	TAL
E. elegantulus	x	x	x	x	x	x	x	x	x	x	x	x
A. trivirgatus	x	x	x	x	x	x	x	x	x	x	x	x
S.oedipus	5	9	12	10	11	6	7	3	2	8	1	4
C. pygerythrus	1	6	4	3	11	10	8	5	2	7	9	12
S. sciureus	3	1	5	2	9	12	6	8	4	10	7	11
M. mulatta	1	2	7	6	11	3	8	5	4	10	9	x
P. troglodytes	4	1	11	6	10	5	7	2	3	9	8	12
G. gorilla	5	1	9	7	11	10	12	6	4	2	3	8
H. sapiens	2	6	7	9	1	3	10	5	4	11	12	8
Average	1	3	7	5	10	6	9	4	2	8	6	11

Appendix 7: Slopes and constants for all males and females.

Male Slopes	HHD	OLCB	CAPD	RHD	ULB	FHD	TRCD	CNDC	PRXTB	DSTTB
E. elegantulus										
HHD		0.57	0.434	0.324	-0.03	0.367	0.315	0.273	0.555	0.138
OLCB	0.491		0.468	0.176	0.068	0.202	0.341	0.325	0.56	0.025
CAPD	0.54	0.675		0.536	0.025	0.371	0.325	0.173	0.703	-0.312
RHD	0.656	0.414	0.873		-0.071	0.431	0.485	0.094	0.6	-0.287
ULB	-0.358	0.941	0.243	-0.416		0.04	0.926	1.02	1.411	-0.333
FHD	0.465	0.297	0.378	0.269	0.004		0.272	0.077	0.462	-0.058
TRCD	0.44	0.553	0.366	0.334	0.108	0.299		0.652	0.866	0.083
CNDC	0.289	0.398	0.147	0.049	0.09	0.064	0.493		0.866	0.106
PRXTB	0.424	0.496	0.432	0.226	0.09	0.279	0.474	0.627		0
DSTTB	0.189	0.039	-0.343	-0.194	-0.038	-0.062	0.081	0.137	-0.001	
A. trivirgatus										
HHD		0.657	0.29	0.506	0.273	0.477	0.596	0.158	0.838	0.326
OLCB	0.585		0.155	0.316	0.092	0.233	0.308	-0.012	0.524	0.128
CAPD	0.851	0.512		0.684	0.221	0.63	0.329	0.579	1.377	0.315
RHD	0.869	0.609	0.4		0.315	0.733	0.428	0.143	1.267	0.344
ULB	0.643	0.242	0.177	0.432		0.44	0.817	0.201	0.761	0.035
FHD	0.98	0.537	0.441	0.876	0.383		0.77	0.323	1.156	0.496
TRCD	0.456	0.265	0.086	0.191	0.266	0.287		-0.025	0.389	0.283
CNDC	0.318	-0.027	0.397	0.167	0.172	0.317	-0.067		0.515	0.099
PRXTB	0.612	0.429	0.343	0.539	0.236	0.411	0.372	0.187		0.212
DSTTB	0.638	0.281	0.21	0.392	0.029	0.473	0.722	0.096	0.568	
S. oedipus										
HHD		0.522	0.303	0.57	0.186	0.81	0.706	0.572	0.88	0.317
OLCB	0.725		0.344	0.685	0.311	0.837	0.964	0.689	0.901	0.38
CAPD	1.404	1.149		1.094	0.496	1.382	1.147	1.105	1.627	0.421
RHD	0.998	0.863	0.413		0.252	1.061	0.896	0.697	1.144	0.382
ULB	0.919	1.108	0.528	0.711		1.114	1.196	0.809	1.143	0.568
FHD	0.898	0.667	0.33	0.671	0.25		0.868	0.642	0.939	0.426
TRCD	0.682	0.669	0.238	0.493	0.234	0.756		0.646	0.729	0.37
CNDC	0.564	0.489	0.235	0.392	0.161	0.571	0.66		0.831	0.363
PRXTB	0.714	0.526	0.284	0.53	0.188	0.688	0.613	0.684		0.356
DSTTB	1.074	0.926	0.308	0.738	0.389	1.301	1.299	1.245	1.487	

Appendix 7: Slopes and constants for all male and females continued.

Male Slopes	HHD	OLCB	CAPD	RHD	ULB	FHD	TRCD	CNDC	PRXTB	DSTTB
C. pygerythrus										
HHD		0.855	0.608	0.98	0.371	0.818	0.984	0.963	1.711	0.538
OLCB	0.296		0.233	0.555	0.362	0.595	0.622	0.594	0.971	0.17
CAPD	0.824	0.91		1.167	0.725	0.924	1.071	1.047	1.794	0.543
RHD	0.426	0.698	0.375		0.257	0.789	0.777	0.906	1.606	0.361
ULB	0.208	0.585	0.299	0.331		0.434	0.536	0.312	0.276	0.377
FHD	0.387	0.812	0.322	0.856	0.367		0.914	0.935	1.553	0.451
TRCD	0.306	0.558	0.246	0.554	0.298	0.601		0.5	0.906	0.376
CNDC	0.351	0.624	0.281	0.758	0.203	0.72	0.586		1.488	0.327
PRXTB	0.219	0.36	0.17	0.473	0.063	0.421	0.374	0.524		0.199
DSTTB	0.437	0.399	0.326	0.673	0.547	0.775	0.982	0.73	1.26	
S. sciureus										
HHD		1.116	0.443	0.41	0.39	0.463	0.62	0.538	1.038	0.368
OLCB	0.315		0.2	0.297	0.18	0.08	0.271	0.154	0.386	0.141
CAPD	0.9	1.442		0.721	0.776	0.417	0.495	0.701	1.318	0.652
RHD	0.693	1.773	0.598		0.444	0.5	0.444	0.598	0.806	0.567
ULB	0.409	0.666	0.399	0.275		0.356	0.377	0.511	0.834	0.296
FHD	0.593	0.361	0.263	0.379	0.435		0.528	0.776	0.83	0.37
TRCD	0.464	0.719	0.182	0.197	0.269	0.309		0.373	0.723	0.241
CNDC	0.464	0.469	0.297	0.305	0.42	0.522	0.429		1.11	0.398
PRXTB	0.444	0.584	0.277	0.204	0.341	0.277	0.413	0.551		0.282
DSTTB	0.575	0.784	0.502	0.525	0.442	0.452	0.505	0.723	1.032	
M. mulatta										
HHD		1.003	0.467	0.458	0.456	0.882	0.476	0.664	1.119	0.259
OLCB	0.57		0.388	0.426	0.419	0.646	0.315	0.415	0.725	0.181
CAPD	0.973	1.421		0.79	0.741	1.153	0.358	0.853	1.157	0.311
RHD	0.976	1.596	0.807		0.901	1.348	0.693	0.829	1.4	0.403
ULB	0.468	0.757	0.365	0.434		0.574	0.518	0.429	0.765	0.137
FHD	0.718	0.926	0.451	0.516	0.456		0.524	0.613	1.093	0.275
TRCD	0.685	0.795	0.247	0.468	0.725	0.925		0.471	0.899	0.261
CNDC	0.934	1.026	0.576	0.548	0.588	1.058	0.461		1.567	0.373
PRXTB	0.542	0.618	0.269	0.318	0.361	0.649	0.303	0.539		0.209
DSTTB	1.328	1.634	0.765	0.972	0.685	1.733	0.932	1.36	2.21	

Appendix 7: Slopes and constants for all males and females continued.

Male Slopes	HHD	OLCB	CAPD	RHD	ULB	FHD	TRCD	CNDC	PRXTB	DSTTB
G. gorilla										
HHD		0.61	0.337	0.503	0.264	0.488	0.562	0.621	0.939	0.188
OLCB	0.559		0.162	0.336	0.123	0.241	0.185	0.474	0.636	0.179
CAPD	1.075	0.565		0.563	0.392	0.504	0.359	0.693	1.001	0.401
RHD	1.266	0.923	0.444		0.405	0.54	0.743	1.116	1.415	0.211
ULB	0.54	0.273	0.251	0.329		0.342	0.472	0.653	0.728	0.063
FHD	1.168	0.63	0.378	0.513	0.4		0.61	0.736	1.124	0.305
TRCD	0.677	0.244	0.136	0.356	0.279	0.307		0.511	0.68	-0.011
CNDC	0.653	0.544	0.228	0.466	0.336	0.323	0.446		0.973	0.129
PRXTB	0.738	0.546	0.247	0.442	0.28	0.369	0.444	0.728		0.168
DSTTB	0.708	0.737	0.475	0.316	0.116	0.481	-0.035	0.462	0.808	
P. troglodytes										
HHD		0.453	0.41	0.509	0.314	0.484	0.218	0.493	0.975	0.269
OLCB	0.988		0.481	0.492	0.334	0.475	0.254	0.492	1.133	0.339
CAPD	1.206	0.649		0.829	0.243	0.631	0.292	0.54	1.157	0.565
RHD	1.141	0.505	0.63		0.395	0.715	0.46	0.743	1.338	0.448
ULB	0.453	0.221	0.119	0.255		0.33	0.574	0.582	0.697	-0.082
FHD	1.044	0.47	0.463	0.689	0.494		0.439	0.613	1.247	0.386
TRCD	0.417	0.222	0.189	0.392	0.759	0.388		0.412	0.733	0.014
CNDC	0.905	0.414	0.337	0.61	0.741	0.522	0.396		1.324	0.253
PRXTB	0.715	0.381	0.288	0.438	0.354	0.424	0.281	0.528		0.242
DSTTB	0.754	0.436	0.538	0.561	-0.16	0.502	0.02	0.387	0.928	
H. sapiens										
HHD		0.351	0.27	0.329	0.139	0.809	0.436	0.686	0.933	0.46
OLCB	0.416		0.291	0.193	0.239	0.368	0.434	0.264	0.557	0.231
CAPD	0.974	0.887		0.761	0.365	0.91	0.419	0.513	0.857	0.351
RHD	1.194	0.594	0.767		0.241	1.028	0.451	1	1.383	0.528
ULB	0.976	1.423	0.713	0.467		0.663	0.807	0.74	1.28	0.254
FHD	1.053	0.404	0.328	0.368	0.122		0.508	0.783	1.138	0.55
TRCD	0.788	0.663	0.21	0.224	0.207	0.706		0.584	0.828	0.429
CNDC	0.798	0.259	0.166	0.321	0.122	0.701	0.377		1.267	0.52
PRXTB	0.573	0.289	0.146	0.234	0.112	0.537	0.281	0.668		0.37
DSTTB	0.853	0.362	0.18	0.269	0.067	0.784	0.44	0.828	1.115	

Appendix 7: Slopes and constants for all males and females continued.

Male Constants	HHD	OLCB	CAPD	RHD	ULB	FHD	TRCD	CNDC	PRXTB	DSTTB
E. elegantulus										
HHD		3.41	-0.03	1.11	1.24	2.46	1.79	2.16	4.19	2.70
OLCB	2.01		-0.77	1.65	0.65	3.07	1.24	1.50	3.49	3.25
CAPD	3.94	4.85		1.59	1.03	3.53	2.69	3.18	5.49	4.09
RHD	3.31	5.19	-0.22		1.28	3.15	2.06	3.30	5.37	4.20
ULB	5.51	5.31	1.93	3.22		4.30	2.40	2.45	5.50	3.77
FHD	3.10	5.04	0.55	1.59	1.07		2.22	3.22	5.03	3.66
TRCD	3.62	4.45	0.95	1.63	0.72	3.32		1.34	4.09	3.12
CNDC	4.09	4.91	1.67	2.59	0.76	4.11	1.65		3.95	3.03
PRXTB	2.14	2.84	-0.85	1.17	0.45	2.38	0.07	-0.85		3.41
DSTTB	4.48	6.20	3.36	3.42	1.21	4.56	3.13	3.09	7.03	
A. trivirgatus										
HHD		2.06	2.56	1.51	0.35	3.37	0.43	5.57	5.14	3.51
OLCB	4.03		3.84	3.39	1.97	5.65	3.15	7.00	8.27	5.31
CAPD	4.22	5.07		2.37	1.56	4.26	3.85	4.00	5.34	4.70
RHD	3.46	4.10	2.71		0.85	3.18	3.02	6.08	4.91	4.29
ULB	6.79	7.00	4.56	4.66		6.26	3.32	6.37	10.24	6.20
FHD	1.22	3.65	1.75	-0.70	-0.18		-0.22	4.51	3.68	2.60
TRCD	6.00	6.19	4.56	4.76	1.21	5.86		7.05	10.13	4.73
CNDC	6.31	7.83	2.29	4.65	1.49	5.25	5.96		8.71	5.61
PRXTB	1.00	2.38	0.83	-0.80	-0.22	2.39	0.94	4.62		3.69
DSTTB	4.49	5.88	3.71	3.35	2.49	4.46	0.96	6.31	8.70	
S. oedipus										
HHD		2.42	1.70	1.03	1.20	0.54	-0.10	1.07	3.33	2.37
OLCB	2.28		1.66	0.75	0.60	0.94	-1.11	0.78	3.81	2.22
CAPD	1.35	1.60		0.72	0.59	0.73	0.28	0.73	3.08	2.88
RHD	1.78	1.73	1.71		1.22	0.78	0.25	1.49	3.64	2.62
ULB	4.28	3.14	2.39	3.01		3.11	1.60	2.83	6.29	3.06
FHD	1.29	1.94	1.75	0.83	0.96		-0.55	1.06	3.60	1.96
TRCD	3.43	2.81	2.59	2.51	1.36	2.41		1.88	5.77	2.76
CNDC	3.79	3.47	2.54	2.85	1.63	3.06	1.33		5.07	2.69
PRXTB	0.04	1.05	1.09	-0.07	0.71	-0.42	-1.06	-1.40		1.20
DSTTB	1.74	1.71	2.30	1.46	0.68	0.04	-1.27	-0.73	2.46	

Appendix 7: Slopes and constants for all males and females continued.

Male Constants	HHD	OLCB	CAPD	RHD	ULB	FHD	TRCD	CNDC	PRXTB	DSTTB
C. pygerythrus										
HHD		0.51	0.26	-4.08	1.64	0.94	-3.66	-1.53	-2.35	2.16
OLCB	10.62		6.05	2.93	2.34	5.10	2.54	4.74	9.85	7.74
CAPD	6.98	4.63		-0.48	0.44	4.40	0.86	2.91	6.12	5.02
RHD	10.14	5.83	5.26		4.40	4.81	2.72	3.26	6.18	6.30
ULB	12.98	8.76	6.94	7.74		9.71	6.79	10.19	20.40	7.29
FHD	9.50	2.50	4.93	-0.85	2.32		-1.11	0.45	2.54	4.18
TRCD	11.21	6.97	6.45	4.22	3.86	6.41		7.10	12.79	5.97
CNDC	10.09	5.13	5.55	0.69	4.48	3.83	3.29		3.93	5.88
PRXTB	9.53	4.82	5.24	-0.50	5.58	3.33	2.19	0.67		5.49
DSTTB	10.09	8.89	5.80	3.37	1.56	5.05	0.79	5.12	9.83	
S. sciureus										
HHD		-2.42	1.29	2.35	-0.36	2.84	0.44	1.84	2.65	2.60
OLCB	6.58		3.74	3.79	1.78	6.39	3.95	5.50	9.04	4.83
CAPD	4.24	0.00		2.25	-0.94	4.80	3.40	2.98	5.04	2.47
RHD	4.79	-3.12	1.65		0.46	3.98	3.32	3.06	7.10	2.48
ULB	7.69	5.49	4.00	5.17		5.88	4.82	5.06	9.35	4.97
FHD	4.83	5.06	3.42	3.39	0.10		2.31	1.24	6.16	3.31
TRCD	6.18	3.27	4.17	4.85	1.53	5.14		4.43	7.63	4.45
CNDC	5.88	4.46	3.28	4.00	0.34	3.52	3.14		4.57	3.25
PRXTB	3.66	0.59	1.94	3.59	-0.93	3.67	1.06	0.07		2.53
DSTTB	5.58	2.96	2.30	2.94	0.54	4.33	3.02	2.40	5.88	
M. mulatta										
HHD		0.39	3.16	4.61	0.43	0.89	4.79	3.47	7.67	7.15
OLCB	7.35		4.39	4.99	0.90	4.77	7.51	7.70	14.33	8.45
CAPD	6.58	1.91		3.70	0.04	3.33	9.13	5.48	14.26	8.19
RHD	5.29	-2.16	1.16		-2.96	-0.65	4.40	4.68	9.67	6.60
ULB	13.73	11.72	8.33	9.04		11.62	8.82	11.58	20.99	10.57
FHD	5.85	2.87	4.00	4.22	0.98		4.57	5.12	9.46	7.19
TRCD	8.66	7.64	8.17	6.54	-1.08	4.28		9.00	15.61	8.28
CNDC	3.48	2.53	2.66	4.39	-0.44	0.39	6.20		3.63	6.06
PRXTB	2.81	1.18	4.04	3.97	-1.41	-1.35	4.90	0.40		6.00
DSTTB	2.12	-1.02	2.46	1.32	0.47	-3.84	2.28	-0.73	1.56	

Appendix 7: Slopes and constants for all males and females continued.

Male Constants	HHD	OLCB	CAPD	RHD	ULB	FHD	TRCD	CNDC	PRXTB	DSTTB
G. gorilla										
HHD		18.62	10.99	3.05	10.38	19.82	4.47	11.08	26.94	20.99
OLCB	31.35		23.05	15.68	20.11	36.94	29.47	23.27	50.01	22.63
CAPD	28.64	39.02		16.73	14.46	34.46	28.49	28.03	54.10	19.90
RHD	19.18	25.07	16.84		12.98	31.92	14.14	11.47	37.05	25.52
ULB	48.75	49.89	25.54	26.01		41.50	27.27	32.74	66.72	31.18
FHD	4.11	25.34	13.16	8.90	6.84		9.14	13.10	29.44	17.40
TRCD	36.26	47.54	26.92	20.68	15.97	38.46		29.96	59.22	33.33
CNDC	30.46	29.86	20.83	11.43	10.19	34.46	17.59		37.39	26.39
PRXTB	-0.45	10.10	11.02	-3.28	2.91	18.83	1.73	-12.48		18.33
DSTTB	40.11	33.08	16.74	24.54	23.33	34.95	41.23	35.26	59.92	
P. troglodytes										
HHD		20.21	4.75	4.15	5.89	14.34	18.71	13.41	18.61	12.67
OLCB	2.66		2.89	5.95	5.82	15.72	17.80	14.54	14.62	10.55
CAPD	15.00	24.79		7.17	13.52	20.55	21.37	21.96	33.63	11.53
RHD	12.42	26.13	5.76		8.88	16.25	16.15	15.01	25.08	12.49
ULB	32.45	34.61	19.29	20.23		27.95	16.89	22.68	45.47	25.23
FHD	5.33	22.71	5.73	1.48	1.90		12.68	12.67	15.96	10.51
TRCD	29.42	32.60	16.29	14.16	-2.24	23.40		22.20	38.26	23.30
CNDC	10.55	24.86	10.20	4.54	-6.12	16.61	14.35		14.07	15.17
PRXTB	-0.89	16.47	4.66	-0.63	-1.96	9.33	11.18	2.67		9.50
DSTTB	23.09	28.43	8.78	11.72	22.54	22.25	27.17	24.42	36.57	
H. sapiens										
HHD		25.41	9.42	8.79	12.48	10.56	13.74	13.46	32.77	9.08
OLCB	29.56		9.90	16.12	8.97	33.17	16.03	34.63	53.26	21.01
CAPD	25.46	22.29		7.40	10.92	28.47	24.95	34.33	57.68	22.95
RHD	18.04	27.51	3.51		13.15	23.67	23.29	21.43	43.11	17.90
ULB	28.44	14.88	8.56	15.35		36.00	18.90	31.62	52.30	25.88
FHD	-4.16	22.27	6.16	6.35	13.05		9.53	7.64	21.33	3.97
TRCD	20.03	19.23	14.91	16.55	11.91	24.42		25.68	48.29	16.01
CNDC	10.50	30.05	14.53	9.59	13.40	16.56	17.02		18.76	6.93
PRXTB	3.06	19.74	10.92	6.32	10.44	7.40	12.66	-5.52		2.38
DSTTB	20.79	30.79	16.57	15.96	16.94	24.51	20.69	20.25	42.37	

Appendix 7: Slopes and constants for all males and females continued.

Female Slopes	HHD	OLCB	CAPD	RHD	ULB	FHD	TRCD	CNDC	PRXTB	DSTTB
E. elegantulus										
HHD		0.782	0.92	0.858	0.073	0.834	0.547	0.549	1.048	0.103
OLCB	0.456		0.535	0.602	-0.074	0.634	0.518	0.326	0.761	-0.019
CAPD	0.754	0.753		0.753	0.04	0.827	0.482	0.426	0.863	0.068
RHD	0.732	0.882	0.784		0.024	0.782	0.452	0.454	0.972	0.068
ULB	0.624	-1.08	0.412	0.239		0.213	-0.194	0.423	0.061	-0.074
FHD	0.492	0.642	0.595	0.54	0.015		0.347	0.367	0.877	0.048
TRCD	0.62	1.009	0.667	0.6	-0.026	0.668		0.27	1.127	-0.22
CNDC	0.578	0.588	0.547	0.56	0.052	0.656	0.25		0.874	0.271
PRXTB	0.471	0.588	0.473	0.512	0.003	0.669	0.447	0.373		-0.063
DSTTB	0.173	-0.056	0.138	0.134	-0.015	0.138	-0.326	0.432	-0.234	
A. trivirgatus										
HHD		0.684	0.385	0.641	0.458	0.849	0.536	0.429	1.097	0.461
OLCB	0.641		0.288	0.534	0.287	0.519	0.326	0.279	0.72	0.223
CAPD	1.368	1.091		1.004	0.684	1.325	0.66	0.586	1.541	0.813
RHD	0.977	0.868	0.431		0.562	1.012	0.57	0.508	1.336	0.58
ULB	1.298	0.866	0.545	1.043		1.252	0.853	0.614	1.766	0.89
FHD	0.943	0.615	0.414	0.737	0.491		0.507	0.5	1.219	0.551
TRCD	0.91	0.59	0.315	0.634	0.511	0.774		0.484	1.052	0.478
CNDC	0.914	0.633	0.352	0.709	0.462	0.959	0.608		1.354	0.444
PRXTB	0.692	0.484	0.274	0.553	0.393	0.692	0.391	0.401		0.377
DSTTB	0.771	0.398	0.383	0.636	0.525	0.829	0.471	0.349	0.999	
S. oedipus										
HHD		0.517	0.315	0.35	0.328	0.83	0.388	-0.052	0.71	0.088
OLCB	0.532		0.299	0.491	0.445	0.455	0.532	0.318	0.796	0.314
CAPD	0.412	0.38		0.309	0.239	0.377	0.31	0.297	0.648	0.144
RHD	0.677	0.922	0.456		0.585	0.826	0.967	0.19	1.199	0.233
ULB	1.032	1.363	0.575	0.952		1.367	0.968	0.244	1.334	0.473
FHD	0.208	0.111	0.072	0.107	0.109		0.122	-0.003	0.256	0.083
TRCD	0.485	0.646	0.297	0.625	0.384	0.609		0.254	0.884	0.187
CNDC	-0.079	0.468	0.345	0.149	0.117	-0.017	0.308		0.613	0.276
PRXTB	0.497	0.541	0.347	0.434	0.296	0.715	0.495	0.283		0.289
DSTTB	0.274	0.946	0.342	0.373	0.465	1.023	0.462	0.564	1.278	

Appendix 7: Slopes and constants for all male and females continued.

Female Slopes	HHD	OLCB	CAPD	RHD	ULB	FHD	TRCD	CNDC	PRXTB	DSTTB
C. pygerythrus										
HHD		0.715	0.389	1.109	0.553	1.035	1.377	0.975	2.565	0.491
OLCB	0.088		0.083	0.19	0.086	0.161	0.164	0.071	0.342	0.047
CAPD	0.654	1.14		1.4	0.678	1.197	1.886	0.923	2.128	0.312
RHD	0.511	0.715	0.384		0.373	0.763	1.232	0.723	1.514	0.308
ULB	0.537	0.682	0.392	0.785		0.73	1.546	0.949	1.703	0.223
FHD	0.444	0.562	0.306	0.71	0.322		1.234	0.651	1.543	0.253
TRCD	0.229	0.222	0.187	0.444	0.265	0.478		0.382	0.828	0.155
CNDC	0.488	0.291	0.275	0.786	0.49	0.761	1.153		1.601	0.3
PRXTB	0.296	0.322	0.146	0.379	0.203	0.416	0.575	0.369		0.149
DSTTB	1.031	0.807	0.39	1.403	0.482	1.236	1.962	1.257	2.711	
S. sciureus										
HHD		0.424	0.343	0.485	0.433	0.704	-0.221	0.498	0.886	0.297
OLCB	0.408		0.199	0.52	0.255	0.504	-0.364	0.613	0.654	0.276
CAPD	0.825	0.499		0.538	0.563	0.981	-0.178	0.734	0.365	0.168
RHD	0.776	0.865	0.358		0.43	0.918	-0.386	0.86	1.054	0.414
ULB	0.84	0.515	0.454	0.522		0.595	0.214	0.646	0.819	0.019
FHD	0.68	0.507	0.394	0.554	0.296		-0.313	0.556	0.88	0.279
TRCD	-0.074	-0.126	-0.025	-0.08	0.037	-0.108		-0.067	-0.139	-0.076
CNDC	0.446	0.571	0.273	0.482	0.298	0.516	-0.179		0.741	0.209
PRXTB	0.508	0.39	0.087	0.378	0.242	0.523	-0.239	0.474		0.238
DSTTB	0.546	0.528	0.128	0.477	0.018	0.531	-0.418	0.428	0.764	
M. mulatta										
HHD		0.575	0.535	0.775	1.458	0.999	0.608	0.914	1.654	0.579
OLCB	0.185		0.268	0.177	0.423	0.383	0.463	0.359	0.741	0.07
CAPD	0.517	0.807		0.551	0.186	0.696	0.855	0.524	1.357	0.377
RHD	0.85	0.606	0.626		1.107	1.088	0.721	1.059	2.016	0.462
ULB	0.108	0.098	0.014	0.075		0.096	0.034	0.083	0.222	0.087
FHD	0.652	0.777	0.47	0.646	0.838		0.677	0.765	1.563	0.271
TRCD	0.331	0.784	0.482	0.358	0.248	0.565		0.455	1.012	0.162
CNDC	0.562	0.686	0.334	0.593	0.686	0.721	0.514		1.67	0.359
PRXTB	0.308	0.43	0.262	0.342	0.556	0.447	0.346	0.506		0.208
DSTTB	1.003	0.378	0.677	0.729	2.037	0.721	0.517	1.011	1.931	

Appendix 7: Slopes and constants for all males and females continued.

Female Slopes	HHD	OLCB	CAPD	RHD	ULB	FHD	TRCD	CNDC	PRXTB	DSTTB
G. gorilla										
HHD		1.053	0.445	0.554	0.5	0.766	0.499	0.829	1.685	0.368
OLCB	0.582		0.244	0.34	0.319	0.402	0.274	0.521	1.124	0.282
CAPD	0.92	0.912		0.62	0.506	0.597	0.515	0.827	1.759	0.555
RHD	1.262	1.402	0.684		0.709	1.152	0.633	1.323	2.692	0.526
ULB	1.045	1.206	0.511	0.649		0.92	0.774	0.908	2.059	0.521
FHD	0.729	0.691	0.275	0.481	0.419		0.52	0.883	1.63	0.298
TRCD	0.672	0.668	0.336	0.374	0.5	0.735		0.611	1.529	0.535
CNDC	0.543	0.617	0.262	0.38	0.285	0.608	0.297		1.54	0.255
PRXTB	0.378	0.456	0.191	0.265	0.221	0.384	0.255	0.528		0.22
DSTTB	0.511	0.709	0.373	0.32	0.347	0.435	0.552	0.54	1.362	
P. troglodytes										
HHD		0.895	0.737	0.342	-0.03	0.452	0.25	0.327	0.848	0.463
OLCB	0.562		0.195	0.188	0.111	0.35	0.407	0.287	0.585	0.319
CAPD	0.353	0.149		0.117	-0.154	0.136	-0.042	0.039	0.175	0.167
RHD	1.623	1.419	1.156		0.129	0.851	0.481	0.433	1.506	0.885
ULB	-0.075	0.443	-0.805	0.068		0.428	0.845	0.194	0.291	-0.088
FHD	0.852	1.051	0.535	0.338	0.322		0.803	0.437	1.107	0.43
TRCD	0.297	0.769	-0.104	0.12	0.401	0.506		0.51	0.556	0.145
CNDC	0.348	0.486	0.087	0.097	0.082	0.247	0.457		0.351	-0.005
PRXTB	0.725	0.796	0.312	0.271	0.1	0.502	0.4	0.282		0.362
DSTTB	0.878	0.963	0.662	0.353	-0.067	0.432	0.231	-0.009	0.801	
H. sapiens										
HHD		0.375	0.254	0.285	0.038	0.954	0.819	0.688	1.048	0.451
OLCB	0.256		0.162	0.117	0.2	0.33	0.364	0.3	0.519	0.161
CAPD	0.91	0.849		0.751	0.264	0.936	0.709	0.156	0.519	0.084
RHD	0.865	0.521	0.637		0.28	0.754	0.777	0.225	0.777	0.471
ULB	0.16	1.219	0.307	0.384		0.082	0.626	0.362	0.95	-0.187
FHD	0.714	0.361	0.196	0.186	0.015		0.584	0.564	0.796	0.44
TRCD	0.501	0.325	0.121	0.156	0.092	0.477		0.412	0.628	0.124
CNDC	0.486	0.31	0.031	0.052	0.061	0.532	0.476		1.364	0.493
PRXTB	0.323	0.235	0.045	0.079	0.07	0.328	0.317	0.596		0.291
DSTTB	0.389	0.203	0.02	0.134	-0.039	0.507	0.175	0.602	0.813	

Appendix 7: Slopes and constants for all males and females continued.

Female Constants	HHD	OLCB	CAPD	RHD	ULB	FHD	TRCD	CNDC	PRXTB	DSTTB
E. elegantulus										
HHD		2.40	-2.52	-1.59	0.73	0.20	0.72	0.75	1.67	2.86
OLCB	2.19		-1.25	-1.07	1.58	0.40	0.20	1.47	2.15	3.50
CAPD	3.46	4.76		1.15	1.02	2.66	2.46	2.63	5.14	3.23
RHD	3.06	3.94	-0.01		1.04	2.28	2.25	2.29	4.31	3.19
ULB	4.41	7.58	1.71	2.51		4.21	3.72	3.08	6.94	3.46
FHD	2.91	3.53	-0.48	0.38	1.04		1.96	1.92	3.11	3.17
TRCD	2.92	2.85	-0.17	0.67	1.20	2.11		2.60	3.06	4.15
CNDC	3.04	4.30	0.22	0.79	0.92	2.12	2.62		3.91	2.42
PRXTB	1.79	2.27	-1.15	-0.81	1.08	-0.24	0.37	0.93		3.82
DSTTB	4.51	6.58	1.70	2.32	1.15	3.98	4.61	2.09	7.80	
A. trivirgatus										
HHD		1.80	1.75	0.40	-1.25	0.13	0.93	3.24	2.88	2.47
OLCB	3.59		2.82	1.77	0.45	3.37	2.99	4.75	6.69	4.67
CAPD	1.59	2.11		0.78	-0.80	0.66	2.15	3.93	4.43	2.29
RHD	2.77	2.53	2.50		-0.64	1.42	2.15	3.91	4.38	2.99
ULB	5.04	5.30	3.57	3.07		4.01	3.22	5.25	7.51	4.03
FHD	1.56	3.09	1.98	0.43	-0.96		1.76	3.21	3.25	2.34
TRCD	3.47	4.35	3.28	2.35	-0.17	3.07		4.22	6.40	3.75
CNDC	2.18	3.23	2.59	0.94	-0.55	0.72	1.29		2.85	3.31
PRXTB	0.04	1.69	1.68	-0.90	-2.15	-1.11	0.71	1.99		1.79
DSTTB	3.54	5.04	2.57	1.77	-0.72	2.02	2.46	4.64	5.79	
S. oedipus										
HHD		2.31	1.56	2.37	0.31	0.27	1.96	5.20	4.29	3.84
OLCB	3.53		1.93	1.86	-0.08	3.12	1.48	3.05	4.41	2.63
CAPD	5.06	4.32		3.54	1.59	4.34	3.38	3.78	6.60	3.90
RHD	3.41	1.40	1.51		-0.27	1.86	0.00	3.97	3.36	3.34
ULB	4.03	2.35	2.22	2.32		2.35	2.13	4.26	5.67	3.26
FHD	5.38	5.07	3.22	4.05	1.84		3.81	4.87	7.49	3.95
TRCD	4.37	2.79	2.30	1.85	0.73	2.97		3.71	4.97	3.58
CNDC	6.95	3.43	1.96	3.94	1.89	5.80	3.01		5.97	3.08
PRXTB	2.11	0.86	0.53	0.78	-0.20	-0.69	0.08	2.32		1.84
DSTTB	5.35	1.52	2.12	3.02	0.40	1.19	2.47	2.36	3.30	

Appendix 7: Slopes and constants for all male and females continued.

Female Constants	HHD	OLCB	CAPD	RHD	ULB	FHD	TRCD	CNDC	PRXTB	DSTTB
C. pygerythrus										
HHD		2.45	3.08	-4.82	-0.82	-1.44	-8.10	-1.26	-11.80	2.63
OLCB	11.17		6.88	6.53	4.95	9.35	6.80	9.79	15.55	8.08
CAPD	7.04	2.23		-2.28	0.61	1.80	-6.10	3.38	2.75	6.17
RHD	7.73	4.94	4.49		2.68	4.54	-2.03	4.33	6.27	5.94
ULB	8.98	7.10	5.49	4.01		6.83	-0.50	4.98	9.30	7.29
FHD	7.20	4.86	4.40	0.74	2.32		-5.11	3.33	2.17	5.79
TRCD	10.17	9.21	6.20	4.81	3.62	7.01		7.28	12.22	7.26
CNDC	6.98	8.05	4.89	0.33	0.72	3.08	-3.57		2.41	5.43
PRXTB	6.41	4.89	4.97	1.30	1.98	3.09	-2.51	3.43		5.71
DSTTB	3.28	4.18	4.45	-3.43	1.76	0.51	-8.25	-0.23	-3.97	
S. sciureus										
HHD		2.34	2.02	1.74	-0.72	0.75	6.95	1.95	3.93	3.00
OLCB	5.72		3.64	2.66	1.31	3.52	7.27	2.44	7.31	3.81
CAPD	4.12	3.37		3.08	0.08	1.74	6.02	2.46	9.33	4.59
RHD	3.68	0.87	2.76		0.34	1.24	7.35	1.11	5.12	3.05
ULB	5.74	4.33	3.52	4.20		4.78	4.58	4.18	8.80	5.34
FHD	3.70	2.50	2.25	2.09	0.87		7.19	2.39	5.41	3.60
TRCD	8.45	6.41	4.91	6.07	2.58	6.99		6.31	11.79	5.79
CNDC	5.40	2.35	3.15	2.78	0.99	3.35	6.24		6.65	4.15
PRXTB	2.44	1.44	3.82	1.47	0.09	0.63	7.82	0.72		2.76
DSTTB	5.12	2.91	4.09	3.08	2.68	3.56	7.43	3.66	6.95	
M. mulatta										
HHD		5.93	1.78	-0.17	-14.09	-0.53	1.94	-0.06	-0.13	2.29
OLCB	12.18		5.84	8.77	1.45	8.76	4.26	8.33	13.71	9.88
CAPD	9.83	6.63		5.98	5.76	7.54	2.65	8.42	11.23	7.23
RHD	5.21	7.59	2.62		-4.99	1.97	2.78	1.51	1.58	5.66
ULB	14.03	13.72	9.61	10.77		13.58	10.70	12.89	22.74	10.23
FHD	5.53	3.35	3.00	2.09	-4.42		1.27	2.58	2.07	7.01
TRCD	11.22	5.87	4.44	7.41	4.84	8.11		8.53	13.34	9.11
CNDC	7.25	5.19	5.21	3.32	-1.71	4.55	4.02		1.85	6.04
PRXTB	7.32	3.97	3.32	2.97	-6.02	3.39	2.50	1.15		5.82
DSTTB	3.92	10.35	2.35	3.39	-14.62	6.45	5.33	2.50	3.39	

Appendix 7: Slopes and constants for all males and females continued.

Female Constants	HHD	OLCB	CAPD	RHD	ULB	FHD	TRCD	CNDC	PRXTB	DSTTB
G. gorilla										
HHD		-8.27	3.16	0.10	-3.29	3.41	8.92	-0.19	-12.79	6.71
OLCB	23.68		14.35	12.44	7.36	23.48	21.44	17.80	20.93	12.49
CAPD	25.93	20.44		11.69	8.55	25.96	20.45	19.70	25.66	10.85
RHD	14.60	5.13	6.34		1.93	9.58	16.10	4.41	-3.56	10.40
ULB	26.71	17.63	14.07	13.39		21.35	16.90	21.08	25.90	13.63
FHD	19.05	14.91	13.66	7.48	4.02		12.07	4.24	2.92	12.48
TRCD	26.44	20.89	13.70	14.65	4.52	16.34		19.94	18.55	6.85
CNDC	26.93	18.27	14.32	11.80	9.66	16.33	21.30		7.41	14.39
PRXTB	22.55	11.44	11.61	8.71	5.77	14.12	15.58	3.65		9.38
DSTTB	36.20	25.64	15.67	19.20	12.58	30.07	19.66	26.95	35.84	
P. troglodytes										
HHD		1.55	-7.33	10.56	18.52	15.24	16.84	18.40	22.75	4.56
OLCB	17.65		13.34	16.75	13.53	19.86	11.95	20.57	33.95	10.69
CAPD	30.17	31.92		20.96	20.51	29.35	26.99	29.80	50.85	18.47
RHD	-0.56	1.84	-6.79		14.41	12.24	14.94	20.49	19.26	1.21
ULB	38.59	27.21	34.17	22.13		24.64	11.45	27.21	49.29	23.38
FHD	9.97	1.21	3.00	12.46	7.08		0.40	16.56	18.87	8.05
TRCD	29.52	14.80	22.87	20.17	6.93	18.86		17.24	39.82	18.05
CNDC	26.64	20.05	17.49	20.34	14.89	24.53	12.17		43.64	22.00
PRXTB	-2.14	-8.36	3.20	8.56	12.00	4.80	4.38	15.27		2.18
DSTTB	18.11	13.88	5.70	15.59	18.87	22.65	21.10	30.79	36.86	
H. sapiens										
HHD		18.65	8.71	9.17	13.99	3.20	-2.46	12.00	24.17	9.02
OLCB	31.69		13.49	16.70	8.79	30.54	18.30	29.64	48.89	21.78
CAPD	23.07	17.66		6.42	10.54	23.91	17.14	36.80	56.58	25.62
RHD	22.47	23.00	5.81		9.76	26.09	14.52	35.11	50.38	17.48
ULB	37.84	14.80	14.18	14.69		40.39	20.84	34.13	51.66	30.11
FHD	10.57	18.70	10.80	12.90	14.93		6.25	16.26	33.26	8.85
TRCD	25.01	23.80	15.26	15.87	12.73	27.09		27.17	47.22	23.41
CNDC	20.99	21.43	17.73	18.57	13.10	20.51	11.66		12.17	7.59
PRXTB	18.84	18.16	15.98	15.40	10.87	19.86	9.51	0.14		7.85
DSTTB	29.75	28.24	18.41	17.02	16.60	27.87	25.82	23.38	44.30	

Appendix 8: All regression output can be found in the supplementary spreadsheet found on the CD-ROM at the back of the thesis.

Appendix 9: Regression plots of FHDxPRXTB for *Aotus trivirgatus, Chlorocebus pygerythrus, Macaca mulatta, Pan troglodytes, Gorilla gorilla, Homo sapiens.*

Appendix 9.1: Scatter graphs of *Aotus trivirgatus* FHDxPRXTB male and female values.

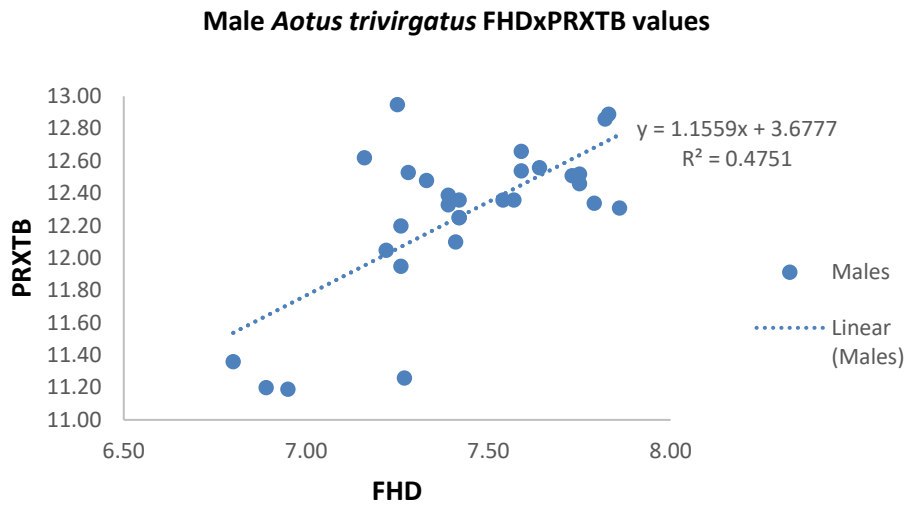

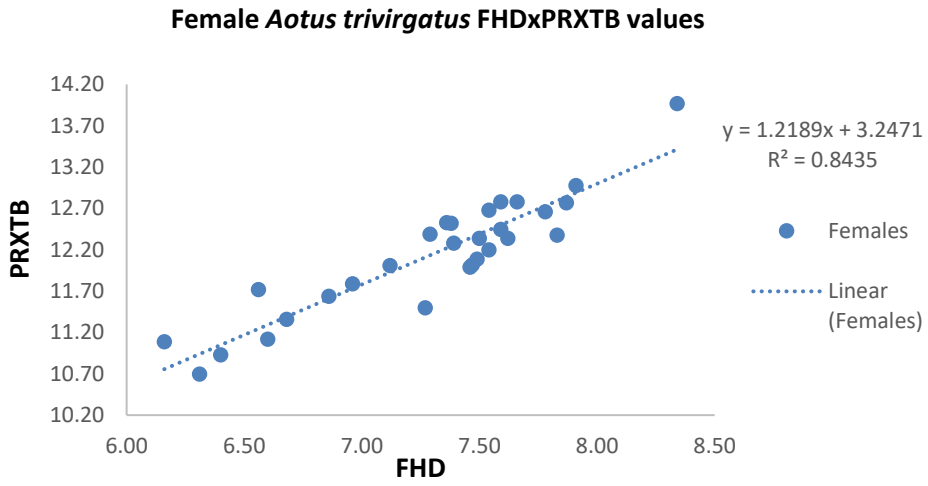

Appendix 9.2: Scatter graphs of *Chlorocebus trivirgatus* FHDxPRXTB male and female values.

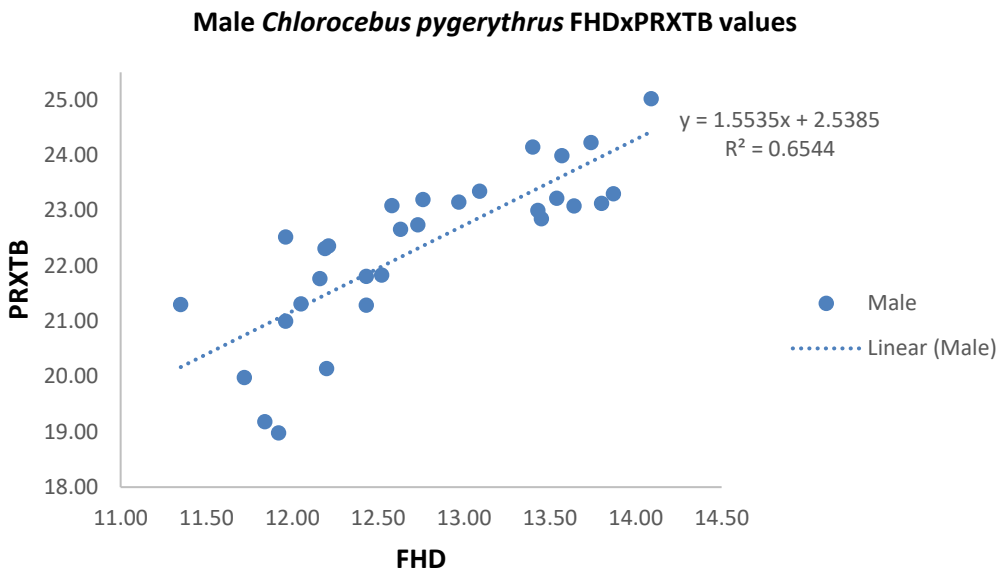

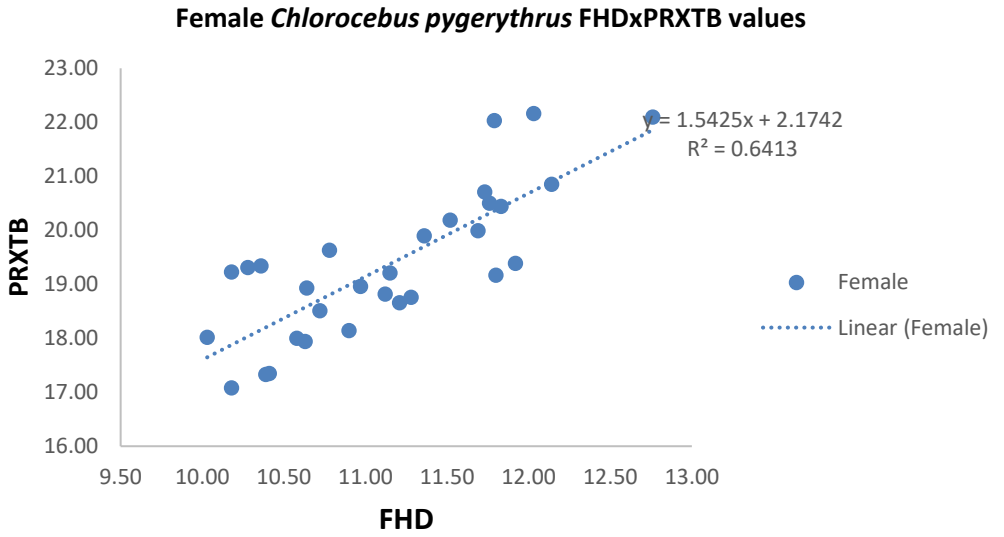

Appendix 9.3: Scatter graphs of *Macaca mulatta* FHDxPRXTB male and female values.

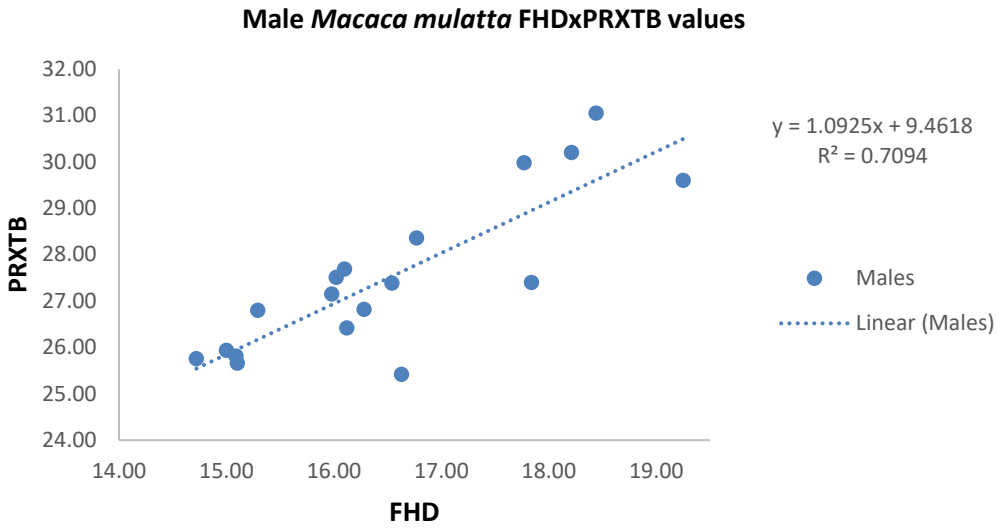

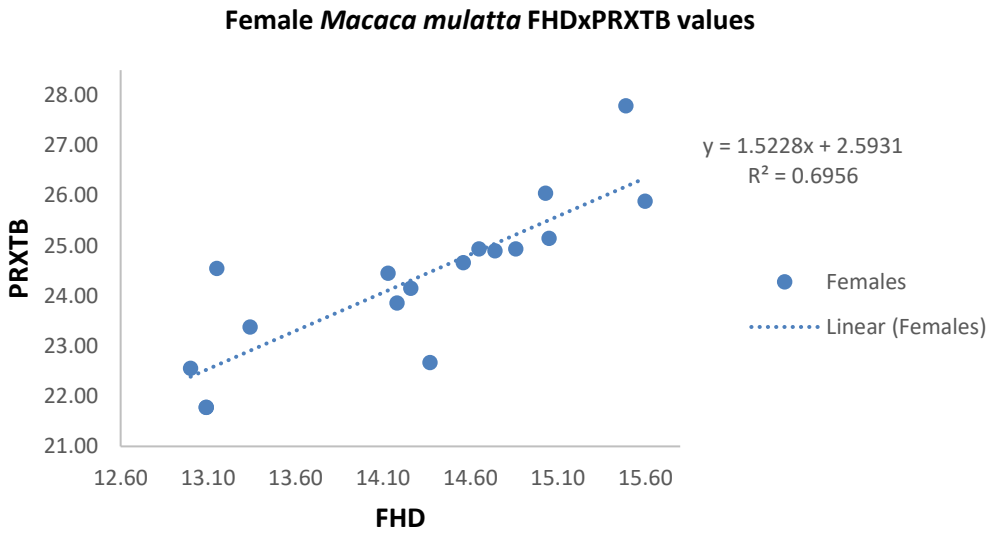

Appendix 9.4: Scatter graphs of *Pan troglodytes* FHDxPRXTB male and female values.

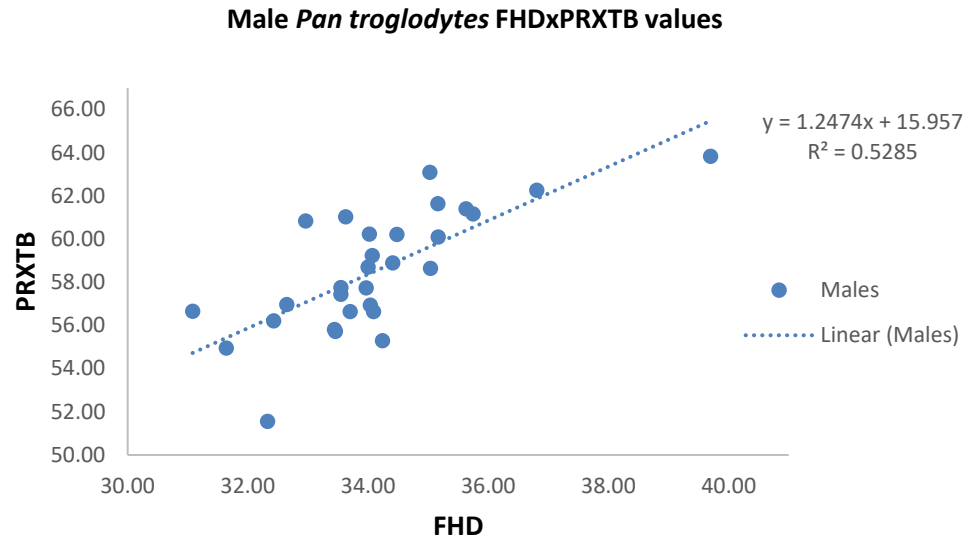

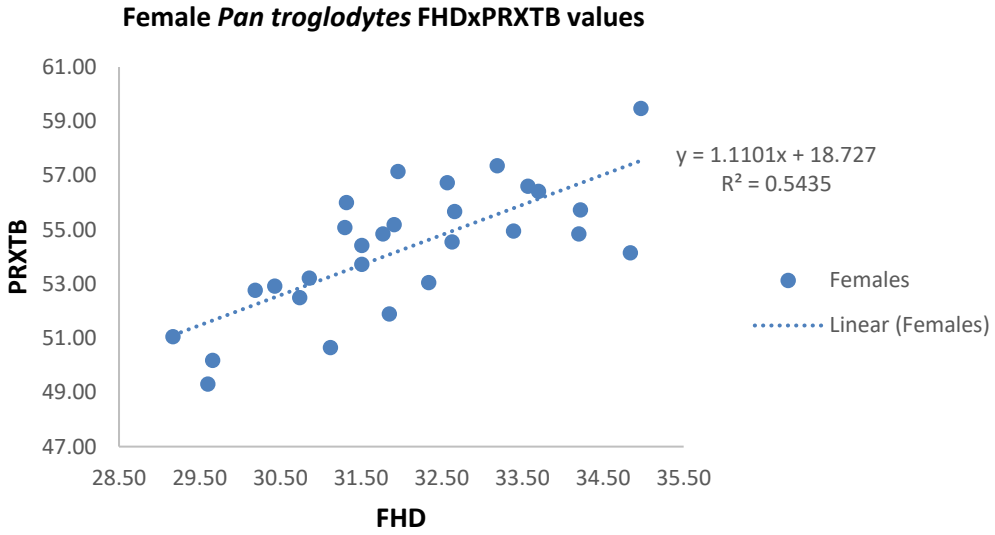

Appendix 9.5: Scatter graphs of *Gorilla gorilla* FHDxPRXTB male and female values.

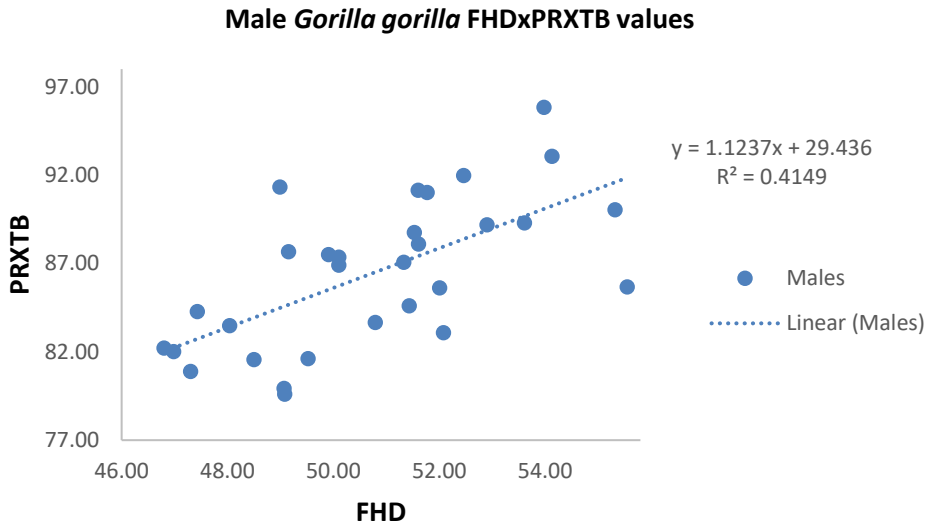

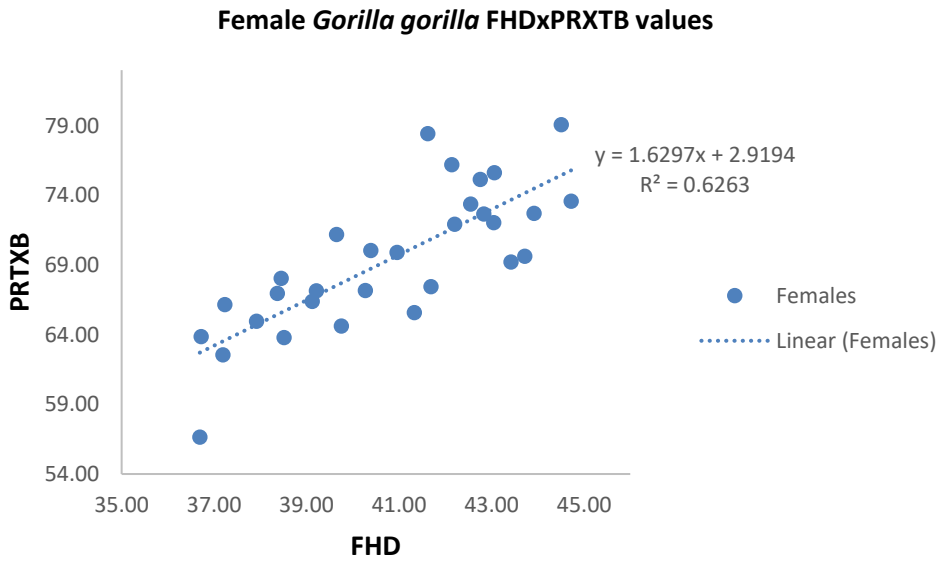

Appendix 9.6: Scatter graphs of *Homo sapiens* FHDxPRXTB male and female values.

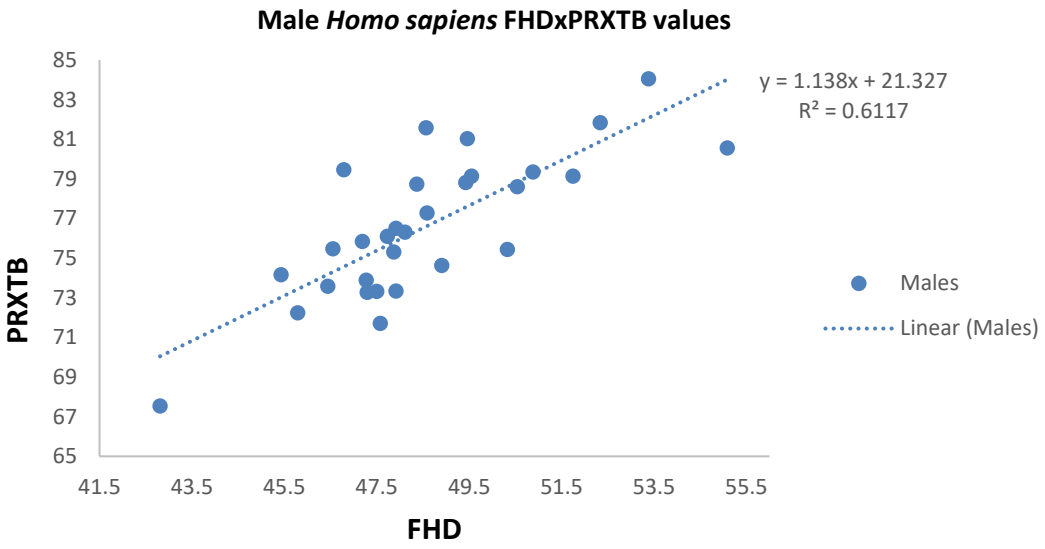

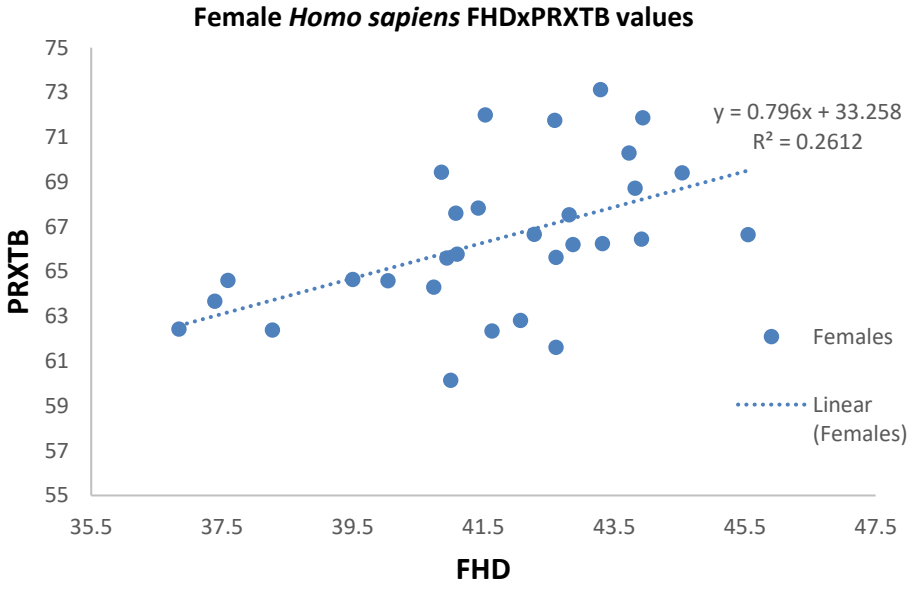

Appendix 10: Scatter graphs of *Euoticus elegantulus* FHDxDSTTB male values, male values without outlier and female values.

Male *Euoticus elegantulus* FHDxDSTTB values

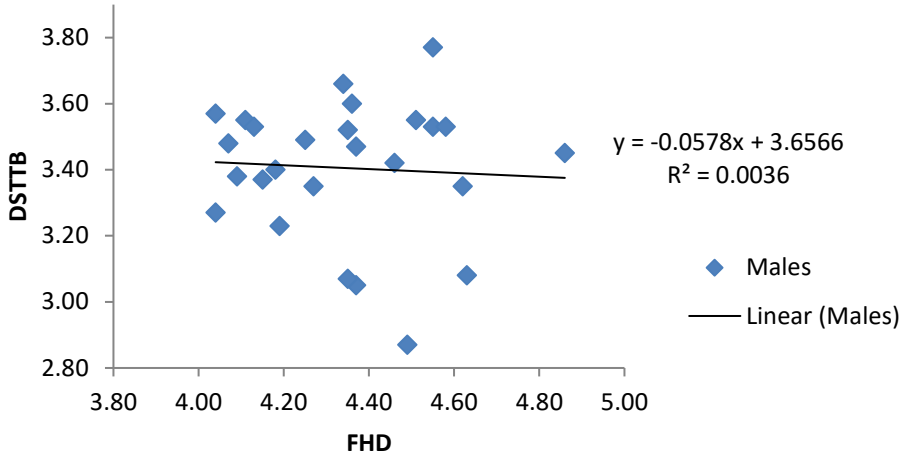

Male *Euoticus elegantulus* FHDxDSTTB values without outlier

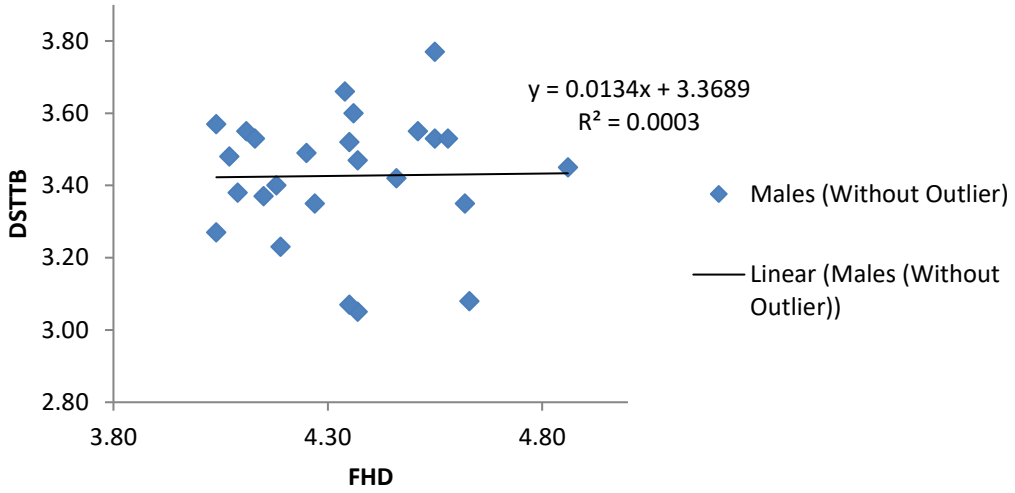

Appendix 10: Scatter graphs of *Euoticus elegantulus* FHDxDSTTB male values, male values without outlier and female values continued.

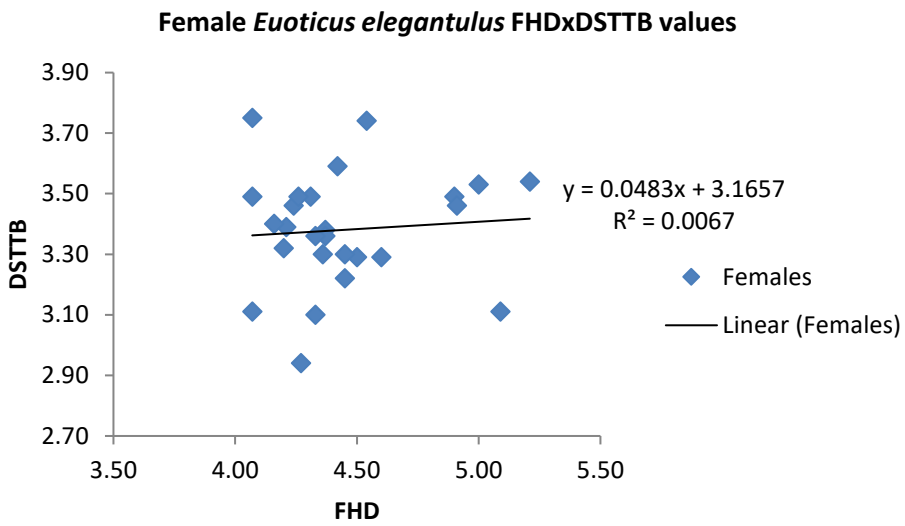

Appendix 11: Comparison scatter graph of male and female *Euoticus elegantulus* OLCBxULB values.

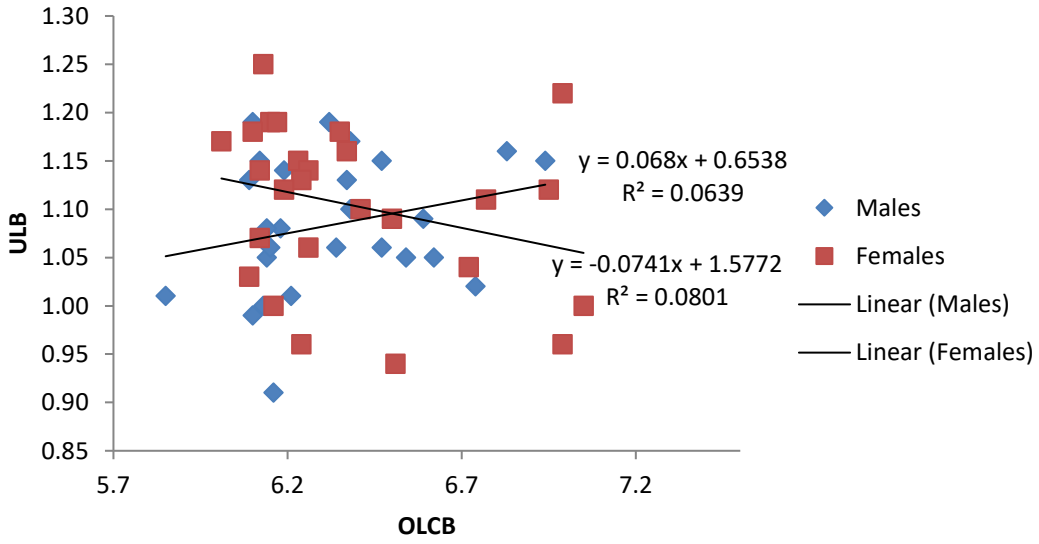

Appendix 12: ANCOVA output for all species.

E.elegantulus	n	F	df (between)	df (within)	Sig.
HHDxOLCB	52	1.223	1	49	0.27
HHDxCAPD	52	0.038	1	49	0.85
HHDxRHD	52	0.366	1	49	0.55
HHDxULB	52	0.897	1	49	0.35
HHDxFHD	52	3.557	1	49	0.07
HHDxTRCD	52	4.516	1	49	0.04
HHDxCNDC	52	0.001	1	49	0.98
HHDxPRXTB	52	0.000	1	49	0.98
HHDxDSTTB	52	0.156	1	49	0.69
OLCBxHHD	52	0.825	1	49	0.37
OLCBxCAPD	52	1.039	1	49	0.31
OLCBxRHD	52	0.044	1	49	0.83
OLCBxULB	52	0.934	1	49	0.34
OLCBxFHD	52	1.432	1	49	0.24
OLCBxTRCD	52	2.470	1	49	0.12
OLCBxCNDC	52	0.198	1	49	0.66
OLCBxPRXTB	52	0.713	1	49	0.40
OLCBxDSTTB	52	0.192	1	49	0.66
CAPDxHHD	52	0.016	1	49	0.90
CAPDxOLCB	52	1.416	1	49	0.24
CAPDxRHD	52	0.573	1	49	0.45
CAPDxULB	52	0.934	1	49	0.34
CAPDxFHD	52	3.991	1	49	0.05
CAPDxTRCD	52	4.516	1	49	0.04
CAPDxCNDC	52	0.000	1	49	0.99
CAPDxPRXTB	52	0.000	1	49	1.00
CAPDxDSTTB	52	0.233	1	49	0.63
RHDxHHD	52	0.434	1	49	0.51
RHDxOLCB	52	0.504	1	49	0.48
RHDxCAPD	52	0.663	1	49	0.42
RHDxULB	52	0.852	1	49	0.36
RHDxFHD	52	2.335	1	49	0.13
RHDxTRCD	52	3.222	1	49	0.08
RHDxCNDC	52	0.044	1	49	0.83
RHDxPRXTB	52	0.208	1	49	0.65
RHDxDSTTB	52	0.188	1	49	0.67

Significant
Not sig.

Appendix 12: ANCOVA output for all species continued.

E.elegantulus	n	F	df (between)	df (within)	Sig.
ULBxHHD	52	0.169	1	49	0.682
ULBxOLCB	52	0.600	1	49	0.442
ULBxCAPD	52	0.229	1	49	0.634
ULBxRHD	52	0.058	1	49	0.810
ULBxFHD	52	1.829	1	49	0.182
ULBxTRCD	52	2.562	1	49	0.116
ULBxCNDC	52	0.107	1	49	0.745
ULBxPRXTB	52	0.133	1	49	0.717
ULBxDSTTB	52	0.141	1	49	0.709
FHDxHHD	52	1.660	1	49	0.204
FHDxOLCB	52	0.001	1	49	0.981
FHDxCAPD	52	2.102	1	49	0.153
FHDxRHD	52	0.415	1	49	0.523
FHDxULB	52	0.720	1	49	0.400
FHDxTRCD	52	1.462	1	49	0.232
FHDxCNDC	52	0.343	1	49	0.561
FHDxPRXTB	52	1.948	1	49	0.169
FHDxDSTTB	52	0.214	1	49	0.645
TRCDxHHD	52	1.682	1	49	0.201
TRCDxOLCB	52	0.134	1	49	0.716
TRCDxCAPD	52	1.705	1	49	0.198
TRCDxRHD	52	0.389	1	49	0.536
TRCDxULB	52	0.554	1	49	0.460
TRCDxFHD	52	0.579	1	49	0.450
TRCDxCNDC	52	0.727	1	49	0.398
TRCDxPRXTB	52	3.340	1	49	0.074
TRCDxDSTTB	52	0.076	1	49	0.784
CNDCxHHD	52	0.108	1	49	0.744
CNDCxOLCB	52	0.699	1	49	0.407
CNDCxCAPD	52	0.130	1	49	0.720
CNDCxRHD	52	0.084	1	49	0.773
CNDCxULB	52	0.943	1	49	0.336
CNDCxFHD	52	2.303	1	49	0.136
CNDCxTRCD	52	3.623	1	49	0.063
CNDCxPRXTB	52	0.038	1	49	0.846
CNDCxDSTTB	52	0.182	1	49	0.672

Significant
Not sig.

Appendix 12: ANCOVA output for all species continued.

E.elegantulus	n	F	df (between)	df (within)	Sig.
PRXTBxHHD	52	0.070	1	49	0.792
PRXTBxOLCB	52	1.181	1	49	0.282
PRXTBxCAPD	52	0.092	1	49	0.763
PRXTBxRHD	52	0.211	1	49	0.648
PRXTBxULB	52	0.930	1	49	0.339
PRXTBxFHD	52	3.931	1	49	0.053
PRXTBxTRCD	52	6.346	1	49	0.015
PRXTBxCNDC	52	0.001	1	49	0.975
PRXTBxDSTTB	52	0.210	1	49	0.649
DSTTBxHHD	52	0.082	1	49	0.776
DSTTBxOLCB	52	0.511	1	49	0.478
DSTTBxCAPD	52	0.181	1	49	0.672
DSTTBxRHD	52	0.047	1	49	0.830
DSTTBxULB	52	0.793	1	49	0.378
DSTTBxFHD	52	1.980	1	49	0.166
DSTTBxTRCD	52	2.742	1	49	0.104
DSTTBxCNDC	52	0.000	1	49	0.983
DSTTBxPRXTB	52	0.066	1	49	0.798

Significant
Not sig.

Appendix 12: ANCOVA output for all species continued.

A.trivirgatus	n	F	df (between)	df (within)	Sig.
HHDxOLCB	58	0.091	1	55	0.765
HHDxCAPD	58	0.004	1	55	0.952
HHDxRHD	58	0.275	1	55	0.602
HHDxULB	58	0.193	1	55	0.662
HHDxFHD	58	2.193	1	55	0.144
HHDxTRCD	58	0.009	1	55	0.923
HHDxCNDC	58	0.160	1	55	0.691
HHDxPRXTB	58	0.549	1	55	0.462
HHDxDSTTB	58	1.459	1	55	0.232
OLCBxHHD	58	0.034	1	55	0.855
OLCBxCAPD	58	0.016	1	55	0.900
OLCBxRHD	58	0.146	1	55	0.704
OLCBxULB	58	0.237	1	55	0.628
OLCBxFHD	58	1.244	1	55	0.270
OLCBxTRCD	58	0.037	1	55	0.849
OLCBxCNDC	58	0.213	1	55	0.647
OLCBxPRXTB	58	0.400	1	55	0.530
OLCBxDSTTB	58	0.831	1	55	0.366
CAPDxHHD	58	0.117	1	55	0.733
CAPDxOLCB	58	0.187	1	55	0.667
CAPDxRHD	58	0.062	1	55	0.804
CAPDxULB	58	0.304	1	55	0.584
CAPDxFHD	58	1.796	1	55	0.186
CAPDxTRCD	58	0.077	1	55	0.782
CAPDxCNDC	58	0.226	1	55	0.636
CAPDxPRXTB	58	0.620	1	55	0.434
CAPDxDSTTB	58	1.020	1	55	0.317
RHDxHHD	58	0.523	1	55	0.473
RHDxOLCB	58	0.451	1	55	0.505
RHDxCAPD	58	0.195	1	55	0.660
RHDxULB	58	0.675	1	55	0.415
RHDxFHD	58	5.145	1	55	0.027
RHDxTRCD	58	0.172	1	55	0.680
RHDxCNDC	58	0.422	1	55	0.519
RHDxPRXTB	58	2.365	1	55	0.130
RHDxDSTTB	58	0.784	1	55	0.380

Significant
Not sig.

Appendix 12: ANCOVA output for all species continued.

A.trivirgatus	n	F	df (between)	df (within)	Sig.
ULBxHHD	58	0.091	1	55	0.765
ULBxOLCB	58	0.110	1	55	0.741
ULBxCAPD	58	0.006	1	55	0.938
ULBxRHD	58	0.242	1	55	0.625
ULBxFHD	58	1.157	1	55	0.287
ULBxTRCD	58	0.000	1	55	0.991
ULBxCNDC	58	0.126	1	55	0.724
ULBxPRXTB	58	0.274	1	55	0.603
ULBxDSTTB	58	1.343	1	55	0.252
FHDxHHD	58	0.876	1	55	0.353
FHDxOLCB	58	0.006	1	55	0.937
FHDxCAPD	58	0.375	1	55	0.543
FHDxRHD	58	3.499	1	55	0.067
FHDxULB	58	0.048	1	55	0.828
FHDxTRCD	58	0.114	1	55	0.737
FHDxCNDC	58	0.025	1	55	0.876
FHDxPRXTB	58	0.186	1	55	0.668
FHDxDSTTB	58	3.629	1	55	0.062
TRCDxHHD	58	0.112	1	55	0.739
TRCDxOLCB	58	0.197	1	55	0.659
TRCDxCAPD	58	0.066	1	55	0.798
TRCDxRHD	58	0.028	1	55	0.868
TRCDxULB	58	0.287	1	55	0.595
TRCDxFHD	58	1.518	1	55	0.223
TRCDxCNDC	58	0.255	1	55	0.615
TRCDxPRXTB	58	0.552	1	55	0.461
TRCDxDSTTB	58	1.038	1	55	0.313
CNDCxHHD	58	0.058	1	55	0.811
CNDCxOLCB	58	0.168	1	55	0.684
CNDCxCAPD	58	0.010	1	55	0.919
CNDCxRHD	58	0.073	1	55	0.788
CNDCxULB	58	0.208	1	55	0.650
CNDCxFHD	58	1.217	1	55	0.275
CNDCxTRCD	58	0.050	1	55	0.823
CNDCxPRXTB	58	0.357	1	55	0.553
CNDCxDSTTB	58	0.904	1	55	0.346

Significant
Not sig.

Appendix 12: ANCOVA output for all species continued.

A.trivirgatus	n	F	df (between)	df (within)	Sig.
PRXTBxHHD	58	0.091	1	55	0.765
PRXTBxOLCB	58	0.012	1	55	0.912
PRXTBxCAPD	58	0.060	1	55	0.807
PRXTBxRHD	58	1.651	1	55	0.204
PRXTBxULB	58	0.013	1	55	0.909
PRXTBxFHD	58	1.033	1	55	0.314
PRXTBxTRCD	58	0.003	1	55	0.953
PRXTBxCNDC	58	0.014	1	55	0.905
PRXTBxDSTTB	58	1.911	1	55	0.172
DSTTBxHHD	58	1.157	1	55	0.287
DSTTBxOLCB	58	0.590	1	55	0.446
DSTTBxCAPD	58	0.605	1	55	0.440
DSTTBxRHD	58	0.238	1	55	0.627
DSTTBxULB	58	1.228	1	55	0.273
DSTTBxFHD	58	4.689	1	55	0.035
DSTTBxTRCD	58	0.634	1	55	0.429
DSTTBxCNDC	58	0.708	1	55	0.404
DSTTBxPRXTB	58	2.065	1	55	0.156

Significant
Not sig.

Appendix 12: ANCOVA output for all species continued.

S.oedipus	n	F	df (between)	df (within)	Sig.
HHDxOLCB	55	4.222	1	52	0.045
HHDxCAPD	55	1.007	1	52	0.320
HHDxRHD	55	3.206	1	52	0.079
HHDxULB	55	0.651	1	52	0.423
HHDxFHD	55	0.162	1	52	0.689
HHDxTRCD	55	0.093	1	52	0.761
HHDxCNDC	55	0.353	1	52	0.555
HHDxPRXTB	55	3.197	1	52	0.080
HHDxDSTTB	55	0.105	1	52	0.747
OLCBxHHD	55	3.596	1	52	0.063
OLCBxCAPD	55	0.000	1	52	0.998
OLCBxRHD	55	0.000	1	52	0.986
OLCBxULB	55	7.571	1	52	0.008
OLCBxFHD	55	2.828	1	52	0.099
OLCBxTRCD	55	2.167	1	52	0.147
OLCBxCNDC	55	2.485	1	52	0.121
OLCBxPRXTB	55	0.022	1	52	0.882
OLCBxDSTTB	55	0.707	1	52	0.404
CAPDxHHD	55	1.575	1	52	0.215
CAPDxOLCB	55	1.150	1	52	0.289
CAPDxRHD	55	0.466	1	52	0.498
CAPDxULB	55	2.203	1	52	0.144
CAPDxFHD	55	0.756	1	52	0.389
CAPDxTRCD	55	0.228	1	52	0.635
CAPDxCNDC	55	1.180	1	52	0.282
CAPDxPRXTB	55	0.254	1	52	0.617
CAPDxDSTTB	55	0.026	1	52	0.874
RHDxHHD	55	3.318	1	52	0.074
RHDxOLCB	55	0.693	1	52	0.409
RHDxCAPD	55	0.015	1	52	0.903
RHDxULB	55	4.117	1	52	0.048
RHDxFHD	55	3.195	1	52	0.080
RHDxTRCD	55	1.507	1	52	0.225
RHDxCNDC	55	1.503	1	52	0.226
RHDxPRXTB	55	0.009	1	52	0.926
RHDxDSTTB	55	0.165	1	52	0.686

Appendix 12: ANCOVA output for all species continued.

S.oedipus	n	F	df (between)	df (within)	Sig.
ULBxHHD	55	0.132	1	52.000	0.718
ULBxOLCB	55	7.649	1	52.000	0.008
ULBxCAPD	55	1.099	1	52.000	0.299
ULBxRHD	55	3.452	1	52.000	0.069
ULBxFHD	55	0.157	1	52.000	0.694
ULBxTRCD	55	0.208	1	52.000	0.650
ULBxCNDC	55	0.299	1	52.000	0.587
ULBxPRXTB	55	2.478	1	52.000	0.122
ULBxDSTTB	55	0.329	1	52.000	0.569
FHDxHHD	55	0.788	1	52.000	0.379
FHDxOLCB	55	4.111	1	52.000	0.048
FHDxCAPD	55	0.822	1	52.000	0.369
FHDxRHD	55	3.744	1	52.000	0.058
FHDxULB	55	1.308	1	52.000	0.258
FHDxTRCD	55	0.009	1	52.000	0.924
FHDxCNDC	55	0.530	1	52.000	0.470
FHDxPRXTB	55	2.567	1	52.000	0.115
FHDxDSTTB	55	0.088	1	52.000	0.768
TRCDxHHD	55	0.822	1	52.000	0.369
TRCDxOLCB	55	3.543	1	52.000	0.065
TRCDxCAPD	55	0.397	1	52.000	0.532
TRCDxRHD	55	2.146	1	52.000	0.149
TRCDxULB	55	1.465	1	52.000	0.232
TRCDxFHD	55	0.111	1	52.000	0.740
TRCDxCNDC	55	0.658	1	52.000	0.421
TRCDxPRXTB	55	1.364	1	52.000	0.248
TRCDxDSTTB	55	0.017	1	52.000	0.895
CNDCxHHD	55	0.451	1	52.000	0.505
CNDCxOLCB	55	3.202	1	52.000	0.079
CNDCxCAPD	55	0.715	1	52.000	0.402
CNDCxRHD	55	1.494	1	52.000	0.227
CNDCxULB	55	0.919	1	52.000	0.342
CNDCxFHD	55	0.005	1	52.000	0.947
CNDCxTRCD	55	0.029	1	52.000	0.865
CNDCxPRXTB	55	2.203	1	52.000	0.144
CNDCxDSTTB	55	0.269	1	52.000	0.606

Appendix 12: ANCOVA output for all species continued.

S.oedipus	n	F	df (between)	df (within)	Sig.
PRXTBxHHD	55	3.540	1	52	0.066
PRXTBxOLCB	55	0.935	1	52	0.338
PRXTBxCAPD	55	0.020	1	52	0.887
PRXTBxRHD	55	0.225	1	52	0.637
PRXTBxULB	55	3.362	1	52	0.072
PRXTBxFHD	55	2.255	1	52	0.139
PRXTBxTRCD	55	0.955	1	52	0.333
PRXTBxCNDC	55	2.437	1	52	0.125
PRXTBxDSTTB	55	0.410	1	52	0.525
DSTTBxHHD	55	0.907	1	52	0.345
DSTTBxOLCB	55	2.122	1	52	0.151
DSTTBxCAPD	55	0.266	1	52	0.608
DSTTBxRHD	55	0.860	1	52	0.358
DSTTBxULB	55	1.663	1	52	0.203
DSTTBxFHD	55	0.263	1	52	0.610
DSTTBxTRCD	55	0.090	1	52	0.766
DSTTBxCNDC	55	0.974	1	52	0.328
DSTTBxPRXTB	55	0.888	1	52	0.350

Significant
Not sig.

Appendix 12: ANCOVA output for all species continued.

S.sciureus	n	F	df (between)	df (within)	Sig.
HHDxOLCB	59	36.031	1	56	0.000
HHDxCAPD	59	2.242	1	56	0.140
HHDxRHD	59	0.099	1	56	0.754
HHDxULB	59	0.035	1	56	0.851
HHDxFHD	59	0.275	1	56	0.602
HHDxTRCD	59	8.052	1	56	0.006
HHDxCNDC	59	2.242	1	56	0.140
HHDxPRXTB	59	0.064	1	56	0.802
HHDxDSTTB	59	4.526	1	56	0.038
OLCBxHHD	59	4.017	1	56	0.050
OLCBxCAPD	59	1.130	1	56	0.292
OLCBxRHD	59	5.921	1	56	0.018
OLCBxULB	59	0.001	1	56	0.981
OLCBxFHD	59	2.666	1	56	0.108
OLCBxTRCD	59	5.471	1	56	0.023
OLCBxCNDC	59	1.389	1	56	0.244
OLCBxPRXTB	59	0.196	1	56	0.660
OLCBxDSTTB	59	2.409	1	56	0.126
CAPDxHHD	59	26.706	1	56	0.000
CAPDxOLCB	59	68.403	1	56	0.000
CAPDxRHD	59	1.080	1	56	0.303
CAPDxULB	59	0.213	1	56	0.646
CAPDxFHD	59	6.814	1	56	0.012
CAPDxTRCD	59	21.028	1	56	0.000
CAPDxCNDC	59	8.966	1	56	0.004
CAPDxPRXTB	59	10.137	1	56	0.002
CAPDxDSTTB	59	13.024	1	56	0.001
RHDxHHD	59	60.587	1	56	0.000
RHDxOLCB	59	141.327	1	56	0.000
RHDxCAPD	59	27.534	1	56	0.000
RHDxULB	59	6.250	1	56	0.015
RHDxFHD	59	16.080	1	56	0.000
RHDxTRCD	59	42.223	1	56	0.000
RHDxCNDC	59	20.373	1	56	0.000
RHDxPRXTB	59	20.326	1	56	0.000
RHDxDSTTB	59	23.684	1	56	0.000

Appendix 12: ANCOVA output for all species continued.

S.sciureus	n	F	df (between)	df (within)	Sig.
ULBxHHD	59	74.887	1	56	0.000
ULBxOLCB	59	144.578	1	56	0.000
ULBxCAPD	59	36.462	1	56	0.000
ULBxRHD	59	13.965	1	56	0.000
ULBxFHD	59	26.344	1	56	0.000
ULBxTRCD	59	38.342	1	56	0.000
ULBxCNDC	59	29.156	1	56	0.000
ULBxPRXTB	59	27.246	1	56	0.000
ULBxDSTTB	59	38.779	1	56	0.000
FHDxHHD	59	38.209	1	56	0.000
FHDxOLCB	59	94.598	1	56	0.000
FHDxCAPD	59	18.050	1	56	0.000
FHDxRHD	59	2.062	1	56	0.157
FHDxULB	59	3.016	1	56	0.088
FHDxTRCD	59	24.883	1	56	0.000
FHDxCNDC	59	9.643	1	56	0.003
FHDxPRXTB	59	10.165	1	56	0.002
FHDxDSTTB	59	17.568	1	56	0.000
TRCDxHHD	59	41.750	1	56	0.000
TRCDxOLCB	59	87.849	1	56	0.000
TRCDxCAPD	59	26.779	1	56	0.000
TRCDxRHD	59	16.128	1	56	0.000
TRCDxULB	59	5.639	1	56	0.021
TRCDxFHD	59	17.733	1	56	0.000
TRCDxCNDC	59	26.044	1	56	0.000
TRCDxPRXTB	59	15.884	1	56	0.000
TRCDxDSTTB	59	24.606	1	56	0.000
CNDCxHHD	59	36.294	1	56	0.000
CNDCxOLCB	59	83.449	1	56	0.000
CNDCxCAPD	59	16.495	1	56	0.000
CNDCxRHD	59	2.234	1	56	0.141
CNDCxULB	59	1.772	1	56	0.189
CNDCxFHD	59	6.137	1	56	0.016
CNDCxTRCD	59	29.192	1	56	0.000
CNDCxPRXTB	59	5.087	1	56	0.028
CNDCxDSTTB	59	14.176	1	56	0.000

Appendix 12: ANCOVA output for all species continued.

S.sciureus	n	F	df (between)	df (within)	Sig.
PRXTBxHHD	59	33.846	1	56	0.000
PRXTBxOLCB	59	82.095	1	56	0.000
PRXTBxCAPD	59	18.637	1	56	0.000
PRXTBxRHD	59	2.856	1	56	0.097
PRXTBxULB	59	1.114	1	56	0.296
PRXTBxFHD	59	7.339	1	56	0.009
PRXTBxTRCD	59	19.486	1	56	0.000
PRXTBxCNDC	59	5.778	1	56	0.020
PRXTBxDSTTB	59	12.959	1	56	0.001
DSTTBxHHD	59	36.516	1	56	0.000
DSTTBxOLCB	59	80.904	1	56	0.000
DSTTBxCAPD	59	18.297	1	56	0.000
DSTTBxRHD	59	2.608	1	56	0.112
DSTTBxULB	59	6.023	1	56	0.017
DSTTBxFHD	59	11.173	1	56	0.001
DSTTBxTRCD	59	24.735	1	56	0.000
DSTTBxCNDC	59	11.691	1	56	0.001
DSTTBxPRXTB	59	9.774	1	56	0.003

Significant

Not sig.

Appendix 12: ANCOVA output for all species continued.

C.pygerythrus	n	F	df (between)	df (within)	Sig.
HHDxOLCB	60	0.016	1	55	0.901
HHDxCAPD	60	0.076	1	55	0.784
HHDxRHD	60	7.206	1	55	0.009
HHDxULB	60	0.027	1	55	0.870
HHDxFHD	60	1.556	1	55	0.217
HHDxTRCD	60	1.595	1	55	0.212
HHDxCNDC	60	1.120	1	55	0.294
HHDxPRXTB	60	7.708	1	55	0.007
HHDxDSTTB	60	0.304	1	55	0.583
OLCBxHHD	60	175.752	1	55	0.000
OLCBxCAPD	60	64.861	1	55	0.000
OLCBxRHD	60	17.036	1	55	0.000
OLCBxULB	60	18.348	1	55	0.000
OLCBxFHD	60	25.839	1	55	0.000
OLCBxTRCD	60	18.225	1	55	0.000
OLCBxCNDC	60	34.065	1	55	0.000
OLCBxPRXTB	60	23.898	1	55	0.000
OLCBxDSTTB	60	61.030	1	55	0.000
CAPDxHHD	60	53.865	1	55	0.000
CAPDxOLCB	60	0.984	1	55	0.325
CAPDxRHD	60	0.254	1	55	0.616
CAPDxULB	60	0.802	1	55	0.374
CAPDxFHD	60	1.403	1	55	0.241
CAPDxTRCD	60	0.245	1	55	0.623
CAPDxCNDC	60	3.270	1	55	0.076
CAPDxPRXTB	60	1.215	1	55	0.275
CAPDxDSTTB	60	14.007	1	55	0.000
RHDxHHD	60	159.065	1	55	0.000
RHDxOLCB	60	4.031	1	55	0.049
RHDxCAPD	60	42.191	1	55	0.000
RHDxULB	60	10.828	1	55	0.002
RHDxFHD	60	9.306	1	55	0.003
RHDxTRCD	60	3.847	1	55	0.055
RHDxCNDC	60	13.520	1	55	0.001
RHDxPRXTB	60	6.815	1	55	0.012
RHDxDSTTB	60	34.851	1	55	0.000

Appendix 12: ANCOVA output for all species continued.

C.pygerythrus	n	F	df (between)	df (within)	Sig.
ULBxHHD	60	143.065	1	55	0.000
ULBxOLCB	60	7.753	1	55	0.007
ULBxCAPD	60	47.397	1	55	0.000
ULBxRHD	60	13.712	1	55	0.000
ULBxFHD	60	19.126	1	55	0.000
ULBxTRCD	60	9.233	1	55	0.004
ULBxCNDC	60	24.216	1	55	0.000
ULBxPRXTB	60	21.101	1	55	0.000
ULBxDSTTB	60	40.999	1	55	0.000
FHDxHHD	60	114.453	1	55	0.000
FHDxOLCB	60	2.417	1	55	0.126
FHDxCAPD	60	31.036	1	55	0.000
FHDxRHD	60	0.692	1	55	0.409
FHDxULB	60	6.535	1	55	0.013
FHDxTRCD	60	0.581	1	55	0.449
FHDxCNDC	60	6.827	1	55	0.011
FHDxPRXTB	60	2.311	1	55	0.134
FHDxDSTTB	60	24.830	1	55	0.000
TRCDxHHD	60	148.339	1	55	0.000
TRCDxOLCB	60	7.577	1	55	0.008
TRCDxCAPD	60	46.277	1	55	0.000
TRCDxRHD	60	6.364	1	55	0.014
TRCDxULB	60	9.161	1	55	0.004
TRCDxFHD	60	11.916	1	55	0.001
TRCDxCNDC	60	19.072	1	55	0.000
TRCDxPRXTB	60	11.910	1	55	0.001
TRCDxDSTTB	60	37.841	1	55	0.000
CNDCxHHD	60	101.230	1	55	0.000
CNDCxOLCB	60	3.732	1	55	0.058
CNDCxCAPD	60	27.474	1	55	0.000
CNDCxRHD	60	0.052	1	55	0.821
CNDCxULB	60	6.026	1	55	0.017
CNDCxFHD	60	2.346	1	55	0.131
CNDCxTRCD	60	2.098	1	55	0.153
CNDCxPRXTB	60	0.600	1	55	0.442
CNDCxDSTTB	60	22.128	1	55	0.000

Appendix 12: ANCOVA output for all species continued.

C.pygerythrus	n	F	df (between)	df (within)	Sig.
PRXTBxHHD	60	139.869	1	55	0.000
PRXTBxOLCB	60	3.292	1	55	0.075
PRXTBxCAPD	60	34.182	1	55	0.000
PRXTBxRHD	60	0.694	1	55	0.408
PRXTBxULB	60	10.731	1	55	0.002
PRXTBxFHD	60	4.629	1	55	0.036
PRXTBxTRCD	60	2.825	1	55	0.098
PRXTBxCNDC	60	7.369	1	55	0.009
PRXTBxDSTTB	60	28.059	1	55	0.000
DSTTBxHHD	60	64.931	1	55	0.000
DSTTBxOLCB	60	4.520	1	55	0.038
DSTTBxCAPD	60	20.783	1	55	0.000
DSTTBxRHD	60	1.077	1	55	0.304
DSTTBxULB	60	2.437	1	55	0.124
DSTTBxFHD	60	2.465	1	55	0.122
DSTTBxTRCD	60	0.585	1	55	0.448
DSTTBxCNDC	60	4.843	1	55	0.032
DSTTBxPRXTB	60	2.488	1	55	0.120

Significant

Not sig.

Appendix 12: ANCOVA output for all species continued.

M.macaca	n	F	df (between)	df (within)	Sig.
HHDxOLCB	35	2.604	1.000	32	0.116
HHDxCAPD	35	0.543	1.000	32	0.467
HHDxRHD	35	0.180	1.000	32	0.674
HHDxULB	35	0.000	1.000	32	0.983
HHDxFHD	35	0.894	1.000	32	0.351
HHDxTRCD	35	2.043	1.000	32	0.163
HHDxCNDC	35	0.853	1.000	32	0.363
HHDxPRXTB	35	0.324	1.000	32	0.573
HHDxDSTTB	35	0.062	1.000	32	0.805
OLCBxHHD	35	8.721	1.000	32	0.006
OLCBxCAPD	35	1.455	1.000	32	0.236
OLCBxRHD	35	0.263	1.000	32	0.612
OLCBxULB	35	0.201	1.000	32	0.657
OLCBxFHD	35	0.181	1.000	32	0.673
OLCBxTRCD	35	3.329	1.000	32	0.077
OLCBxCNDC	35	0.390	1.000	32	0.537
OLCBxPRXTB	35	0.436	1.000	32	0.514
OLCBxDSTTB	35	1.952	1.000	32	0.172
CAPDxHHD	35	15.126	1.000	32	0.000
CAPDxOLCB	35	9.170	1.000	32	0.005
CAPDxRHD	35	0.713	1.000	32	0.405
CAPDxULB	35	0.967	1.000	32	0.333
CAPDxFHD	35	1.803	1.000	32	0.189
CAPDxTRCD	35	8.130	1.000	32	0.008
CAPDxCNDC	35	1.597	1.000	32	0.215
CAPDxPRXTB	35	2.199	1.000	32	0.148
CAPDxDSTTB	35	1.684	1.000	32	0.204
RHDxHHD	35	22.822	1.000	32	0.000
RHDxOLCB	35	14.707	1.000	32	0.001
RHDxCAPD	35	6.484	1.000	32	0.016
RHDxULB	35	0.758	1.000	32	0.391
RHDxFHD	35	2.550	1.000	32	0.120
RHDxTRCD	35	10.122	1.000	32	0.003
RHDxCNDC	35	1.969	1.000	32	0.170
RHDxPRXTB	35	2.735	1.000	32	0.108
RHDxDSTTB	35	2.310	1.000	32	0.138

Significant
Not sig.

Appendix 12: ANCOVA output for all species continued.

M.macaca	n	F	df (between)	df (within)	Sig.
ULBxHHD	35	34.802	1	32	0.000
ULBxOLCB	35	25.124	1	32	0.000
ULBxCAPD	35	15.524	1	32	0.000
ULBxRHD	35	8.140	1	32	0.008
ULBxFHD	35	11.232	1	32	0.002
ULBxTRCD	35	16.793	1	32	0.000
ULBxCNDC	35	8.825	1	32	0.006
ULBxPRXTB	35	10.591	1	32	0.003
ULBxDSTTB	35	9.294	1	32	0.005
FHDxHHD	35	21.087	1	32	0.000
FHDxOLCB	35	12.134	1	32	0.001
FHDxCAPD	35	5.672	1	32	0.023
FHDxRHD	35	0.730	1	32	0.399
FHDxULB	35	1.423	1	32	0.242
FHDxTRCD	35	7.161	1	32	0.012
FHDxCNDC	35	0.834	1	32	0.368
FHDxPRXTB	35	0.998	1	32	0.325
FHDxDSTTB	35	1.993	1	32	0.168
TRCDxHHD	35	14.778	1	32	0.001
TRCDxOLCB	35	9.253	1	32	0.005
TRCDxCAPD	35	6.079	1	32	0.019
TRCDxRHD	35	1.975	1	32	0.170
TRCDxULB	35	0.118	1	32	0.734
TRCDxFHD	35	1.343	1	32	0.255
TRCDxCNDC	35	2.365	1	32	0.134
TRCDxPRXTB	35	1.900	1	32	0.178
TRCDxDSTTB	35	2.405	1	32	0.131
CNDCxHHD	35	25.822	1	32	0.000
CNDCxOLCB	35	16.444	1	32	0.000
CNDCxCAPD	35	8.834	1	32	0.006
CNDCxRHD	35	3.094	1	32	0.088
CNDCxULB	35	2.420	1	32	0.130
CNDCxFHD	35	3.807	1	32	0.060
CNDCxTRCD	35	12.016	1	32	0.002
CNDCxPRXTB	35	1.771	1	32	0.193
CNDCxDSTTB	35	2.116	1	32	0.156

Significant

Not sig.

Appendix 12: ANCOVA output for all species continued.

M.macaca	n	F	df (between)	df (within)	Sig.
PRXTBxHHD	35	22.024	1	32	0.000
PRXTBxOLCB	35	14.069	1	32	0.001
PRXTBxCAPD	35	7.471	1	32	0.010
PRXTBxRHD	35	2.077	1	32	0.159
PRXTBxULB	35	2.100	1	32	0.157
PRXTBxFHD	35	2.173	1	32	0.150
PRXTBxTRCD	35	9.234	1	32	0.005
PRXTBxCNDC	35	0.070	1	32	0.794
PRXTBxDSTTB	35	1.712	1	32	0.200
DSTTBxHHD	35	27.539	1	32	0.000
DSTTBxOLCB	35	21.577	1	32	0.000
DSTTBxCAPD	35	11.194	1	32	0.002
DSTTBxRHD	35	5.399	1	32	0.027
DSTTBxULB	35	4.734	1	32	0.037
DSTTBxFHD	35	7.113	1	32	0.012
DSTTBxTRCD	35	14.496	1	32	0.001
DSTTBxCNDC	35	3.996	1	32	0.054
DSTTBxPRXTB	35	5.457	1	32	0.026

Significant

Not sig.

Appendix 12: ANCOVA output for all species continued.

P.troglodytes	n	F	df (between)	df (within)	Sig.
HHDxOLCB	57	4.713	1	54	0.034
HHDxCAPD	57	1.329	1	54	0.254
HHDxRHD	57	0.016	1	54	0.899
HHDxULB	57	0.628	1	54	0.432
HHDxFHD	57	0.371	1	54	0.545
HHDxTRCD	57	0.338	1	54	0.564
HHDxCNDC	57	5.581	1	54	0.022
HHDxPRXTB	57	1.332	1	54	0.254
HHDxDSTTB	57	1.883	1	54	0.176
OLCBxHHD	57	4.146	1	54	0.047
OLCBxCAPD	57	3.854	1	54	0.055
OLCBxRHD	57	2.613	1	54	0.112
OLCBxULB	57	0.948	1	54	0.334
OLCBxFHD	57	1.727	1	54	0.194
OLCBxTRCD	57	0.002	1	54	0.967
OLCBxCNDC	57	7.446	1	54	0.009
OLCBxPRXTB	57	4.054	1	54	0.049
OLCBxDSTTB	57	2.351	1	54	0.131
CAPDxHHD	57	8.095	1	54	0.006
CAPDxOLCB	57	11.563	1	54	0.001
CAPDxRHD	57	1.573	1	54	0.215
CAPDxULB	57	2.365	1	54	0.130
CAPDxFHD	57	2.702	1	54	0.106
CAPDxTRCD	57	0.678	1	54	0.414
CAPDxCNDC	57	14.315	1	54	0.000
CAPDxPRXTB	57	7.988	1	54	0.007
CAPDxDSTTB	57	4.339	1	54	0.042
RHDxHHD	57	11.797	1	54	0.001
RHDxOLCB	57	15.631	1	54	0.000
RHDxCAPD	57	6.316	1	54	0.015
RHDxULB	57	1.383	1	54	0.245
RHDxFHD	57	3.975	1	54	0.051
RHDxTRCD	57	0.940	1	54	0.337
RHDxCNDC	57	11.847	1	54	0.001
RHDxPRXTB	57	10.160	1	54	0.002
RHDxDSTTB	57	5.805	1	54	0.019

Significant

Not sig.

Appendix 12: ANCOVA output for all species continued.

P.troglodytes	n	F	df (between)	df (within)	Sig.
ULBxHHD	57	29.987	1	54	0.000
ULBxOLCB	57	31.302	1	54	0.000
ULBxCAPD	57	23.214	1	54	0.000
ULBxRHD	57	15.902	1	54	0.000
ULBxFHD	57	15.316	1	54	0.000
ULBxTRCD	57	1.990	1	54	0.164
ULBxCNDC	57	23.926	1	54	0.000
ULBxPRXTB	57	26.795	1	54	0.000
ULBxDSTTB	57	23.049	1	54	0.000
FHDxHHD	57	11.621	1	54	0.001
FHDxOLCB	57	13.913	1	54	0.000
FHDxCAPD	57	6.977	1	54	0.011
FHDxRHD	57	3.444	1	54	0.069
FHDxULB	57	0.415	1	54	0.522
FHDxTRCD	57	0.017	1	54	0.896
FHDxCNDC	57	11.825	1	54	0.001
FHDxPRXTB	57	9.595	1	54	0.003
FHDxDSTTB	57	6.714	1	54	0.012
TRCDxHHD	57	28.716	1	54	0.000
TRCDxOLCB	57	29.005	1	54	0.000
TRCDxCAPD	57	20.163	1	54	0.000
TRCDxRHD	57	14.659	1	54	0.000
TRCDxULB	57	1.437	1	54	0.236
TRCDxFHD	57	14.130	1	54	0.000
TRCDxCNDC	57	23.122	1	54	0.000
TRCDxPRXTB	57	25.865	1	54	0.000
TRCDxDSTTB	57	18.291	1	54	0.000
CNDCxHHD	57	9.512	1	54	0.003
CNDCxOLCB	57	12.138	1	54	0.001
CNDCxCAPD	57	10.886	1	54	0.002
CNDCxRHD	57	3.624	1	54	0.062
CNDCxULB	57	0.030	1	54	0.863
CNDCxFHD	57	4.138	1	54	0.047
CNDCxTRCD	57	0.006	1	54	0.941
CNDCxPRXTB	57	7.002	1	54	0.011
CNDCxDSTTB	57	10.771	1	54	0.002

Significant

Not sig.

Appendix 12: ANCOVA output for all species continued.

P.troglodytes	n	F	df (between)	df (within)	Sig.
PRXTBxHHD	57	2.951	1	54	0.092
PRXTBxOLCB	57	6.334	1	54	0.015
PRXTBxCAPD	57	2.848	1	54	0.097
PRXTBxRHD	57	0.214	1	54	0.646
PRXTBxULB	57	0.090	1	54	0.766
PRXTBxFHD	57	0.234	1	54	0.631
PRXTBxTRCD	57	0.000	1	54	0.990
PRXTBxCNDC	57	4.901	1	54	0.031
PRXTBxDSTTB	57	2.613	1	54	0.112
DSTTBxHHD	57	13.271	1	54	0.001
DSTTBxOLCB	57	14.495	1	54	0.000
DSTTBxCAPD	57	8.574	1	54	0.005
DSTTBxRHD	57	5.102	1	54	0.028
DSTTBxULB	57	6.328	1	54	0.015
DSTTBxFHD	57	6.556	1	54	0.013
DSTTBxTRCD	57	3.167	1	54	0.081
DSTTBxCNDC	57	19.144	1	54	0.000
DSTTBxPRXTB	57	12.212	1	54	0.001

Significant

Not sig.

Appendix 12: ANCOVA output for all species continued.

G.gorilla	n	F	df (between)	df (within)	Sig.
HHDxOLCB	60	3.471	1	57	0.068
HHDxCAPD	60	4.419	1	57	0.040
HHDxRHD	60	0.116	1	57	0.735
HHDxULB	60	0.781	1	57	0.380
HHDxFHD	60	2.231	1	57	0.141
HHDxTRCD	60	0.557	1	57	0.458
HHDxCNDC	60	0.018	1	57	0.892
HHDxPRXTB	60	0.008	1	57	0.927
HHDxDSTTB	60	14.910	1	57	0.000
OLCBxHHD	60	21.804	1	57	0.000
OLCBxCAPD	60	20.945	1	57	0.000
OLCBxRHD	60	10.451	1	57	0.002
OLCBxULB	60	6.694	1	57	0.012
OLCBxFHD	60	19.456	1	57	0.000
OLCBxTRCD	60	5.407	1	57	0.024
OLCBxCNDC	60	3.744	1	57	0.058
OLCBxPRXTB	60	6.255	1	57	0.015
OLCBxDSTTB	60	23.020	1	57	0.000
CAPDxHHD	60	23.304	1	57	0.000
CAPDxOLCB	60	21.202	1	57	0.000
CAPDxRHD	60	12.392	1	57	0.001
CAPDxULB	60	5.324	1	57	0.025
CAPDxFHD	60	20.985	1	57	0.000
CAPDxTRCD	60	5.434	1	57	0.023
CAPDxCNDC	60	6.877	1	57	0.011
CAPDxPRXTB	60	10.151	1	57	0.002
CAPDxDSTTB	60	21.178	1	57	0.000
RHDxHHD	60	19.491	1	57	0.000
RHDxOLCB	60	12.317	1	57	0.001
RHDxCAPD	60	14.077	1	57	0.000
RHDxULB	60	3.446	1	57	0.069
RHDxFHD	60	14.287	1	57	0.000
RHDxTRCD	60	0.824	1	57	0.368
RHDxCNDC	60	0.496	1	57	0.484
RHDxPRXTB	60	2.937	1	57	0.092
RHDxDSTTB	60	28.647	1	57	0.000

Significant

Not sig.

Appendix 12: ANCOVA output for all species continued.

G.gorilla	n	F	df (between)	df (within)	Sig.
ULBxHHD	60	72.757	1	57	0.000
ULBxOLCB	60	52.759	1	57	0.000
ULBxCAPD	60	50.045	1	57	0.000
ULBxRHD	60	44.359	1	57	0.000
ULBxFHD	60	51.198	1	57	0.000
ULBxTRCD	60	9.393	1	57	0.003
ULBxCNDC	60	20.089	1	57	0.000
ULBxPRXTB	60	34.515	1	57	0.000
ULBxDSTTB	60	67.130	1	57	0.000
FHDxHHD	60	16.369	1	57	0.000
FHDxOLCB	60	15.673	1	57	0.000
FHDxCAPD	60	16.882	1	57	0.000
FHDxRHD	60	8.935	1	57	0.004
FHDxULB	60	2.681	1	57	0.107
FHDxTRCD	60	0.662	1	57	0.419
FHDxCNDC	60	1.731	1	57	0.194
FHDxPRXTB	60	2.925	1	57	0.093
FHDxDSTTB	60	22.406	1	57	0.000
TRCDxHHD	60	94.138	1	57	0.000
TRCDxOLCB	60	68.749	1	57	0.000
TRCDxCAPD	60	68.389	1	57	0.000
TRCDxRHD	60	56.377	1	57	0.000
TRCDxULB	60	20.634	1	57	0.000
TRCDxFHD	60	65.236	1	57	0.000
TRCDxCNDC	60	28.570	1	57	0.000
TRCDxPRXTB	60	45.885	1	57	0.000
TRCDxDSTTB	60	83.143	1	57	0.000
CNDCxHHD	60	52.682	1	57	0.000
CNDCxOLCB	60	32.666	1	57	0.000
CNDCxCAPD	60	36.979	1	57	0.000
CNDCxRHD	60	25.585	1	57	0.000
CNDCxULB	60	9.034	1	57	0.004
CNDCxFHD	60	34.206	1	57	0.000
CNDCxTRCD	60	5.686	1	57	0.020
CNDCxPRXTB	60	17.408	1	57	0.000
CNDCxDSTTB	60	49.604	1	57	0.000

Significant
Not sig.

Appendix 12: ANCOVA output for all species continued.

G.gorilla	n	F	df (between)	df (within)	Sig.
PRXTBxHHD	60	27.084	1	57	0.000
PRXTBxOLCB	60	14.592	1	57	0.000
PRXTBxCAPD	60	18.752	1	57	0.000
PRXTBxRHD	60	9.010	1	57	0.004
PRXTBxULB	60	3.106	1	57	0.083
PRXTBxFHD	60	14.355	1	57	0.000
PRXTBxTRCD	60	0.790	1	57	0.378
PRXTBxCNDC	60	0.053	1	57	0.820
PRXTBxDSTTB	60	25.239	1	57	0.000
DSTTBxHHD	60	29.707	1	57	0.000
DSTTBxOLCB	60	17.039	1	57	0.000
DSTTBxCAPD	60	15.097	1	57	0.000
DSTTBxRHD	60	20.112	1	57	0.000
DSTTBxULB	60	9.650	1	57	0.003
DSTTBxFHD	60	20.296	1	57	0.000
DSTTBxTRCD	60	7.352	1	57	0.009
DSTTBxCNDC	60	9.822	1	57	0.003
DSTTBxPRXTB	60	10.231	1	57	0.002

Significant

Not sig.

Appendix 12: ANCOVA output for all species continued.

H.sapiens	n	F	df (between)	df (within)	Sig
HHDxOLCB	60	31.633	1	57	0.000
HHDxCAPD	60	7.866	1	57	0.007
HHDxRHD	60	9.814	1	57	0.030
HHDxULB	60	39.888	1	57	0.000
HHDxFHD	60	6.230	1	57	0.015
HHDxTRCD	60	0.001	1	57	0.970
HHDxCNDC	60	2.797	1	57	0.100
HHDxPRXTB	60	10.266	1	57	0.002
HHDxDSTTB	60	0.350	1	57	0.557
OLCBxHHD	60	11.019	1	57	0.002
OLCBxCAPD	60	4.465	1	57	0.039
OLCBxRHD	60	12.821	1	57	0.001
OLCBxULB	60	14.565	1	57	0.000
OLCBxFHD	60	13.329	1	57	0.001
OLCBxTRCD	60	0.114	1	57	0.737
OLCBxCNDC	60	9.209	1	57	0.004
OLCBxPRXTB	60	12.156	1	57	0.001
OLCBxDSTTB	60	3.342	1	57	0.073
CAPDxHHD	60	17.691	1	57	0.000
CAPDxOLCB	60	35.224	1	57	0.000
CAPDxRHD	60	10.745	1	57	0.002
CAPDxULB	60	40.335	1	57	0.000
CAPDxFHD	60	22.786	1	57	0.000
CAPDxTRCD	60	5.118	1	57	0.028
CAPDxCNDC	60	21.711	1	57	0.000
CAPDxPRXTB	60	30.939	1	57	0.000
CAPDxDSTTB	60	9.866	1	57	0.003
RHDxHHD	60	10.152	1	57	0.002
RHDxOLCB	60	34.441	1	57	0.000
RHDxCAPD	60	2.131	1	57	0.150
RHDxULB	60	36.296	1	57	0.000
RHDxFHD	60	16.085	1	57	0.000
RHDxTRCD	60	2.899	1	57	0.094
RHDxCNDC	60	10.702	1	57	0.002
RHDxPRXTB	60	18.069	1	57	0.000
RHDxDSTTB	60	3.746	1	57	0.058

Significant

Not sig.

Appendix 12: ANCOVA output for all species continued.

H.sapiens	n	F	df (between)	df (within)	Sig
ULBxHHD	60	13.487	1	57	0.001
ULBxOLCB	60	10.843	1	57	0.002
ULBxCAPD	60	4.498	1	57	0.038
ULBxRHD	60	10.532	1	57	0.002
ULBxFHD	60	20.646	1	57	0.000
ULBxTRCD	60	1.005	1	57	0.320
ULBxCNDC	60	9.883	1	57	0.030
ULBxPRXTB	60	12.966	1	57	0.001
ULBxDSTTB	60	9.204	1	57	0.004
FHDxHHD	60	0.496	1	57	0.484
FHDxOLCB	60	26.333	1	57	0.000
FHDxCAPD	60	6.008	1	57	0.017
FHDxRHD	60	9.123	1	57	0.004
FHDxULB	60	40.051	1	57	0.000
FHDxTRCD	60	0.013	1	57	0.911
FHDxCNDC	60	1.774	1	57	0.188
FHDxPRXTB	60	7.306	1	57	0.009
FHDxDSTTB	60	0.001	1	57	0.977
TRCDxHHD	60	44.889	1	57	0.000
TRCDxOLCB	60	76.029	1	57	0.000
TRCDxCAPD	60	39.429	1	57	0.000
TRCDxRHD	60	49.529	1	57	0.000
TRCDxULB	60	85.519	1	57	0.000
TRCDxFHD	60	55.072	1	57	0.000
TRCDxCNDC	60	32.152	1	57	0.000
TRCDxPRXTB	60	53.116	1	57	0.000
TRCDxDSTTB	60	15.090	1	57	0.000
CNDCxHHD	60	13.716	1	57	0.000
CNDCxOLCB	60	45.028	1	57	0.000
CNDCxCAPD	60	23.840	1	57	0.000
CNDCxRHD	60	22.661	1	57	0.000
CNDCxULB	60	51.723	1	57	0.000
CNDCxFHD	60	19.438	1	57	0.000
CNDCxTRCD	60	1.984	1	57	0.164
CNDCxPRXTB	60	17.138	1	57	0.000
CNDCxDSTTB	60	0.533	1	57	0.468

Appendix 12: ANCOVA output for all species continued.

H.sapiens	n	F	df (between)	df (within)	Sig
PRXTBxHHD	60	5.699	1	57	0.020
PRXTBxOLCB	60	26.997	1	57	0.000
PRXTBxCAPD	60	14.186	1	57	0.000
PRXTBxRHD	60	12.620	1	57	0.001
PRXTBxULB	60	32.643	1	57	0.000
PRXTBxFHD	60	8.918	1	57	0.004
PRXTBxTRCD	60	0.422	1	57	0.519
PRXTBxCNDC	60	1.434	1	57	0.236
PRXTBxDSTTB	60	0.018	1	57	0.894
DSTTBxHHD	60	40.752	1	57	0.000
DSTTBxOLCB	60	77.023	1	57	0.000
DSTTBxCAPD	60	41.981	1	57	0.000
DSTTBxRHD	60	46.019	1	57	0.000
DSTTBxULB	60	98.109	1	57	0.000
DSTTBxFHD	60	49.846	1	57	0.000
DSTTBxTRCD	60	11.743	1	57	0.001
DSTTBxCNDC	60	25.922	1	57	0.000
DSTTBxPRXTB	60	47.265	1	57	0.000

Significant

Not sig.

Appendix 13: Tables of *Homo sapiens* and *Saimiri sciureus* male correlation coefficient values with similar values between the species (<0.1 difference) highlighted.

	Upper Limb Metrics					Lower Limb Metrics				
H. sapiens	HHD	OLCB	CAPD	RHD	ULB	FHD	TRCD	CNDC	PRXTB	DSTTB
HHD		0.382	0.513	0.626	0.368	0.923	0.586	0.740	0.731	0.627
OLCB	0.382		0.508	0.339	0.583	0.385	0.536	0.262	0.402	0.289
CAPD	0.513	0.508		0.764	0.510	0.546	0.297	0.292	0.353	0.251
RHD	0.626	0.339	0.764		0.336	0.615	0.318	0.566	0.569	0.377
ULB	0.368	0.583	0.510	0.336		0.285	0.409	0.301	0.378	0.130
FHD	0.923	0.385	0.546	0.615	0.285		0.599	0.741	0.782	0.657
TRCD	0.586	0.536	0.297	0.318	0.409	0.599		0.469	0.483	0.435
CNDC	0.740	0.262	0.292	0.566	0.301	0.741	0.469		0.920	0.657
PRXTB	0.731	0.402	0.353	0.569	0.378	0.782	0.483	0.920		0.642
DSTTB	0.627	0.289	0.251	0.377	0.130	0.657	0.435	0.657	0.642	

	Upper Limb Metrics					Lower Limb Metrics				
S. sciureus	HHD	OLCB	CAPD	RHD	ULB	FHD	TRCD	CNDC	PRXTB	DSTTB
HHD		0.593	0.631	0.533	0.399	0.524	0.537	0.500	0.679	0.460
OLCB	0.593		0.537	0.725	0.346	0.170	0.441	0.268	0.475	0.333
CAPD	0.631	0.537		0.657	0.557	0.331	0.300	0.456	0.604	0.572
RHD	0.533	0.725	0.657		0.349	0.435	0.296	0.427	0.406	0.546
ULB	0.399	0.346	0.557	0.349		0.394	0.318	0.463	0.533	0.361
FHD	0.524	0.170	0.331	0.435	0.394		0.404	0.636	0.480	0.409
TRCD	0.537	0.441	0.300	0.296	0.318	0.404		0.400	0.546	0.349
CNDC	0.500	0.268	0.456	0.427	0.463	0.636	0.400		0.782	0.536
PRXTB	0.679	0.475	0.604	0.406	0.533	0.480	0.546	0.782		0.539
DSTTB	0.460	0.333	0.572	0.546	0.361	0.409	0.349	0.536	0.539	

Appendix 14: Tables of *Homo sapiens* and *Macaca mulatta* lower limb correlation coefficient difference values with similar values between the species (<0.1 difference) highlighted.

H. sapiens	FHD	TRCD	CNDC	PRXTB	DSTTB
FHD		0.072	0.193	0.271	0.184
TRCD	0.072		0.027	0.036	0.288
CNDC	0.193	0.027		0.018	0.112
PRXTB	0.271	0.036	0.02		0.155
DSTTB	0.184	0.288	0.112	0.155	

M. mulatta	FHD	TRCD	CNDC	PRXTB	DSTTB
FHD		0.077	0.062	0.007	0.248
TRCD	0.077		-0.017	-0.070	0.204
CNDC	0.062	-0.017		0.000	0.110
PRXTB	0.007	-0.070	0.000		0.046
DSTTB	0.248	0.204	0.110	0.046	